

ROADWAY SHALLOW WATER FLOW MODELING BY
VELOCITY DISTRIBUTION

by

CHIRAKARN SIRIVITMAITRIE

Presented to Faculty the Graduate School of
The University of Texas at Arlington in Partial Fulfillment
of the Requirements
for the Degree of

DOCTOR OF PHILOSOPHY

THE UNIVERSITY OF TEXAS AT ARLINGTON

August 2007

Copyright © by Chirakarn Sirivitmaitrie 2007

All Rights Reserved

ACKNOWLEDGMENTS

I would like to express my appreciation to my supervising professor, Dr. Ernest C. Crosby, for providing valuable assistance and suggestions. This research could not have taken place without his support and encouragement. His experience and knowledge guided me throughout the entire period of my graduate study. I would also like to express my appreciation to the members of the dissertation committee, Dr. Max Spindler, Dr. Laureano R. Hoyos, Dr. Melanie L. Sattler, and Dr. Chien Pai Han for their comments and suggestions.

A special word of appreciation is due to Texas Department of Transportation roadway Manning's n-value analysis project for providing the graduate research assistantship and all the roadway data used in this research.

I wish to thank my cousin and his wife, Dr. Manus and Suwanna Chaiprasert, for their guidance and support.

Finally, I cannot express in words my deepest appreciation to my parents, Kitti and Chiravadi Sirivitmaitrie, and my sister and brother for everything they did for me during my years of study.

July 16, 2007

ABSTRACT

ROADWAY SHALLOW WATER FLOW MODELING BY VELOCITY DISTRIBUTION

Publication No. _____

Chirakarn Sirivitmaitrie, Ph.D.

The University of Texas at Arlington, 2007

Supervising Professor: Ernest C. Crosby

Manning's equation is a widely used method for determining flow discharge in a channel with unconfined gravity flow. The roughness value, n-value, is a critical factor for Manning's equation to obtain the accurate amount of flow. A precise estimation of Manning "n" is difficult to obtain and varies by investigator justification and experience. Flow on a roadway is a type of open channel flow normally determined by Manning's equation. To ensure reliability and highway safety, the hydraulic geometry dimensions such as spread, depth and discharge must be accurately estimated.

A Texas Department of Transportation Manning's n-value research project collected data on surface roughness and estimate n-value of four different types of

roadway sections; asphalt, asphalt treatment, smooth (worn) concrete and TxDOT's standard concrete surface. This research used full scale roadway sections with the varied flows and longitudinal and transverse slopes. This study focused on estimating n-values for the entire roadway flow width.

A velocity distribution method is used as an alternative method to study the flow characteristic and estimate n-values of each roadway cross-section. The velocity distribution equations use basic geometry data from the TxDOT research. The data for the four types of roadways from TxDOT Manning's n-value research were used as input for the velocity distribution modeling.

The percent accuracy of model simulation is estimated from a comparison of result, discharge and n-value, between the velocity method result and the original TxDOT research data. The modeling utilizes theoretical survey, statistical-analysis, numerical-analysis and flow methods to simulate roadway flow. Statistical analysis such as normality, data cleaning, and outlier detection, were used to improve results.

The results indicate velocity distribution equations are potentially a good method for estimating discharge and n-values for a roadway section. It shows comparable discharge volumes and average n-values to the original TxDOT laboratory result with an acceptable percent of error.

TABLE OF CONTENTS

ACKNOWLEDGEMENTS.....	iii
ABSTRACT.....	iv
LIST OF ILLUSTRATIONS.....	x
LIST OF TABLES.....	xiv
Chapter	
1. INTRODUCTION.....	1
1.1 Background.....	1
1.2 Flow Simulation with Velocity Distribution Method.....	2
1.3 Statement of the Problem.....	6
1.4 Objective of the Study.....	7
1.5 Approach.....	8
2. LITERATURE REVIEW.....	10
2.1 Manning's n-value.....	10
2.2 Velocity Distribution.....	14
2.2.1 Flow Resistance Equation Transformation.....	15
2.2.2 Friction Velocity.....	23
2.2.3 Prandtl-von Karman Velocity Distribution Equation.....	23
2.3 Roughness Dimension.....	27

2.4 Method of Estimating Average Manning's n-value.....	30
2.4.1 Horton and Einstein's Equation.....	31
2.4.2 Pavlovski, Muhlhofer, Einstein and Banks's Equation.....	32
2.4.3 Lotter's Equation.....	32
2.4.4 Krishnamurthy and Christensen's Equation.....	33
2.4.5 Other Methods of Averaging n-values.....	33
2.5 Statistical Analysis.....	35
2.5.1 Histogram Plot.....	36
2.5.2 Normality Distribution Plot (Q-Q Plot).....	36
2.5.3 Scatter Plots.....	37
2.5.4 Outlier Detection.....	37
2.5.5 Correlation Coefficient.....	37
2.5.6 Transformation to Near Normality.....	39
3. METHODOLOGY.....	42
3.1 Data Collection and Preparation.....	42
3.2 Calculation Process and Modeling.....	43
3.2.1 Obtain Geometry Data.....	46
3.2.2 Surface Roughness Estimation.....	47
3.2.3 Calculate Roadway Cross-Section and Sub-Section Areas.....	54
3.2.3.1 Water Surface.....	58
3.2.4 Friction Velocity.....	58
3.2.5 Critical Roughness Height.....	59

3.2.6 Surface Roughness Condition.....	60
3.2.7 Vertical Velocity Profile.....	60
3.2.8 Calculate Sub-Section Average Velocity.....	62
3.2.8.1 Total Cross-Section Velocity Distribution.....	63
3.2.9 Sub-Section Manning’s n-value Calculation.....	66
3.2.10 Sub-Section Discharges Calculation.....	67
3.2.11 Total Cross-Section Discharge and Average Manning’s n-value Calculation.....	68
3.3 Mathematic Statistical Analysis.....	68
3.3.1 Obtain and Rearrange Data Sets.....	70
3.3.2 Construct Histogram Plot.....	70
3.3.3 Construct a Normal Probability Plot (Q-Q Plot).....	72
3.3.4 Construct Scatter Plots.....	74
3.3.5 Calculate Correlation Coefficient.....	76
3.3.6 Check Hypothesis of Normality.....	78
3.3.6.1 Detect Outliers.....	79
3.3.6.2 Data Cleaning.....	81
3.3.7 Calculate Statistical Result.....	81
4. MODEL VERIFICATION AND RESULT ANALYSIS.....	84
4.1 Model Calibration and Verification.....	84
4.2 Theoretical Manning’s n-value.....	86
4.3 Velocity Distribution Methods Comparison.....	90
4.4 Manning’s n-values Estimated by Various Averaging Methods.....	99

4.5 Discharges Estimated by Velocity Distribution Methods' n-values.....	105
4.6 Affect of Roadway Slopes.....	111
5. CONCLUSIONS AND RECOMMENDATIONS.....	115
5.1 Conclusion.....	115
5.2 Recommendation for Future Research.....	117
Appendix	
A. ESTIMATED DISCHARGE PLOTS.....	118
B. ROADWAY DATA TABLES.....	137
C. MANNING'S N-VALUES ESTIMATED BY PRANDTL-VON KARMAN VELOCITY METHOD.....	161
D. COMPARISON BETWEEN MEASURED AND PRANDTL-VON KARMAN VELOCITY METHOD DISCHARGES.....	188
E. HISTOGRAM PLOTS OF MANNING'S N-VALUES.....	201
REFERENCES.....	210
BIOGRAPHICAL INFORMATION.....	215

LIST OF ILLUSTRATIONS

Figure	Page
1.1 TxDOT roadway roughness research study.....	3
1.2 Asphalt roadway surface (longitudinal cross-section).....	4
1.3 TxDOT concrete roadway surface (longitudinal cross-section).....	4
1.4 Smooth concrete roadway surface (longitudinal cross-section).....	5
1.5 Asphalt treatment roadway surface (longitudinal cross-section).....	5
2.1 Development of the boundary layer.....	19
2.2 Velocity profile of flow.....	20
2.3 Projections of roughness value k , k_c in different conditions.....	28
2.4 Three basic types of rough surface flow.....	30
2.5 Histogram plot of smooth concrete n-value (lab result).....	40
2.6 Histogram plot of smooth concrete n-value (Prandtl-von Karman velocity method and depth-weight averaging method).....	41
3.1 Velocity distribution calculation process.....	45
3.2 Longitudinal TxDOT concrete roadway surface profiles.....	50
3.3 Longitudinal asphalt roadway surface profiles.....	51
3.4 Longitudinal smooth concrete roadway surface profiles.....	52
3.5 Longitudinal asphalt treatment roadway surface profiles.....	53
3.6 Methods of cross-section area estimation.....	54

3.7	Total cross-section, sub section areas, heights, widths, and water elevation of the roadway cross-section.....	55
3.8	Roadway sub-section area dimensions.....	56
3.9	Roadway curb-section dimensions.....	56
3.10	Roadway longitudinal slope calculation.....	57
3.11	Vertical velocity profiles across the roadway cross-section.....	61
3.12	Plan view of average velocity in each station from curb on left hand side to the end of water on right hand side of roadway cross-section.....	63
3.13	Velocity distributions across a roadway cross-section.....	65
3.14	Process of statistical analysis.....	69
3.15	Histogram plot of smooth concrete n-value by Manning's equation and measure discharge.....	71
3.16	Normality plot (Q-Q plot) of n-values (before detecting outliers and cleaning data).....	73
3.17	Normality plot (Q-Q plot) of n-values (after detecting outliers and cleaning data).....	73
3.18	Scatter plots of TxDOT concrete roadway n-values with no-rain, 1-inch/hr, 3-inch/hr, and 6-inch/hr.....	75
3.19	Result of TxDOT concrete discharge comparison before cleaning process.....	82
3.20	Result of TxDOT concrete discharge comparison after cleaning process.....	82
3.21	Comparison of average n-values by various averaging methods (before and after cleaning data).....	83
4.1	Cross-sectiona areas estimated by spread and depth methods.....	86
4.2	Estimated Manning's n-value for asphalt surface.....	88

4.3	Estimated Manning's n-value for asphalt treatment surface.....	88
4.4	Estimated Manning's n-value for TxDOT concrete surface.....	89
4.5	Estimated Manning's n-value for smooth concrete surface.....	89
4.6	Comparison of velocity profiles by various flow resistance equations.....	91
4.7	Discharge estimated by various flow resistance equations.....	92
4.8	Average percent discharge error comparisons by various flow resistance equations.....	94
4.9	Vertical velocity profiles calculated by different roughness values (k).....	97
4.10	Vertical velocity profiles calculated by different longitudinal slopes.....	97
4.11	Vertical velocity profiles estimated by different transverse slopes.....	98
4.12	Vertical velocity profiles calculated by different roughness values (k) and longitudinal slopes.....	98
4.13	Relationships between local geometries and methods of averaging n-values.....	100
4.14	Average Manning's n-values by various averaging methods.....	102
4.15	Example of sub-section n-values across the roadway cross-section by Prandtl-von Karman velocity distribution method.....	104
4.16	Example of averaging parameters across the entire roadway cross-section.....	104
4.17	Plots of average variable and constant n-values.....	107
4.18	Percent discharge error by various methods of averaging n-value.....	109
4.19	Comparison of percent error between variable and constant n-value by various averaging methods.....	110
4.20	Comparison of roadway cross-section areas by different transverse slopes.....	112

4.21	Comparison of roadway cross-section areas with different longitudinal slopes.....	112
4.22	Percent error of estimated discharge by various velocity method n-values in different transverse slopes (TxDOT concrete surface).....	113
4.23	Percent error of estimated discharge by various velocity method n-values in different longitudinal slopes (TxDOT concrete surface).....	114

LIST OF TABLES

Table	Page
2.1 Critical points for the Q-Q plot correlation coefficient test for normality.....	39
3.1 Correlation coefficient calculation table.....	77
3.2 Critical point for the Q-Q plot correlation coefficient test for normality.....	78
3.3 Standardized and generalized distance values for TxDOT concrete roadway surface with no-rain, 1-in/hr, 3-in/hr, 6-in/hr.....	80
4.1 Estimated Manning’s n-values.....	87
4.2 Average percent discharge errors from various velocity methods.....	93
4.3 Estimated average Manning’s n-values for four types of roadway surfaces by Prandtl-von Karman velocity distribution and various averaging methods.....	101

CHAPTER 1

INTRODUCTION

1.1 Background

Manning's equation has been used for a number of years. It is used in hydraulics to estimate channel discharge. Manning's equation can be used to estimate discharge accurately if the correct roughness, n-value, is used. Innumerable researches have studied channels with the intention to determine exact n-values. Manning's n-values are obtained from roughly estimating channel bottom surfaces and local channel geometry. For natural channels, a bottom surface roughness is estimated through observation of the bed material. Bottom surface roughness is difficult to estimate and often inaccurate due to the vast variable geometric condition of natural channels. Increasing the number of bed material samples can help improve the accuracy of roughness estimation, but increases cost.

A roadway is considered a type of channel flow. It's designed to remove water from the roadway surface. Because of public safety and reliability, a roadway needs to be designed to have adequate discharge capacity. The flow capacity of a roadway depends on both Manning's n-value and the cross-section geometry. An incorrect n-value leads to either under or over estimation of roadway geometry and flow capacity.

Changing longitudinal and transverse slopes significantly change the roadway discharge capacity. In order to achieve sufficient flow capacity, a roadway should be designed with as accurate n-value and factors of safety as possible.

1.2 Flow Simulation with Velocity Distribution Method

The velocity distribution method is found to be very useful to obtain a stream velocity without numerous physical measurements. It is used to calculate average discharges of a channel. This method considers many geometry conditions such as longitudinal slope, surface roughness, hydraulic depth, and cross-section area of a channel. The velocity distribution method is capable of simulating flow distributions in any shape of channel such as triangular, rectangular, and trapezoidal, including symmetric and non-symmetric cross-section channels. It uses average surface roughness height to calculate flow in channels. Since the velocity distribution technique requires many conditional parameters such as friction velocity, average roughness height, and critical roughness, it can provide accurate discharge estimations.

This research expands upon the TxDOT roadway roughness project. The TxDOT project studied flow over roadway roughness surfaces and evaluated a single Manning's n-value for each roadway surface. The TxDOT project was constructed in a hydraulic laboratory at the University of Texas at Arlington. It was composed of two standard full-scale roadway lanes with an overall size of 64 feet by 17 feet, as shown in Figure 1.1. The roadway slopes varied, and were set and checked by survey methods. The slopes were adjustable in the longitudinal and transverse axis. Two 60 horse-power

centrifugal pumps provided constant discharge, ranging from 1-11cfs for the roadway. Flow geometry data, spread and depth, was collected and used to compute Manning's n-values. The TxDOT project studied four types of roadway surfaces: smooth (worn) concrete, TxDOT concrete, asphalt, and asphalt treatment surfaces as shown in Figure 1.2-1.5. The curb and roadway surfaces were built according to TxDOT roadway standards.



Figure 1.1 TxDOT roadway roughness research study



Figure 1.2 Asphalt roadway surface (longitudinal cross-section)

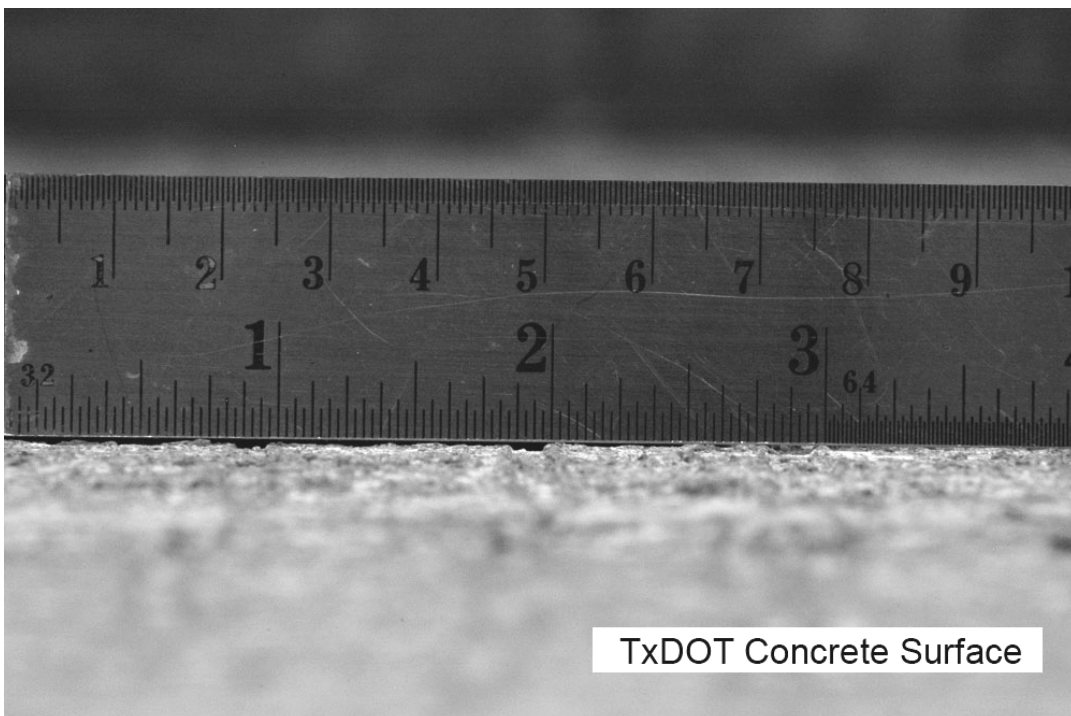


Figure 1.3 TxDOT concrete roadway surface (longitudinal cross-section)

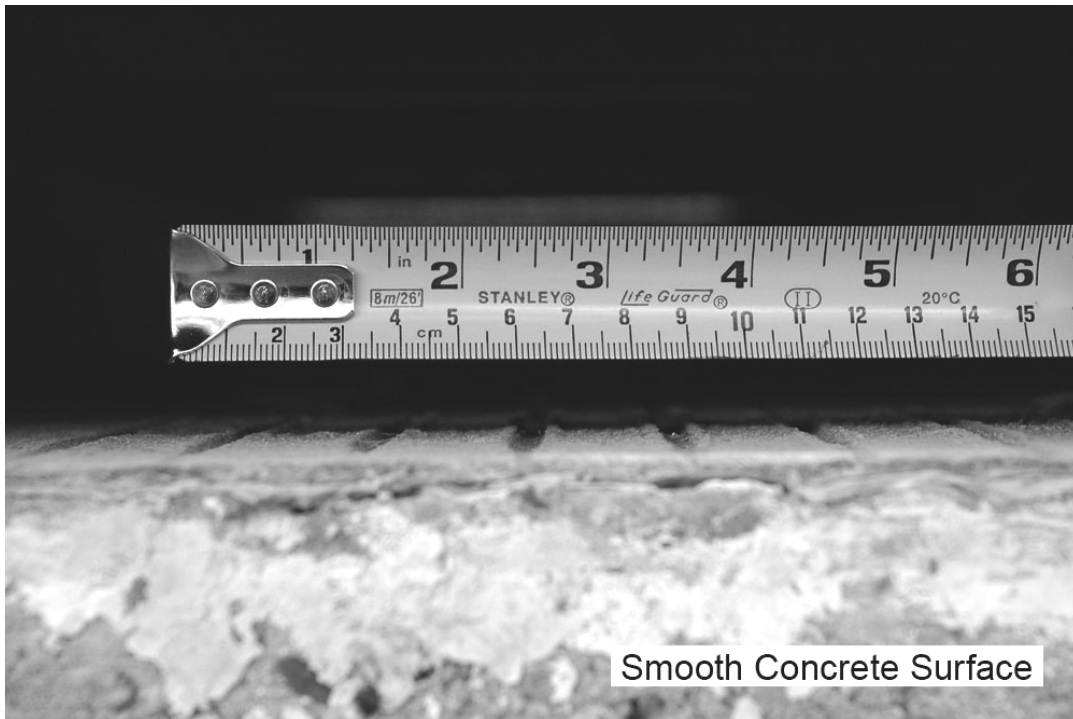


Figure 1.4 Smooth concrete roadway surface (longitudinal cross-section)

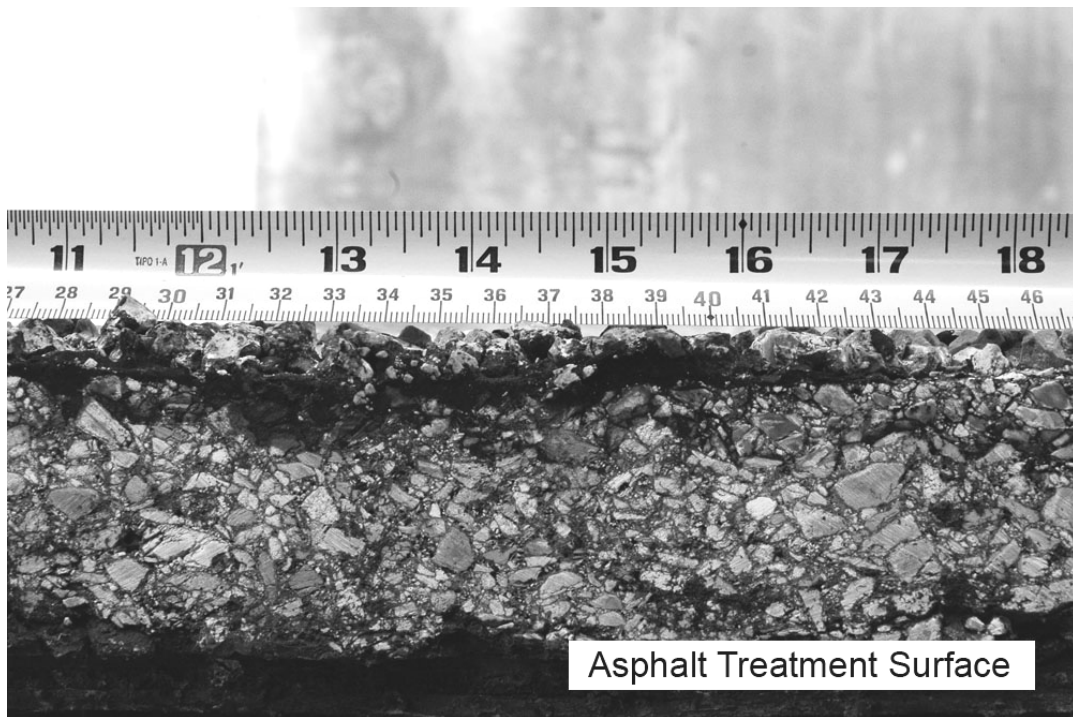


Figure 1.5 Asphalt treatment roadway surface (longitudinal cross-section)

In this research project, roadway and flow geometry data are taken from the TxDOT study. The data consists of roadway cross-section geometries such as depth, spread, longitudinal slope and transverse slopes, along with flows and determined n-values. The TxDOT concrete roadway was also tested with a rainfall simulator to determine the impact of rainfall on Manning's n-value. The rainfall simulator provided rainfall equivalents of one, three and six inches per hour over the roadway.

1.3 Statement of the Problem

Manning's equation is used in roadway design and has been for many years. Manning's n-values have been assigned to past roadway surfaces as a constant value. Present methods of roadway construction including material, equipment, technique, and environment have improved and changed as the result of new technologies and higher standard requirements. These improvements can alter roadway n-values. As roadway surfaces age they change n-values. Roadway designs are based on new surface standards.

The velocity distribution method is an alternative method for calculating discharges. This method uses the same basic geometry data as the Manning's equation. The roughness estimation is determined differently. Instead of using Manning's n-value for surface roughness value, the velocity distribution method utilizes actual roughness height (k) in measurable units. The actual roughness dimension (k) is obtained directly from vertical roughness dimension of a roadway longitudinal cross-section. The

roughness dimension (k) of the velocity distribution method can be transformed to a Manning's n -value.

This research proposes to compare total discharges and average n -values from the velocity distribution method to the original TxDOT roadway data for difference and reliability.

1.4 Objective of the Study

Prandtl-von Karman velocity distribution method is used to simulate vertical velocity profiles of flow in a roadway channel. These velocity profiles can be used to estimate an average velocity and a total cross-section flow of a roadway channel.

A roadway channel is considered to be an irregular channel. It is made up of small non-symmetric sub-sections adjacent to each other throughout the entire cross-section. An entire roadway cross-section profile is established from a theoretical survey calculation. This study focuses on using an estimated roughness dimension (k) for velocity distribution equations. The roughness value (k) is estimated directly from channel bed material. It is converted to Manning's n -value by theoretical equation conversion. The converted n -value can be used to estimate the average cross-section n -value of a roadway channel.

Unlike Manning's n -value, the roughness value (k) is limited to physical measuring of the actual bottom roughness dimension on roadway surfaces. The roughness value (k) is considered to be uniform and constant for the entire surface and highly affects the flow. It's not a variable due to changing of cross-section geometries

or flow environments. On the contrary, Manning's n-value can be changed by flow environments such as states of flow, geometry dimensions, and slopes. Theoretically, Manning's n-value is a constant average index value of an individual roughness surface.

This research is designed to find affects of flow environments to Manning's n-value. It's possible that Manning's n-value can be changed due to variation of flow stages from laminar to turbulent flow. For constant discharge and bottom surface roughness, velocity and depth of flow are varied by roadway longitudinal and transverse slopes. The validation of n-value variation is determined by comparison of roughness value (k) to Manning's n-value and discharge comparison.

Another study topic is the Manning's n-value cross-section averaging method. Averaging methods of n-values are significant factors and highly affect the outcome of the average cross-section n-value. Weighting parameters such as, area, depth, wetted-perimeter, hydraulic-radius, discharge, and velocity for each sub-section are key factors in determining averaging methods effect. In order to justify the specific methods of average, various discharge and n-value comparisons are considered.

1.5 Approach

The proposed simulation will be performed in the following steps:

1. Collect necessary geometry data such as depth, spread, slopes, and discharge from the TxDOT roadway study and use as input to a velocity distribution method for flow calculations.

2. Develop a roadway geometric model to simulate flow calculation. Perform discharge and n-value calculations using this model.

3. Using both sets of discharge and n-value results, perform statistical analysis and display the result comparison of the two methods.

CHAPTER 2

LITERATURE REVIEW

2.1 Manning's n-value

Manning's n-value represents roughness a value of channel bottom material. This value is used with Manning's equation as shown in equation 2.1. The main purpose of Manning's equation is to estimate channel velocity and thus flow discharge. The Manning's equation consists of n-value, longitudinal slope (S), and hydraulic radius (R) in order to find average velocity (V) of a channel. An n-value can be obtained by carefully determining the bottom roughness material of a channel.

$$V = \frac{1.486}{n} S^{1/2} R^{2/3} \text{ Manning's equation (Sturm, 2001)} \quad \text{eq.2.1}$$

V = velocity

n = Manning's n-value

S = slope

R = hydraulic radius

A number of researchers have written about Manning's n-values. It has been a research topic for many years. Often the purpose was to estimate the most precise n-value for a particular channel. Much of the literatures is about natural and man made channels with various bottom materials. Some are about artificial channels, specially constructed for research purposes. The approach of each is very specific depending on

its particular geometries and the bottom surface material. Because each location presents unique basic geometry and surface conditions, n-values are estimated based on the unique conditions to achieve acceptable accuracy.

Boyer is one of the early n-value researchers. He purposes an equation for solving n-value in natural channels by using a velocity ratio as shown in equation 2.2. His estimation is based on natural river data. The equation contains no physical roughness parameter of the channel's bottom material. Since Boyer's equation was derived based on a velocity distribution equation, n-values can be similar to the Prandtl-von Karman estimation.

$$n = \frac{(x-1)y^{1/2}}{6.78(x+0.95)} \quad (\text{Boyer, 1954), Mississippi river} \quad \text{eq.2.2}$$

Where $x = u_{0.2}/u_{0.8}$; $y =$ depth of water,

$u_{0.2}, u_{0.8} =$ velocity at 20% and 80% of the depth from the surface of water.

Many researches suggest an n-value estimated from dimensions of channel bottom material, depth or hydraulic radius. These n-value equations are derived from experimental natural channel data. Equations 2.2-2.13 show various equations of n-value estimation based on empirical natural river data.

$$n = 0.034 d_{50}^{1/6} \quad (\text{Strickler, 1923): Gravel-bed river in Switzerland} \quad \text{eq.2.3}$$

where $d_{50,75}$ and $90 =$ mean grain size of bed material which correspond to 50%, 75% and 90% finer respectively.

$$n = 0.032 d_{90}^{1/6} \quad \text{Meyer-Peter, (Mueller, 1948): Sand mixtures in flumes} \quad \text{eq.2.4}$$

$$n = 0.039 d_{75}^{1/6} \text{ (Lane-Carlson, 1953): Canals lined with cobbles} \quad \text{eq.2.5}$$

$$n = 0.104 R^{1/6} \left(\frac{R^{-0.297}}{d_{50}} \right) \left(\frac{P^{-1.03}}{R} \right) \quad \text{eq.2.6}$$

(Griffiths, 1981): Gravel and cobble bed rivers in USA, Canada, New Zealand, and England.

where P = wetted-perimeter, and

R = hydraulic radius.

$$n = 0.048 d_{50}^{0.179} \text{ (Bray, 1979): Gravel-bed river in Alberta, Canada} \quad \text{eq.2.7}$$

$$n = 0.126 R^{1/6} \left(\frac{R^{-0.281}}{d_{50}} \right) \text{ (Bray, 1979): Gravel-bed river in Alberta, Canada} \quad \text{eq.2.8}$$

$$n = \frac{0.0927 R^{1/6}}{0.248 + 2.36 \log_{10} \left(\frac{R}{d_{50}} \right)} \text{ (Bray, 1979): Gravel-bed rivers in Alberta, Canada} \quad \text{eq.2.9}$$

$$n = \frac{0.0927 R^{1/6}}{0.76 + 1.98 \log_{10} \left(\frac{R}{d_{50}} \right)} \text{ (Griffiths, 1981)} \quad \text{eq.2.10}$$

Gravel and cobble bed rivers in USA, Canada, New Zealand and England

$$n = \frac{0.0927 R^{1/6}}{0.035 + 2.03 \log_{10} \left(\frac{R}{d_{50}} \right)} \text{ (Limerinos, 1970): Gravel-bed river in California} \quad \text{eq.2.11}$$

$$n = 0.39 S^{0.38} R^{-0.16} \text{ (Jarrett, 1983)} \quad \text{eq.2.12}$$

Steep streams in CO with cobble sand small boulders

$$n = 0.245 R^{0.14} \left(\frac{R^{-0.44}}{d_{50}} \right) \left(\frac{T^{-0.3}}{R} \right) \text{ (Froehlich, 1978)} \quad \text{eq.2.13}$$

Gravel and cobble bed rivers in USA.

where T = top spread width

In natural channels, channel geometry conditions are difficult to determine. Due to various geometry conditions, non-symmetrical shape of natural channels, bottom materials, average slopes, and obstructions, an average velocity can be difficult to simulate. Water flow distribution within a channel comes from unequal velocity distribution as a result of the local bottom material and geometries. An average velocity is considered the best representation of flow. It is often used to estimate the total cross-section discharge.

A roadway represents a specific type of an artificial channel. It consists of a uniform consistent slope and roughness through out the entire cross-section area. Roadway slopes are designed as a function of the drainage required, reliability desired and safety required. Because of these limiting conditions, roadway Manning's n-values must be estimated more precisely than natural channels. A roadway cross-section is unlike other channel types in that they are a shallow non-symmetry triangular channel. Flow over a roadway is intentionally shallow to improve the traffic handling and reduce drainage safety issue such as hydroplaning.

2.2 Velocity Distribution

Velocity distribution method has been used for a number of years for non roadway channel. A number of researches have worked on this methodology. The velocity distribution is a very useful method for measuring and determining flow velocities in an open channel. This method is an alternative for determining a flow rate in channel without using Manning's n-value. Many roughness equations have been proposed in the literatures for natural rivers as shown in equations 2.15, 2.17, 2.20, 2.24 and 2.26. These equations can be rearranged in to the form of the velocity distribution equation as shown in equation 2.14. The transformations of roughness equations such as Bathurst (1985), Bray (1979), Griffiths (1981), Hey (1979), Limerinos (1970) and Keulegan (1938) into flow resistance equations are shown in equation 2.16, 2.19, 2.21, 2.23, 2.25 and 2.27 by Bettess (2002). These flow resistance equations are based on experimental studies of natural channels. The derivations are based on the logarithm function and friction velocity of channel bed material. After the transformation, every equation is in the similar velocity distribution equation form, eq.2.14. Most flow resistance equations produce similar velocity profiles depends upon the equation parameters. Comparisons of discharge with various velocity distribution equations are provided in chapter 4.

The general flow resistance equation form is

$$V = \sqrt{\alpha g R S} \log\left(\frac{\beta d}{k}\right) \quad \text{or} \quad V = \sqrt{\alpha g R S} \log\left(\frac{\beta R}{k}\right) \quad \text{eq.2.14}$$

where α and β = estimated parameters,

k = roughness dimension,

V = flow velocity,

g = gravity,

S = longitudinal slope, and

Hydraulic radius (R) = depth (d) for broad wide channel and infinitesimal differential area.

2.2.1 Flow Resistance Equation Transformation

The following is an example of roughness equation to be transformed into a velocity distribution equation.

Limerinos (1970) roughness equation is

$$n = \frac{0.113 d^{1/6}}{1.16 + 2.00 \log_{10} \left(\frac{d}{D_{84}} \right)}. \quad (\text{Limerinos, 1970), Gravel-bed river} \quad \text{eq.2.15}$$

Roughness is considered to approximate a function of the diameter of grain size used to define the bed roughness as seen in eq.2.15.

$$k \approx 3D_{50, 84 \text{ or } 90}$$

$D_{50, 84 \text{ or } 90}$ = estimated bed material diameter, and

K = average roughness height.

From Manning's equation $V = \frac{1}{n} d^{2/3} S^{1/2}$ (SI-units)

$$\frac{d^{2/3} S^{1/2}}{V} = \frac{0.113 d^{1/6}}{1.16 + 2.00 \log_{10} \left(\frac{d}{D_{84}} \right)},$$

$$V = \frac{d^{2/3} S^{1/2}}{0.113 d^{1/6}} \left(1.16 + 2.00 \log_{10} \left(\frac{3d}{k} \right) \right),$$

$$V = 8.84 d^{1/2} S^{1/2} 2 \left(0.58 + \log_{10} \left(\frac{3d}{k} \right) \right),$$

$$V = 17.699 d^{1/2} S^{1/2} \left(\log_{10}(3.80) + \log_{10} \left(\frac{3d}{k} \right) \right),$$

$$V = \sqrt{31.93 g d S} \log_{10} \left(\frac{11.4d}{k} \right) \text{ Based on Limerinos's (1970) equation.} \quad \text{eq.2.16}$$

Brays's (1979) roughness equation is shown below.

$$\frac{1}{\sqrt{f}} = 1.26 + 2.16 \log_{10} \left(\frac{d}{D_{90}} \right) \quad \text{eq.2.17}$$

f = roughness value

Literature (Sturm, 2002) shows that the friction value (f) can be expressed as an equation below.

$$\text{where } f = \frac{8gRS}{V^2}, \text{ (Sturm, 2002)} \quad \text{eq.2.18}$$

g = gravity,

R = hydraulic radius,

V = velocity, and

S = slope.

After transforming Bray's roughness equation, eq.2.17, the flow resistance equation is shown below as, eq.2.19.

Bray's transformed equation is

$$V = \sqrt{37.32 g R S} \log_{10} \left(\frac{11.49 d}{k} \right). \quad \text{eq.2.19}$$

Griffiths's (1981) roughness equation is

$$\frac{1}{\sqrt{f}} = 0.760 + 1.98 \log_{10} \left(\frac{R}{D_{90}} \right). \quad \text{eq.2.20}$$

Griffith's transformed equation is

$$V = \sqrt{31.36 g R S} \log_{10} \left(\frac{9.68 R}{k} \right). \quad \text{eq.2.21}$$

Keulegan's (1938) velocity equation is

$$V = \sqrt{g d S} \left[6.25 + 5.75 \log_{10} \left(\frac{d}{k} \right) \right]. \quad \text{eq.2.22}$$

Keulegan's transformed equation is

$$V = \sqrt{33.06 g d S} \log_{10} \left(\frac{12.22 d}{k} \right). \quad \text{eq.2.23}$$

Hey's (1979) roughness equation is

$$\frac{1}{\sqrt{f}} = 2.03 \log_{10} \left(\frac{a R}{3.5 D_{84}} \right). \quad \text{eq.2.24}$$

Where $12.95 < a < 15.70$ depends on shape of channel.

Hey's transformed equation is

$$V = \sqrt{32.97 g R S} \log_{10} \left(\frac{a R}{k} \right). \quad \text{eq.2.25}$$

Bathurst's (1985) roughness equation is

$$\sqrt{\frac{8}{f}} = 5.62 \log_{10} \left(\frac{d}{D_{84}} \right) + 4. \quad \text{eq.2.26}$$

Bathurst's transformed equation is

$$V = \sqrt{31.6 g R S} \log_{10} \left(\frac{15.44 d}{k} \right). \quad \text{eq.2.27}$$

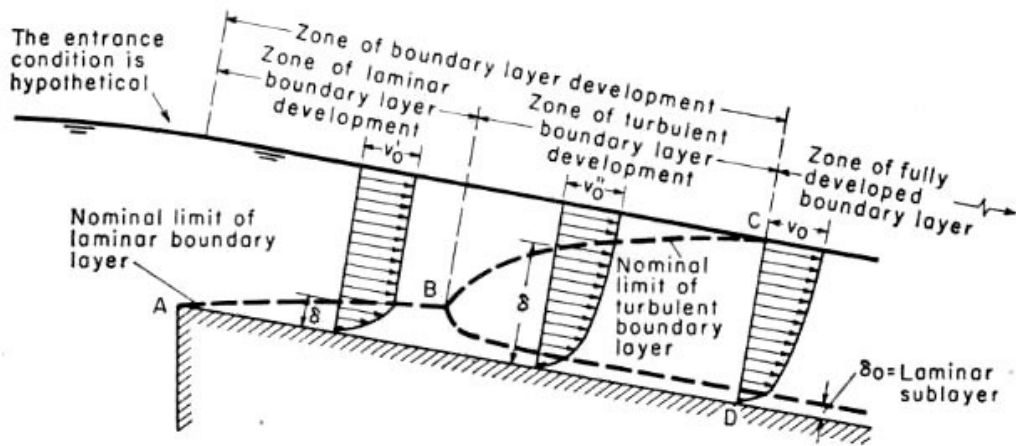
Colebrook's (1939) velocity equation is

$$V = \sqrt{32 g R S} \log_{10} \left(\frac{14.8 R}{k} \right). \quad \text{eq.2.28}$$

In this research, Prandtl-von Karman (1989) velocity distribution equations, equation 2.35 and 2.36, were selected based on consistency and accuracy of the discharge calculation. The results, discharges and n-values, comparison are discussed in chapter 4.

In one dimensional flow, a velocity profile represents logarithm vertical flow velocity distribution in one-dimension parallel to the flow direction. Velocity distribution equations or so called flow resisting equations are based on shear forces emanating at the bottom surface of channel. These equations can be used with an open channel or a gravity flow. With no restriction of geometry conditions, velocity profiles can be used for any type of channel with a known bottom roughness value. In a small sub-section of a channel, a velocity profile starts from channel bottom and progress upward to the water surface.

Figure 2.1 shows various stages of gravity flow behavior in a channel. At the beginning point, water starts entering a channel assumed to be laminar and uniform velocity. At this point, a small laminar layer starts developing along the channel bottom. This laminar layer is shown in region from point A to B. This zone is called “laminar boundary layer”. The velocity distribution in this layer (below A to B to C) is assumed to be parabolic. The flow distribution above line ABC is constant.



Development of the boundary layer in an open channel with an ideal entrance condition.

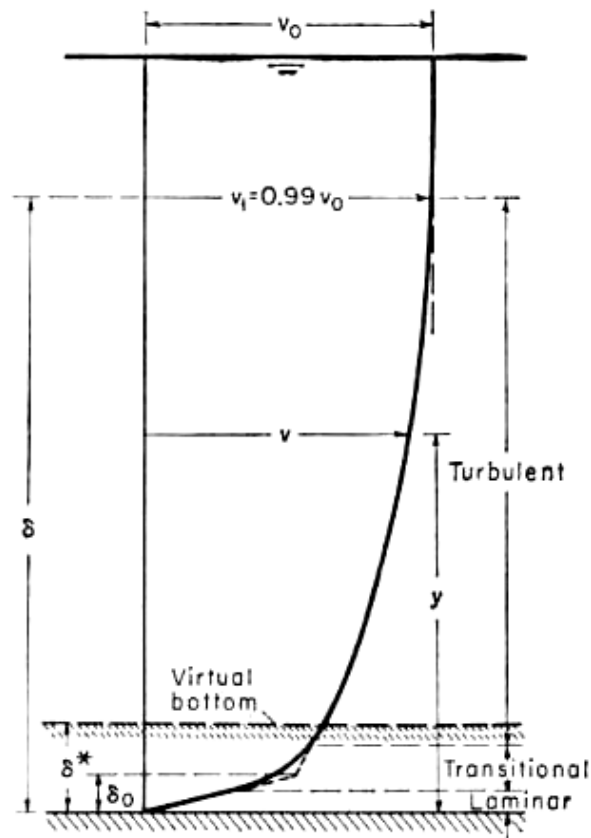
Figure 2.1 Development of the boundary layer (Chow, 1959)

From the channel entrance, the effect of bottom surface roughness on flow distribution is shown under the line ABC. Flow under the line ABC is called the “boundary layer” of δ height.

After the stream reaches a certain velocity, a turbulent zone starts developed from point B to C. In this zone, a very thin laminar layer can developed at the channel bottom due to a smooth bottom roughness surface. This bottom layer is called “laminar sub-layer”, δ^* or δ_0 . Velocity in this zone (below B to C) is approximate as logarithmic.

If flow in a channel becomes uniform, a fully developed turbulent zone is assumed to occurred, after point C. (Chow, 1959)

The velocity profile (Figure 2.2) shows various states of flow from laminar, transition, and turbulent. A laminar layer is a bottom layer of a flow. It represents a very thin layer relative to the whole depth of flow. A velocity at this level is highly resisted by bottom roughness.



Distribution of velocity over a smooth channel surface (not in scale).

Figure 2.2 Velocity profile of flow (Chow, 1959)

where v_0 = water surface velocity
 v_1 = velocity at boundary layer ($v_1 = 0.99v_0$)
 δ = boundary layer
 δ^* = displacement thickness
 δ_0 = laminar sub-layer

The next level of velocity is the transition zone or diverting zone. In every turbulent flow, the transition zone is a turning point of velocity profile. Flow in this transition zone is still under a great influence from bottom roughness. In this zone, the laminar zone and turbulent zone can be separated approximately by both top and bottom boundaries of this layer.

The top layer of a fully developed turbulent flow is a turbulent zone. The turbulent zone is defined by relationship of both roughness and flow conditions. Slopes of a bottom surface also have a great influence on flow in this zone. Turbulent flow develops from under a virtual bottom zone same as other layers. The reason that it dominates a flow is because of a greater flow layer. In fully turbulent flow, the turbulent layer contains more than 90 percent of flow discharge.

“The effect of boundary layer on the flow is equivalent to a fractious upward displacement of the channel bottom to a virtual position by an amount equal to the so called “displacement thickness”, δ^* , (Chow, 1959) as shown in Figure 2.2.

Water flows from a higher level to a lower level as a function of gravitation. Surface roughness and slopes of a channel affect a flow as a function of the earth’s gravity. In open channel flow, surface roughness and slopes of a channel have

significant effects on the flow velocity. Roughness dimension and slopes of channel are normally constant for a channel. Hydraulic depth is a key identifier of the flow conditions. For gravitation flow, velocity is a function of roughness, slope and hydraulic depth. Flow velocity increases as depth increases from the bottom of the channel. This is possible only at the point that bottom roughness doesn't disturb the flow anymore, after that velocity will be a function of slope and gravity.

Three parts of the velocity profile, turbulent, transition, and laminar are developed in the channel as shown in Figure 2.2. These layers of flow define characteristics of fluid flow in three different stages. When water begins entering the channel, it also starts to increase velocity. The velocity develops over a period of time up to a definite speed. The velocity of flow depends on conditions of channel such as, a longitudinal slope and roughness.

Some literature suggests resistance force between air and the top water surface is also present. As water flows in a channel, air is flowing above the water. Friction force can be created between these two flowable materials. This phenomenal could create a convex velocity curve at the surface of water. Especially for a steady gravitation flow layer, where roughness and a slope are constant, air particle resistance could have an effect on water flow. Water flow over a roadway is a very shallow water flow type. Unless the air has significant velocity, the air would have a minimal effect to this type of flow.

2.2.2 Friction Velocity

The friction velocity, V_f , is a result of resistance force created between the liquid and surface friction at the channel bottom. The geometries of roadway, such as longitudinal slope and hydraulic radius, have significant effects on friction velocity. For a roadway surface, a cross-section is divided into small vertical sub-sections beginning with the curb to the end of water on the roadway surface. In this situation, the hydraulic radius is equal to the water depth at each location.

Friction velocity varies with basic geometries of channel such as longitudinal slope, bottom surface roughness, side surface roughness, and hydraulic depth. Transverse slope has an indirect effect to friction velocity. Changing the transverse slope changes the hydraulic depth by changing flow spread. Different types of surface roughness provide different vertical velocity profiles. Surface roughness is estimated by bed material, such as average grain size for natural channels and roughness height for streets and artificial channels. The derivation of friction velocity is shown in the next topic.

2.2.3 Prandtl-von Karman Velocity Distribution Equation

The vertical velocity distribution is a result of local geometry conditions such as depth, hydraulic radius, slopes and surface roughness. Turbulence in the liquid takes a role in justifying distributions of velocity profile. Prandtl-von Karman (1926) derived flow resistance equation based on shear stress of bottom surface roughness. Prandtl introduced a shear stress for turbulent flow as follow.

Shear stress in flow equation

$$\tau = \rho l^2 \left(\frac{dv}{dy} \right)^2 \quad (\text{Prandtl-von Karman, 1926}) \quad \text{eq.2.29}$$

where τ = Shear stress,

ρ = Mass density = w/g ,

w = Unit weight of the fluid,

g = Gravity,

l = Mixing length, and

$\frac{dv}{dy}$ = Velocity gradient at depth (y) from water surface.

“Assume the mixing length is proportional to depth and that the shear stress is constant, $\tau = \tau_0$ ” (Prandtl, 1926). Equation 2.29 can be rewritten as follow.

$$du = \frac{1}{k} \sqrt{\frac{\tau_0}{\rho}} \frac{dy}{y} \quad \text{eq.2.30}$$

Where k is a constant that varies with mixing length and depth, then

$$V = 2.5 \sqrt{\frac{\tau_0}{\rho}} \ln \left(\frac{y}{y_0} \right), \quad \text{eq.2.31}$$

$$\text{By using } \sqrt{\frac{\tau_0}{\rho}} = \sqrt{gRS} = V_f, \quad (\text{Chow, 1959}) \quad \text{eq.2.32}$$

where V_f = friction velocity,

R = hydraulic radius,

d = hydraulic depth, and

S = slope.

it can be shown that:

$$V = 2.5 V_f \ln\left(\frac{y}{y_0}\right). \quad \text{eq.2.33}$$

For a broad channel, hydraulic radius (R) can be assumed equivalent to depth (d). Then equation 2.32 can be shown as;

$$\sqrt{\frac{\tau_0}{\rho}} = \sqrt{g d S} = \sqrt{g R S} = V_f. \quad \text{eq.2.32}$$

The vertical velocity profile equation is divided into two types, roughness surface and smooth surfaces. These two types are result of roughness, viscosity and turbulent in individual channel. Roughness and channel slopes play a critical role in determining the type of vertical velocity profile. Because each individual channel has its own unique slope and roughness, vertical velocity profile must be individually determined.

“When surface is smooth, y_0 is depended on the friction velocity and kinematic viscosity” (Chow, 1959). In equation 2.33, y_0 is a constant defined as follow;

$$y_0 = \frac{mv}{V_f}, \quad \text{eq.2.34}$$

where m = constant value; “equal to 1/9 for smooth surface and 1/30 for rough surface”, (Chow, 1959)

ν = kinematic viscosity, and

V_f = friction velocity.

After inputting $y_0 = \frac{m\nu}{V_f}$, the equation can be shown below.

Flow velocity in smooth surface,

$$V = 5.75 V_f \log\left(\frac{9y V_f}{\nu}\right). \text{ (Prandtl-von Karman, 1926)} \quad \text{eq.2.35}$$

For a rough surface, y_0 mainly depends on texture height,

$$y_0 = mk$$

where k = average surface roughness.

Inputting y_0 , gets the flow velocity in rough surface as shown below.

$$V = 5.75 V_f \log\left(\frac{30y}{k}\right), \text{ (Prandtl-von Karman, 1926)} \quad \text{eq.2.36}$$

Prandtl introduced velocity distribution equations based on the shear stress equation in turbulent flow as shown in equation 2.35 and 2.36. These two equations are used to calculate velocity distribution base on geometry conditions and roughness.

2.3 Roughness Dimension

Roughness dimension is the key to define uniform types of surface. It has a direct affect on flow in a channel. There are three types of surface roughness, rough, wavy and smooth surface conditions. In the velocity distribution method, the surface roughness condition is defined through comparison of an actual roughness (k) to a critical roughness (k_c). The critical roughness is described as a layer of roughness magnitude influence. The actual roughness (k) will have an influence beyond the laminar layer if the critical roughness height (k_c) is less than the roughness height (k) (Chow, 1959). Schlichting (1923) defines the smooth flow condition (eq.2.37) from his experiment in pipe flow for smooth flow condition as below.

$$\frac{V_f k}{\nu} < 5 \quad \text{or} \quad k < \frac{5\nu}{V_f}, \text{ (Schlichting, 1923)} \quad \text{eq.2.37}$$

where V_f = friction velocity

ν = kinematic viscosity, and

k = Roughness value.

Schlichting gives estimation of the critical roughness to be $k_c = 100 \nu/V$,

Inputting Chezy's equation to transformed equation 2.37, a critical roughness equation can be shown as.

Critical roughness with Chezy's C . is

$$k_c = \frac{5\nu}{V_f} = \frac{5\nu}{\sqrt{gRS}} = \frac{5\nu C}{\sqrt{g} V} \text{ (Chow, 1959)} \quad \text{eq.2.38}$$

where C = Chezy's C , ($u = C\sqrt{RS}$),

ν = kinematic viscosity,

V = average velocity,

g = gravity, and

k_c = critical roughness.

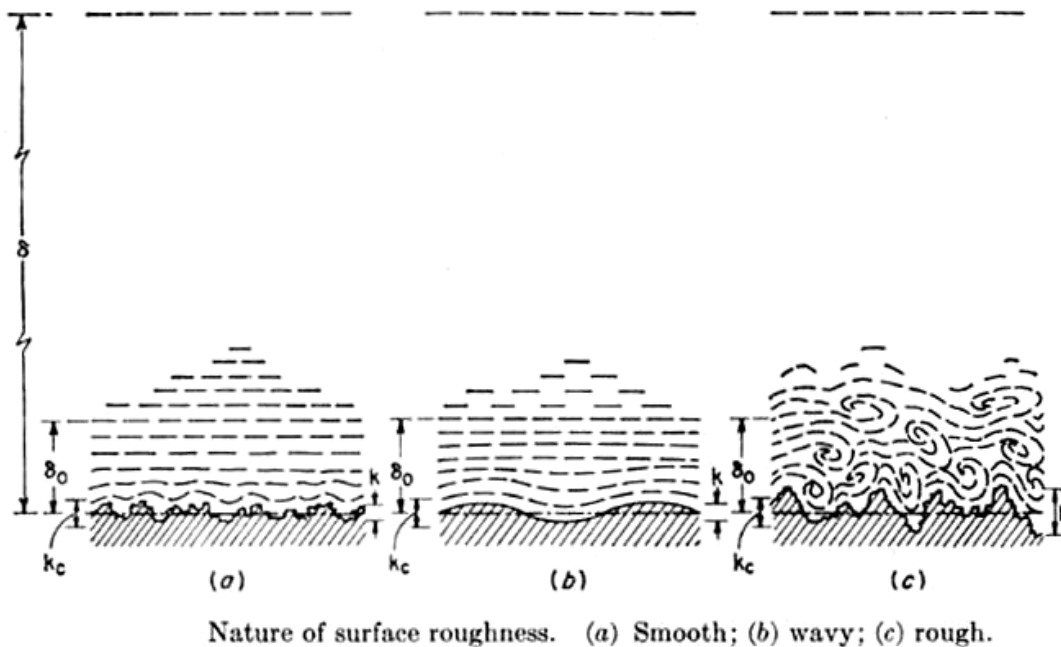


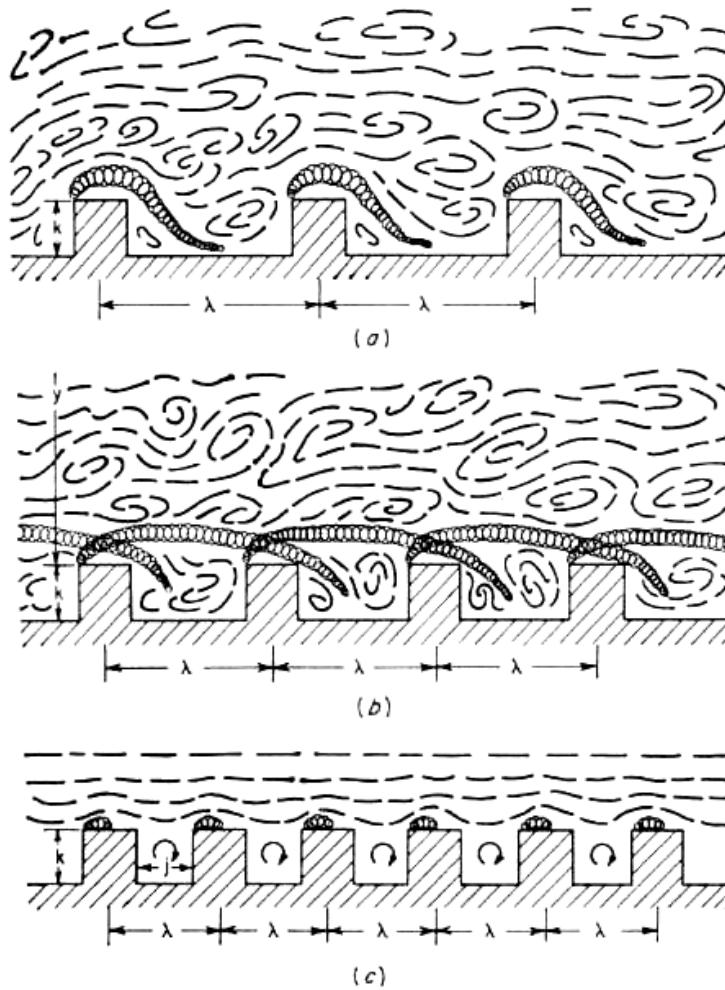
Figure 2.3 Projections of roughness value k , k_c in different conditions (Chow, 1959)

Three types of roughness are shown in Figure 2.3. The relationships between a critical roughness (k_c), a roughness height (k) and laminar layer (δ^* or δ_0) explain conditions of surface roughness. When the roughness height (k) is in the boundary of a critical roughness (k_c), a smooth surface is presented. From equation 2.38, a critical roughness (k_c) is a function of Chezy's C , kinematic viscosity, average velocity and

gravity. With a constant critical roughness, surface roughness height is sufficient to identify types of roughness. In smooth surface, flow shows minimal influences due to the bottom surface roughness as shown in Figure 2.3a.

A wavy roughness condition shows almost equivalent height between a roughness height and a critical roughness as shown in Figure 2.3b. The surface roughness influences the flow but is still under the laminar sub-layer. The last type of surface, Figure 2.3c, is a rough surface. It shows a fully disturbed influence of roughness through out the bottom layer of a flow. In this type of surface, the roughness height is higher than a critical roughness.

Longitudinal spacing of roughness, λ , is an important consideration to determine types of flow. Chow, V. T. defines spacing of roughness as three types. These types of roughness are assumed to have equivalent roughness height (k) with three different spacing. The first type, Figure 2.4a, is an iso-lated roughness. In this type, roughness spacing is so far from each others. Influence of roughness height is less than an average spacing. Therefore, a ratio of k/λ will take place to account the effect as shown. The second type of roughness is a wake-interference flow as shown in Figure 2.4b. Spacing of roughness is close together. The roughness creates great effect to turbulent flow. Quasi-smooth flow is the last type of roughness spacing, Figure 2.4c. The roughness spacing is so close together, that it causes minimal effect to the flow.



Sketches showing concept of three basic types of rough-surface flow: (a) isolated-roughness flow; (b) wake-interference flow; (c) quasi-smooth flow.

Figure 2.4 Three basic types of rough surface flow (Chow, 1959)

2.4 Method of Estimating Average Manning's n-value

A total roadway cross-section average n-value can be estimated by averaging the sub-section n-values. Each sub-section n-value represents a local surface roughness of a sub-section. A sub-section n-value is the result of the unique physical flow condition of

each individual sub-section. In determining an average n-value of the entire cross-section, the method of evaluation has a significantly impact on the overall n-value.

An estimation of the total cross-section roughness can be calculated from a weighting n-value with the geometry parameters for example depth, area, wetted-perimeter, discharge, velocity, or hydraulic radius across the entire roadway cross-section. Weighting parameters are as significant as methods of estimation. It shows significant effects on the outcome of the resulting n-value. The values of weighting parameter are varied from the curb to the end of roadway water. The variation of weighting parameters is caused by changing the basic geometry inputs such as depth and wetted-perimeter along the transverse slope. Hydraulic depth and wetted-perimeter are the basic geometry inputs of a channel calculation. Other parameters, hydraulic radius and area, are calculated from these basic geometry inputs.

Several methods of estimation are observed in literature. Most literature considered basic parameters such as depth and wetted-perimeter of local sections along with their conceptual assumptions. These assumptions are made to improve the compatibility of the geometry conditions. There are also equations used to estimate n-values of composite bottom channels. These equations are based on each individual conclusion.

2.4.1 Horton and Einstein's Equation

Horton and Einstein (1933) suggested an equation to evaluate cross-section n-value as shown in equation 2.39. This equation is based on an assumption that velocity

of each sub-section is equivalent. This method uses only wetted-perimeter as a weighting parameter.

$$n_{\text{Average}} = \left[\frac{\sum_1^N (P_i n_i^{1.5})}{P} \right]^{2/3} = \frac{(P_1 n_1^{1.5} + P_2 n_2^{1.5} + \dots + P_N n_N^{1.5})^{2/3}}{P^{2/3}} \quad \text{eq.2.39}$$

(Horton and Einstein, 1933)

2.4.2 Pavlovski, Muhlhofer, Einstein and Banks's Equation

Equation 2.40 is based on assumption that the total resisting force is equal to sum of the resisting force each sub-section. It was introduced by Pavlovski, Muhlhofer, Einstein and Banks (1931). The total resisting force of channel is as follows.

$$n_{\text{Average}} = \left[\frac{\sum_1^N (P_i n_i^2)}{P^{1/2}} \right]^{1/2} = \frac{(P_1 n_1^2 + P_2 n_2^2 + \dots + P_N n_N^2)^{1/2}}{P^{1/2}} \quad \text{eq.2.40}$$

(Pavlovski, Muhlhofer, Einstein and Banks, 1931)

2.4.3 Lotter's Equation

By considering only discharges of a channel, Lotter (1933) suggested equation 2.41 for equivalent roughness. This equation is based on the assumption that the total discharge is equal to sum of the sub-section discharges. This method considers two parameter, wetted-perimeter and hydraulic-radius.

$$n_{\text{Average}} = \frac{PR^{5/3}}{\sum_1^N \left(\frac{P_i R_i^{5/3}}{n_i} \right)} = \frac{PR^{5/3}}{\frac{P_1 R_1^{5/3}}{n_1} + \frac{P_2 R_2^{5/3}}{n_2} + \dots + \frac{P_N R_N^{5/3}}{n_N}} \quad (\text{Lotter, 1933}) \quad \text{eq.2.41}$$

2.4.4 Krishnamurthy and Christensen's Equation

Krishnamurthy and Christensen (1972) introduced another equation for averaging n-value in 1972. An equation is based on the logarithmic velocity distribution as shown in equation 2.42. Two significant parameters, wetted perimeter and depth are used in a weighting process. As far as velocity distribution equation

$$\ln(n_{\text{Average}}) = \frac{\sum_1^N (P_i y_i^{3/2} \ln(n_i))}{\sum_1^N P_i y_i^{3/2}}$$

$$= \frac{P_1 y_1^{3/2} \ln(n_1) + P_2 y_2^{3/2} \ln(n_2) + \dots + P_N y_N^{3/2} \ln(n_N)}{P y^{3/2}} \quad \text{eq.2.42}$$

(Krishnamurthy and Christensen, 1972)

2.4.5 Other Methods of Averaging n-values

$$\text{Area weighted n-value; } n_{\text{Area-weight}} = \frac{\sum_1^N n_i A_i}{\sum_1^N A_i} \quad \text{eq.2.43}$$

$$\text{Depths weighted n-value; } n_{\text{Depth-weight}} = \frac{\sum_1^N n_i d_i}{\sum_1^N d_i} \quad \text{eq.2.44}$$

$$\text{Wetted-perimeter weighted n-value; } n_{\text{Wetted-perimeter weighted}} = \frac{\sum_1^N n_i P_i}{\sum_1^N P_i} \quad \text{eq.2.45}$$

$$\text{Velocity weighted n-value; } n_{\text{Velocity-weight}} = \frac{\sum_1^N n_i u_i}{\sum_1^N u_i} \quad \text{eq.2.46}$$

$$\text{Discharge weighted n-value; } n_{\text{Discharge-weight}} = \frac{\sum_1^N n_i q_i}{\sum_1^N q_i} \quad \text{eq.2.47}$$

$$\text{Hydraulic radius weighted n-value; } n_{\text{Hydraulic-radius-weight}} = \frac{\sum_1^N n_i R_i}{\sum_1^N R_i} \quad \text{eq.2.48}$$

$$\text{Numerical average n-value; } n_{\text{Numerical average}} = \frac{\sum_1^N n_i}{N} \quad \text{eq.2.49}$$

Manning's equation average n-value using the actual discharge;

$$n_{\text{Manning equation with measured discharge}} = \frac{1.486 S^{1/2} R^{2/3}}{\left(\frac{Q_{\text{measured}}}{A_{\text{total cross-section}}} \right)} \quad \text{eq.2.50}$$

Manning's equation average n-value using velocity estimated discharge;

$$n_{\text{Manning equation with velocity estimated discharge}} = \frac{1.486 S^{1/2} R^{2/3}}{\left(\frac{Q_{\text{estimated}}}{A_{\text{total cross-section}}} \right)} \quad \text{eq.2.51}$$

Most of these equations provide very similar results. The impacts and comparisons of averaging methods will be discussed in chapter 4.

2.5 Statistical Analysis

Generally, data taken from field or laboratory contains error. The sources of error are from factors such as human and equipments. Mostly human error is caused by insufficient experience. Error such as incorrect reading and measurement are varies by person.

Another type of error is from measuring-equipment. The measuring-equipment error is caused by variation or limitation of equipment accuracy. The equipment accuracy is a result the equipment design. It also caused by the equipment age. Therefore, the measuring-equipment should be maintained and calibrated to minimize possible error.

Some sources of error can be observed shown in a data plot as unrelated points or outliers. Typically, the data error can be analyzed and identified by mathematic statistical analysis. The statistical analysis such as histogram, normality distribution (Q-Q plot) and scatter plots are useful to analyze the normal distribution of a data set.

2.5.1 Histogram Plot

The histogram plot is data groups plotted in intervals. The plot shows data frequency within the interval ranges. The normal distribution of a data set can be seen when the plot appear as a convex and symmetric shape with the maximum at a median point as shown in Figure 2.5. (Montgomery, Runger and Hubele, 2004)

2.5.2 Normality Distribution Plot (Q-Q Plot)

A normality distribution plot (Q-Q plot) is a special plot used to determine the statistic normality. The Q-Q plot is composed of pairs of observed data and standard quantiles. The normal probability plot indicates normality distribution of a data set. Equal probability ($P_{(j)}$) of every data point in Q-Q plot reveals the data relationship, consistency and outliers. A straight line and equal spacing between points are indications of a normal distribution. The outliers are normally seen on the ends of the Q-Q plot. Normal distribution and standard quantiles are related by equation 2.52. (Johnson, 2002)

$$P[Z \leq q_{(j)}] = \int_{-\infty}^{q_{(j)}} \frac{1}{\sqrt{2\pi}} e^{-\frac{z^2}{2}} dz = P_{(j)} = \frac{j - \frac{1}{2}}{n} \quad (\text{Johnson, 2002}) \quad \text{eq.2.52}$$

where $P_{(j)}$ = probability level

$q_{(j)}$ = standard quantiles

j = 1, 2, 3,, n

n = Total numbers of sample

2.5.3 Scatter Plots

Scatter plots represent plots of multiple data series. The plots are related pairs from data sets plotted side by side and arranged in a matrix n by n (n = numbers of data set). Outliers of a single data set can be easily identified by examination of the unrelated points. In order to construct scatter plots, data sets should have the same sample number and data range.

2.5.4 Outlier Detection

The data error points or outliers are unusual points created by many different factors. Most laboratory data sets contain a minimal percent of error. A data set with a significantly large percent of error is unusual. Elimination of the outliers is a significant process to achieve the normality distribution and accurate statistical analysis. Outliers can be recognized by the unusually large or small magnitude of the number, and unrelated variance from the majority data in the plots. Several methods can be used to identify outliers in addition to the histogram plot, a normal probability plot and scatter plots. (discussed in section 2.5.3)

2.5.5 Correlation Coefficient

The straightness of a normal probability plot (Q-Q plot) can be determined by the correlation coefficient (r_Q). The correlation coefficient of data set can be calculated by equation 2.53. The critical point of normality distribution is defined as a critical

correlation coefficient as shown in table 2.1. The critical correlation coefficient varies by number of samples and significant level (α). Therefore normality can be checked by comparison between the correlation coefficient (r_Q) and the critical correlation coefficient. (Johnson, 2002)

$$r_Q = \frac{\sum_{j=1}^n (x_{(j)} - \bar{x})(q_{(j)} - \bar{q})}{\sqrt{\sum_{j=1}^n (x_{(j)} - \bar{x})^2} \sqrt{\sum_{j=1}^n (q_{(j)} - \bar{q})^2}} \quad \text{(Filliben, 1975)} \quad \text{eq.2.53}$$

where r_Q = correlation coefficient,

x = data point,

\bar{x} = numerical average of data,

$q_{(j)}$ = standard quantiles,

\bar{q} = numerical average of standard quantiles,

j = 1, 2, 3, ..., n, and

n = total number of samples.

Table 2.1 Critical points for the Q-Q plot correlation coefficient test for normality (Johnson, 2002)

Sample size <i>n</i>	Significance levels α		
	.01	.05	.10
5	.8299	.8788	.9032
10	.8801	.9198	.9351
15	.9126	.9389	.9503
20	.9269	.9508	.9604
25	.9410	.9591	.9665
30	.9479	.9652	.9715
35	.9538	.9682	.9740
40	.9599	.9726	.9771
45	.9632	.9749	.9792
50	.9671	.9768	.9809
55	.9695	.9787	.9822
60	.9720	.9801	.9836
75	.9771	.9838	.9866
100	.9822	.9873	.9895
150	.9879	.9913	.9928
200	.9905	.9931	.9942
300	.9935	.9953	.9960

2.5.6 Transformation to Near Normality

The transformation to near normality is an alternative method of data treatment. It is a way to treat non-normal distribution data. Figures 2.5 and 2.6 demonstrate the histogram plots of normality and non-normality distribution of n-values. Methods of transformation are depended on type of distribution and character of outliers. For non-normality distribution data, changing a unit of the data set may change the data distribution. The data sets can be changed by a power transformation with a parameter λ . For example if $\lambda = -1$, then $x^\lambda = x^{-1}$. The power transformation either shrinks the large

value or increases the large value of data. The proper weighted parameter (λ) may help transform the data distribution. Methods of transformation are shown below.

....., X^{-1} , $\ln X$, $X^{1/4}$, $X^{1/2}$ Shrink large values of data

X^2 , X^3 , .. Increase large values of data

After a transformation, data set may show normal distribution and be suitable for statistical analysis. Since methods of transformation affect data units, the statistical analysis of transformed data can not be compared with data in the original units. Therefore the method of transformation is not used in this project.

Outliers can be identified and should be removed only from normal distribution data sets. For non-normal distribution data sets, numerical average (\bar{x}) are calculated with no transformation treated. The numerical average (\bar{x}) from a non-normal distribution data set is the only statistic which should be compared. Other statistics of non-normal distribution are not valid.

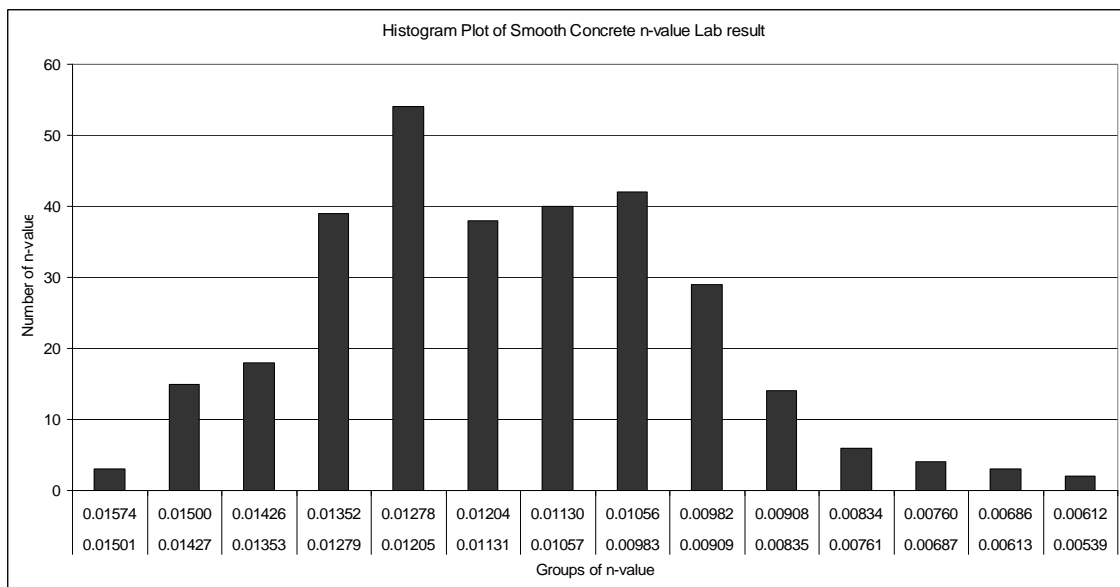


Figure 2.5 Histogram plot of smooth concrete n-value (lab result)

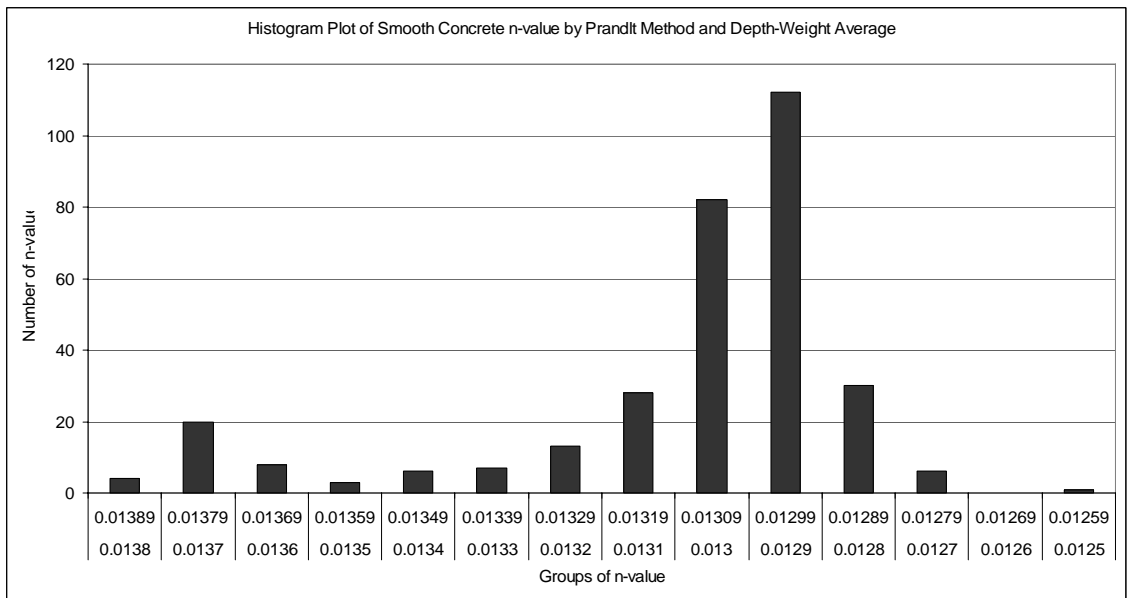


Figure 2.6 Histogram plot of smooth concrete n-value (Prandtl-von Karman velocity method and depth-weight averaging method)

CHAPTER 3

METHODOLOGY

3.1 Data Collection and Preparation

This project studies four types of roadway surfaces, TxDOT standard concrete, smooth (worn) concrete, asphalt, and asphalt treatment surface experiments. Each roadway surface represents one data set for analysis and inputs to this study. All data for this research was obtained from a TxDOT roadway roughness simulation project. The raw data included roadway basic geometry, discharge values, and flow cross-sections, which originally obtained by physical measurement.

Actual discharge values were obtained from ultrasonic meter readings. The ultrasonic meters were adjusted and calibrated by volumetric flow rate measurement. The meters provide flow rates measurements with minimum percent of error (<3.0%). Flow rate readings were acquired after establishing uniform and steady flow. Uniform flows on roadway were observed a short time after flow initiation. Time to achieve steady uniform flow varies as a result of slopes of roadway, flow rates, and pump stability. This data is used to study and verify the velocity distribution model approach.

All the data was analyzed for numerical averages and errors. Outlier detection and data cleaning were part of the statistical analysis. Inputs, discharges and n-values, were processed to achieve the maximum accuracy. Statistical analysis can indicate

percentage of normality and data consistency. Resulting analysis showed some deviation of data. These irregular points could lead to erroneous future analysis. Therefore outliers were processed and removed. The normality of this data set is controlled by percent acceptability within a significant level (α) of 0.05. After cleaning the data set, results should noticeably improve in terms of accuracy and consistency.

Ultimate outputs of the velocity distribution model from this project, such as n-values and discharge, will be compared to original TxDOT project results for verification and analysis.

3.2 Calculation Process and Modeling

The simulation of flow on each roadway surface was performed in several steps. The process is shown in Figure 3.1. These steps are performed using Microsoft Excel spread-sheets.

In the flow calculation, there are two methods to estimate roadway cross-section n-values and discharges. The first method calculates average velocity and area by velocity distribution method and laboratory geometries. The n-values and discharges are calculated from each average velocity and area. The entire roadway cross-section n-value is estimated from various averaging methods as shown in chapter 2. The total roadway cross-section discharge is sum of sub-section discharges.

The second method, a total discharge is a constant input. The entire roadway cross-section geometries, depths and spreads, are estimated by trial and error according to the total discharge. Each average velocity is calculated by velocity distribution

method according to estimated sub-section depths. The sub-section n-values are calculated from the estimated sub-section geometries. The total cross-section n-value is calculated from various averaging methods as shown in chapter 2.

The first method is the only method used this research due to accurate discharges and n-values compared to the original TxDOT project result.

Velocity Distribution Calculation Process

3.2.1. Obtain Geometry Data

3.2.2. Estimate Average
Roughness (k) Over Total Surface

3.2.3. Calculate Total Cross-
Section (A_t) and Sub-Section

3.2.4. Calculate Friction Velocity
(V_f)

3.2.5. Calculate Critical
Roughness Height (k_c)

3.2.6. Assign a Roughness
Condition

3.2.7. Calculate Sub-Section
Velocity Profiles

3.2.8. Calculate Average Sub-
Section Velocities

3.2.9. Calculate Sub-Section'
Manning N-values

3.2.10. Calculate sub-section
discharges

3.2.11. Calculate Total Cross-Section
Discharge and Average N-value

Figure 3.1 Velocity distribution calculation process

3.2.1. Obtain Geometry Data

Basic geometry data in this project is obtained from TxDOT roadway roughness study. All TxDOT geometry data is shown in Appendix B. In TxDOT study, geometric data is a basic input for calculating area of cross-section, height of roughness, and slopes. Original cross-section geometries were surveyed with an accuracy of 0.01 foot.

A measuring procedure was developed and constantly used to take consistent data reading. Since flow is a shallow water flow over a roadway. Water waves were developed by the affect of surface roughness across the roadway cross-section. The flow geometric readings of depth and spread are affected by these waves. A procedure of taking minimum and maximum readings was used to estimate an average flow reading. Flow and geometry data was repeatedly taken several times for each single setting of flow and roadway slopes to achieve the maximum accuracy.

Additionally, rainfall data was physically simulated on the TxDOT concrete surface. A rainfall simulator was used to simulate rainfall over this roadway. The rainfall simulator consists of special sprinklers distributing simulation over the roadway area. The rainfall rate and amounts are estimated from roadway area and time period of rainfall. Rainfall rate investigated were one, three, and six inches per hour.

In TxDOT research, results are analyzed from basic data consisting of depth, spread, and discharge. Flow cross-section area was obtained from basic geometric data. By inputting area, slope, discharge, and hydraulic radius data into Manning's equation (eq.2.1), the average Manning's n-value for the total cross-section can be obtained as follow.

$$\text{Manning } n - \text{value} = \frac{1.486}{Q} S^{\frac{1}{2}} R^{\frac{2}{3}} A \quad \text{Manning's Equation (Sturm, 2001)} \quad \text{eq.3.1}$$

Q = velocity,

n = Manning's n-value,

S = longitudinal slope,

R = hydraulic radius, and

A = area.

The second method used to approach Manning's n-value determination is to use the Prandtl-von Karman velocity distribution method. This method is based on shear force between the liquid and the surface roughness of the roadway cross-section. The result from the TxDOT study and this Prandtl method calculation can then be compared in term of the total cross-section discharge.

3.2.2. Surface Roughness Estimation

Surface roughness plays a significant role in open channel flow estimation. It dramatically changes in energy dissipation through turbulence. Roughness estimation is always a tricky part of open channel design. It's an important part of many flow equations. Each channel requires study of roughness for accurate estimation.

Roadway flow design is considered to be open channel flow with uniform geometric conditions. A good estimate of some roadway surface roughness such as asphalt treatment, and smooth concrete surfaces can be difficult. Surface roughness value (k) is a direct physical measure of an actual height of surface roughness. The

roughness value is often estimated from an average grain size of sand diameter in the channel or pipe bottom. The roadway surface roughness were estimated according to average uniform distribute of roughness through out the channel bottom. Roughness uniformity greatly affects the roughness value. Since the entire roadway surface was made at the same time the roughness is considered to be uniform roughness. For uniform roadway surfaces, roughness is divided in to two cases, sequence and non-sequence.

A uniform non-sequence roughness surface can be found in asphalt, asphalt treatment and TxDOT concrete surfaces. These surface roughness values can be calculated from an actual average height of roughness found in the direct measure of a surface cross-section image. (Figure 3.2, 3.3 and 3.5)

The other type of roughness is uniform sequence roughness (Figure3.4). It is found in the smooth (worn) concrete surface. This surface may contain one or two types of roughness, smooth or rough. For this type of surface, roughness height (k) can be estimated by visually observing the overall average height of longitudinal roughness from the lowest to the highest point.

A range of roughness values are pre-selected from visual inspection of roughness dimension. The maximum, minimum and average values of dimension are determined from vertical distance of roughness dimension as shown in Figure 3.2-3.5. These figures are actual longitudinal cross-sections of the roadway profile taken from the actual footage photography of roadway cross-sections.

The longitudinal surface profile presents the surface of roadway. For Figure 3.2, 3.3, and 3.4, the TxDOT concrete, asphalt, and smooth concrete surface, the surface profile represents projection of roughness from the bottom to the top. In these types of a roadway surface, roughness heights are projections of difference in vertical distances of a surface profile.

In Figure 3.5, treatment roadway profiles show projections of bottom surface profiles and top roughness profiles. Dash lines between the bottom surface and the top roughness profile show estimated projections of material in between levels.

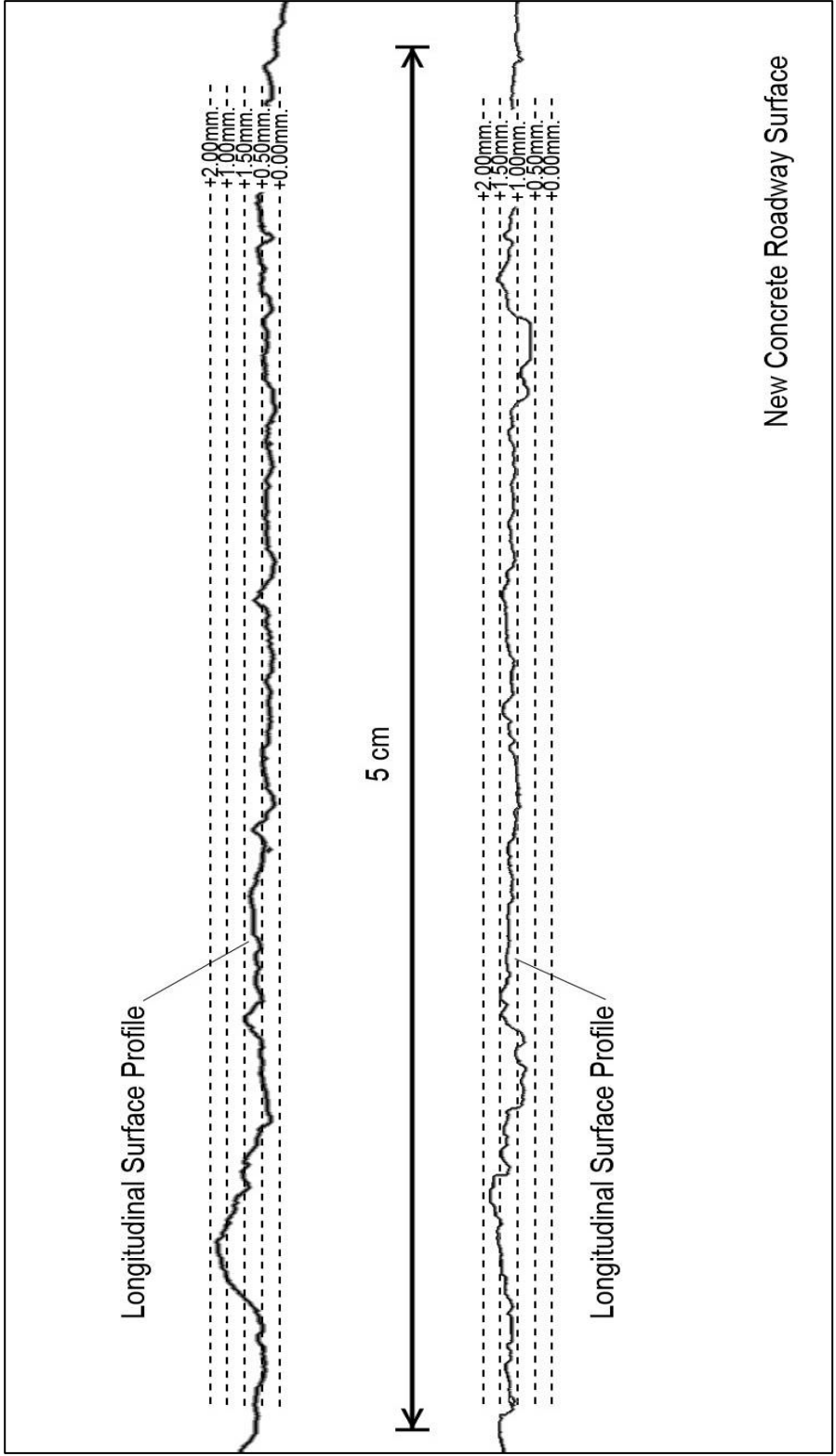


Figure 3.2 Longitudinal TxDOT concrete roadway surface profiles

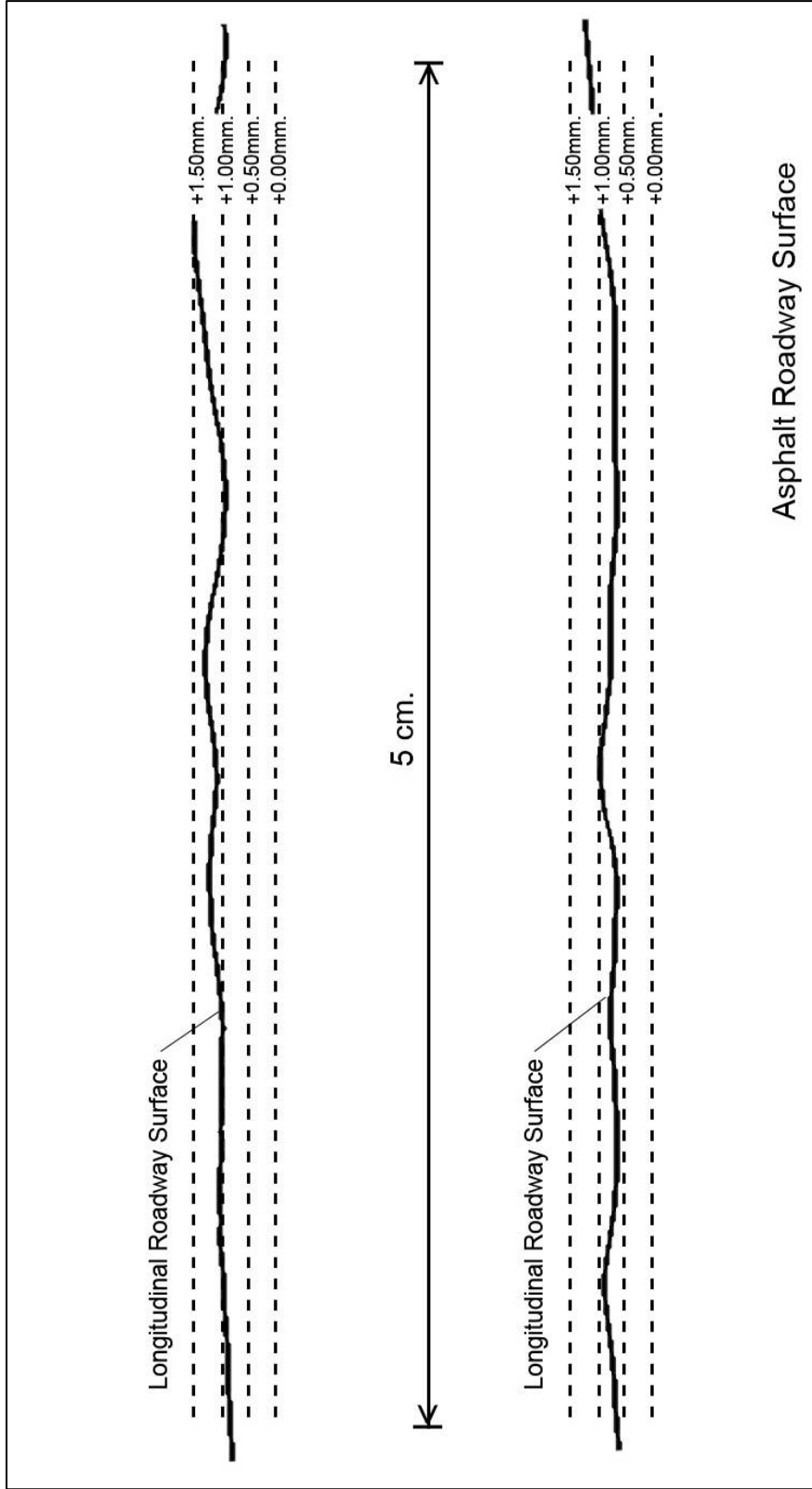


Figure 3.3 Longitudinal asphalt roadway surface profiles

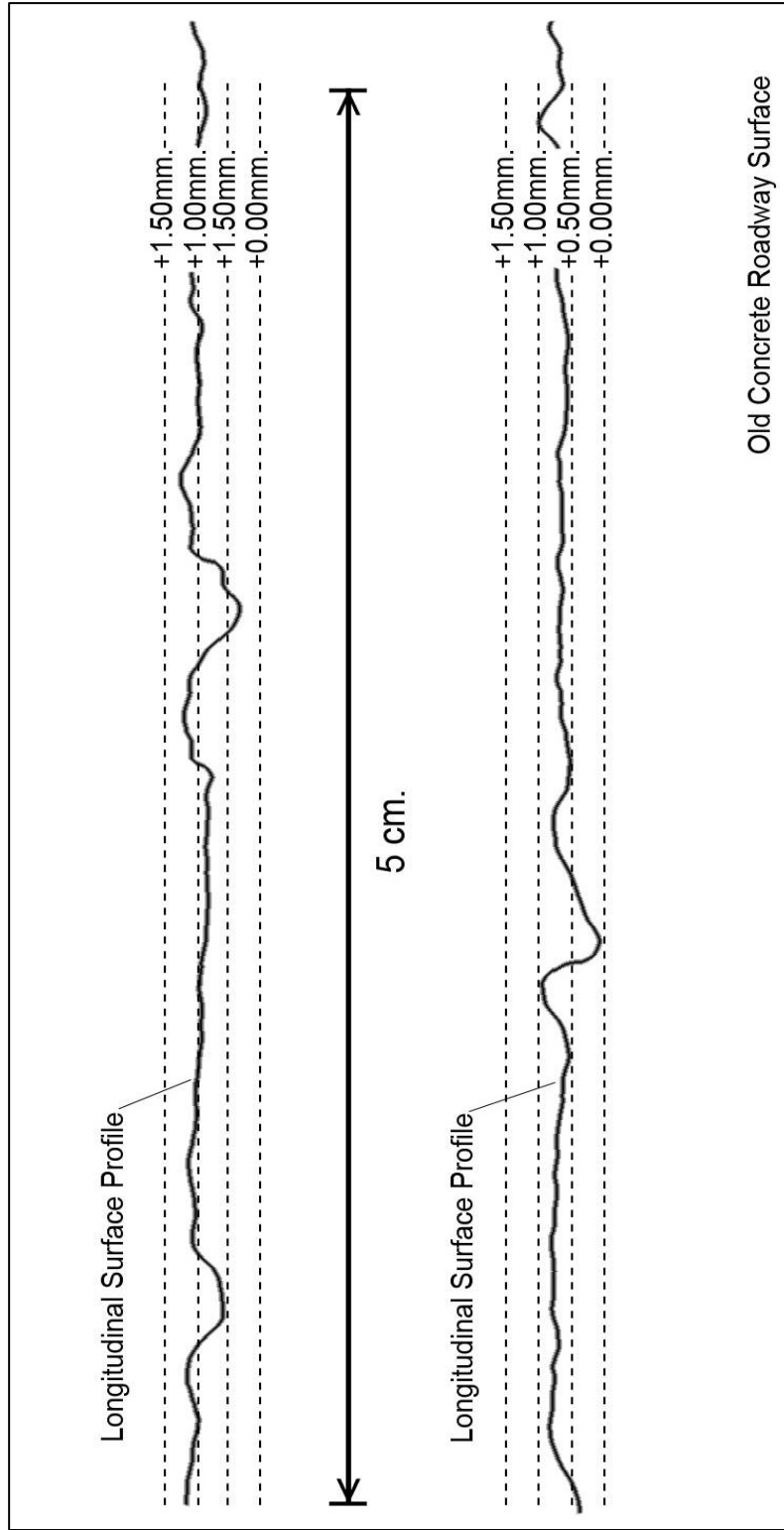


Figure 3.4 Longitudinal smooth concrete roadway surface profiles

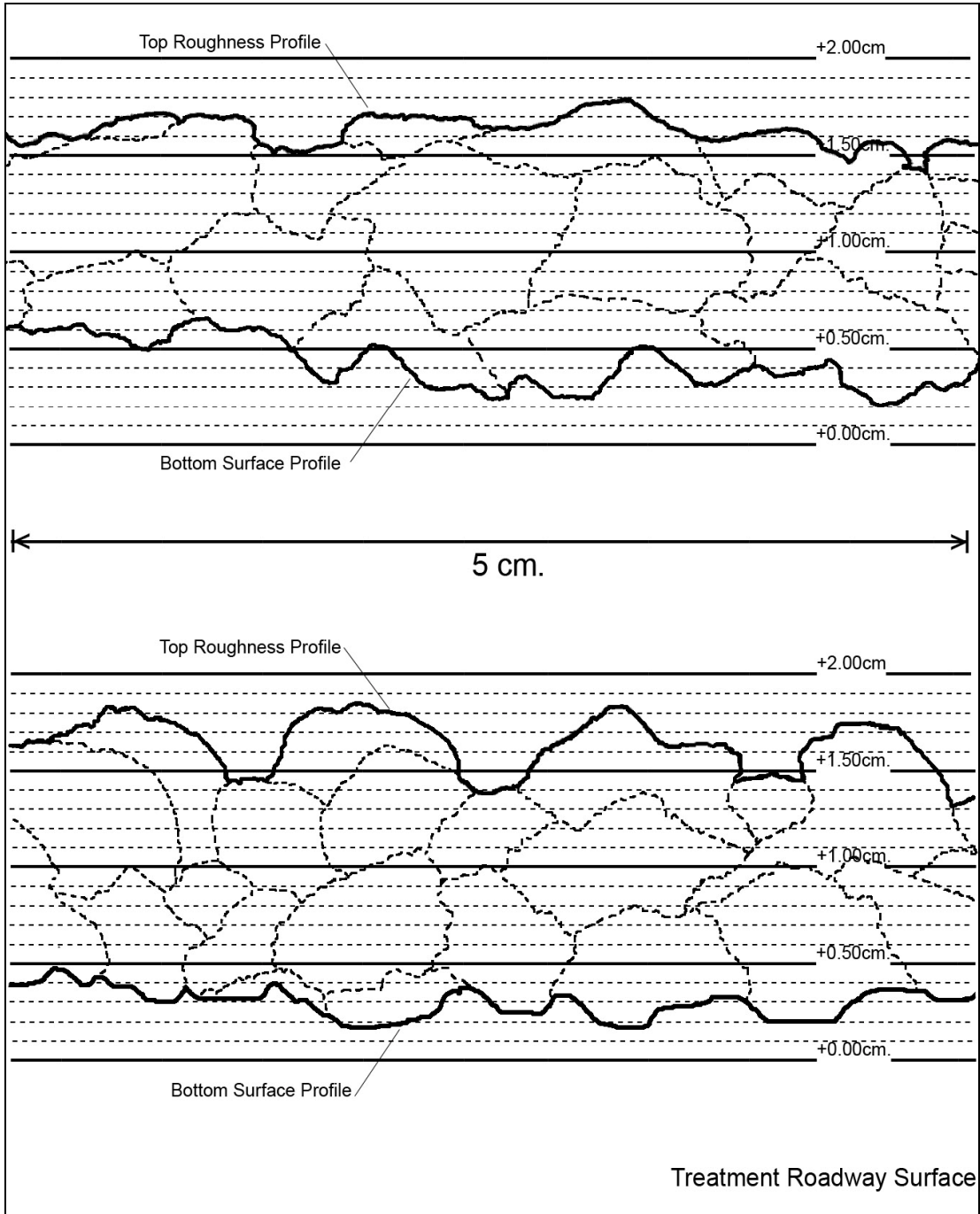


Figure 3.5 Longitudinal asphalt treatment roadway surface profiles

3.2.3 Calculate Roadway Cross-Section and Sub-Section Areas

For a steady state flow, no increase or decrease in velocity, depth, and discharge, occurs. A single cross-section is used to calculate discharge. The total cross-section area is a product of hydraulic depth and total spread. Discharge is the product of total average cross-section velocity multiple by total cross-section area.

The spread can be determined by two methods, depth or spread method, see Figure 3.6. Using the depth-method, total spread is estimated from the product of depth and measured transverse slope. Using the spread-method the total spread is obtained from an actual laboratory measurement as shown in Figure 3.6. The different methods can produce results that vary some what.

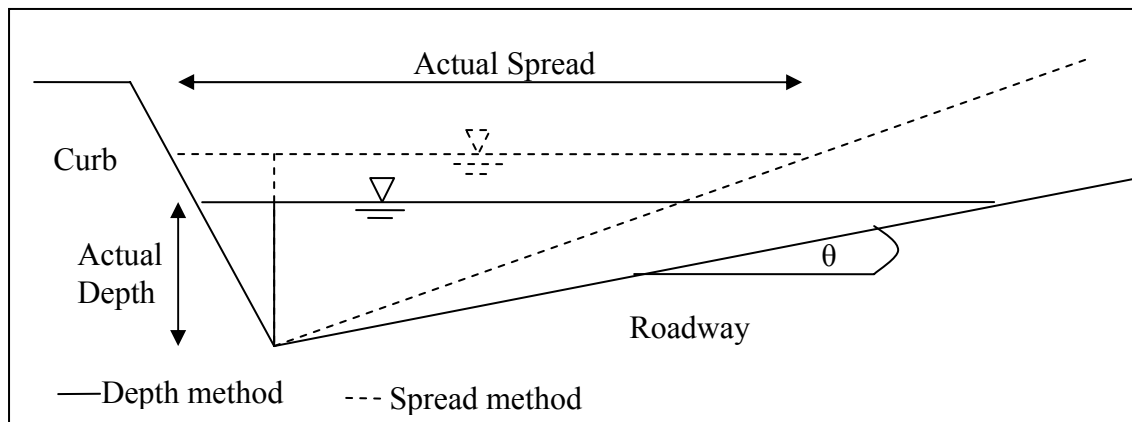


Figure 3.6 Methods of cross-section area estimation

In this research, the total roadway cross-section is divided into small vertical slices having an interval of 1 ft width in the roadway cross-section's transverse direction as shown in Figure 3.7. The sub-section area adjacent to the curb is calculated by the summation of two parts, the triangular and the trapezoidal areas, which are shown in Figure 3.8.

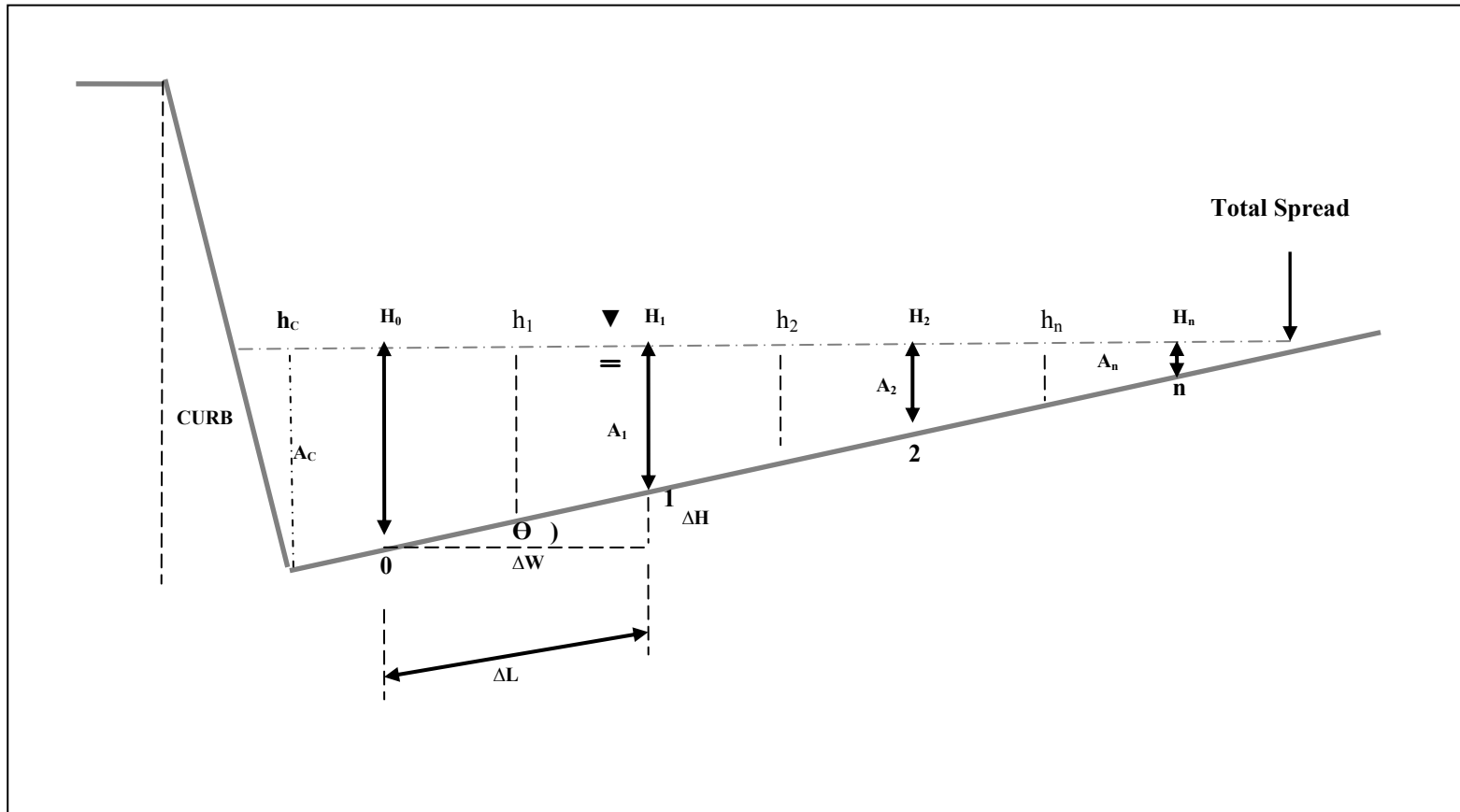


Figure 3.7 Total cross-section, sub section areas, heights, widths, and water elevation of the roadway cross-section

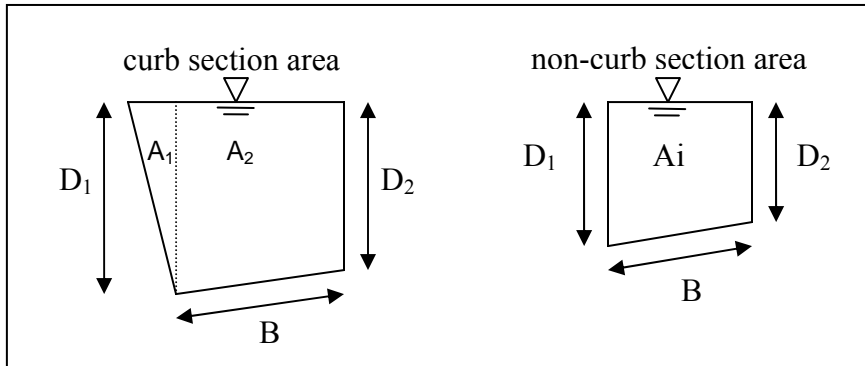


Figure 3.8 Roadway sub-section area dimensions

Figure 3.9 shows dimension of the TxDOT standard roadway curb.

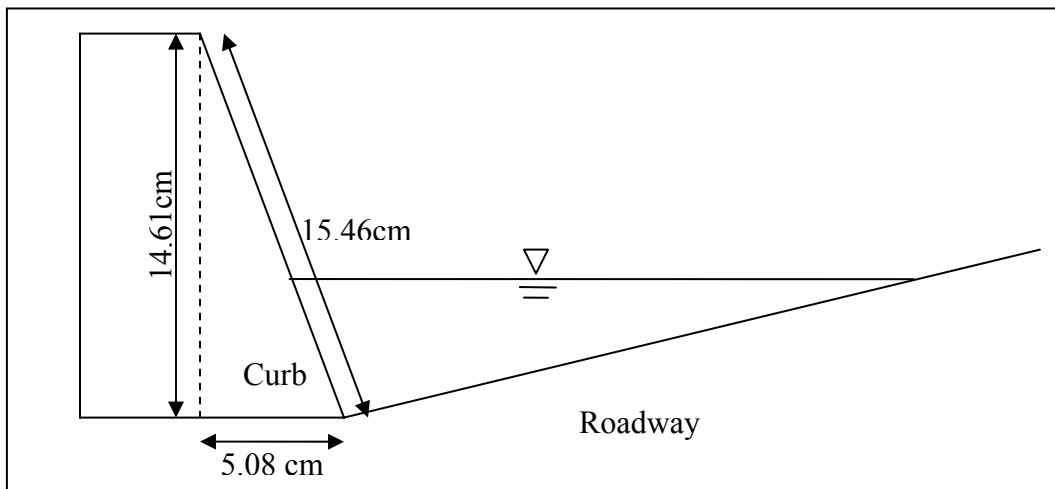


Figure 3.9 Roadway curb-section dimensions

The curb-area calculation is shown below.

$$\text{curb-area } (A_c) = A_1 + A_2 \quad \text{eq.3.2}$$

$$\text{where } A_1 = 0.5 D_1 \left(D_1 \frac{5.08 \text{ cm}}{14.61 \text{ cm}} \right) = 0.1738 D_1^2, \quad \text{eq.3.3}$$

$$A_2 = \frac{(D_1 + D_2)}{2} B, \quad \text{eq.3.4}$$

B = length of bottom surface, and

D_1, D_2 = hydraulic depth on left and right sides of section.

For other vertical sub-sections, areas are the product of average depth on both sides of section multiple by bottom length of section. For small transverse angles, the horizontal length between depths is similar to the bottom roadway surface length.

$$\text{non-curb section area } A = \frac{(D_1 + D_2)}{2} B \quad \text{eq.3.5}$$

The geometry data obtained from laboratory use depth (Y) in vertical distances. The conversion of vertical depth to hydraulic depth is shown below.

Hydraulic depth is $D = Y \cos(\theta)$.

$$\text{where } \theta = \left[\tan^{-1} \frac{H}{100} \right], \quad \text{eq.3.6}$$

D = hydraulic depth,

Y = vertical depth of water,

θ = degree slope angle, and

$$H = \text{percent longitudinal slope; percent slope} = \frac{H \text{ (ft)}}{100 \text{ (ft)}}.$$

Figure 3.10 shows relationship between a vertical water depth, hydraulic depth and roadway longitudinal slope.

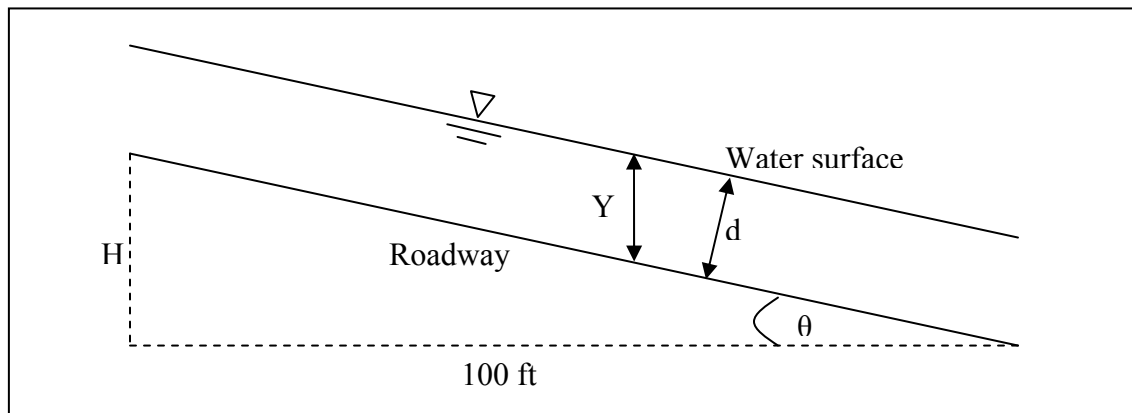


Figure 3.10 Roadway longitudinal slope calculation

3.2.3.1 Water Surface

There are two techniques of calculating surface water level in this project. Both techniques use the cross-section depth measurements obtained in the TxDOT roadway project.

For asphalt, asphalt treatment and smooth concrete roadway surface one water depth measurement was made. It was located adjacent to the curb at the deepest point of the channel. For the TxDOT concrete roadway surface, multiple water depths were taken along the transverse slope.

Additionally, all cross-sectional roadway surfaces were surveyed at several locations along the transverse direction from the curb. This survey data allows the development of a representative transverse slope for the entire cross-section or a subsection.

The spread was measured for all roadway surfaces. The depth at the curb when convoluted with the transverse slope did not always equal to the measured spread. This is a result of the minor wave action, surface variation in the transverse slope and the shallower flow as distance progressed from the curb. Figure 3.13 shows this phenomenon in that the water surface profile does not connect with the roadway.

3.2.4 Friction Velocity

The friction velocity is described in a chapter 2. Equation 2.32 presents friction velocity.

$$\sqrt{\frac{\tau_0}{\rho}} = \sqrt{gRS} = \sqrt{gdS} = V_f \quad \text{Friction velocity (Chow, 1959)} \quad \text{eq.2.32}$$

where hydraulic radius (R) = depth (d) for a broad channel,

R = hydraulic radius,

d = hydraulic depth,

S = slope,

ρ = mass density = w/g,

w = unit weight of fluid, and

g = gravity.

3.2.5 Critical Roughness Height

Critical roughness height is a function of roughness value, kinematic viscosity, gravity, and average velocity. It represents a unique condition of flow in channel. The critical roughness height is described in chapter 2. The critical roughness equation is presented in equation 2.38.

$$k_c = \frac{5Cv}{\sqrt{gV}} \quad (\text{Chow, 1959}) \quad \text{eq.2.38}$$

where C = Chezy's C,

v = kinematic viscosity,

V = average velocity,

g = gravity, and

k_c = critical roughness.

3.2.6 Surface Roughness Condition

Surface roughness can be separated into two types, a rough and smooth condition. In the velocity distribution method, the surface roughness condition can be defined through comparison of the critical roughness (k_c) and the roughness height (k). The following equation (eq.2.37) indicates the surface condition, a smooth condition and rough condition.

$$\frac{V_f k}{\nu} < 5 \quad \text{or} \quad k < \frac{5\nu}{V_f} \quad \text{Smooth flow condition, (Schlichting, 1923)} \quad \text{eq.2.37}$$

where k = roughness height,

ν = kinematic viscosity, and

V_f = friction velocity.

If the value of the term $\frac{V_f k}{\nu}$ is less than 5, the surface is in smooth condition.

If the value of the term $\frac{V_f k}{\nu}$ is more than 5 a surface is in rough condition.

Since k is almost constant in a particular channel section and ν minimally changes, friction velocity has the greatest effect to define the surface roughness conditions. (Chow, 1959)

3.2.7 Vertical Velocity Profile

Vertical velocity distributions are flow resistance equations, which represent the relationship of velocity and roughness. They are the direct result of channel geometry conditions. Local sub-section flow and geometry such as depth, kinetic viscosity and

surface roughness are used to evaluate the velocity profile. The local geometries of each roadway sub-section vary section by section due to the non-symmetric triangular shape of the roadway. The vertical velocity profile equation is divided into two types, roughness surface and smooth surface. Two types of flow equation used in this project are shown in equation 2.35 (smooth surface condition) and 2.36 (rough surface condition). These two types are result from different roughness, viscosity and turbulence in an individual channel. The velocity profile methodology is explained in chapter 2. Figure 3.11 demonstrates vertical velocity profiles of every sub-section across the roadway.

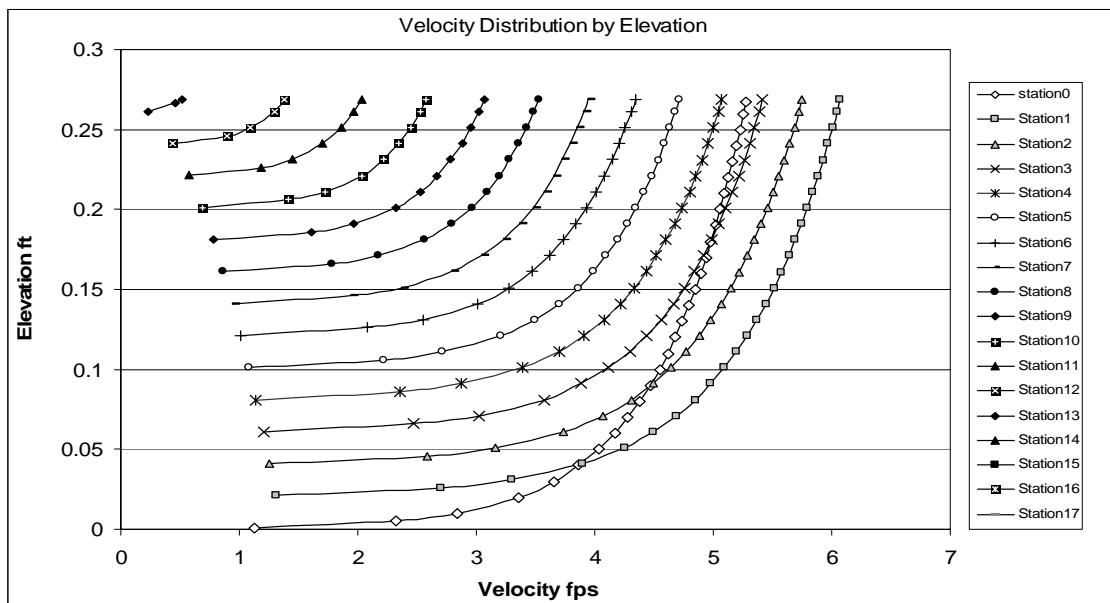


Figure 3.11 Vertical velocity profiles across the roadway cross-section

The velocity profile starting approximately at elevation 0 ft is nearest to the curb. Elevation represents the height on a profile above the channel lowest point near the curb where a velocity can be found. Each additional profile starts at the next elevation is located further out along the transverse slope.

$$V = 5.75 V_f \log\left(\frac{9yV_f}{\nu}\right) \text{ for smooth surface (Prandtl-von Karman, 1926)} \quad \text{eq.2.35}$$

$$V = 5.75 V_f \log\left(\frac{30y}{k}\right) \text{ for rough surface (Prandtl-von Karman, 1926)} \quad \text{eq.2.36}$$

3.2.8 Calculate Sub-Section Average Velocity

A roadway cross-section is a non-symmetric triangular channel. Each vertical velocity profile is individually calculated from the station depth. The USGS recommended average velocity method (Wahl, Thomas and Hirsh, 1995) is used in this research. The average velocity can be obtained by taking the velocity at 0.6 of the depth or an average of the 0.2 and 0.8 of the depth from the surface of water.

Another method for averaging velocity is an integration of vertical velocity profile. Integration will give the total area of vertical velocity curve, which when divided by the total depth estimated the average velocity. An average velocity can be obtained from equation 3.7. This method gives a very close estimation to the USGS method.

$$\text{Average sub-section velocity} = \frac{\int_0^d V dy}{d_i} \quad \text{eq.3.7}$$

Figure 3.12 shows sub-section average velocities across the roadway cross-section. The average velocity at the curb-section is dropped due to the increasing

wetted-perimeter at the curb-section. The section next to the curb shows the highest average velocity. Sub-section average velocities decrease along the transverse slope due to the decreasing of water depth.

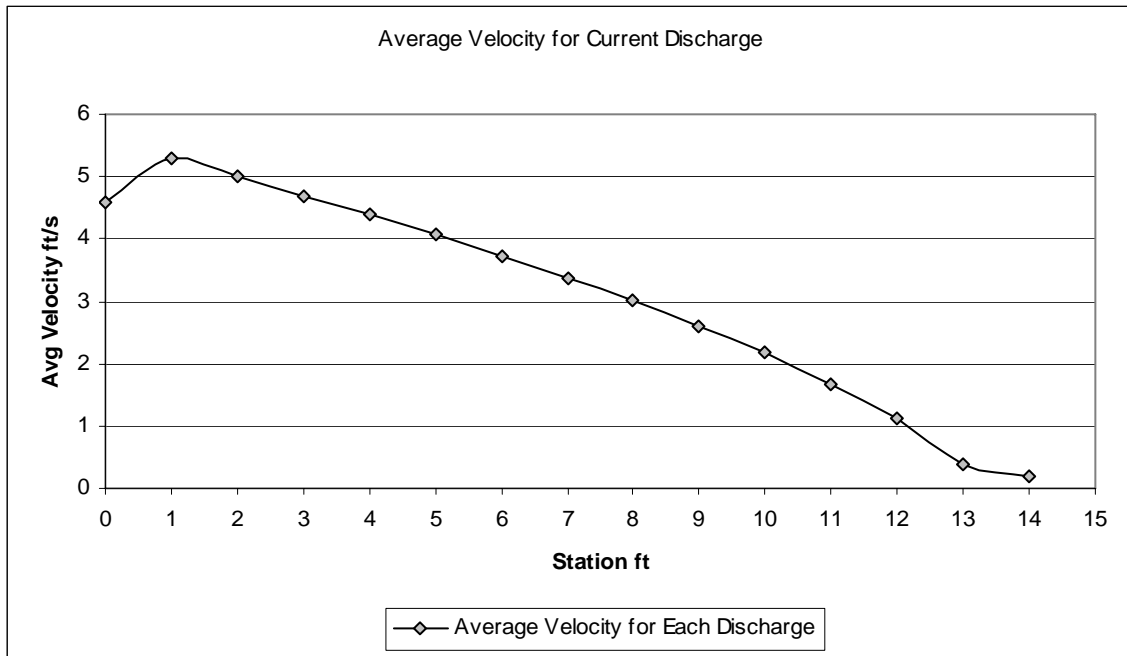


Figure 3.12 Plan view of average velocity in each station from curb on left hand side to the end of water on right hand side of roadway cross-section

3.2.8.1 Total Cross-Section Velocity Distribution

A cross-section velocity distribution can be display by plotting local geometries of roadway such as elevation, transverse slope and sub-section vertical velocity profiles as shown in Figure 3.13. The roadway cross-section velocity distribution demonstrates details of isolated-velocity, depth of flow and water surface across the entire cross-section. It also shows location of super-critical, critical (Froude number = 1), and sub-critical state of flow.

$$\text{Froude number} = F = \frac{V}{(gd/\alpha)^{1/2}} \quad (\text{Sturm, 2001}) \quad \text{eq.3.8}$$

where F = Froude number,

V = velocity,

g = gravity,

d = depth, and

α = specific gravity.

In Figure 3.13, the water surface varies with the depth measurement. The fitted equation best represents the water surface. It also indicates potential shallow flow area that could easily be missed during measurement. Notice that the Froude number in this diagram can be representation of super and sub-critical flow location.

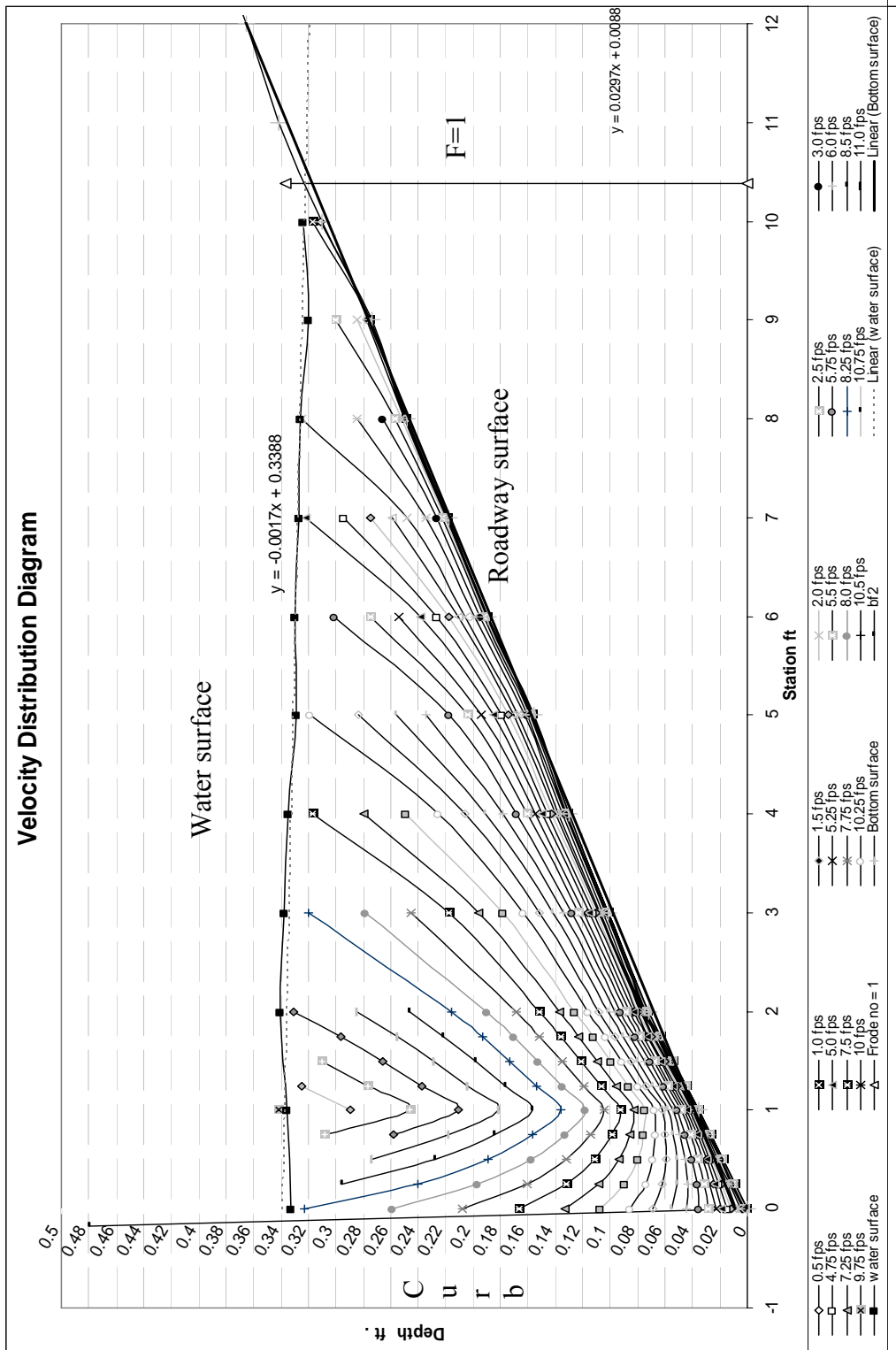


Figure 3.13 Velocity distributions across a roadway cross-section

3.2.9. Sub-Section Manning's n-value Calculation

In every sub-section, n-value is separately calculated based on local geometries of sub-section. The local geometries consist of water depth, surface elevation, surface area, longitudinal, and transverse slopes. The sub-section n-value is estimated from the Prandtl-von Karman velocity equations. The transformations of velocity and Manning's equations are shown below. The equation 3.9 shows the calculation of sub-section n-value based on Prandtl-von Karman velocity distribution equations.

Manning's equation (eq.2.1) can be used to calculate an average sub-section velocity (V_i) by inputting sub-section geometries as shown below.

$$V_i = \frac{1.486}{n_i} S^{1/2} R_i^{2/3} \quad (\text{Sturm, 2001}) \quad \text{eq.3.9}$$

where V_i = sub-section velocity

n_i = sub-section Manning's n-value

S = longitudinal slope

R_i = sub-section hydraulic radius

The average sub-section velocity also can be estimated from Prandtl-von Karman velocity equation (equation 2.35 and 2.36).

By assuming an average velocity is located at 0.4 of depth from the bottom surface ($y = 0.4d$), equation 2.36 can be rewritten in eq.3.10.

Average velocity by velocity distribution equation (rough condition)

$$V_i = 5.75 V_{f_i} \log \frac{30(0.4d_i)}{k} \quad \text{eq.3.10}$$

By substitute average velocity (V_i) in Manning's equation (eq.2.1) by Prandtl-von Karman average velocity equation (eq.3.10), the relationship of roughness value (k) and n -value can be shown in equation below.

$$\frac{1.486}{n_i} S^{1/2} R_i^{2/3} = 5.75 V_{f,i} \log \frac{30(0.4 d_i)}{k} \quad \text{eq.3.11}$$

Then solving for n -value

Manning's n -value by Prandtl's rough surface equation is

$$n_i = \frac{1.486 S^{1/2} R_i^{2/3}}{5.75 V_{f,i} \log \left(\frac{30(0.4 d_i)}{k} \right)} \quad \text{eq.3.12}$$

The smooth surface condition (eq.2.35) can be similarly derived giving in equation 3.13, Manning's n -value by Prandtl's smooth surface equation is

$$n_i = \frac{1.486 S^{1/2} R_i^{2/3}}{5.75 V_{f,i} \log \left(\frac{9(0.4 d_i) V_{f,i}}{v} \right)} \quad \text{eq.3.13}$$

3.2.10. Sub-Section Discharges Calculation

The vertical velocity profile of sub-sections is estimated by Prandtl-von Karman velocity method. The average velocity and area of sub-section is shown in “*average velocity calculation*” and “*sub-section area calculation*” sections. Each sub-section discharge is obtained by multiplied average sub-section velocity by the sub-section area for each sub-section across the roadway cross-section. As shown below.

$$\text{Sub - section discharge } (q_i) = V_{i- \text{average}} * A_i \quad \text{eq.3.14}$$

3.2.11 Total Cross-Section Discharge and Average Manning's n-value Calculation

Total cross-section discharge of a roadway can be obtained by sum of all sub-section discharge as shown below.

$$Total\ discharge\ (Q_{total}) = \sum_1^n Sub - section\ discharge \quad eq.3.15$$

A sub-section n-value is multiplied by a local geometry such as depth, wetted-perimeter, hydraulic-radius, velocity, discharge and area in order to weight effects of local geometry in that section. These factors are parts of the local geometry inputs and calculation results. There are several methods to obtaining average n-value of the entire cross-section. The methods of averaging n-value are associated with local geometries of a roadway. Some literatures suggest using a depth or a wetted-perimeter for a weight-parameter in estimating a cross-section average n-value. Each method gives different results of an average n-value. All methods used for averaging cross-section n-value are discussed in the chapter 2.

3.3 Mathematic Statistical Analysis

Before any analysis, all TxDOT roadway and velocity distribution data sets, n-values and discharges, have to be analyzed statistically. The processes such as normality distribution, detect outliers, scatter plot, cleaning outliers, and normality evaluation were used to analyze data. The statistical analysis is a step to minimize errors in the results. The statistical analysis process steps are shown in Figure 3.14.

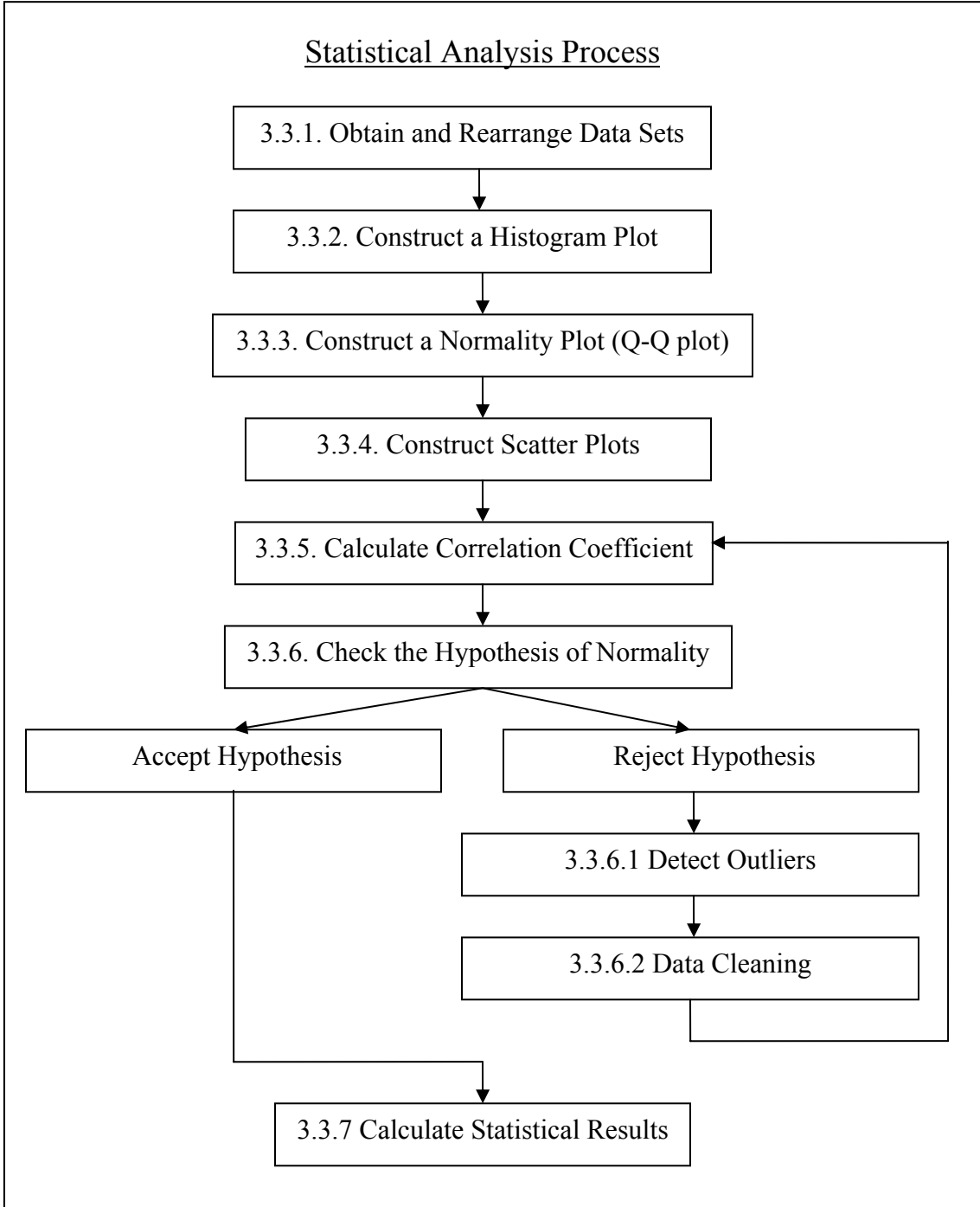


Figure 3.14 Process of statistical analysis

3.3.1 Obtain and Rearrange Data Sets

All series of average cross-section n-values and discharges from TxDOT laboratory and velocity distribution method are rearranged in order from low value to high value. Histogram and probability plots are developed from these data sets.

3.3.2 Construct Histogram Plot

In this research, the total cross-section n-values are used in histogram plots. The total range of n-value is based on the overall maximum and minimum n-value. The n-value interval is roughly estimated to be about 0.001. All the histogram plots of total roadway cross-section n-value indicate sign of normal distribution with some outliers. The highest column in the histogram plot shows the largest interval of n-value data frequency. An example histogram plot is shown in Figure 3.15 and Appendix E.

A histogram plot can be constructed as follow.

1. Divide the continuous range of data in to equal intervals. Too many or too few data intervals make it difficult to recognize normality distribution.
2. Group data into the interval ranges. The number of data in each interval range represents the data frequency.
3. Plot a bar graph between numbers of data and the interval ranges in y and x coordinates respectively. Montgomery, (Runger and Hubele, 2004)

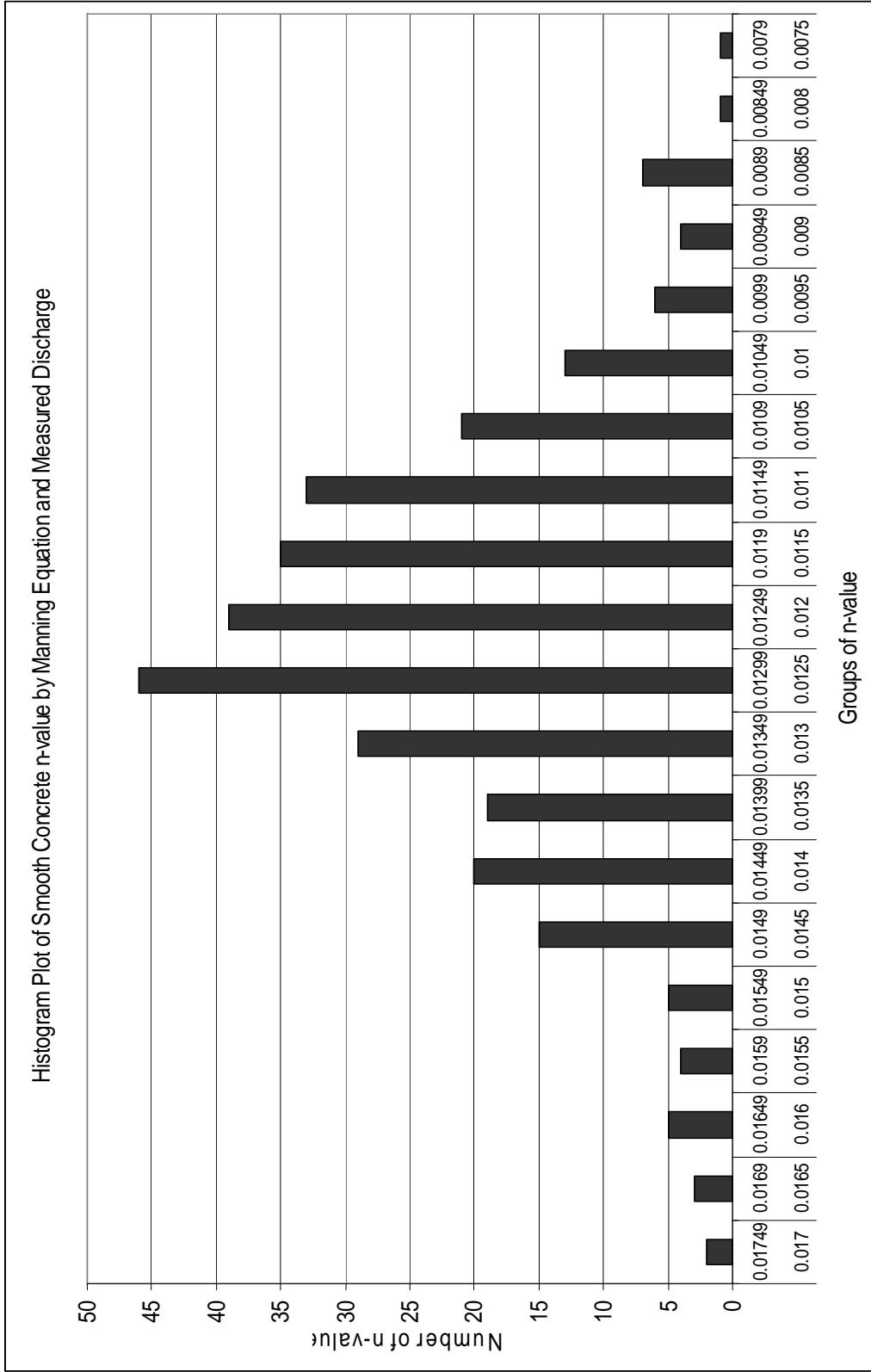


Figure 3.15 Histogram plot of smooth concrete n-value by Manning's equation and measure discharge

3.3.3 Construct a Normal Probability Plot (Q-Q Plot)

In this research, normality plots of n-value and discharge are developed for all sets of roadway data. Example plots of normal probability are shown in Figures 3.16 (before cleaning data) and Figure 3.17 (after cleaning data). The normality plot is constructed by the following steps.

1. Order the original observations to get $x_{(1)}, x_{(2)}, \dots, x_{(n)}$ and their corresponding probability values $(1-1/2)/n, (2-1/2)/n, \dots, (n-1/2)/n$;
2. Calculate the standard normal quantiles $q_{(1)}, q_{(2)}, \dots, q_{(n)}$
3. Plot the pairs of observations $(q_{(1)}, x_{(1)}), (q_{(2)}, x_{(2)}), \dots, (q_{(n)}, x_{(n)})$, and examine the “straightness” of the outcome. (Johnson, 2002)

Probability level is related to standard quantiles as shown in equation 2.52.

$$P[Z \leq q_{(j)}] = \int_{-\infty}^{q_{(j)}} \frac{1}{\sqrt{2\pi}} e^{-z^2/2} dz = P_{(j)} = \frac{j - \frac{1}{2}}{n} \quad (\text{Johnson, 2002}) \quad \text{eq.2.52}$$

- where $P_{(j)}$ = probability level,
 $q_{(j)}$ = standard quantiles,
 Z = probability,
 j = 1, 2, 3, ..., n, and
 n = total number of samples.

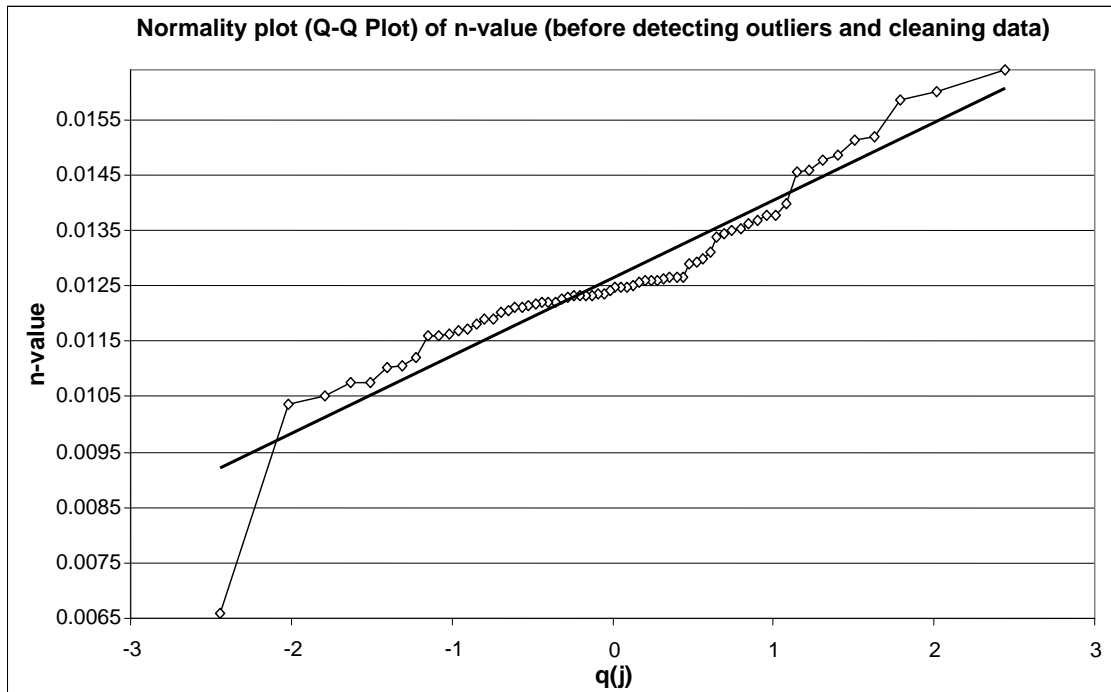


Figure 3.16 Normality plot (Q-Q plot) of n-values (before detecting outliers and cleaning data)

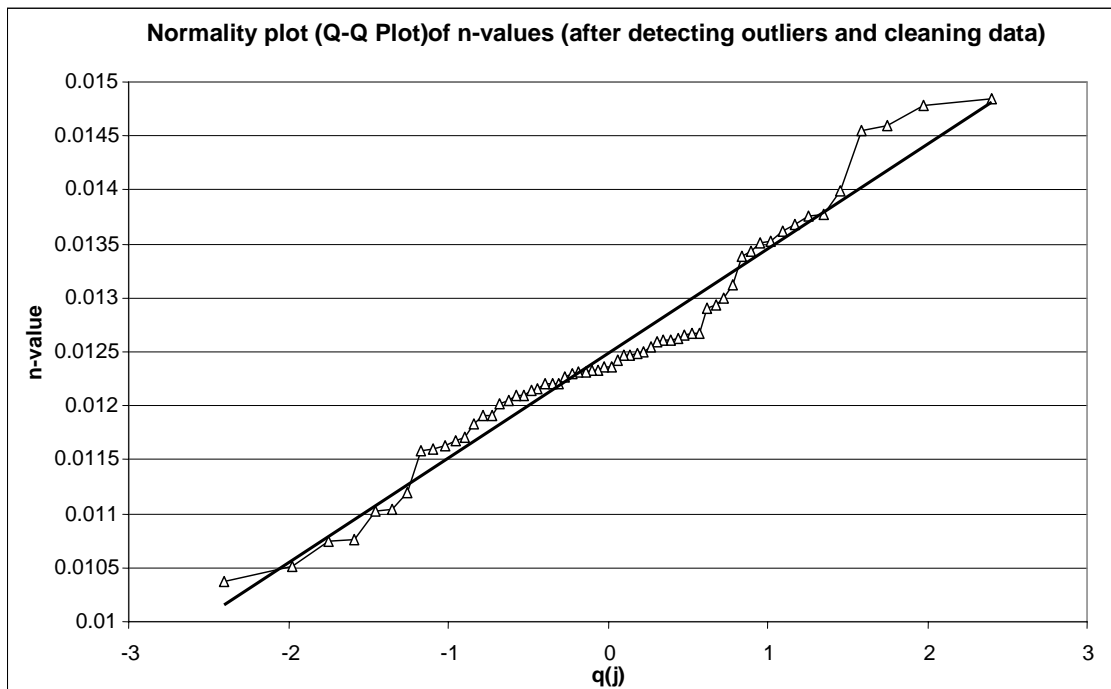


Figure 3.17 Normality plot (Q-Q plot) of n-values (after detecting outliers and cleaning data)

3.3.4 Construct Scatter Plots

A scatter plot compares one set of data with a second set of data taken under similar conditions. In this study, four similar sets of data existed for the TxDOT concrete roadway. The data sets differed only by the amount of rainfall each experiment. Each data set experiment only one of the following rainfall rates; 0, 1, 3 and 6 inches per hour. These four data sets were plotted one on one in scatter plots as shown in Figure 3.18.

X_1 is no-rainfall data plotted against no-rainfall data.

X_2 is 1-in/hr rainfall data plotted against 1-in/hr rainfall data.

X_3 is 3-in/hr rainfall data plotted against 3-in/hr rainfall data.

X_4 is 6-in/hr rainfall data plotted against 6-in/hr rainfall data.

The top row is X_1 , no-rain vs 1-in/hr, no-rain vs 3-in/hr, no-rain vs 6-in/hr.

The left column is X_1 , 1-in/hr vs no-rain, 3-in/hr vs no-rain, 6-in/hr vs no-rain.

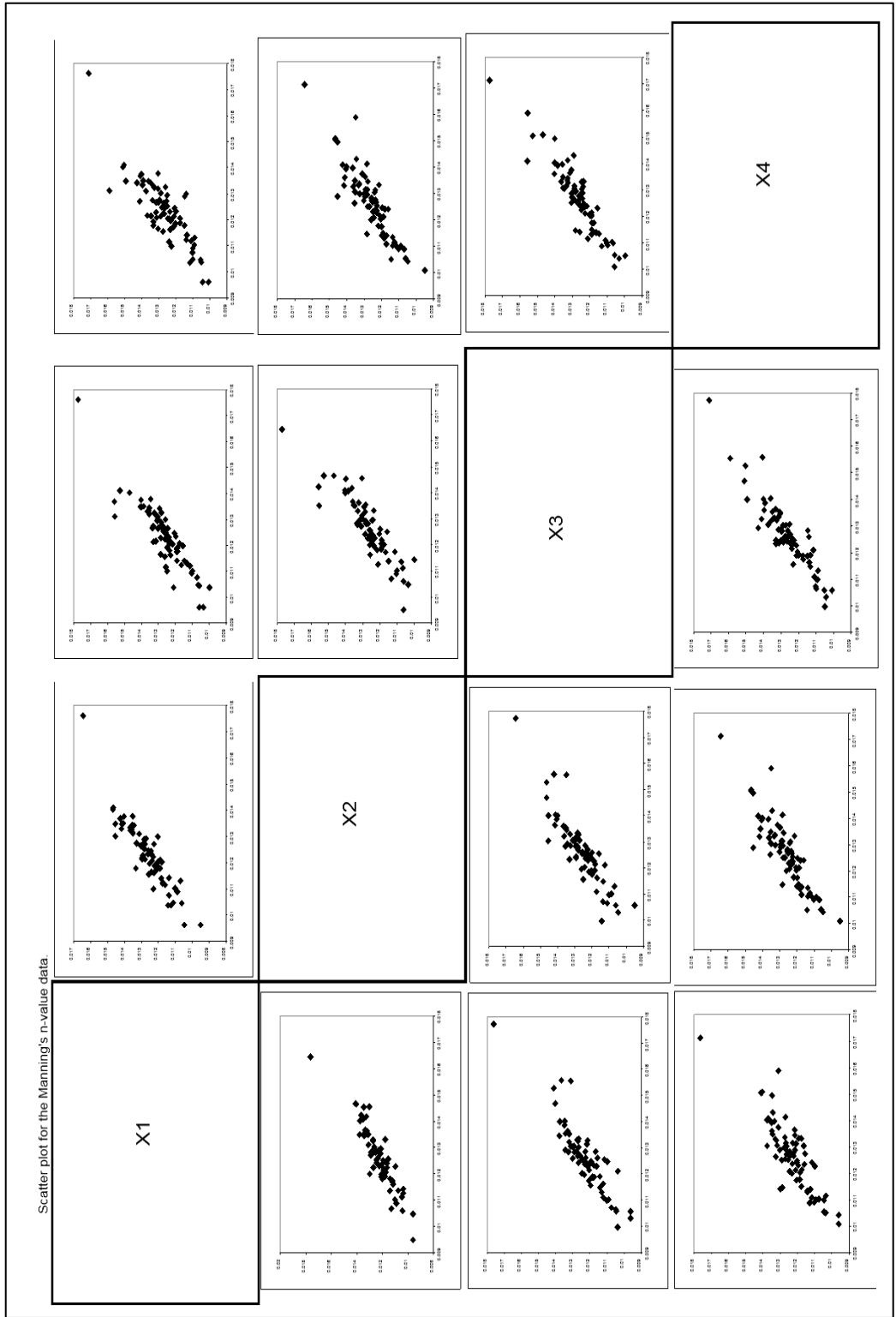


Figure 3.18 Scatter plots of TxDOT concrete roadway n-values with no-rain, 1-inch/hr, 3-inch/hr, and 6-inch/hr

3.3.5 Calculate Correlation Coefficient

The correlation coefficient is used to estimate normality distribution of data set before and after removing outliers. Correlation coefficient is a method used to calculate after most of outliers were taken out. An equation 2.53 provides a calculation of correlation coefficient of data set. Several of methods, such as histogram, normal probability plot, and scatter plots were used to identify and remove outliers. The process of removing outlier is described in topic 3.3.6.1. Table 3.1 shows correlation coefficient calculation samples.

$$r_Q = \frac{\sum_{j=1}^n (x_{(j)} - \bar{x})(q_{(j)} - \bar{q})}{\sqrt{\sum_{j=1}^n (x_{(j)} - \bar{x})^2} \sqrt{\sum_{j=1}^n (q_{(j)} - \bar{q})^2}} \quad (\text{Filliben, 1975}) \quad \text{eq.2.53}$$

where r_Q = correlation coefficient,

x = data point,

\bar{x} = numerical average of data,

$q_{(j)}$ = standard quantiles,

\bar{q} = numerical average of standard quantiles,

j = 1, 2, 3... n, and

n = total number of samples.

Table 3.1 Correlation coefficient calculation table

no.	n-value	$(x_{(j)} - \bar{x}) q_{(j)}$	$(x_{(j)} - \bar{x})^2$	$q_{(j)}$	$q_{(j)}^2$
1	0.010578	0.003476	0.000004	-1.827880	3.341145
2	0.010578	0.003178	0.000004	-1.671644	2.794393
3	0.010654	0.002826	0.000003	-1.548003	2.396313
4	0.010720	0.002541	0.000003	-1.444321	2.086064
5	0.010982	0.002028	0.000002	-1.354190	1.833831
6	0.011028	0.001849	0.000002	-1.273889	1.622794
7	0.011105	0.001651	0.000002	-1.201055	1.442534
8	0.011310	0.001327	0.000001	-1.134090	1.286160
9	0.011478	0.001073	0.000001	-1.071858	1.148880
10	0.011560	0.000932	0.000001	-1.013522	1.027227
11	0.011632	0.000812	0.000001	-0.958446	0.918619
12	0.011750	0.000661	0.000001	-0.906134	0.821079

73	0.012101	0.000209	0.000000	-0.551806	0.304490
74	0.012150	0.000169	0.000000	-0.512776	0.262939
Σ		0.045037	0.000048		43.613574
correlation coefficient (r_q)=			0.968		
In table 3.1, at 74 samples and $\alpha = 0.05$; critical point = 0.983					

3.3.6 Check Hypothesis of Normality

Hypothesis of normality is used to separate types of data series distribution. For a normal distributed data set, correlation coefficient value will be compared to a critical correlation coefficient value at significant level (α) of 0.05 for acceptance level. Table 3.2 shows critical points for correlation coefficient value with various significance levels (α) and sample sizes. For different sample size, the critical correlation coefficient is obtained by interpolation. In order to accept a data set, the correlation value has to be higher or equal to critical values in the table. Data sets with a lower correlation coefficient value than a critical value will need further data cleaning analysis or rejected as a non-normal distribution.

Table 3.2 Critical points for the Q-Q plot correlation coefficient test for normality (Johnson 2002)

Sample size <i>n</i>	Significance levels α		
	.01	.05	.10
5	.8299	.8788	.9032
10	.8801	.9198	.9351
15	.9126	.9389	.9503
20	.9269	.9508	.9604
25	.9410	.9591	.9665
30	.9479	.9652	.9715
35	.9538	.9682	.9740
40	.9599	.9726	.9771
45	.9632	.9749	.9792
50	.9671	.9768	.9809
55	.9695	.9787	.9822
60	.9720	.9801	.9836
75	.9771	.9838	.9866
100	.9822	.9873	.9895
150	.9879	.9913	.9928
200	.9905	.9931	.9942
300	.9935	.9953	.9960

3.3.6.1 Detect Outliers

Outliers are unusual data points that can be identified by histogram plot, probability plot, scatter plot, and chi-square plot. In the probability plot, outliers can be found on both ends of data sets as shown in Figure 3.16. Those unusual points greatly affect the outcome of analysis. The results are unpredictable with interruption sources. The only way to treat these unused points is carefully remove them out from the analysis. The unusual points can be found as uneven spacing or further out from a main line plot.

The following steps are for standardized and generalized distances calculation. They are used for detecting outliers in data sets with very similar data range. Therefore, these steps were used only TxDOT concrete roadway data with no-rain, 1-in/hr, 3-in/hr and 6-in/hr.

1. Make a dot plot for each variable.
2. Make a scatter plot for each pair of variables.
3. Calculate the standardized values $z_{jk} = (x_{jk} - x_k) / \sqrt{s_{kk}}$ for $j = 1, 2, \dots, n$ and each column $k = 1, 2, \dots, p$ examine these standardized values for large or small values.
4. Calculate the generalized squared distances $d_j^2 = (x_{(j)} - \bar{x})' S^{-1} (x_{(j)} - \bar{x})$.

Examine these distances for unusually large values. (Johnson, 2002)

Table 3.3 shows standardized, generalized distances and n-values of TxDOT roadway surface with no-rain, 1-in/hr, 3-in/hr, 6-in/hr.

Table 3.3 Standardized and generalized distance values for TxDOT concrete roadway surface with no-rain, 1-in/hr, 3-in/hr, 6-in/hr

no-rain	1-in/hr	3-in/hr	6-in/hr	no.					
X ₁	X ₂	X ₃	X ₄		Z ₁	Z ₂	Z ₃	Z ₄	d _j ²
0.01411	0.01466	0.01527	0.0150	1	1.611	1.816	2.403	2.154	5.0424
0.01375	0.01401	0.01401	0.01401	2	1.288	1.235	1.253	1.223	3.2260
0.01178	0.01331	0.0123	0.01331	3	-0.474	0.617	-0.282	0.589	0.4360
0.01192	0.01214	0.01246	0.0133	4	-0.349	-0.428	-0.162	0.588	0.2362
0.01292	0.01271	0.01305	0.01250	5	0.548	0.078	0.382	-0.142	0.5837
0.01348	0.01411	0.01403	0.01359	6	1.046	1.326	1.271	0.848	2.1278
0.01266	0.01282	0.01334	0.01313	7	0.315	0.175	0.644	0.432	0.1928
0.01204	0.01196	0.01234	0.01246	8	-0.234	-0.588	-0.267	-0.176	0.1067
0.01164	0.01239	0.01285	0.01304	9	-0.592	-0.203	0.200	0.350	0.6820
0.01270	0.01224	0.01269	0.01254	10	0.354	-0.337	0.051	-0.105	0.2439
0.01271	0.01283	0.01325	0.01412	11	0.359	0.184	0.566	1.322	0.2501
0.01090	0.01088	0.01102	0.01000	12	-1.256	-1.555	-1.470	-1.504	3.0656
0.01115	0.01160	0.01255	0.01239	13	-1.035	-0.908	-0.075	-0.239	2.0833
0.01377	0.01349	0.01345	0.01304	14	1.311	0.772	0.749	0.344	3.3387
0.01322	0.0136	0.01322	0.01325	15	0.819	0.894	0.535	0.536	1.3024
0.01310	0.01349	0.0155	0.01588	16	0.713	0.772	2.658	2.922	0.9887
0.01368	0.01423	0.01558	0.01407	17	1.226	1.431	2.689	1.279	2.9205
0.01334	0.01366	0.01359	0.01396	18	0.924	0.922	0.870	1.182	1.6593
0.01216	0.01295	0.01314	0.01364	19	-0.132	0.294	0.460	0.895	0.0336
0.01347	0.01453	0.01399	0.01494	20	1.043	1.703	1.240	2.064	2.1133
0.01402	0.01465	0.01469	0.01508	21	1.528	1.808	1.877	2.191	4.5358
0.01223	0.01230	0.01242	0.01265	22	-0.069	-0.283	-0.198	-0.002	0.0093
.
.
.
0.01102	0.01101	0.01098	0.01090	69	-1.151	-1.435	-1.512	-1.591	2.5749
0.01130	0.01069	0.01131	0.01088	70	-0.902	-1.723	-1.213	-1.612	1.5798
0.01213	0.01277	0.01327	0.01343	71	-0.158	0.130	0.582	0.704	0.0487
0.01045	0.01060	0.01057	0.01053	72	-1.658	-1.801	-1.881	-1.926	5.3413
0.01762	0.01644	0.01772	0.01711	73	4.741	3.397	4.645	4.032	43.690
0.01299	0.01199	0.01258	0.01140	74	0.607	-0.560	-0.050	-1.134	0.7167
0.01231	0.01262	0.01263	0.01266	<= average n-value					

3.3.6.2 Data Cleaning

Normally, laboratory or field raw data contains unusual point as shown in detect outliers step. The methods to identify outliers such as detecting outliers and scatter plots show location of unrelated points. These unrelated points or outliers can be removed out of the data sets to improve the normality. Figure 3.16, 3.17, 3.19, 3.20 and 3.21 show plots of result, discharge and n-value, before and after data cleaning process.

3.3.7 Calculate Statistical Result

The statistical result of analyzed data shows improvement of normality distribution and minimal numbers of outliers. The percentage of error is reduced on account of the reduction of outliers in data series. Then the analyzed data sets are ready for display and numerical average calculation. An average n-value of each data set is calculated from numerical average. After an average n-value for each TxDOT study and velocity method data set are calculated, data comparison can be done. All data sets of n-value after removed outliers are plotted in normal scale graph and shown in Appendix C. The comparisons of discharge between measured and velocity method four types of the roadway surface are shown in Figure 3.19, 3.20 and Appendix D.

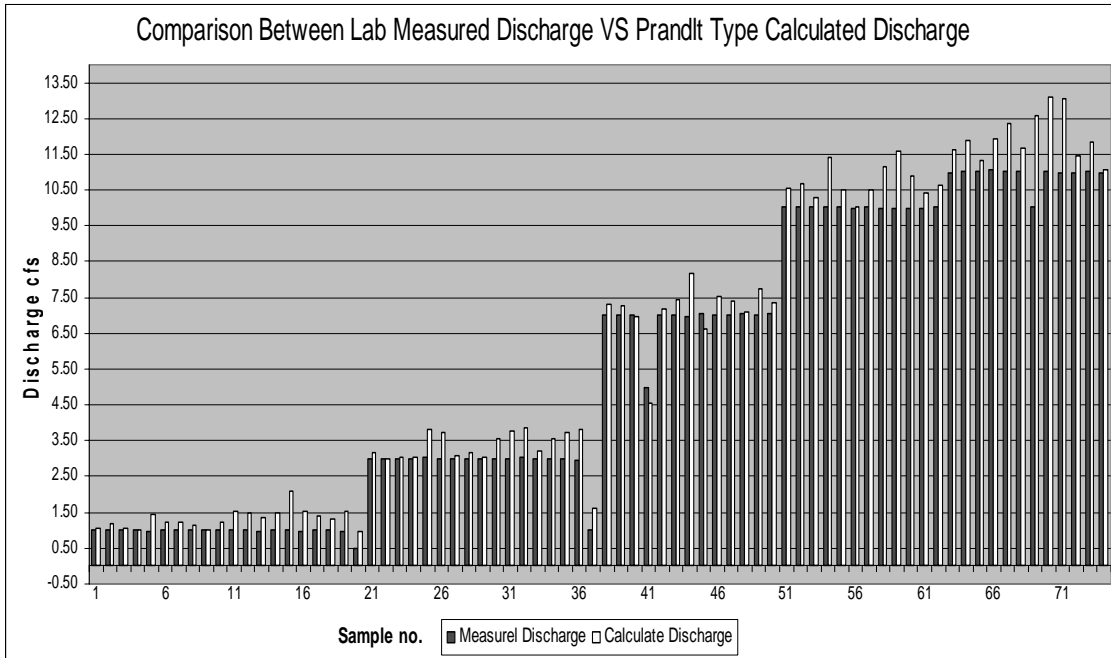


Figure 3.19 Result of TxDOT concrete discharge comparison before cleaning process

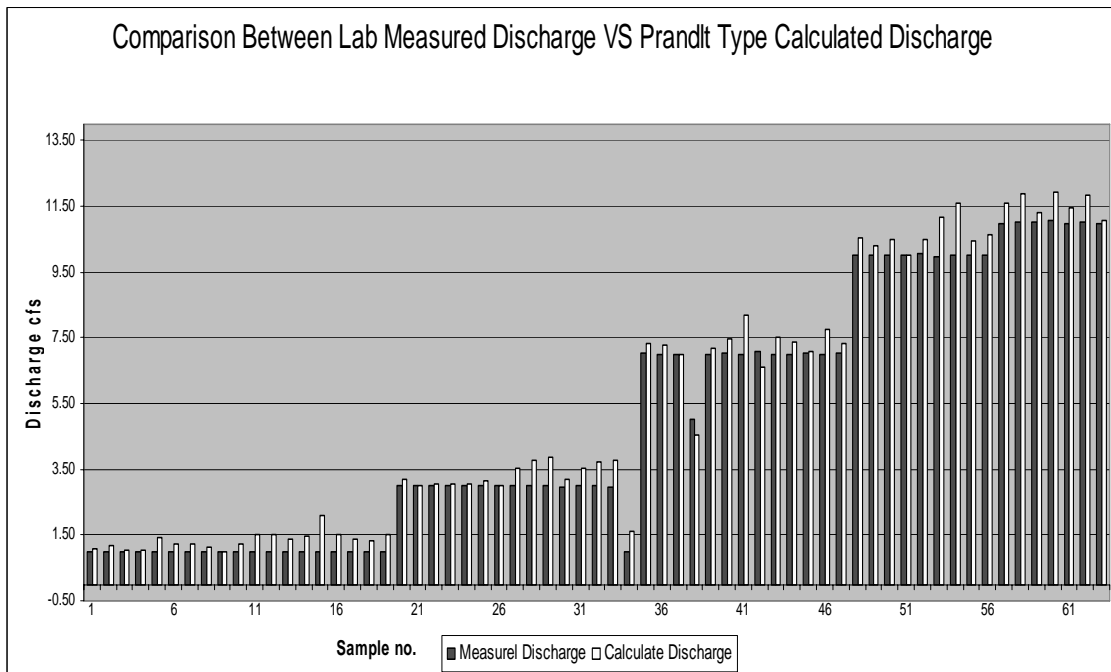


Figure 3.20 Result of TxDOT concrete discharge comparison after cleaning process

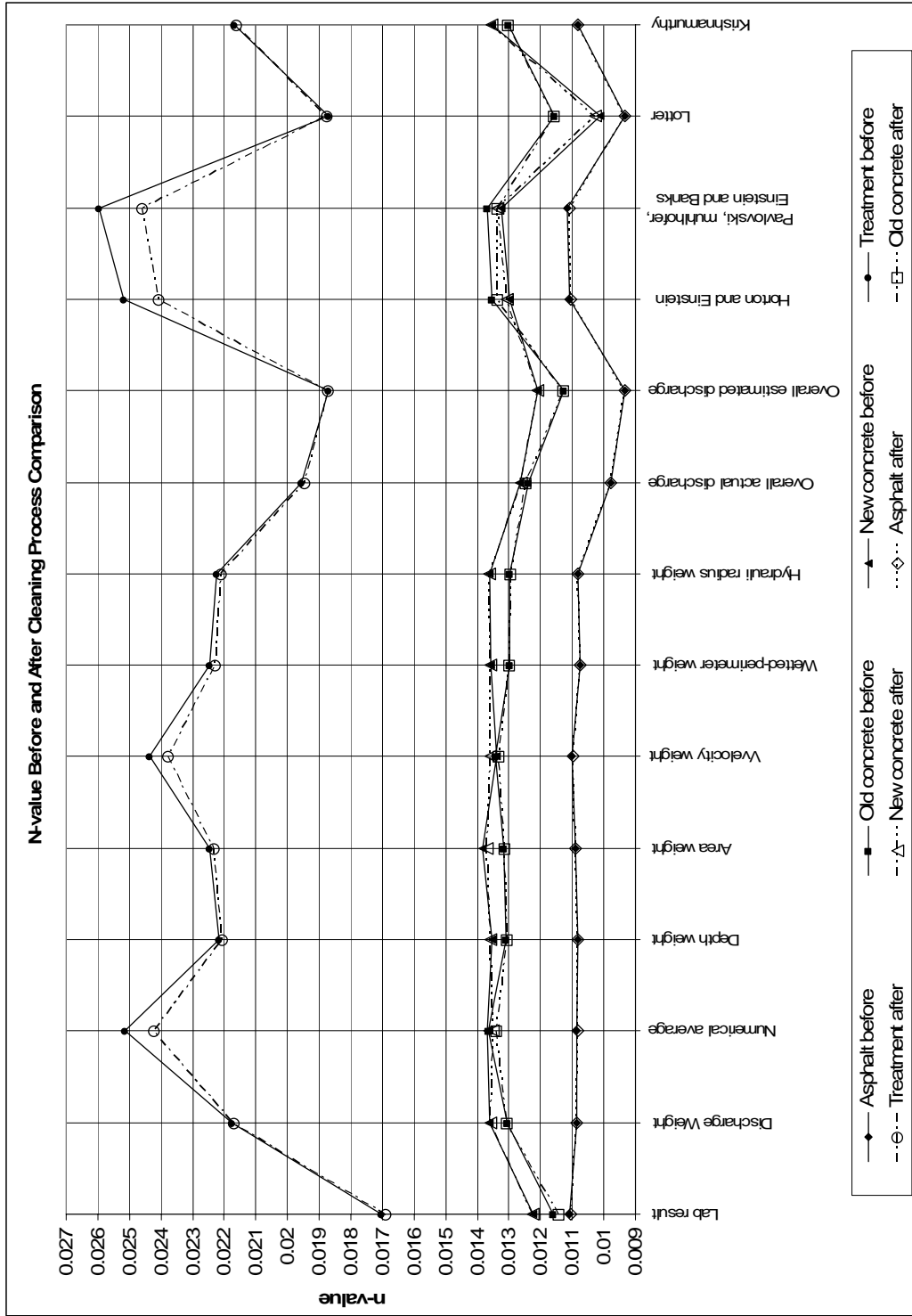


Figure 3.21 Comparison of average n-values by various averaging methods (before and after cleaning data)

CHAPTER 4

MODEL VERIFICATION AND RESULT ANALYSIS

4.1 Model Calibration and Verification

The TxDOT roadway roughness project geometry data for the roadway surfaces, new concrete, smooth concrete, asphalt, and asphalt treatment are used in the velocity distribution model. Geometry data is used for the Manning's roughness analysis. Two methods are used to estimate cross-section n-values and discharges.

The first method calculates average sub-section velocity by velocity distribution method. Calculate sub-section area by sub-section's geometry, depth and spread. The sub-section n-values and discharges are calculated from each average sub-section velocity and sub-section area. The entire roadway cross-section n-value is estimated from various averaging methods as shown in chapter 2. The total roadway cross-section discharge is sum of sub-section discharges.

The second method, a total discharge is a constant input. The entire roadway cross-section geometries, depths and spreads, are estimated by trial and error according to the total discharge. Each average velocity is calculated by velocity distribution method according to estimated sub-section depths. The sub-section n-values are calculated from the estimated sub-section geometries. The total cross-section n-value is calculated from various averaging methods as shown in chapter 2

The first method is the only method used this research. It provides accurate discharges and n-values compared to the original TxDOT project result.

In the TxDOT project, some geometry conditions such as curb surface roughness, actual transverse slope and the actual water surface were not used in the total cross-section n-value estimation. As a result, the TxDOT project's n-value is differ from the velocity distribution's n-value.

The laboratory result consists of two methods of total area calculation, depth-analysis and spread-analysis as shown in Figure 3.6. These methods have different assumptions to estimate the total cross-section geometries. Depth-analysis is based on a curb station depth and transverse slope. Then the total cross-section spread is calculated by dividing the curb-depth by the transverse slope. The total cross-sectional area is a one half product of the curb-depth and the spread width.

The second technique, spread-analysis, a total spread is estimated from average laboratory readings. The total cross-section area is calculated the same way as previous method. Figure 4.1 demonstrates the difference between two area estimation methods, depth-analysis and spread-analysis. These two techniques always show similar but different total cross-sectional areas. An average value from these methods might be a better estimation of the total area.

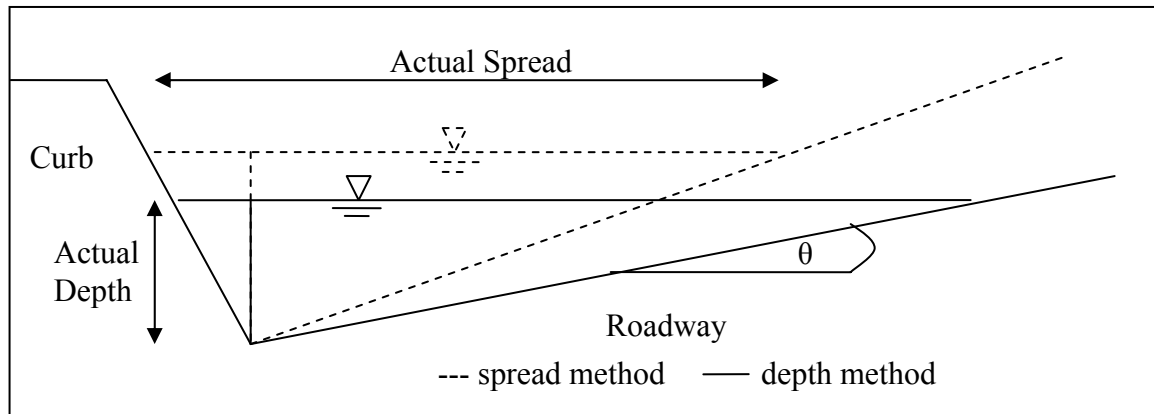


Figure 4.1 Cross-sectional areas estimated by spread and depth methods

4.2 Theoretical Manning's n-value

Literature suggests several equations to estimate roughness n-value for all types of channels. Due to complexities of natural channel geometries, it is almost impossible to estimate accurately the actual n-value. Most purposed techniques for finding average n-values are based on empirical data as well as theoretical assumptions. The experimental field data helps improve accuracy of n-value estimations.

There are two types of theoretical equations for estimating n-values, variable and constant roughness equations. The constant roughness equation calculates n-value from the average grain size of bed material. Estimations of n-values by the constant roughness equations are shown in table 4.1. The roughness value (k) was obtained by estimating roadway roughness height as shown in chapter 3. The n-values are then calculated from equation 2.3, 2.4, 2.5, and 2.7. These equations are based on Strickler (1923), Meyer-Peter (1948), Lane (1953), and Bray (1979) assumptions respectively. These constant n-values do not vary as a function of channel geometry but vary a

function of the average bed material diameter. Since bed material of roadways rarely changes quickly, the estimated n-values from the constant roughness equation remain constant.

Table 4.1 Estimated Manning's n-values

	Estimated n-value			
	Asphalt	Smooth concrete	TxDOT concrete	Treatment
Roughness value, k	0.5mm	1.6mm	2mm	17mm
Strickler (1923)	0.01168	0.01417	0.01471	0.02102
Meyer-Peter, Muller (1948)	0.01099	0.01334	0.01385	0.01978
Lane-Carlson (1953)	0.01339	0.01626	0.01687	0.02411
Bray (1979)	0.01523	0.01876	0.01952	0.02863

A second type of roughness equation exists, which contains more geometry information such as depth, hydraulic radius, and width of channel. Estimated n-values from these equations are more representative of the channel cross-section geometries. Some of these equations are not compatible with this research, such as the Jarret (1983) equation (assuming steep longitudinal slope) and the Forehlich (1975) equation (containing a special estimated parameter). Some of these variable n-value equations such as equation 2.6, 2.8, 2.9, 2.10 and 2.11 are more practicable to estimate n-values. Figure 4.2-4.5 show n-value estimation for four types of roadway surfaces. The Bray (1979), Limerinos (1970) and Griffiths (1981) equations show different n-value estimation. Limerinos (1970) equation shows higher n-values than Bray (1979) and Griffith (1981) equations. All equations show high estimated n-values at low discharge and vise versa.

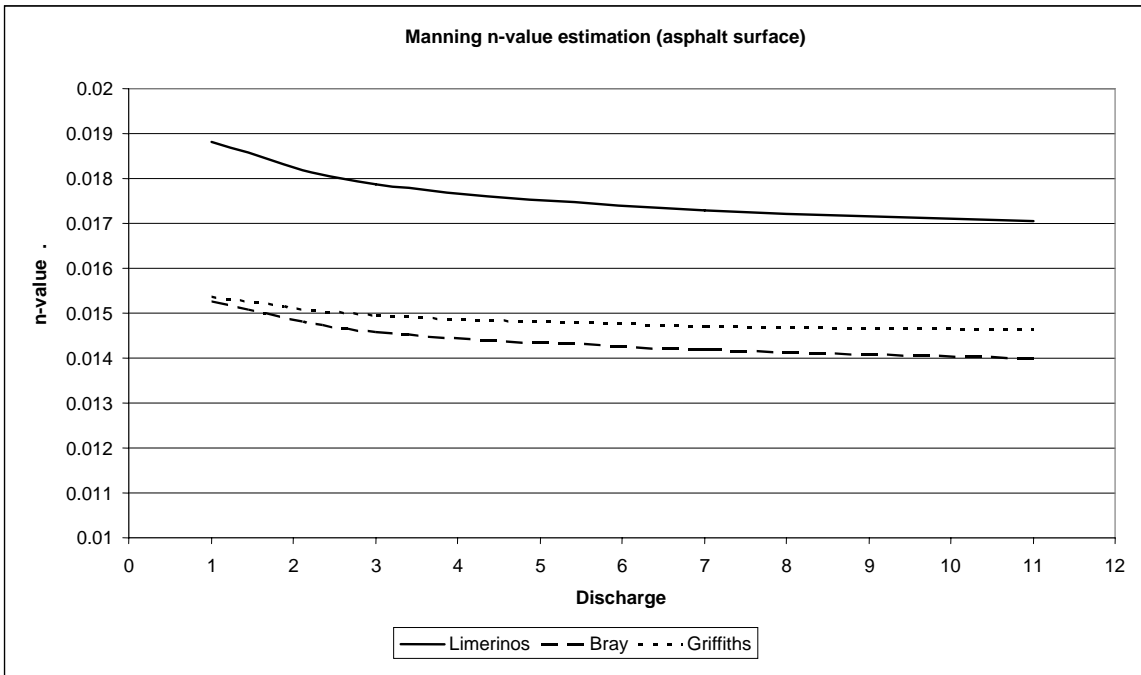


Figure 4.2 Estimated Manning's n-value for asphalt surface

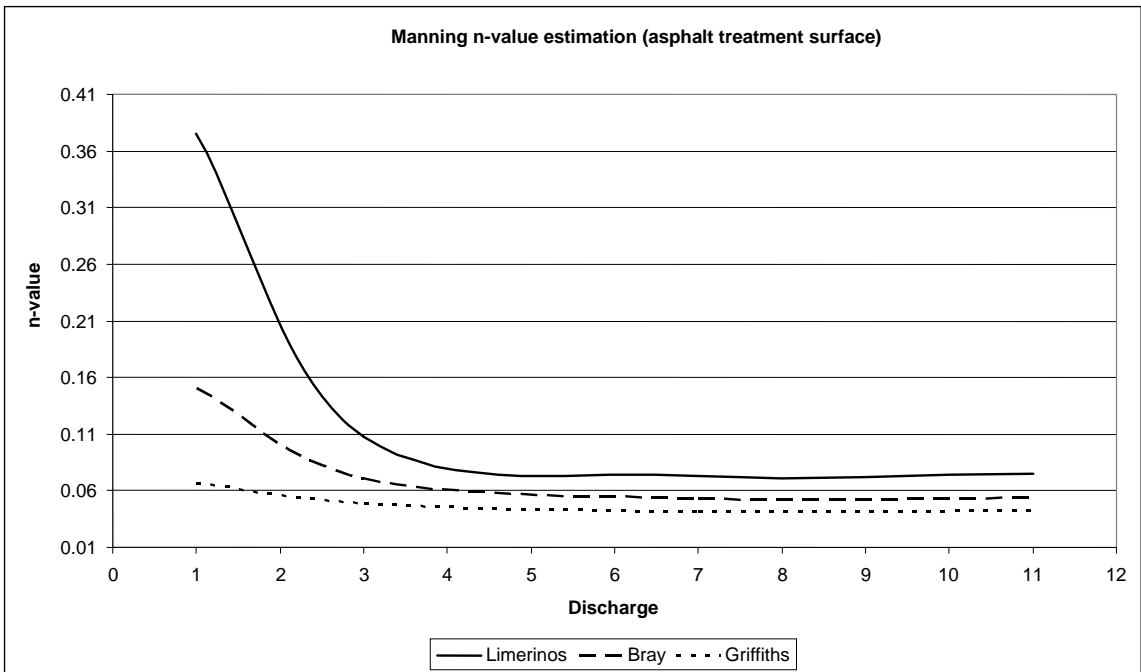


Figure 4.3 Estimated Manning's n-value for asphalt treatment surface

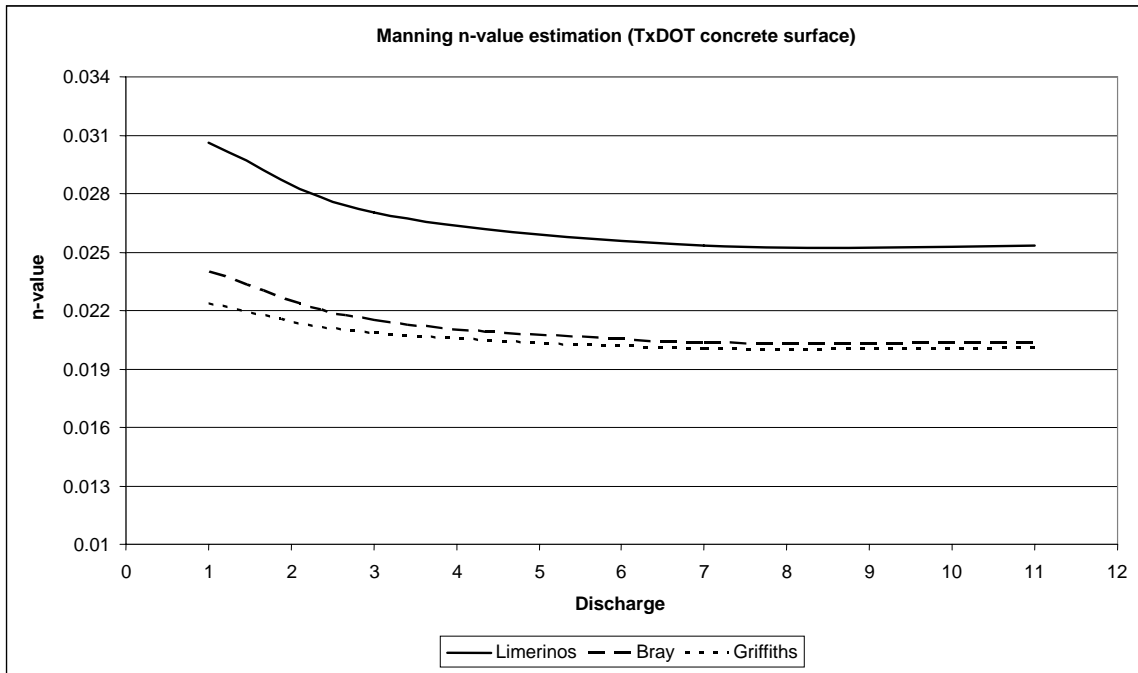


Figure 4.4 Estimated Manning's n-value for TxDOT concrete surface

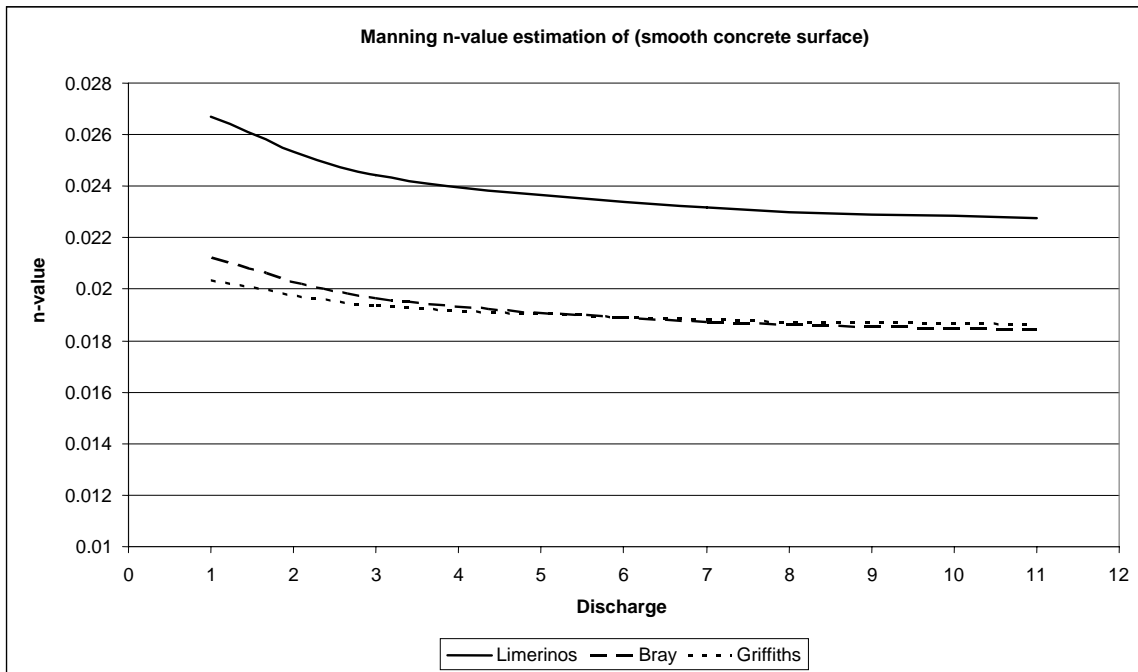


Figure 4.5 Estimated Manning's n-value for smooth concrete surface

4.3 Velocity Distribution Methods Comparison

All the flow resistance equations, equation 2.16, 2.19, 2.21, 2.23, 2.25, 2.27, 2.28, 2.35 and 2.36 from the chapter two were analyzed and compared by percent error of total estimated discharge. In order to estimate accuracy of velocity equations, flow of all four types of roadways, TxDOT concrete, smooth concrete, asphalt, and asphalt treatment were used in the comparison of these velocity equations. All the roadway data provide variety of roughness and geometry inputs to these velocity equations.

The flow resistance equations, eq.2.16, 2.19, 2.21, 2.23, 2.25, 2.27, 2.28, 2.35 and 2.36 are in a logarithmic form with two estimated variables α and β . The equation found from literature defined α and β as shown in eq.2.14. These parameters affect the outcome in different ways. Some flow equations use hydraulic-radius in stead of hydraulic-depth inside the logarithm term of the equation. These variances of α and β are a major cause of the velocity variation shown in Figure 4.6.

These equations simulate different velocity profiles with varied slopes and surface roughness with the same input parameters. Figure 4.6 shows plots of theoretical velocity profiles for all the methods investigated. In this specific figure, Griffiths's velocity equation produces the minimum velocity for a constant depth. Prandtl-von Karman velocity equation shows the maximum velocity profile. The rest of the velocity profiles are located between these curves. The velocity profiles shown in Figure 4.6 are not constant, since they vary with the geometry of the cross-section. The actual velocity distributions change with actual geometry conditions of the channels. Optimization of α and β could produce better flow estimations.

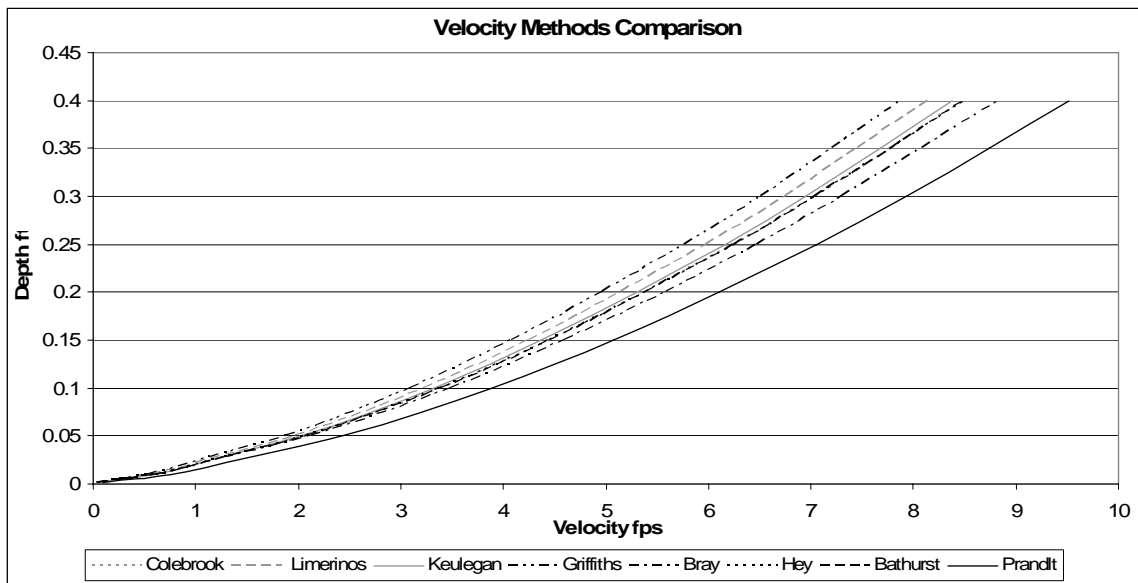


Figure 4.6 Comparison of velocity profiles by various flow resistance equations

Figure 4.7 shows the plots of eight velocity method estimated discharges for the TxDOT concrete surface. The negative and positive percent errors show over and under estimation of discharge respectively. All methods show both over and under estimated discharge. The trend lines of estimated error appear to align parallel to each other. This variance in flow appears to result from the variation of estimated parameters (α and β) in the velocity equations.

Most methods tend to under estimate at the lower flow rate and over estimated at the high flow rate. The calculated discharges by various velocity equations are compared to the actual discharge with average percent of error as shown in table 4.2. Plots of average percent error of all roadway surfaces are plotted in Figure 4.8. Each equation shows comparable results based on its parameters and functions.

Table 4.2 Average percent discharge errors from various velocity methods

	Average Percent Discharge Error							
Roadway type	Colebrook	Limerinos	Keulegan	Griffiths	Bray	Hey	Bathurst	Prandtl
Asphalt	14.06%	11.11%	11.08%	15.61%	11.11%	11.07%	11.30%	13.73%
Smooth Concrete	11.08%	10.81%	10.46%	16.15%	10.39%	10.44%	10.64%	13.69%
TxDOT Concrete	8.40%	8.70%	7.62%	14.51%	6.53%	6.53%	7.64%	10.48%
Asphalt Treatment	19.42%	24.00%	19.92%	31.99%	19.46%	16.84%	17.53%	10.43%
Average Percent Error	13.24%	13.66%	12.27%	19.56%	11.87%	11.22%	11.78%	12.08%

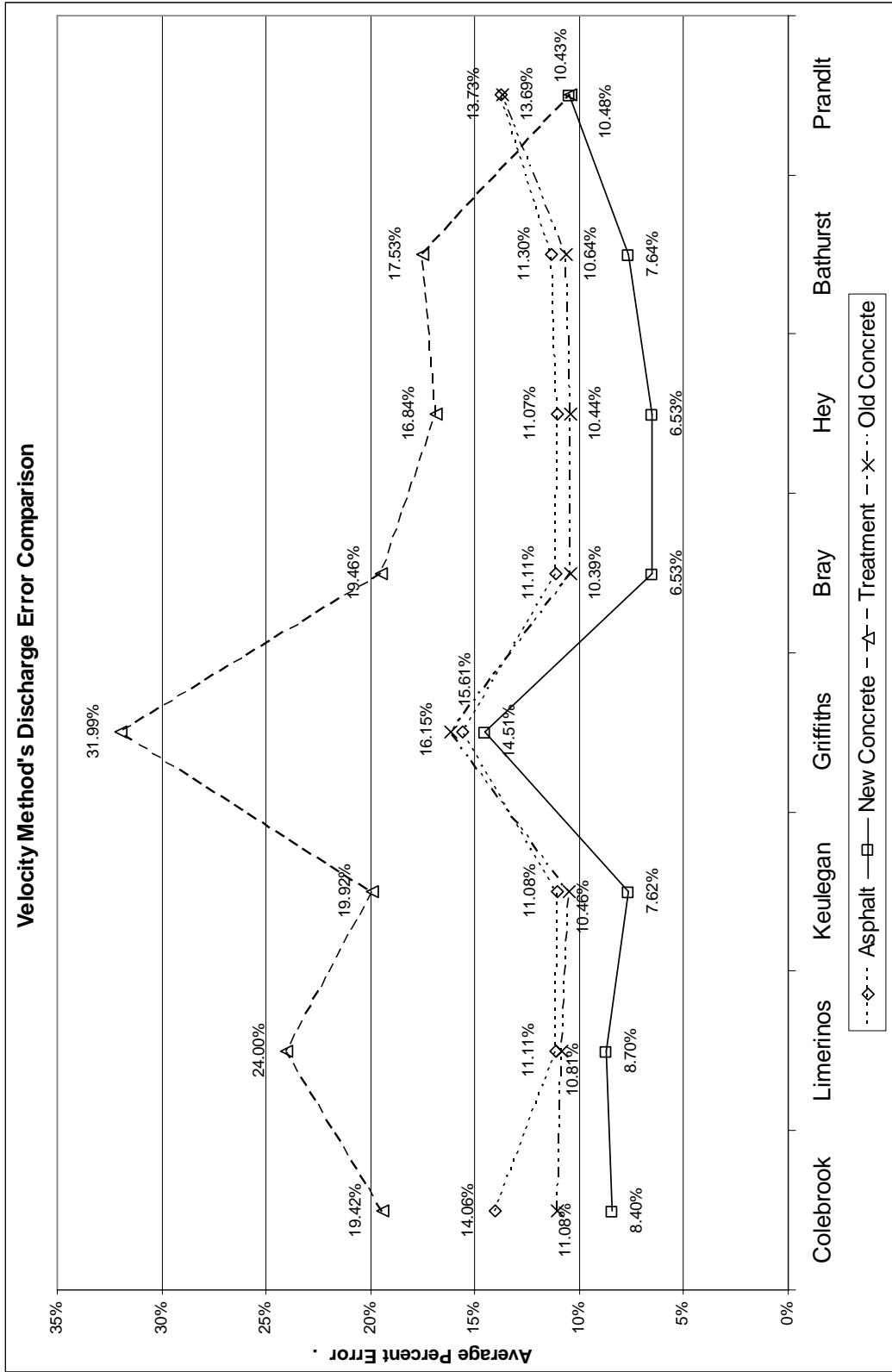


Figure 4.8 Average percent discharge error comparisons by various flow resistance equations

Table 4.2 and Figure 4.8 show average error of all methods ranges from about 6.5 to 32 percent. Some velocity equations are suitable only for low roughness value such as TxDOT concrete, asphalt and smooth concrete surfaces. Consequently, these equations show high error for higher roughness such as the asphalt treatment surface. In order to select the flow resistance method, justifications are determined not only from the overall accuracy but also from the most consistent estimated discharges.

Bray (1979) and Hey (1979) equations show the best result on the TxDOT concrete roadway. Their equations are among the best results shown for asphalt and smooth concrete surfaces. Nevertheless, these two equations are not used due to inconsistent results on the treatment surface. The same inconsistency scenario applied to most others such as Colebrook (1937), Limerinos (1970), Keulegan (1938), Griffiths and Bathurst (1985) equations.

Prandtl-von Karman velocity equation was selected for this research. The selection was made since they displayed the most consistency and accuracy of all the methods as shown in Figure 4.8. Even though this method produces a moderate overall accuracy result, the consistence is better than other methods. This velocity method shows average errors of about 10 to 14 percent for all the surfaces. Most errors for all surface types are related to over estimated discharge.

Figure 4.9, 4.10, 4.11, 4.12 and 4.13 are based on Prandtl-von Karman universal velocity method. The figures show effects of one variable condition to velocity profile with constant environment. Depths of velocity profile were estimated from velocity distribution program calculation in order to archive the same discharge. Average

velocities are estimated at the depth of 0.6 (0.6d) from the surface of water. The average velocity line connects the average velocities of every velocity profile. The average velocity line is shown in a linear straight line across the velocity profiles.

Effect of variable bottom roughness heights to velocity profiles with constant discharge, transverse slope and longitudinal slope is shown in Figure 4.9. The velocity decreases according to increase of the channel bottom roughness. Water depth is increased by increase the channel bottom roughness.

Figure 4.10 and 4.11 shows affect of longitudinal and transverse slopes respectively. The velocity increases according to increase of the longitudinal or transverse slopes. In Figure 4.10, water depth is increased by decrease longitudinal slope. Depth of water is decreased by decrease transverse slope in Figure 4.11.

Figure 4.12 shows the effects of various roughness dimensions and longitudinal slopes at constant transverse slop and discharge. By increasing longitudinal slope, the surface velocity and the water depth remain the same by decreasing bottom roughness height. They were calculated from different roughness and longitudinal slopes. These velocity curves demonstrate the average velocities and velocity profiles could be different at the same depth and water surface velocity. This effect is created from roughness values and longitudinal slopes.

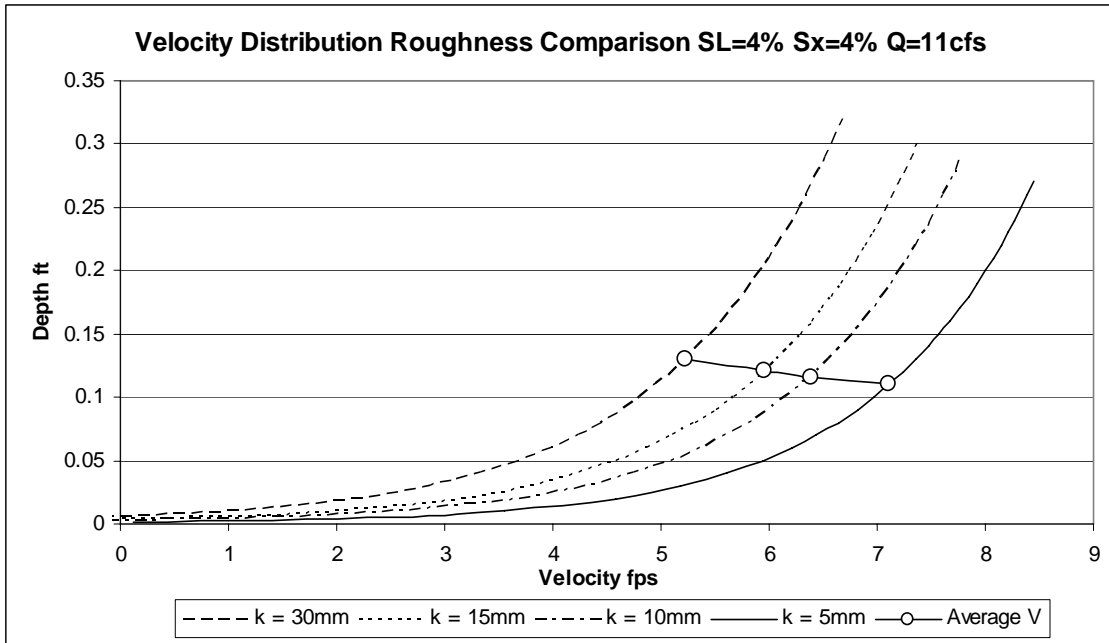


Figure 4.9 Vertical velocity profiles calculated by different roughness values (k)

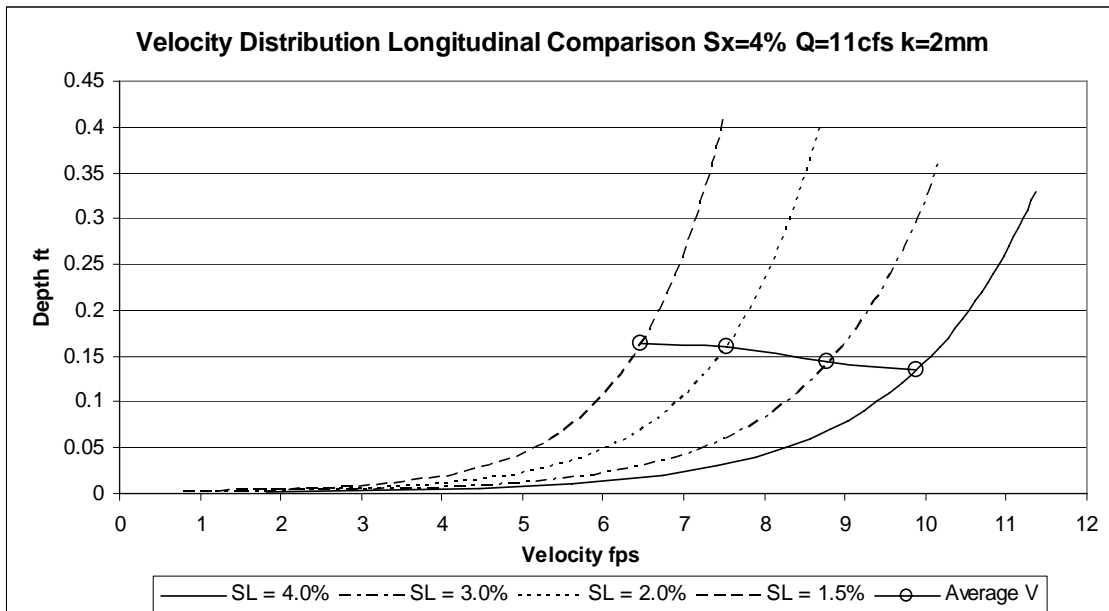


Figure 4.10 Vertical velocity profiles calculated by different longitudinal slopes

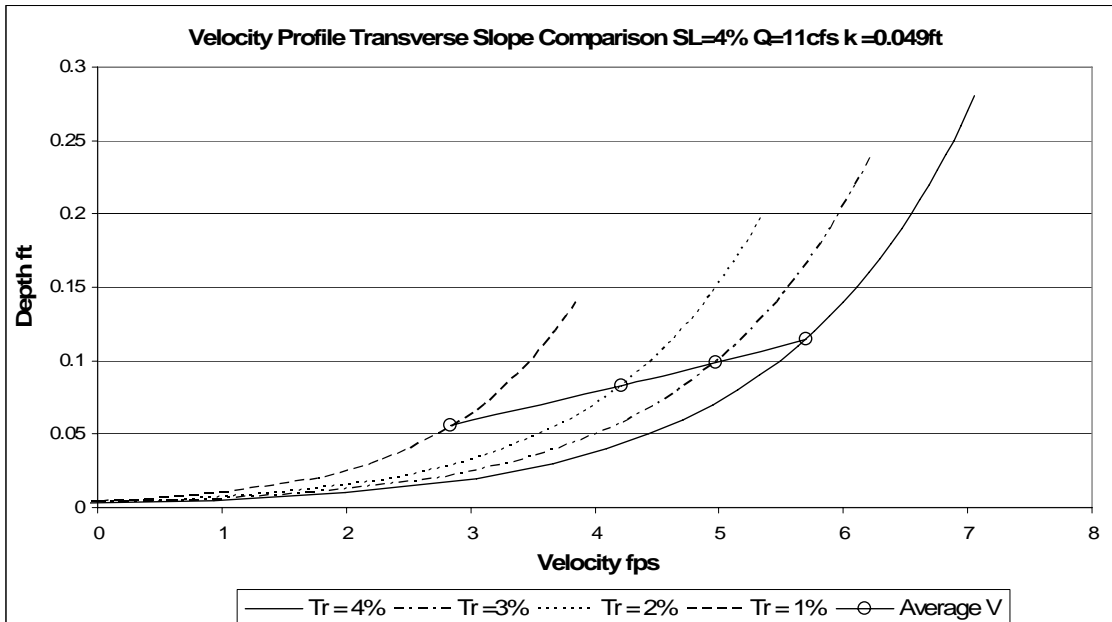


Figure 4.11 Vertical velocity profiles estimated by different transverse slopes

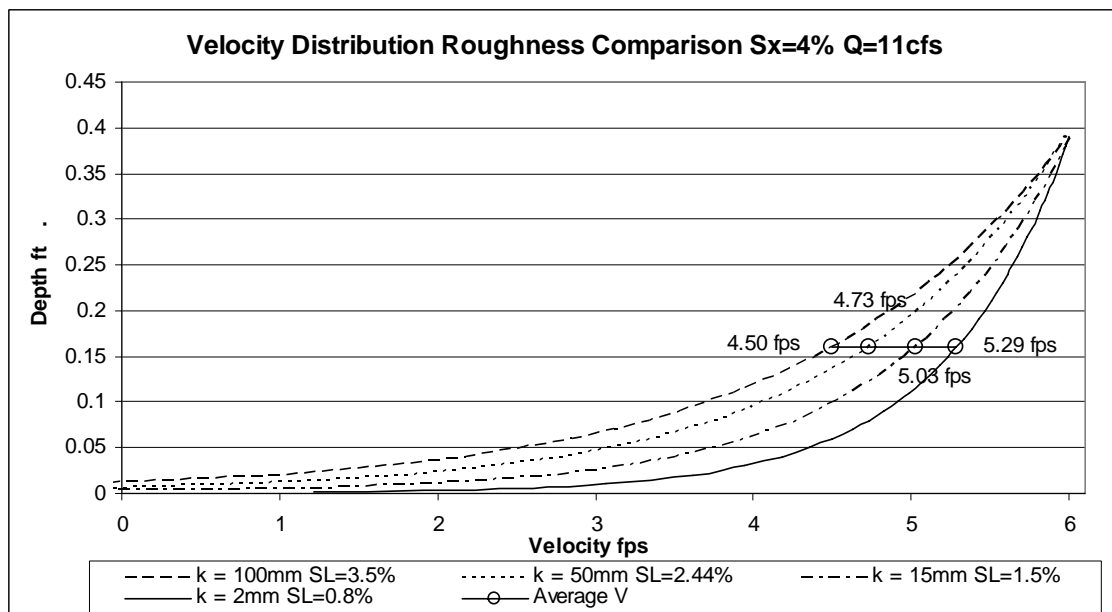


Figure 4.12 Vertical velocity profiles calculated by different roughness values (k) and longitudinal slopes

4.4 Manning's n-values Estimated by Various Averaging Methods

All methods for estimating the average cross-sectional n-value are shown in chapter 2 in equation 2.39 to 2.49. Some methods are suggested by literatures based on their empirical data and geometry assumptions. The averaging methods highly affect the outcome of average n-value. All averaging methods use the local geometry parameters of the sub-sections to calculate the total cross-section n-value. The relationships of local geometries and averaging methods are displayed in Figure 4.13. Wetted-perimeter and hydraulic depth are the basic geometry inputs. Sub-section geometries, such as velocity, discharge, hydraulic radius and area are calculated from the basic geometry. Average cross-section n-values are calculated by sub-section n-values and various sub-section geometries.

Results of average cross-section n-values estimated by Prandtl-von Karman (1926) velocity method and various averaging methods on the four roadway surface types are shown in table 4.3 and Figure 4.14.

Table 4.3 shows average cross-section n-values after cleaning process. The asphalt treatment n-value series shows the maximum variation and percent error from the lab result. Most averaging methods estimate n-value consistently higher than the lab result except the asphalt surface series.

Average cross-section n-values by averaging methods before and after cleaning data are shown in Figure 4.14. The decrease or increase value of Manning "n" is a result of the outlier reduction. Krishnamurthy (1972) averaging method is selected based on the accuracy and consistency of estimated discharges. (discussed in section 4.5)

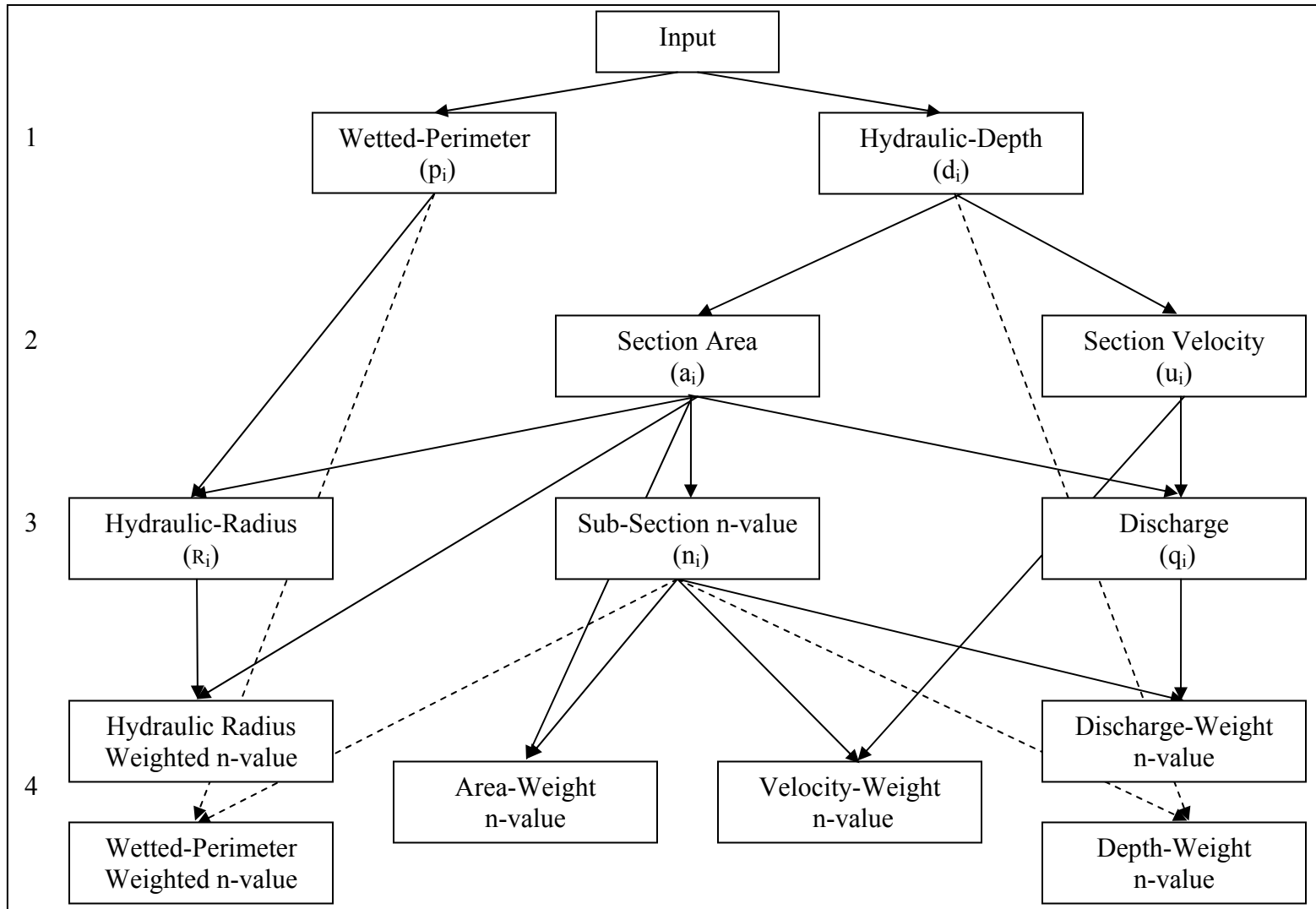


Figure 4.13 Relationships between local geometries and methods of averaging n-values

Table 4.3 Estimated average Manning's n-values for four types of roadway surfaces by Prandtl-von Karman velocity distribution and various averaging methods

	Asphalt surface		TxDOT Concrete surface		Smooth Concrete		Asphalt Treatment surface	
	n-value	% error from Lab result	n-value	% error from lab result	n-value	% error from lab result	n-value	%error from lab result
Lab result	0.01103		0.01222		0.01142		0.01687	
Discharge-weight	0.01086	1.52%	0.01359	11.19%	0.01306	14.30%	0.02169	28.60%
Numerical average	0.01084	1.70%	0.01351	10.59%	0.01338	17.11%	0.02421	43.55%
Depth-weight	0.01083	1.78%	0.01357	11.08%	0.01307	14.39%	0.02206	30.76%
Area-weight	0.01088	1.30%	0.01367	11.90%	0.01314	15.03%	0.02232	32.31%
Velocity-weight	0.01098	0.40%	0.01359	11.20%	0.01331	16.51%	0.02375	40.78%
Wetted-perimeter weighted	0.01075	2.48%	0.01358	11.13%	0.01296	13.45%	0.02229	32.15%
Hydraulic-radius weighted	0.01083	1.78%	0.01362	11.45%	0.01294	13.30%	0.02208	30.88%
Manning's equation and actual discharge	0.00976	11.46%	0.01262	3.26%	0.01245	8.95%	0.01946	15.34%
Manning's equation and estimated discharge	0.00933	15.38%	0.01210	0.97%	0.01126	1.47%	0.01871	10.95%
Horton and Einstein	0.01105	0.24%	0.01306	6.86%	0.01334	16.79%	0.02407	42.69%
Pavlovski, muhlhofer, Einstein and Banks	0.01105	0.23%	0.01334	9.12%	0.01335	16.89%	0.02457	45.65%
Lotter	0.00934	15.31%	0.01026	16.06%	0.01157	1.27%	0.01873	11.04%
Krishnamurthy	0.01082	1.84%	0.01353	10.68%	0.01300	13.82%	0.02161	28.12%
Average percent Of discharge error	13.73%		10.48%		13.69%		10.43%	

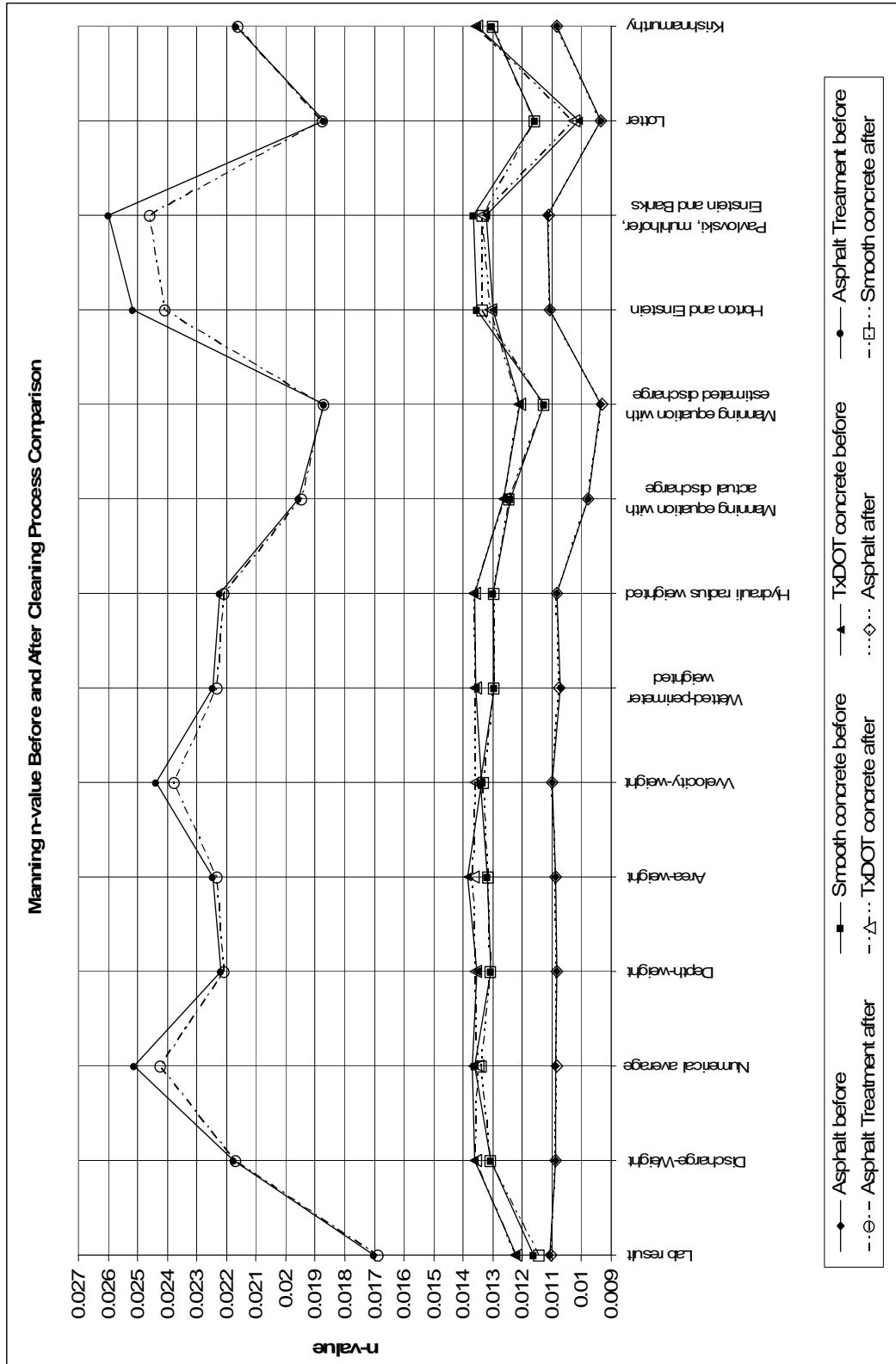


Figure 4.14 Average Manning's n-values by various averaging methods

Figure 4.15 shows the typical patterns of sub-section n-values across the entire roadway cross-section estimated by Prandtl-von Karman (1926) velocity distribution equation. The n-value at the curb section is significantly dropped because of an increasing of local wetted-perimeter in the curb sub-section. In other sections, n-values retain the same average. The n-values at the end of water are significantly increased. This phenomenon is caused by the logarithm depth term, i.e. the increasing shallow depth. As the depth is decreased then flow often changes from super-critical to sub-critical stage.

Since a depth of water decreases along the roadway lateral slope, the velocity tends to decrease noticeably as a logarithm function. Therefore the n-value increases according to decrease of velocity. Figure 4.16 shows example values of parameters across the cross-section. These values are used in methods of average n-value estimation. The parameter values across the roadway cross-section demonstrate the affect of geometry parameters to the average cross-section n-value.

Because the flow sections are divided in one-foot intervals, wetted-perimeters of sub-section are almost constant throughout the cross-section. In this case, results from the wetted-perimeter weight method and numerical average method would be close to each other. Other parameters vary from the curb to the end of water, because of hydraulic depth decrease along the transverse slope. Most parameters decrease as a function of depth.

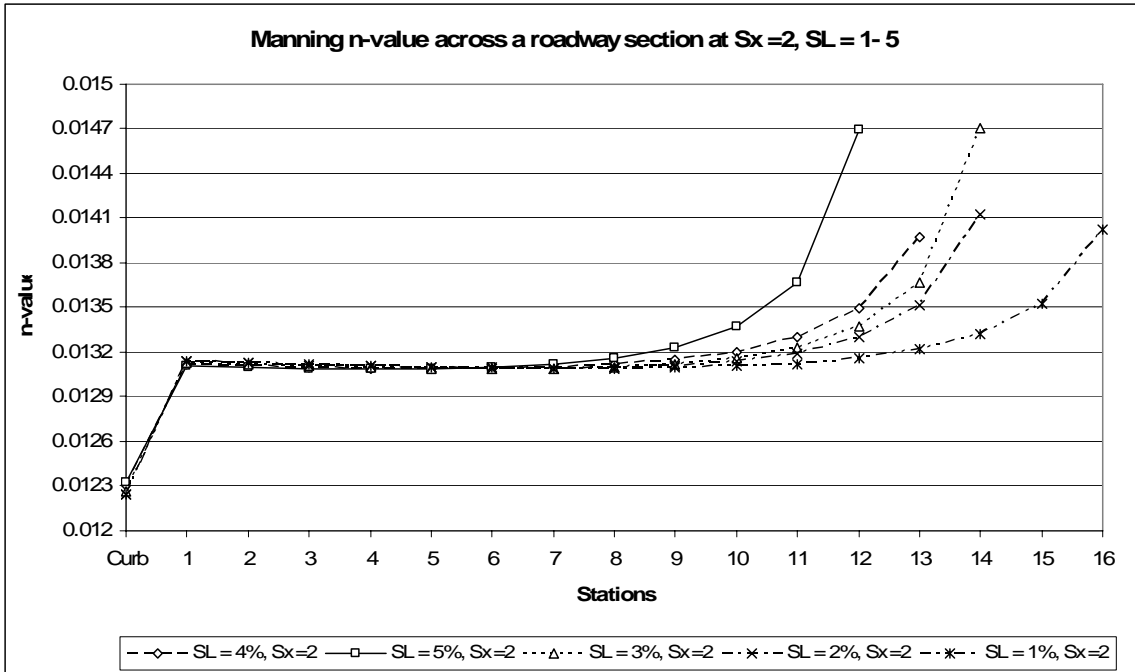


Figure 4.15 Example of sub-section n-values across the roadway cross-section by Prandtl-von Karman velocity distribution method

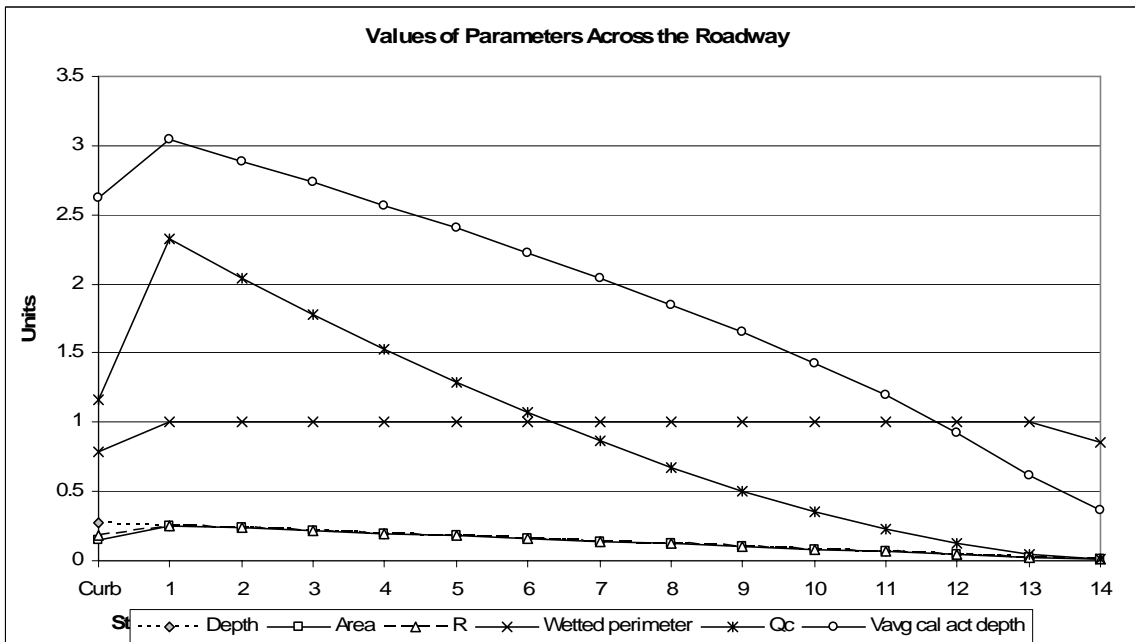


Figure 4.16 Example of averaging parameters across the entire roadway cross-section

4.5 Discharge Estimated by Velocity Distribution Methods' n-values

In the pervious section, various methods of averaging were used to estimating the average cross-section Manning's n-values. The type of estimation method considerably impacted the outcome of the average n-value. After the analysis, the overall average n-values (design n-values) by each method were determined. These overall average n-values were put back in to the Manning's equation to estimate discharges. A new discharge value is determined using the value of design n-values. The new discharges indicate the overall outcome of the estimated accuracy for that design n-value. The n-value estimated discharges of all roadway types are shown in Figure 4.17. The most accuracy can be obtained by the overall average n-value by actual discharge method. This method calculates n-values by directly inputting the actual discharge, total area, longitudinal slope and total wetted-perimeter in to Manning's equation. The result is the most accurate discharge possible. This estimation is comparable to a traditional design calculation. Where flow rate is calculated by average velocity of cross-section. Other methods are comparable with higher percent error.

According to Figure 4.17, most methods provide exceptional result of discharge. However, this research investigated performance of averaging system. Therefore the finest method for averaging shallow water flow over roadway was picked according to overall accuracy, consistency, and reliability. The averaging method by Krishnamurthy and Christensen was selected to be the finest method. Even though, this method

provides moderate average result of all roadway types. It shows the most accuracy and consistency available.

Krishnamurthy-Christensen (1926) method was derived according to logarithm of the velocity distribution method. It shows more compatibility than other methods. Methods are limited by their empirical and basic assumptions, so they might not be suitable in this type of calculation. Some other methods such as discharge, depth, area, velocity and hydraulic-depth weights are consider good alternative for average n-value estimation. These methods provide good accuracy and consistency to the discharge result. The discharge results for four types of surfaces are shown in Appendix D.

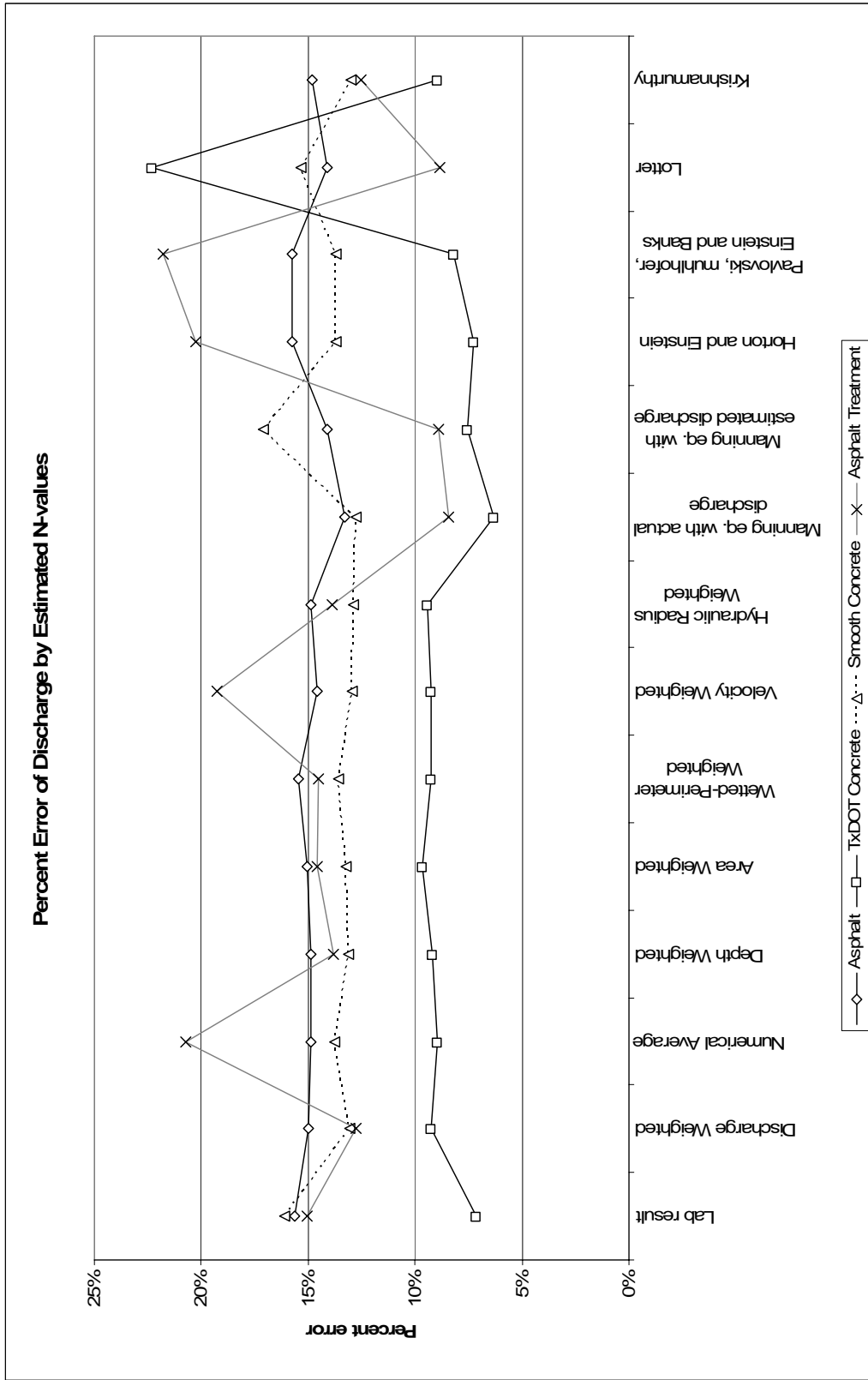


Figure 4.17 Percent discharge error by various methods of averaging n-value

There are two types of average n-values, constant and variable n-values. Figure 4.18 shows plots of n-values, the average constant n-value and the average variable n-values estimated by Prandtl-von Karman (1926) velocity method and Manning's equation with the actual discharge.

The constant n-value is estimated by numerical average of all n-values from each roadway surface. The actual numbers for constant n-value are shown in table 4.3. These constant n-values are not adapted to changing of discharge along the trend of n-value. In fact, it is constant throughout the range of flow. The logarithm trend line shows high-value at the low flow and low-value at the high flow compare to the constant n-value. Consequently, results should be an over estimated at the low flow and under estimated at high flows. This type of n-value is a practical case for most standard design purposes. This unchanged n-value provides simplicity and enough reliability to normal design method. Accuracy from constant n-value is in acceptable range of error.

Another type of n-value is variable value. The n-values in this set are variable by estimated logarithm function on average trend line as shown in Figure 4.18. The variable functions were determined by an average logarithm plot of n-values. An equation of n-values varies with discharge can be obtained from least-square fit of data distribution. This method of n-value adapted to the change of discharge from low flow to high flow rate.

The accuracy of n-values and calculated discharges are noticeable improved over the constant method as shown in Figure 4.19. The results of discharge error by constant and variable n-value methods for the TxDOT concrete surface are shown in

Figure 4.19. Most averaging methods with variable n-values show improvement over the constant n-values. The variable n-value method can easily be done by adding an estimated variable n-value equation to the Manning's equation.

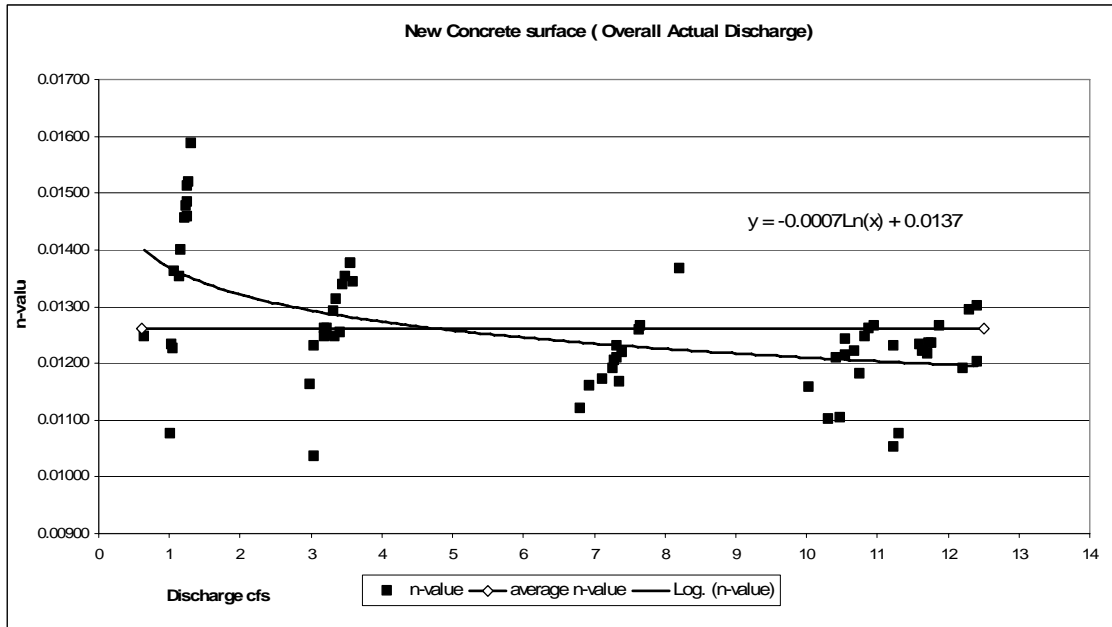


Figure 4.18 Plots of average variable and constant n-values

The variable n-value method is not a practical method for traditional design calculation. The improvement of discharge accuracy is so small and may not worth the complexity in the traditional design calculation.

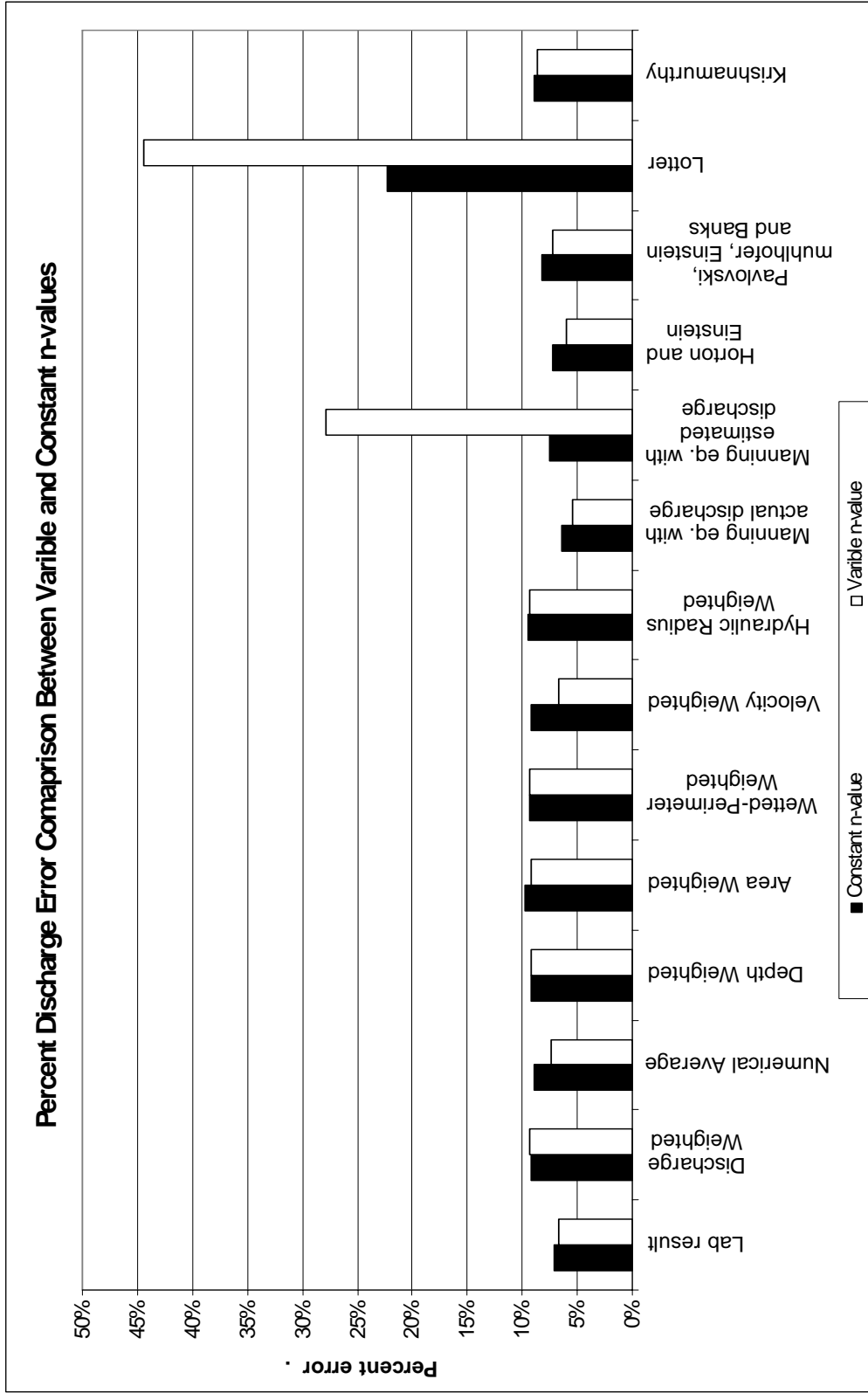


Figure 4.19 Comparison of percent error between variable and constant n-value by various averaging methods

4.6 Affect of Roadway Slopes

Longitudinal slope and surface roughness of a roadway are main parameters for flow equation. Both longitudinal and transverse slopes affect the results of discharge calculations. The roadway slopes are indirect area-affects that results in different depth of water. In this research, an average velocity is estimated by the velocity distribution method. This method tends to generate more errors for low velocity calculation. Transverse slope tends to change the depth of water more rapidly than longitudinal slope. This is due to the fact that a percent adjust of transverse slope likely changed the water depth more than the same percent adjust of longitudinal slope. With increases or decreases of the water depth, velocity profiles change as the slope increases or decreases.

Figure 4.20 and 4.21 show effect of changing transverse and longitudinal slopes to the flow cross-section. The hydraulic depth and flow velocity change as a result of changing cross-section area and longitudinal slope. Flow velocity is increased by increase the longitudinal or transverse slope. Water depth is increased by increase the transverse slope or decrease the longitudinal slope.

Calculated discharge plots for the design n-value for TxDOT roadway surface are shown in Figure 4.22-4.23 and Appendix A. The percent discharge errors are arranged in different transverse or longitudinal slopes. A change in transverse slope tends to have more variation in discharge estimations than a change of longitudinal slope. Low transverse slope tends to have more error fluctuation than high transverse slope.

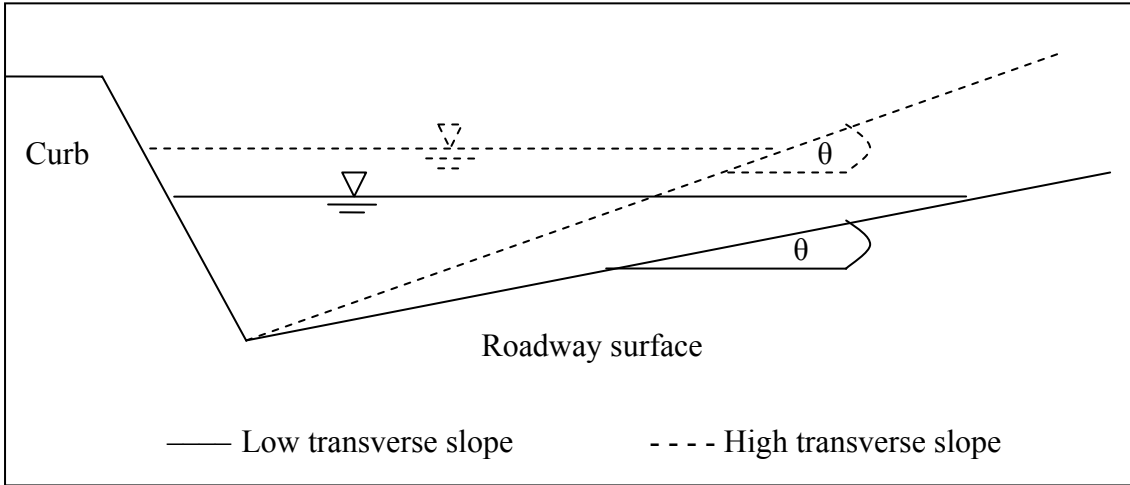


Figure 4.20 Comparison of roadway cross-section areas by different transverse slopes

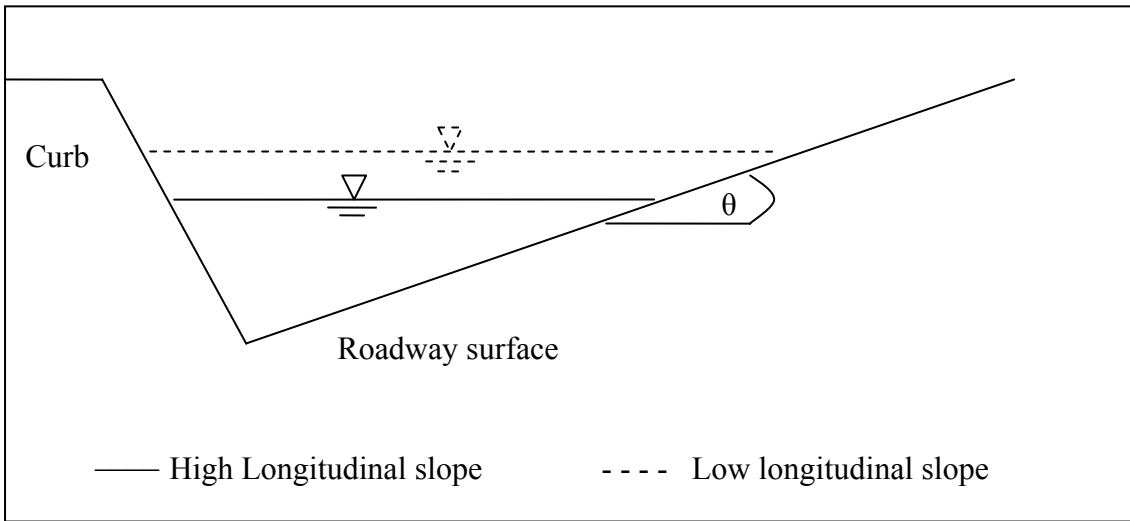


Figure 4.21 Comparison of roadway cross-section areas with different longitudinal slopes

CHAPTER 5

CONCLUSIONS AND RECOMMENDATIONS

5.1 Conclusion

The Prandtl-von Karman velocity distribution method provides acceptable results for estimating flows and n-values of roadway cross-section. Although, the roadway channel is a non-symmetry triangular channel, irregularly shaped channel, compared to typical man-made or natural channels, results still retain high accuracy of discharges compared to measured data. Accuracy and consistency of discharge and n-value calculations for all types of roadway surface are similar. These results imply the method is practicable. Thus, the velocity distribution method is appropriate to calculate flow discharge of these roadway cross-sections.

The discharge calculated from the velocity distribution method is verified with the measured discharge. The result shows consistency with minimal error percentage. The result also shows accuracy and consistency. Consequently a direct conversion of roughness dimension, k , to Manning “ n ” by theoretical equation transformation can be done with a theoretical transformation using equation 3.12 and 3.13.

This paper also analyzes various average methods of n-values to obtain a single cross-section n-value. The methods of estimating average n-values significantly impact the outcome. The percent error increases significantly by altering the averaging method.

Some methods provide outstanding accuracy on one surface but lack of consistency on the others. As a result, Krishnamurthy and Christensen's method, equation 2.42, was selected based on the most accuracy and consistency of discharge result. Krishnamurthy and Christensen's method n-values show minimum affect due to various flows and transverse and longitudinal slopes as shown in Figure C1.1-1.4 in Appendix C.

Laboratory n-values are shown to vary with increased discharge, and also vary at the same discharge value. Consequently, Krishnamurthy and Christensen's averaging method lacked to indicate discharge and slopes affects. The discharges calculated from constant n-value of all roadway surfaces, Figure 4.22, 4.23 and Appendix A, show the result of increasing percent error along the increasing transverse slope percent and decreasing of discharges.

Since the laboratory n-values show variation due to the discharge and slope. Two methods of n-value, constant and variable, are used in calculating discharge. The results of these two methods are shown in Figure 4.19. The comparison shows improvement of discharge accuracy from variable n-values. The improvement of discharge accuracy from variable n-values is small. It still implies practical uses of variable n-values for the design purposes. The achievement of variable n-value method over the contemporary method, constant n-value, is useful for roadway design. However, benefits of variable n-value might not be sufficient to override the use of constant n-value. Consequently, justification of use varies by the necessity discharge accuracy. It is conclusive that discharge and both slopes have effects on Manning's n-

value method and they appears to be the most significant factors for roadway hydraulic design calculation.

5.2 Recommendation for Future Research

The velocity distribution model could be applied to other types of channel or surfaces for further verification. This will extend the velocity distribution method to other types of channel.

Because of water waves, the total spread of the roadway section is estimated from an average of the maximum and minimum spread. This phenomenal creates the overestimated of the total spread. Elimination of water waves is recommended to improve the accuracy.

In this research, the longitudinal slope is based on theoretical survey estimation. The actual longitudinal slope variation can be used to improve calculation accuracy.

In the velocity equations, the estimated parameters, α and β , have the main affect to the outcome. These parameters can be optimized for the unique characteristic of the roadway surfaces, thus establishing a roughness value (k) for roadways. The optimization of α and β values should improve the accuracy and consistency of estimated discharges and n -values.

The rainfall effects should be evaluated with the velocity distribution method. This could provide incite on n -value impact. The amount of affect then should be compared to normal n -value and velocity distribution calculation.

APPENDIX A
ESTIMATED DISCHARGE PLOTS

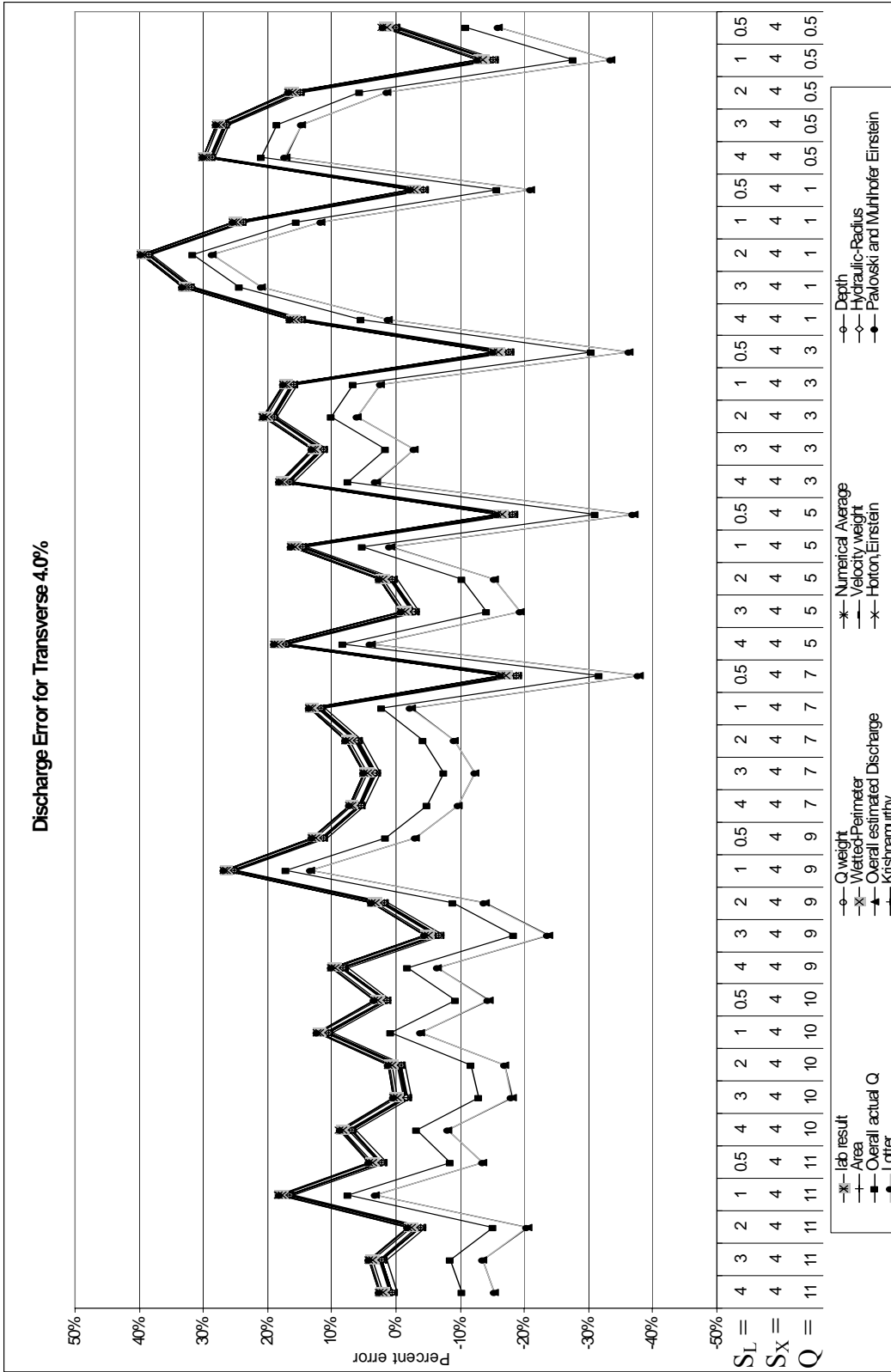


Figure A1.1 Velocity methods discharge estimations (asphalt surface)

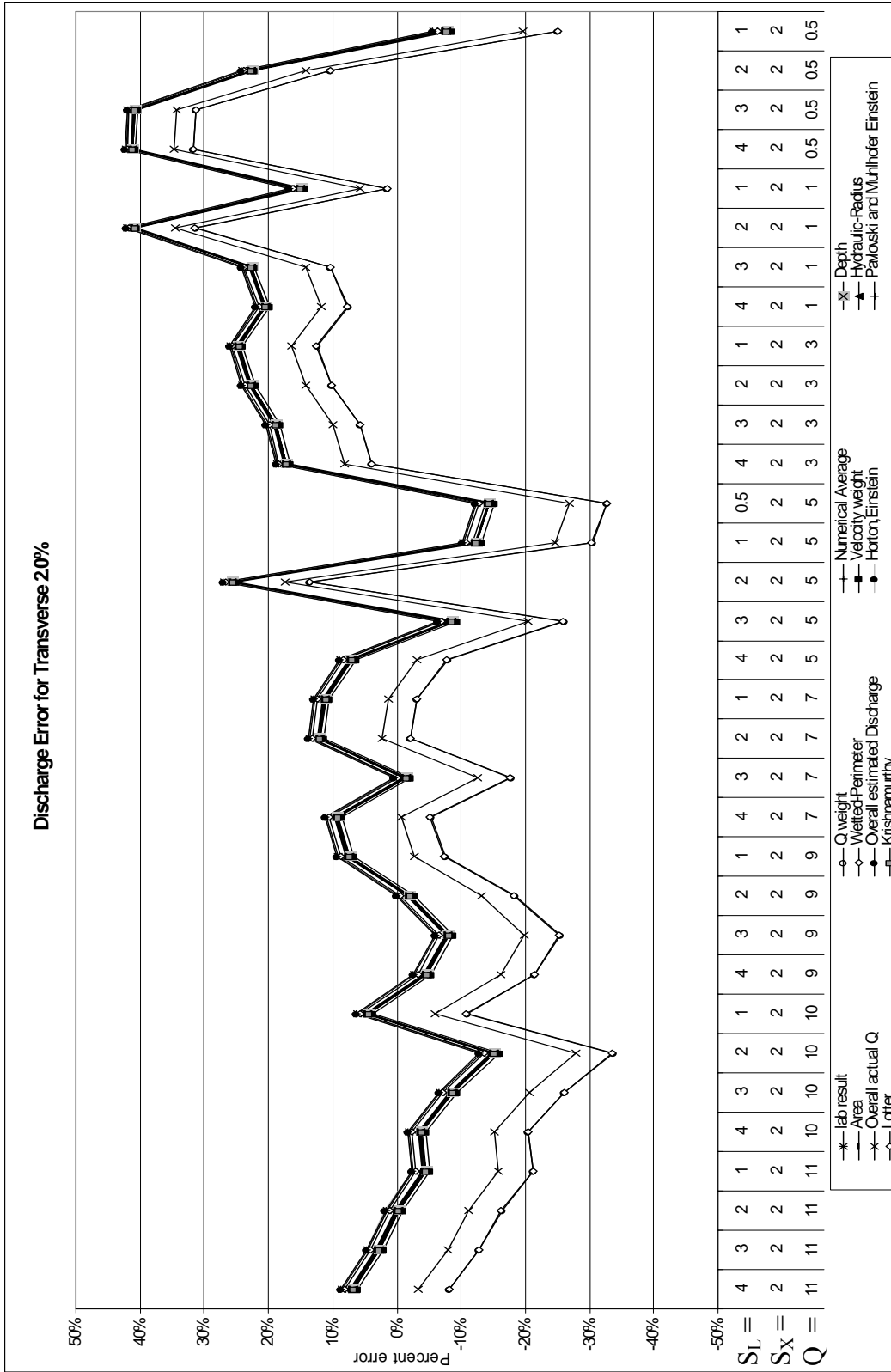


Figure A1.4 Velocity methods discharge estimations (asphalt surface)

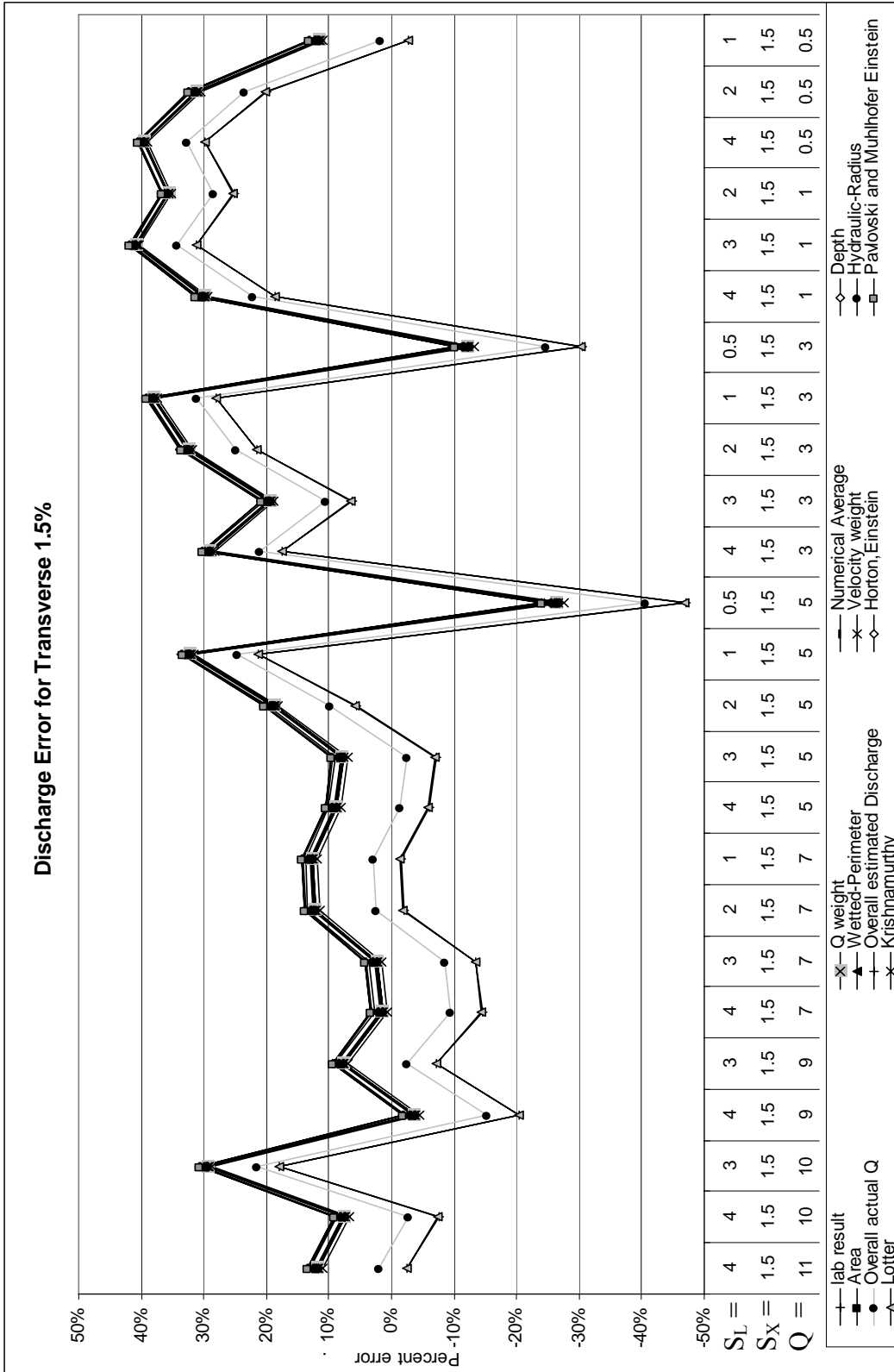


Figure A1.5 Velocity methods discharge estimations (asphalt surface)

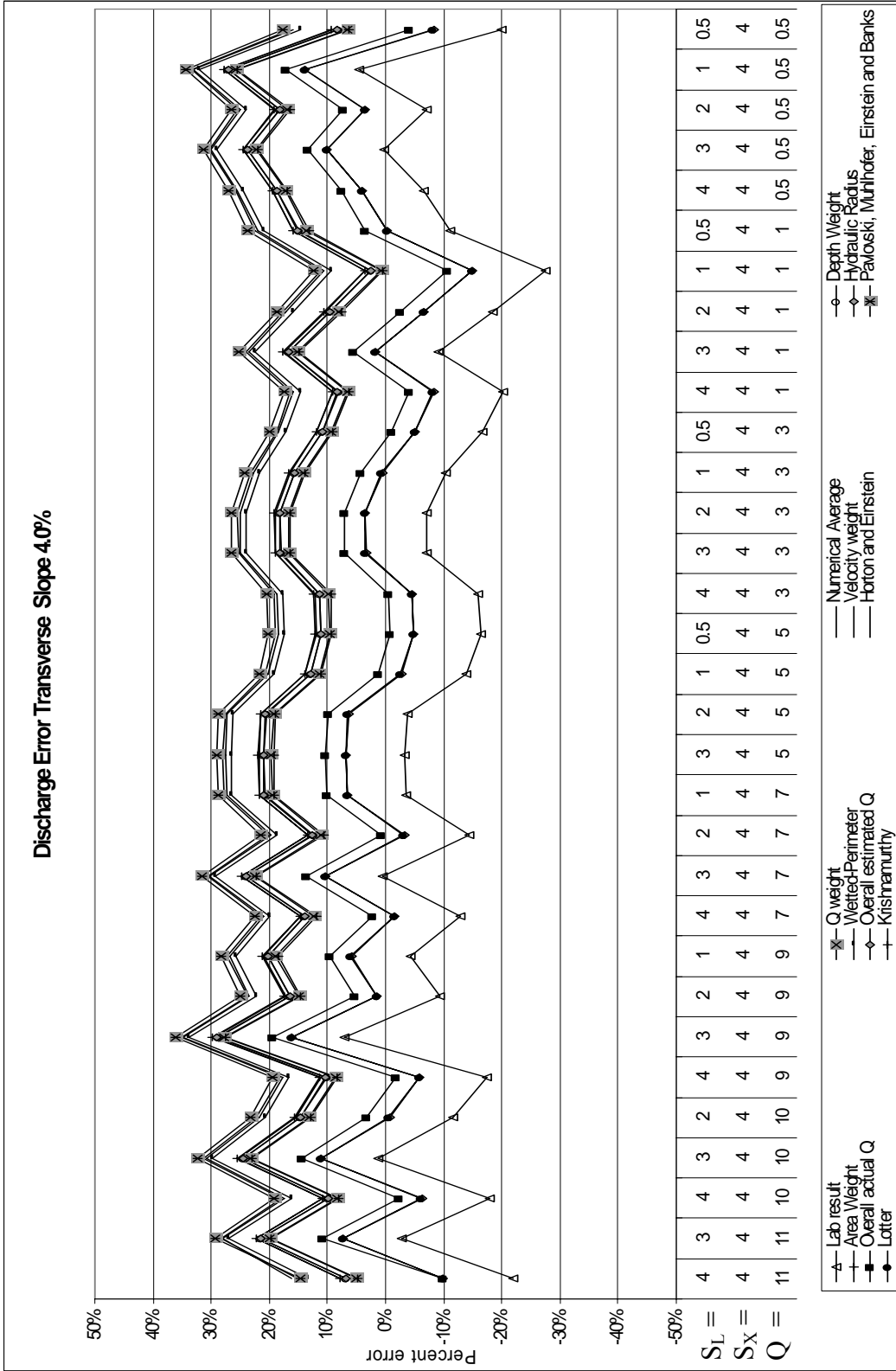


Figure A2.1 Velocity methods discharge estimations (asphalt treatment surface)

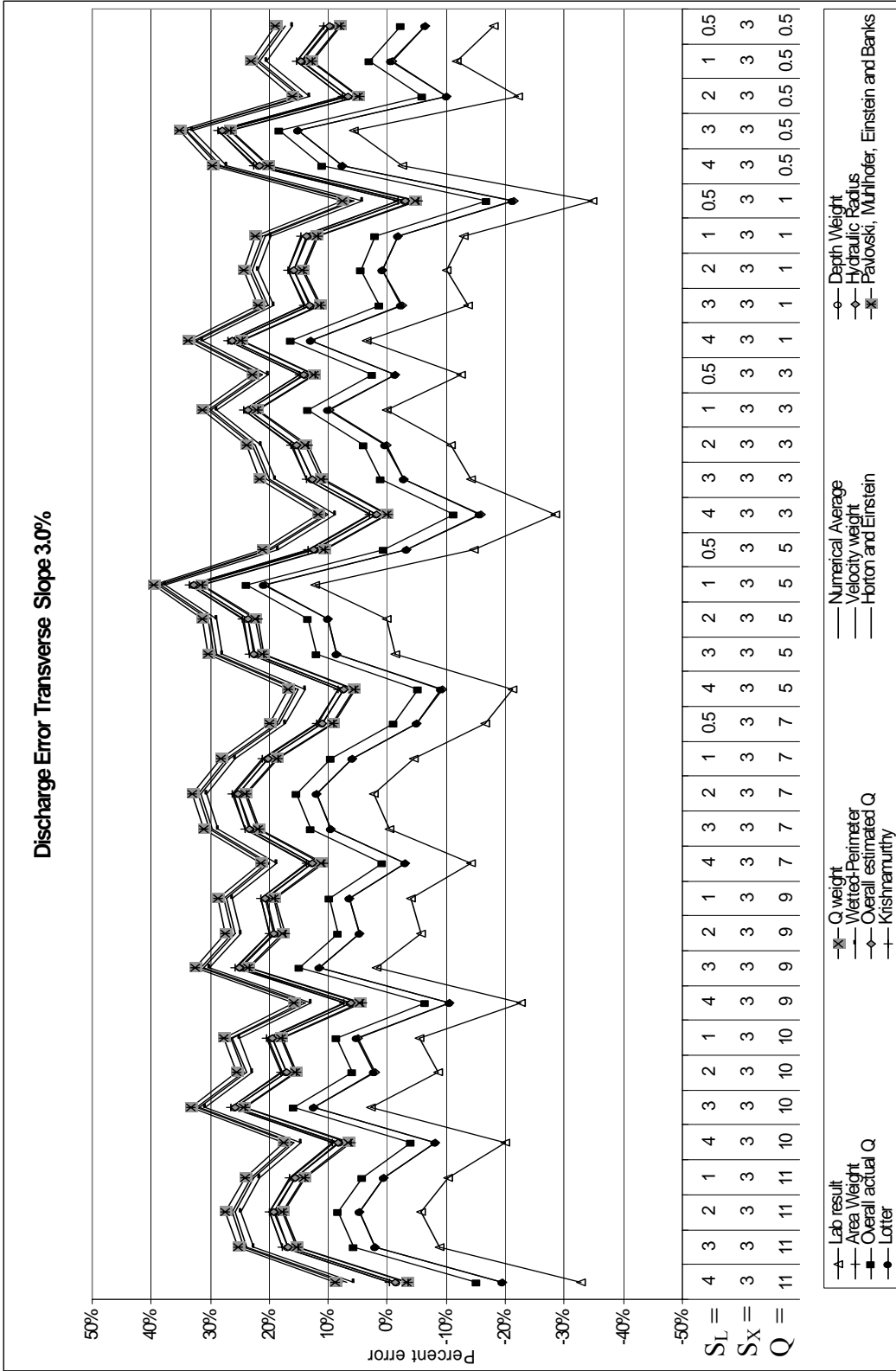


Figure A2.2 Velocity methods discharge estimations (asphalt treatment surface)

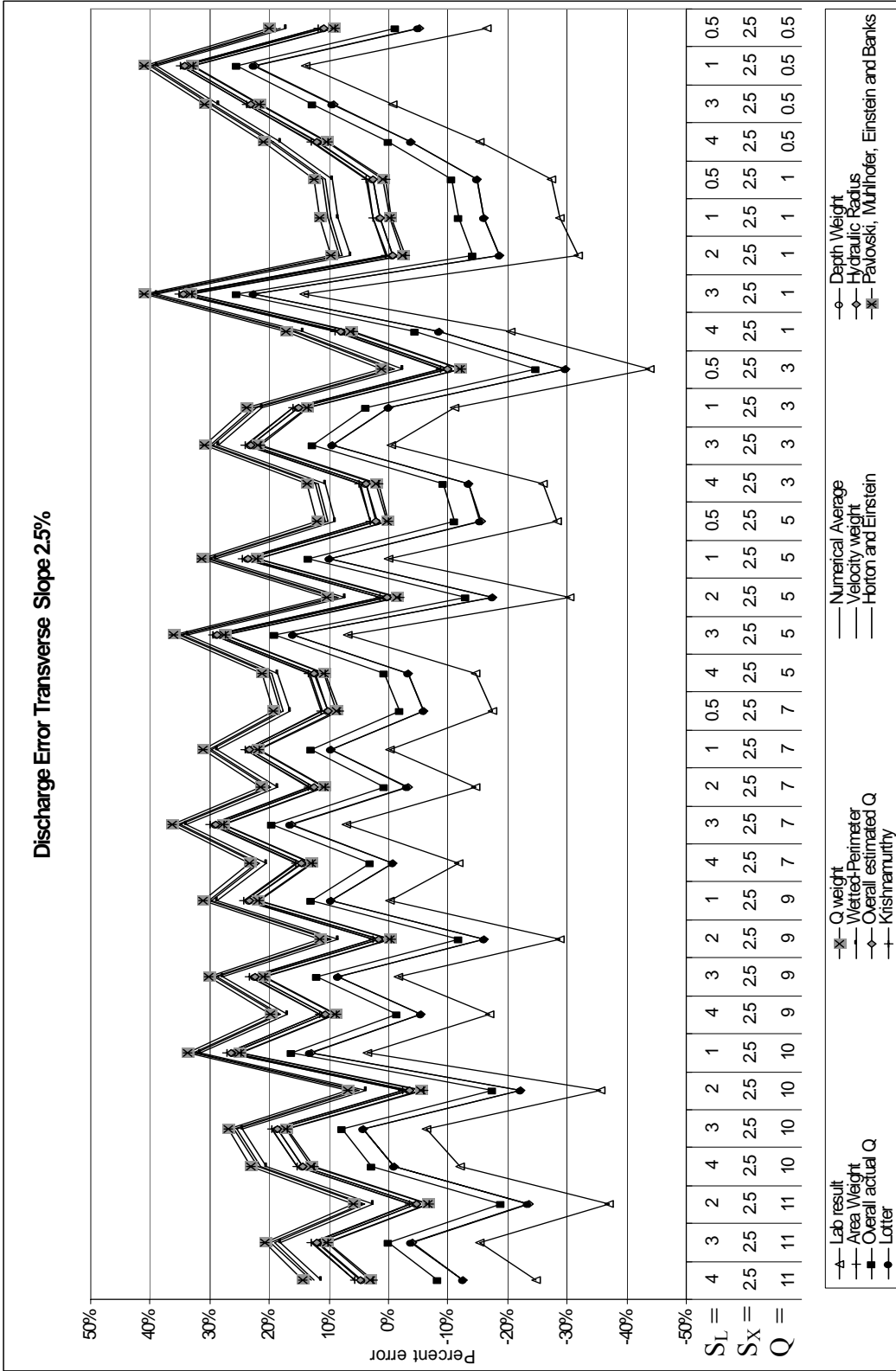


Figure A2.3 Velocity methods discharge estimations (asphalt treatment surface)

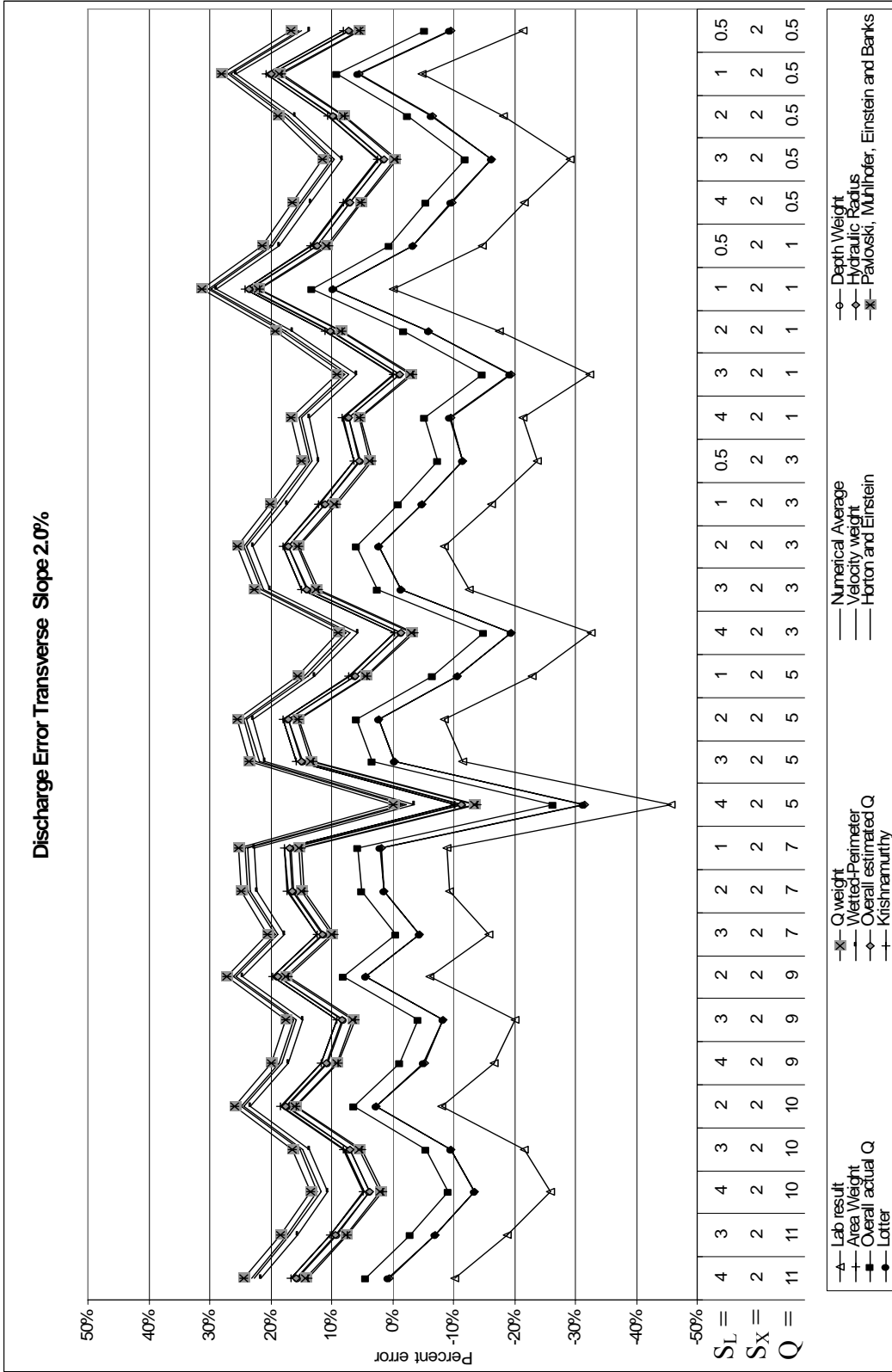


Figure A2.4 Velocity methods discharge estimations (asphalt treatment surface)

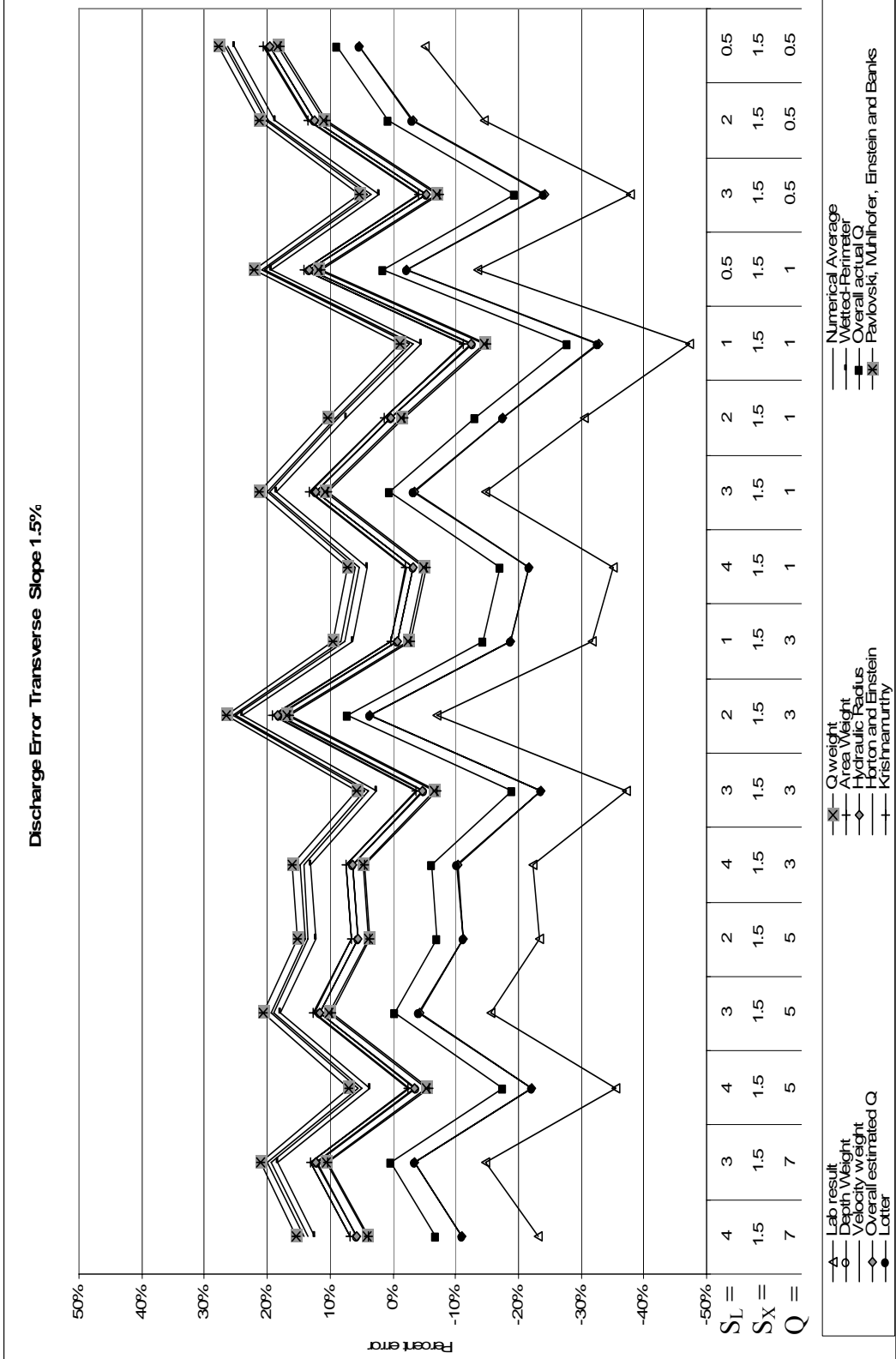


Figure A2.5 Velocity methods discharge estimations (asphalt treatment surface)

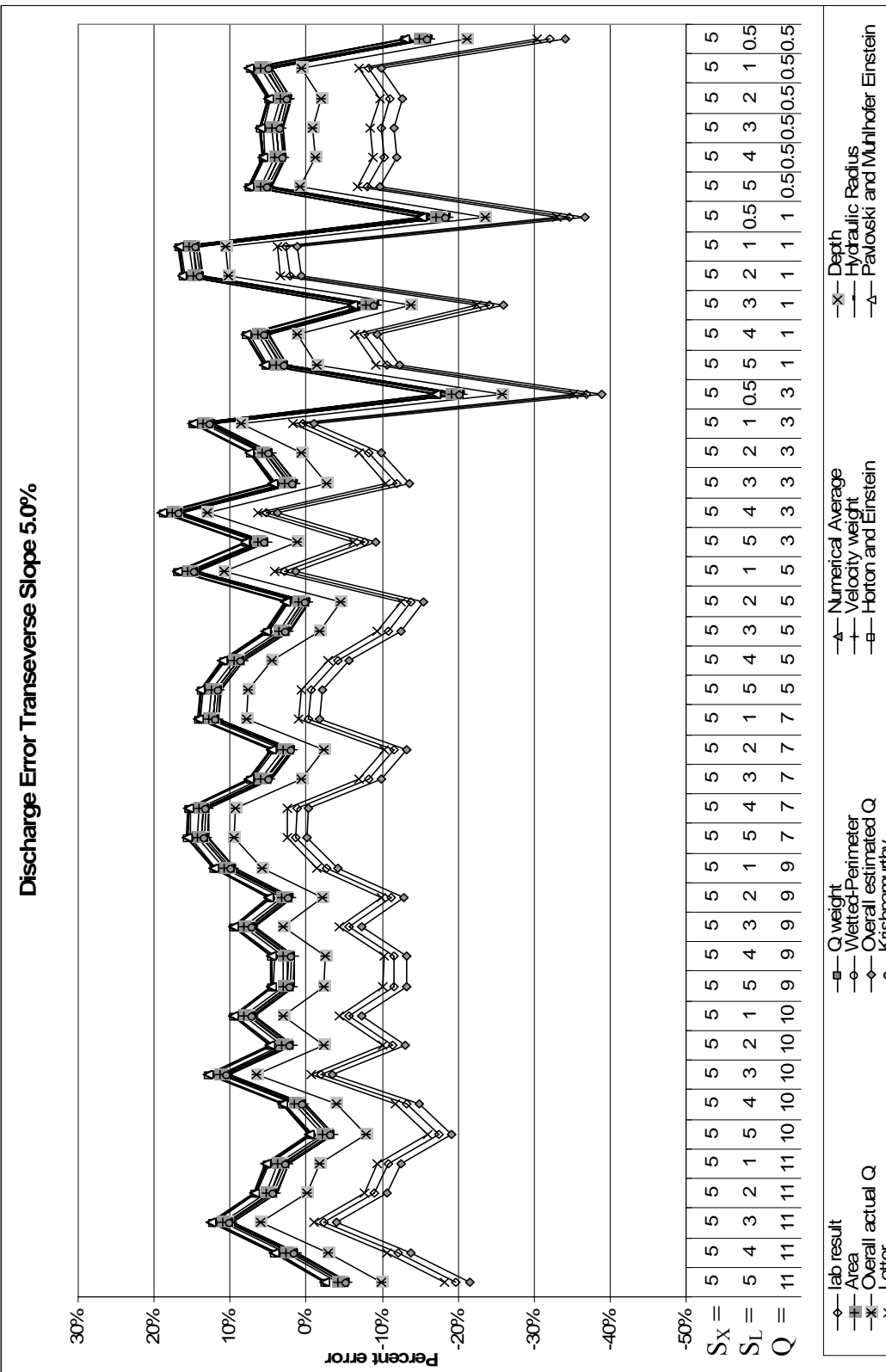


Figure A3.1 Velocity methods discharge estimations (smooth concrete surface)

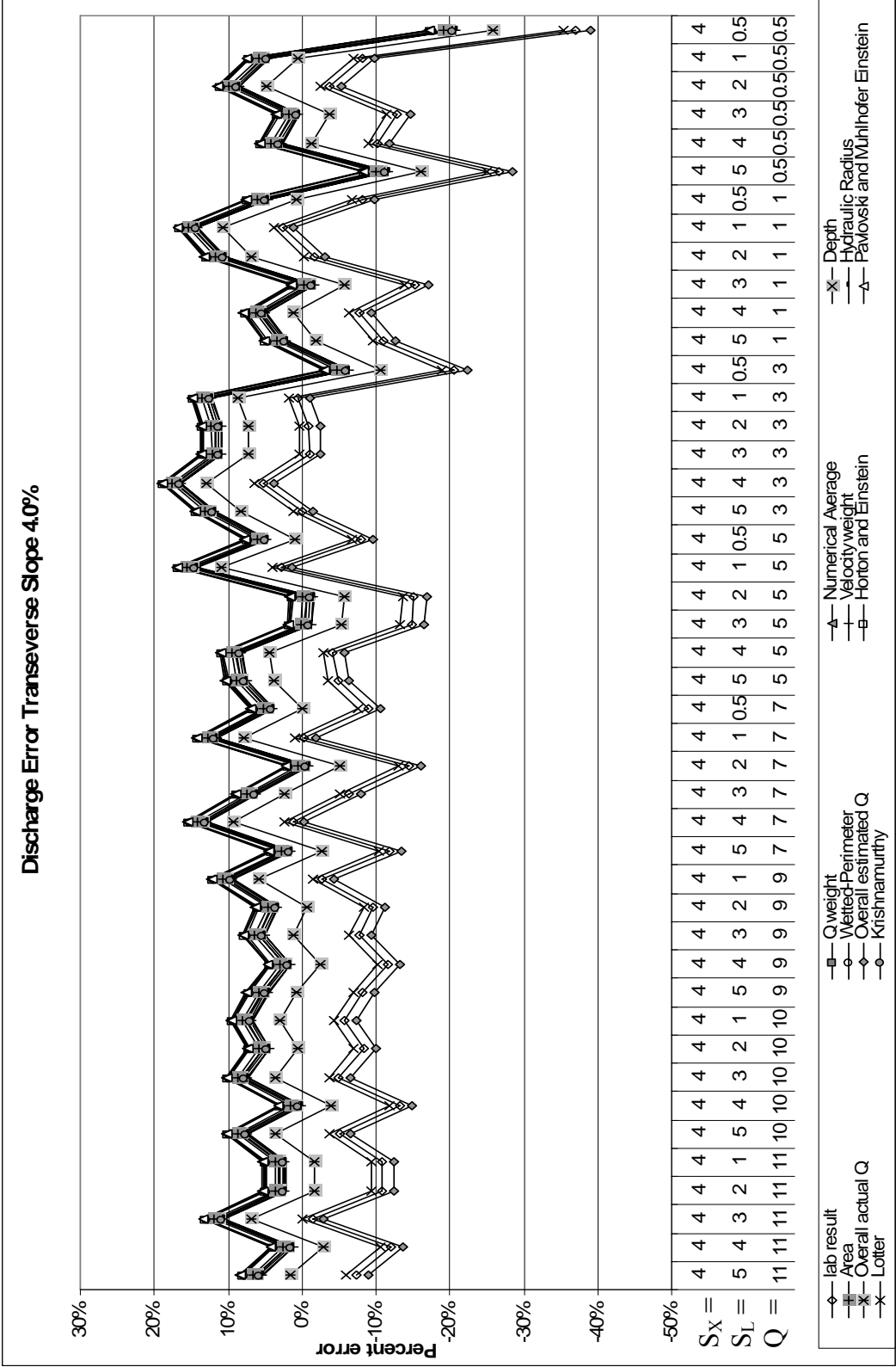


Figure A3.2 Velocity methods discharge estimations (smooth concrete surface)

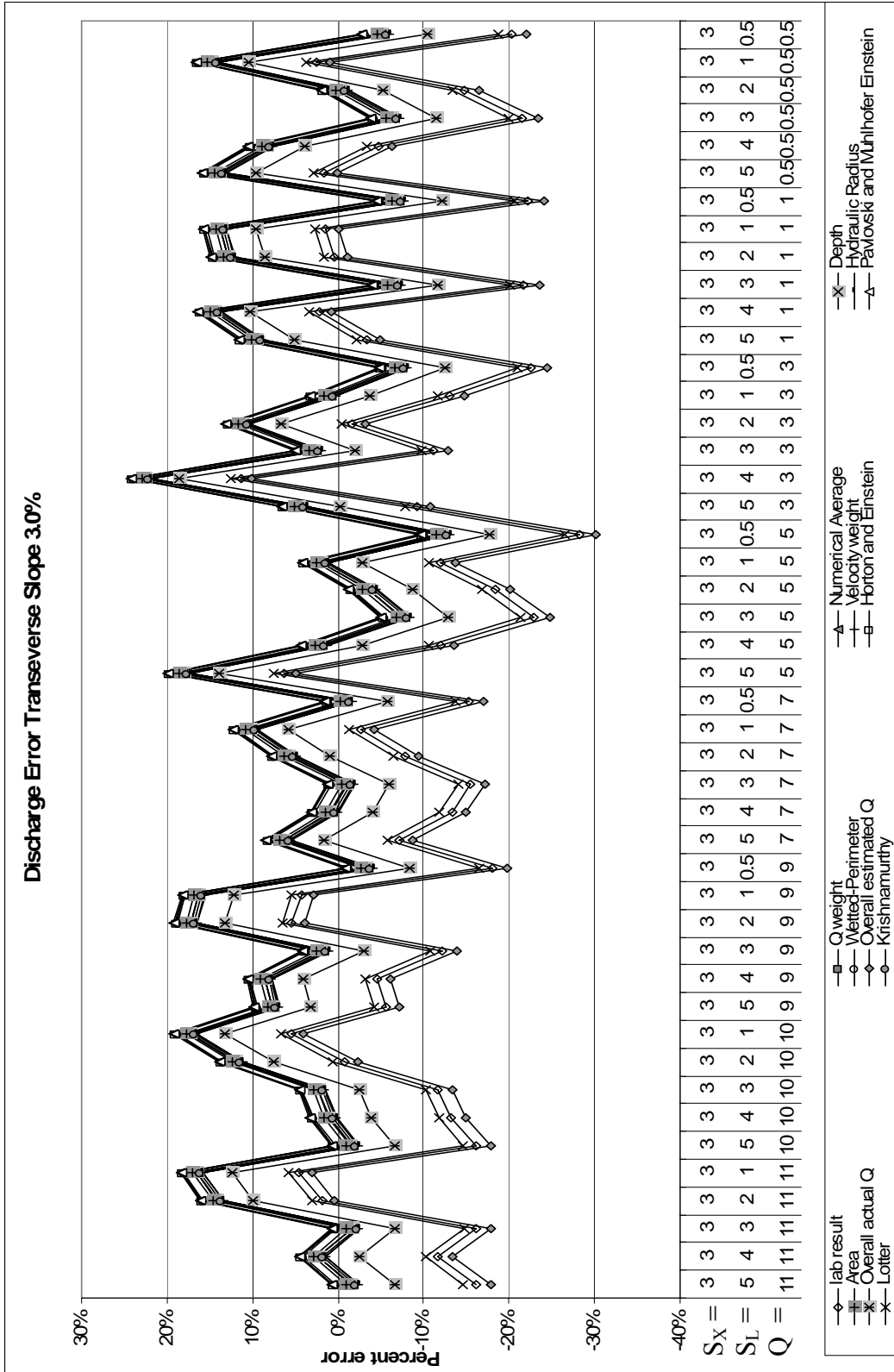


Figure A3.3 Velocity methods discharge estimations (smooth concrete surface)

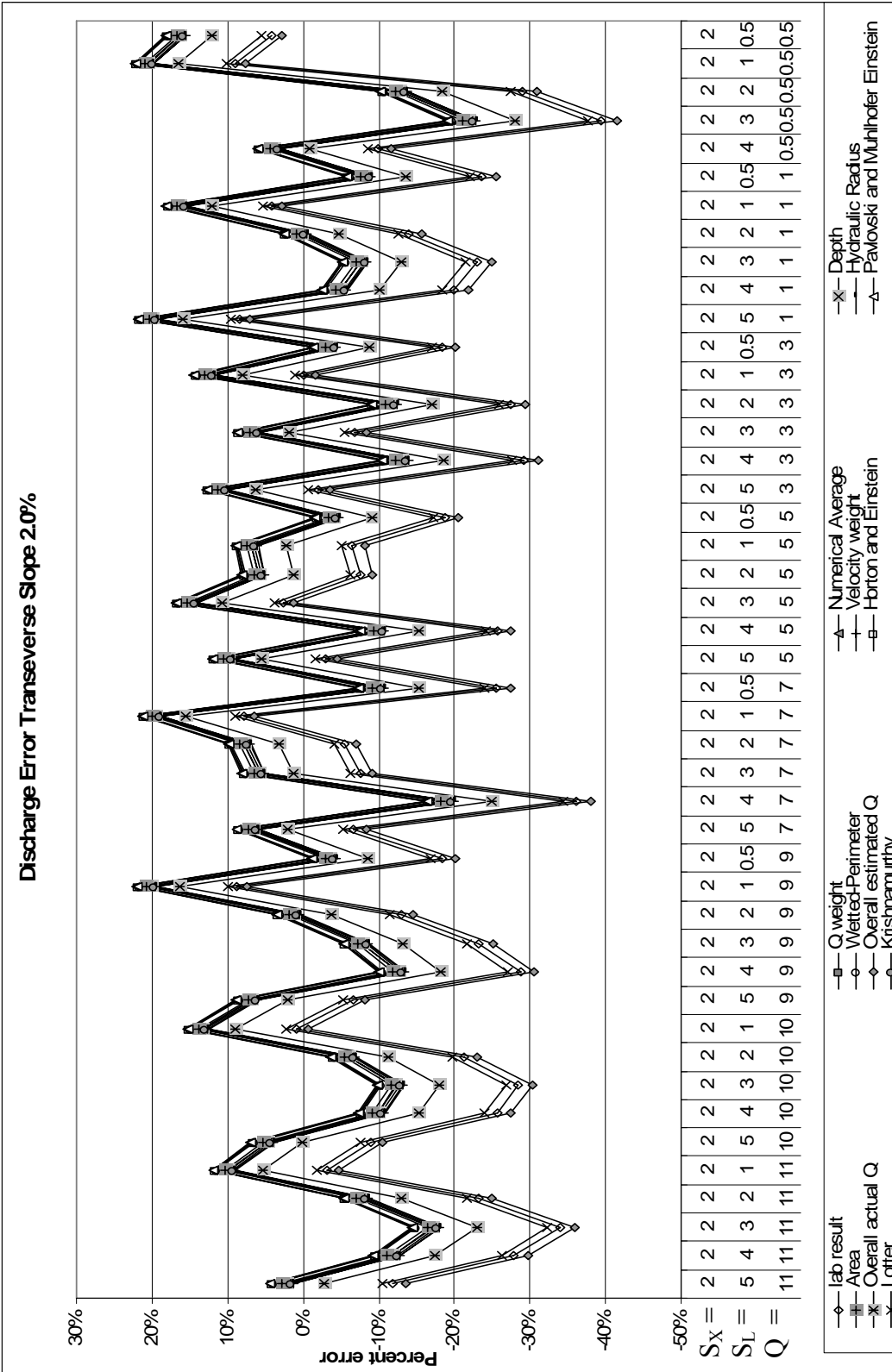


Figure A3.5 Velocity methods discharge estimations (smooth concrete surface)

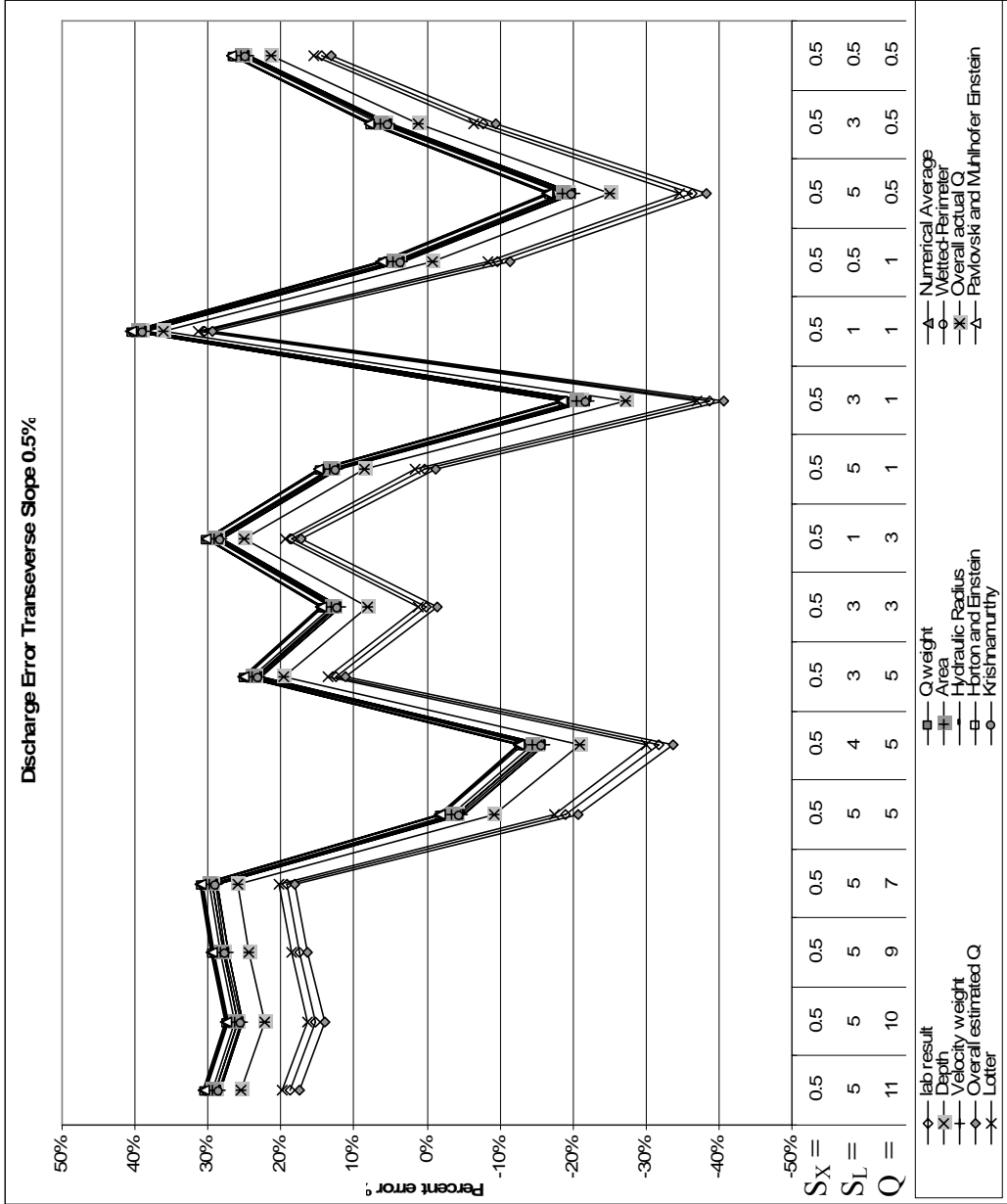


Figure A3.8 Velocity methods discharge estimations (smooth concrete surface)

APPENDIX B
ROADWAY DATA TABLES

Table B1.4 Smooth concrete surface data

Discharge/actual O/CFS	O/CFS	High Flow		Low Flow		Average		Depth (ft)	Spread Dist (ft)		Curb Distance (ft)		Spread Dist (ft)		AVG		n value		
		Initial	Final	Initial	Final	1st run	2nd run		1st run	2nd run	1st run	2nd run	1st run	2nd run	1st run	2nd run		1st run	2nd run
0.5	0.5%	14.94	14.94	14.94	14.94	14.94	14.94	0.65	0.65	29.85	29.85	29.85	29.85	29.85	29.85	174.156	174.156	174.156	0.00964
1	3.0%	14.94	14.94	14.94	14.94	14.94	14.94	0.65	0.65	29.85	29.85	29.85	29.85	29.85	29.85	174.156	174.156	174.156	0.00964
3	3.0%	14.94	14.94	14.94	14.94	14.94	14.94	0.65	0.65	29.85	29.85	29.85	29.85	29.85	29.85	174.156	174.156	174.156	0.00964
5	3.0%	14.94	14.94	14.94	14.94	14.94	14.94	0.65	0.65	29.85	29.85	29.85	29.85	29.85	29.85	174.156	174.156	174.156	0.00964
7	3.0%	14.94	14.94	14.94	14.94	14.94	14.94	0.65	0.65	29.85	29.85	29.85	29.85	29.85	29.85	174.156	174.156	174.156	0.00964
9	3.0%	14.94	14.94	14.94	14.94	14.94	14.94	0.65	0.65	29.85	29.85	29.85	29.85	29.85	29.85	174.156	174.156	174.156	0.00964
11	3.0%	14.94	14.94	14.94	14.94	14.94	14.94	0.65	0.65	29.85	29.85	29.85	29.85	29.85	29.85	174.156	174.156	174.156	0.00964
0.5	0.5%	14.94	14.94	14.94	14.94	14.94	14.94	0.65	0.65	29.85	29.85	29.85	29.85	29.85	29.85	174.156	174.156	174.156	0.00964
1	3.0%	14.94	14.94	14.94	14.94	14.94	14.94	0.65	0.65	29.85	29.85	29.85	29.85	29.85	29.85	174.156	174.156	174.156	0.00964
3	3.0%	14.94	14.94	14.94	14.94	14.94	14.94	0.65	0.65	29.85	29.85	29.85	29.85	29.85	29.85	174.156	174.156	174.156	0.00964
5	3.0%	14.94	14.94	14.94	14.94	14.94	14.94	0.65	0.65	29.85	29.85	29.85	29.85	29.85	29.85	174.156	174.156	174.156	0.00964
7	3.0%	14.94	14.94	14.94	14.94	14.94	14.94	0.65	0.65	29.85	29.85	29.85	29.85	29.85	29.85	174.156	174.156	174.156	0.00964
9	3.0%	14.94	14.94	14.94	14.94	14.94	14.94	0.65	0.65	29.85	29.85	29.85	29.85	29.85	29.85	174.156	174.156	174.156	0.00964
11	3.0%	14.94	14.94	14.94	14.94	14.94	14.94	0.65	0.65	29.85	29.85	29.85	29.85	29.85	29.85	174.156	174.156	174.156	0.00964
0.5	0.5%	14.94	14.94	14.94	14.94	14.94	14.94	0.65	0.65	29.85	29.85	29.85	29.85	29.85	29.85	174.156	174.156	174.156	0.00964
1	3.0%	14.94	14.94	14.94	14.94	14.94	14.94	0.65	0.65	29.85	29.85	29.85	29.85	29.85	29.85	174.156	174.156	174.156	0.00964
3	3.0%	14.94	14.94	14.94	14.94	14.94	14.94	0.65	0.65	29.85	29.85	29.85	29.85	29.85	29.85	174.156	174.156	174.156	0.00964
5	3.0%	14.94	14.94	14.94	14.94	14.94	14.94	0.65	0.65	29.85	29.85	29.85	29.85	29.85	29.85	174.156	174.156	174.156	0.00964
7	3.0%	14.94	14.94	14.94	14.94	14.94	14.94	0.65	0.65	29.85	29.85	29.85	29.85	29.85	29.85	174.156	174.156	174.156	0.00964
9	3.0%	14.94	14.94	14.94	14.94	14.94	14.94	0.65	0.65	29.85	29.85	29.85	29.85	29.85	29.85	174.156	174.156	174.156	0.00964
11	3.0%	14.94	14.94	14.94	14.94	14.94	14.94	0.65	0.65	29.85	29.85	29.85	29.85	29.85	29.85	174.156	174.156	174.156	0.00964

Table B1.6 Smooth concrete surface data

Discharge/actual Q (%)	SK (%)	High Flow (CFS)		Low Flow (CFS)		Average		Depth (ft)		Spread Dist (ft)		Curb Distance (ft)		Spread Dist (ft)		AVG		n value			
		Initial	Final	Initial	Final	1st run	2nd run	1st run	2nd run	1st run	2nd run	1st run	2nd run	1st run	2nd run	1st run	2nd run		1st run	2nd run	
0.5	5.0%	0.61	0.61	14.105	14.175	14.105	14.175	0.061	0.061	0.051	0.071	29.75	29.75	29.75	29.75	176.188	176.188	176.188	176.188	0.01668	0.02267
1	5.0%	0.61	0.61	14.122	14.164	14.122	14.164	0.061	0.061	0.051	0.071	29.75	29.75	29.75	29.75	176.188	176.188	176.188	176.188	0.01668	0.02267
3	5.0%	0.61	0.61	14.122	14.164	14.122	14.164	0.061	0.061	0.051	0.071	29.75	29.75	29.75	29.75	176.188	176.188	176.188	176.188	0.01668	0.02267
5	5.0%	0.61	0.61	14.122	14.164	14.122	14.164	0.061	0.061	0.051	0.071	29.75	29.75	29.75	29.75	176.188	176.188	176.188	176.188	0.01668	0.02267
7	5.0%	0.61	0.61	14.122	14.164	14.122	14.164	0.061	0.061	0.051	0.071	29.75	29.75	29.75	29.75	176.188	176.188	176.188	176.188	0.01668	0.02267
9	5.0%	0.61	0.61	14.122	14.164	14.122	14.164	0.061	0.061	0.051	0.071	29.75	29.75	29.75	29.75	176.188	176.188	176.188	176.188	0.01668	0.02267
11	5.0%	0.61	0.61	14.122	14.164	14.122	14.164	0.061	0.061	0.051	0.071	29.75	29.75	29.75	29.75	176.188	176.188	176.188	176.188	0.01668	0.02267
0.5	5.0%	0.61	0.61	14.122	14.164	14.122	14.164	0.061	0.061	0.051	0.071	29.75	29.75	29.75	29.75	176.188	176.188	176.188	176.188	0.01668	0.02267
1	5.0%	0.61	0.61	14.122	14.164	14.122	14.164	0.061	0.061	0.051	0.071	29.75	29.75	29.75	29.75	176.188	176.188	176.188	176.188	0.01668	0.02267
3	5.0%	0.61	0.61	14.122	14.164	14.122	14.164	0.061	0.061	0.051	0.071	29.75	29.75	29.75	29.75	176.188	176.188	176.188	176.188	0.01668	0.02267
5	5.0%	0.61	0.61	14.122	14.164	14.122	14.164	0.061	0.061	0.051	0.071	29.75	29.75	29.75	29.75	176.188	176.188	176.188	176.188	0.01668	0.02267
7	5.0%	0.61	0.61	14.122	14.164	14.122	14.164	0.061	0.061	0.051	0.071	29.75	29.75	29.75	29.75	176.188	176.188	176.188	176.188	0.01668	0.02267
9	5.0%	0.61	0.61	14.122	14.164	14.122	14.164	0.061	0.061	0.051	0.071	29.75	29.75	29.75	29.75	176.188	176.188	176.188	176.188	0.01668	0.02267
11	5.0%	0.61	0.61	14.122	14.164	14.122	14.164	0.061	0.061	0.051	0.071	29.75	29.75	29.75	29.75	176.188	176.188	176.188	176.188	0.01668	0.02267

Table B2.1 Asphalt surface data

Diehard/SL actual Q	SV (%)	OVAL (CFS)		Offloor (CFS)		Ortal AVG CFS	Depth (ft)		Spread Dist T1 (in)		Curb Distance (in)		Spread Dist T2 (in)		AVG Spread In	n value		
		Initial	Final	Initial	Final		1st run	2nd run	1st run	2nd run	1st run	2nd run	1st run	2nd run			1st run	2nd run
0.5	0.5%	0.485	0.485	0.485	0.485	0	0	0.49488	0.0785	0.0785	28.9875	28.9875	28.9875	28.9875	154.125	155.188	0.00606	
1	0.5%	1.0055	1.0055	1.006	1.006	0	0	1.00975	0.0945	0.0945	28.7188	28.7188	28.7188	28.7188	237.313	237.313	0.00972	
3	0.5%	0.5	0.5	0.5	0.5	0	0											
5	0.5%	0.5	0.5	0.5	0.5	0	0											
7	0.5%	0.5	0.5	0.5	0.5	0	0											
9	0.5%	0.5	0.5	0.5	0.5	0	0											
10	0.5%	0.5	0.5	0.5	0.5	0	0											
11	0.5%	0.5	0.5	0.5	0.5	0	0											
0.5	0.5%	1.0%	0.485	0.486	0.486	0	0	0.4855	0.1075	0.1075	28.8438	28.8438	28.8438	28.8438	151.489	151.781	0.01548	
1	0.5%	1.0%	1.025	1.03	1.04	1.05	0	0	1.0325	0.14	0.1425	28.6563	28.6563	28.6563	28.6563	173.313	175.083	0.01358
3	0.5%	1.0%	3.028	3.023	3.022	3.022	0	0	3.02225	0.2075	0.2125	28.3125	28.3125	28.3125	28.3125	237.313	237.313	0.01421
5	0.5%	1.0%					0	0										
7	0.5%	1.0%					0	0										
9	0.5%	1.0%					0	0										
10	0.5%	1.0%					0	0										
11	0.5%	1.0%					0	0										
0.5	0.5%	1.5%	0.49	0.489	0.489	0	0	0.4885	0.145	0.145	29.4063	29.4063	29.4063	29.4063	143.438	143.438	0.02864	
1	0.5%	1.5%	0.976	0.976	0.971	0.971	0	0.97325	0.16	0.1675	28.6563	28.6563	28.6563	28.6563	157.813	158.888	0.02863	
3	0.5%	1.5%	2.887	2.887	2.889	2.889	0	2.888	0.225	0.235	28.7813	28.7813	28.7813	28.7813	198.206	198.206	0.01624	
5	0.5%	1.5%	5.03	5.03	5.03	5.03	0	5.03	0.29	0.31	28.7813	28.7813	28.7813	28.7813	237.313	237.313	0.0143	
7	0.5%	1.5%					0	0										
9	0.5%	1.5%					0	0										
10	0.5%	1.5%					0	0										
11	0.5%	1.5%					0	0										
0.5	0.5%	2.0%	0.513	0.51	0.5	0.489	0	0.5055	0.135	0.145	40.3125	40.3125	40.3125	40.3125	125.594	125.594	0.01781	
1	0.5%	2.0%	1.006	1.009	1.01	1.01	0	1.00625	0.18	0.195	40.25	40.25	40.25	40.25	135.188	136.719	0.0262	
3	0.5%	2.0%	3.001	2.987	2.974	2.976	0	2.987	0.265	0.285	38.7813	38.7813	38.7813	38.7813	171.813	171.813	0.0288	
5	0.5%	2.0%	4.938	4.837	4.811	4.81	0	4.924	0.29	0.31	39.125	39.125	39.125	39.125	214.75	215.563	0.01705	
7	0.5%	2.0%	6.25	6.25	6.25	6.25	0	6.25	0.38	0.425	38.8438	38.8438	38.8438	38.8438	230.5	232.563	0.01486	
9	0.5%	2.0%					0	0										
10	0.5%	2.0%					0	0										
11	0.5%	2.0%					0	0										
0.5	0.5%	2.5%	0.544	0.544	0.525	0.525	0	0.5395	0.115	0.125	38.0313	38.0313	38.0313	38.0313	107.594	107.594	0.0195	
1	0.5%	2.5%	1.126	1.126	1.115	1.115	0	1.125	0.165	0.175	38.0313	38.0313	38.0313	38.0313	115.125	115.125	0.01473	
3	0.5%	2.5%	3.11	3.11	3.101	3.101	0	3.1055	0.27	0.3	37.8125	37.8125	37.8125	37.8125	157.813	157.813	0.0164	
5	0.5%	2.5%	5.006	5.006	5.004	5.004	0	5.005	0.295	0.335	37.8125	37.8125	37.8125	37.8125	179.5	183.656	0.01137	
7	0.5%	2.5%	8.819	8.819	8.812	8.812	0	8.819	0.34	0.375	37.4375	37.4375	37.4375	37.4375	195.813	195.813	0.01208	
9	0.5%	2.5%	2.895	2.889	2.889	2.889	0	2.895	0.425	0.48	37.3125	37.3125	37.3125	37.3125	205.594	205.594	0.01181	
10	0.5%	2.5%					0	0										
11	0.5%	2.5%					0	0										
0.5	0.5%	3.0%	0.487	0.489	0.489	0.489	0	0.488	0.125	0.125	38.3438	38.3438	38.3438	38.3438	100.188	100.625	0.01548	
1	0.5%	3.0%	1.045	1.048	1.048	1.048	0	1.045	0.175	0.185	38.1875	38.1875	38.1875	38.1875	123.594	123.594	0.01661	
3	0.5%	3.0%	2.867	2.867	2.866	2.866	0	2.8615	0.265	0.32	37.5938	37.5938	37.5938	37.5938	147.938	147.938	0.01459	
5	0.5%	3.0%	5.05	5.051	5.03	5.03	0	5.0425	0.32	0.38	37.625	37.625	37.625	37.625	167.125	167.125	0.01515	
7	0.5%	3.0%	8.814	8.814	8.834	8.834	0	8.834	0.38	0.425	37.4375	37.4375	37.4375	37.4375	181.25	181.25	0.01638	
9	0.5%	3.0%	2.933	2.929	2.929	2.929	0	2.933	0.44	0.49	37.1875	37.1875	37.1875	37.1875	202.625	202.625	0.01503	
10	0.5%	3.0%	3.93	3.93	3.914	3.914	0	3.93	0.475	0.53	37.5938	37.5938	37.5938	37.5938	214.75	214.75	0.01431	
11	0.5%	3.0%	4.855	4.855	4.854	4.854	0	4.855	0.475	0.53	37.5938	37.5938	37.5938	37.5938	230.5	230.5	0.01319	
0.5	0.5%	4.0%	0.517	0.51	0.513	0.509	0	0.512	0.16	0.17	38.125	38.125	38.125	38.125	87.4063	87.4063	0.0126	
1	0.5%	4.0%	1.0245	1.0265	1.021	1.025	0	1.02383	0.21	0.22	37.9375	37.9375	37.9375	37.9375	100.188	100.625	0.01481	
3	0.5%	4.0%	2.865	2.866	2.866	2.870	0	2.8613	0.33	0.34	37.3125	37.3125	37.3125	37.3125	123.594	123.594	0.01474	
5	0.5%	4.0%	5.028	5.028	5.036	5.016	0	5.0228	0.405	0.415	37.9688	37.9688	37.9688	37.9688	145.188	145.188	0.01578	
7	0.5%	4.0%	8.821	8.822	8.821	8.824	0	8.821	0.46	0.46	37.1875	37.1875	37.1875	37.1875	167.125	167.125	0.01629	
9	0.5%	4.0%	2.8	2.899	2.92	2.921	0	2.899	0.43	0.44	38.125	38.125	38.125	38.125	181.25	181.25	0.0128	
10	0.5%	4.0%	3.744	3.743	3.742	3.742	0	3.743	0.47	0.48	37.5938	37.5938	37.5938	37.5938	202.625	202.625	0.0128	
11	0.5%	4.0%	4.785	4.786	4.786	4.786	0	4.785	0.49	0.5	37.1875	37.1875	37.1875	37.1875	230.5	230.5	0.01284	

Table B2.2 Asphalt surface data

Discharge (actual) cfs	SX (%)	GVALL (CFS)		Color (CFS)		Qtotal	Depth (ft)		Spread Dist T1 (in)		Curb Distance (in)		Spread Dist T2 (in)		AVG Spread In	n value	Geomet integrate		
		Initial 1st run	Final 2nd run	Initial 1st run	Final 2nd run		AVG CFS	Min 1st run	Max 2nd run	T1min 1st run	T1max 2nd run	Cmin 1st run	Cmax 2nd run	T2min 1st run				T2max 2nd run	
0.5	1.0%	5.08	0.87	0.50	0.01	0	0	0	0.905	0.999	0.097	0.099	39.125	121.438	127.875	121.438	86.4531	0.0184	
1	1.0%	1.011	2.927	2.927	2.927	0	0	1.008	0.1	0.1	0.1	0.1	39.25	141.666	131.375	141.666	96.2031	0.0147	
3	1.0%	2.887	2.692	2.692	2.692	0	0	0.299275	0.155	0.155	0.155	0.155	39.25	178.25	163.031	178.25	122.633	0.0688	
5	1.0%	5.016	5.015	5.011	5.011	0	0	5.013	0.205	0.2	0.205	0.205	37.125	181.031	210.344	181.031	124.456	0.0669	
7	1.0%	3.833	4.855	4.833	4.833	6.281	6.281	7.11125	0.245	0.245	0.245	0.245	37.125	181.031	210.344	181.031	124.456	0.0669	
9	1.0%	4.887	4.887	4.887	4.887	0	0	0	0	0	0	0	37.125	181.031	210.344	181.031	124.456	0.0669	
10	1.0%	4.887	4.887	4.887	4.887	0	0	0	0	0	0	0	37.125	181.031	210.344	181.031	124.456	0.0669	
11	1.0%	4.887	4.887	4.887	4.887	0	0	0	0	0	0	0	37.125	181.031	210.344	181.031	124.456	0.0669	
0.5	2.0%	4.92	0.483	0.489	0.489	0	0	0	0.49075	0.12	0.1265	0.1215	38.2813	100.688	102.719	101.156	103.569	63.8516	0.0188
1	2.0%	1.001	1.001	0.989	0.989	0	0	1	0.14	0.1435	0.1405	0.14	37.8438	100.688	102.719	101.156	103.569	63.8516	0.0188
3	2.0%	2.979	2.975	2.97	2.979	0	0	0.297575	0.19	0.2	0.2	0.2	37.4375	100.688	102.719	101.156	103.569	63.8516	0.0188
5	2.0%	5.005	5.007	5.019	5.018	0	0	5.013	0.2775	0.28	0.2775	0.28	37.2188	100.688	102.719	101.156	103.569	63.8516	0.0188
7	2.0%	3.829	4.831	4.821	4.821	6.144	6.144	6.153	0.28	0.28	0.28	0.28	37.2188	100.688	102.719	101.156	103.569	63.8516	0.0188
9	2.0%	4.887	4.887	4.887	4.887	6.127	6.127	6.146	0.3	0.3	0.3	0.3	37.125	100.688	102.719	101.156	103.569	63.8516	0.0188
10	2.0%	4.887	4.887	4.887	4.887	6.127	6.127	6.146	0.3	0.3	0.3	0.3	37.125	100.688	102.719	101.156	103.569	63.8516	0.0188
11	2.0%	4.887	4.887	4.887	4.887	6.105	6.105	6.129	0.33	0.33	0.33	0.33	37.125	100.688	102.719	101.156	103.569	63.8516	0.0188
0.5	2.5%	1.018	1.017	1.013	1.013	0	0	0.50025	0.135	0.135	0.135	0.135	37.75	100.688	102.719	101.156	103.569	63.8516	0.0188
1	2.5%	2.989	2.989	2.982	2.983	0	0	1.0475	0.14	0.14	0.14	0.14	37.75	100.688	102.719	101.156	103.569	63.8516	0.0188
3	2.5%	4.98	4.983	4.97	4.97	0	0	4.97575	0.26	0.275	0.26	0.26	37.75	100.688	102.719	101.156	103.569	63.8516	0.0188
5	2.5%	0.951	0.945	0.945	0.943	6.16	6.16	6.165	0.285	0.305	0.285	0.285	37.75	100.688	102.719	101.156	103.569	63.8516	0.0188
7	2.5%	3.828	2.827	2.821	2.823	6.154	6.155	6.15	0.31	0.31	0.31	0.31	37.75	100.688	102.719	101.156	103.569	63.8516	0.0188
9	2.5%	3.821	3.818	3.819	3.819	6.126	6.126	6.15	0.35	0.35	0.35	0.35	37.75	100.688	102.719	101.156	103.569	63.8516	0.0188
10	2.5%	4.848	4.848	4.837	4.837	6.129	6.129	6.108	0.35	0.35	0.35	0.35	37.75	100.688	102.719	101.156	103.569	63.8516	0.0188
11	2.5%	4.848	4.848	4.837	4.837	6.129	6.129	6.108	0.35	0.35	0.35	0.35	37.75	100.688	102.719	101.156	103.569	63.8516	0.0188
0.5	3.0%	0.512	0.511	0.511	0.511	0	0	0.51125	0.14	0.14	0.14	0.14	37.75	100.688	102.719	101.156	103.569	63.8516	0.0188
1	3.0%	1.002	1.002	1.002	1.002	0	0	1.00075	0.15	0.15	0.15	0.15	37.75	100.688	102.719	101.156	103.569	63.8516	0.0188
3	3.0%	3.042	3.043	3.021	3.022	0	0	3.032	0.225	0.225	0.225	0.225	37.75	100.688	102.719	101.156	103.569	63.8516	0.0188
5	3.0%	5.015	5.016	5.02	5.021	0	0	5.018	0.285	0.285	0.285	0.285	37.75	100.688	102.719	101.156	103.569	63.8516	0.0188
7	3.0%	0.915	0.915	0.915	0.915	6.18	6.18	6.195	0.3	0.3	0.3	0.3	37.75	100.688	102.719	101.156	103.569	63.8516	0.0188
9	3.0%	2.975	2.975	2.968	2.968	6.18	6.18	6.18	0.35	0.35	0.35	0.35	37.75	100.688	102.719	101.156	103.569	63.8516	0.0188
10	3.0%	3.98	3.98	3.97	3.97	6.176	6.176	6.18	0.35	0.35	0.35	0.35	37.75	100.688	102.719	101.156	103.569	63.8516	0.0188
11	3.0%	4.985	4.985	4.985	4.985	6.155	6.155	6.14	0.38	0.38	0.38	0.38	37.75	100.688	102.719	101.156	103.569	63.8516	0.0188
0.5	4.0%	0.5	0.488	0.482	0.482	0	0	0.48925	0.135	0.135	0.135	0.135	37.75	100.688	102.719	101.156	103.569	63.8516	0.0188
1	4.0%	1.033	1.038	1.044	1.043	0	0	1.0395	0.15	0.15	0.15	0.15	37.75	100.688	102.719	101.156	103.569	63.8516	0.0188
3	4.0%	2.981	2.982	3.004	3.006	0	0	2.98825	0.23	0.24	0.24	0.24	37.75	100.688	102.719	101.156	103.569	63.8516	0.0188
5	4.0%	5.001	5.003	5.03	5.028	0	0	5.01675	0.305	0.315	0.305	0.305	37.75	100.688	102.719	101.156	103.569	63.8516	0.0188
7	4.0%	0.92	0.921	0.922	0.923	6.174	6.183	6.185	0.345	0.35	0.345	0.345	37.75	100.688	102.719	101.156	103.569	63.8516	0.0188
9	4.0%	2.92	2.919	2.913	2.913	6.172	6.175	6.173	0.4	0.4	0.4	0.4	37.75	100.688	102.719	101.156	103.569	63.8516	0.0188
10	4.0%	3.928	3.901	3.903	3.903	6.167	6.167	6.163	0.39	0.4	0.39	0.39	37.75	100.688	102.719	101.156	103.569	63.8516	0.0188
11	4.0%	4.952	4.883	4.883	4.883	6.169	6.164	6.165	0.39	0.4	0.39	0.4	37.75	100.688	102.719	101.156	103.569	63.8516	0.0188

Table B2.3 Asphalt surface data

Discharge actual CFS	St. (%)	SX (%)	GWALL (CFS)		Color (CFS)		Qtotal AVG CFS	Depth (ft)		Spread Dist T1 (in)		Curb Distance (in)		Spread Dist T2 (in)		AVG Spread in	n value Geomet integrate					
			Initial 1st run	Final 2nd run	Initial 1st run	Final 2nd run		Min 1st run	Max 2nd run	T1min 1st run	T1max 2nd run	Cmin 1st run	Cmax 2nd run	T2min 1st run	T2max 2nd run							
0.5	2.0%	1.5%	0.49	0.487	0.488	0	0	0.488	0.085	0.085	37.8125	38.0338	38.5125	104.469	104.344	107.661	67.0547	0.0146				
1	2.0%	1.5%	1.027	1.027	1.022	0	0	1.02475	0.095	0.095	37.8125	37.8438	38.5125	121.626	121.626	127.616	86.8938	0.0148				
3	2.0%	1.5%	3.071	3.071	3.014	0	0	3.01725	0.14	0.15	37.8125	37.8638	38.5125	172.813	172.813	177.031	123.977	0.0118				
5	2.0%	1.5%	5.062	5.061	5.055	0	0	5.05725	0.1625	0.19	37.125	37.8438	38.5125	151.084	151.084	151.084	103.921	0.0121				
7	2.0%	1.5%	7.052	7.052	7.023	0	0	7.023	0.205	0.215	37.1875	37.5313	38.5125	181.563	181.563	181.563	130.423	0.0120				
9	2.0%	1.5%	9.042	9.042	9.013	0	0	9.013	0.245	0.255	37.1875	37.5313	38.5125	205.166	205.166	205.166	150.423	0.0120				
10	2.0%	1.5%	11.032	11.032	11.003	0	0	11.003	0.285	0.295	37.1875	37.5313	38.5125	229.769	229.769	229.769	174.923	0.0119				
11	2.0%	1.5%	13.022	13.022	13.003	0	0	13.003	0.325	0.335	37.1875	37.5313	38.5125	254.372	254.372	254.372	199.423	0.0118				
0.5	2.0%	2.0%	0.486	0.488	0.483	0	0	0.48613	0.1	0.1	37.8125	38.4375	37.7613	38.4275	38.5625	86.6563	86.4375	86.6563	48.4766	0.0082		
1	2.0%	2.0%	0.98	0.981	0.98	0	0	0.98	0.109	0.109	37.8125	37.9063	38.5125	38.5625	38.625	38.625	101.084	103.625	101.084	103.625	64.5445	0.0083
3	2.0%	2.0%	2.993	3	3.007	0	0	3.00125	0.181	0.181	38.3438	38.4063	39.3125	39.9063	39.9375	39.9125	129.106	136.563	129.106	136.563	95.3938	0.0086
5	2.0%	2.0%	5.008	5.008	5.005	0	0	5.003	0.203	0.203	37.8125	37.9688	39.3125	39.9688	39.975	39.9125	153.906	169.666	154.188	169.666	123.08	0.0088
7	2.0%	2.0%	7.023	7.023	7.023	0	0	7.023	0.245	0.245	37.5625	37.6563	37.4375	37.5938	38.75	38.75	177.688	177.688	177.688	177.688	145.088	0.0087
9	2.0%	2.0%	9.042	9.042	9.042	0	0	9.042	0.285	0.285	37.5625	37.6563	38.0625	38.0625	38.75	38.75	206.938	222.375	206.938	222.375	176.423	0.0086
10	2.0%	2.0%	11.061	11.061	11.061	0	0	11.061	0.325	0.325	37.5625	37.6563	38.4688	38.4688	38.75	38.75	231.813	247.25	231.813	247.25	199.423	0.0085
11	2.0%	2.0%	13.080	13.080	13.080	0	0	13.080	0.365	0.365	37.5625	37.6563	38.875	38.875	38.75	38.75	256.706	272.143	256.706	272.143	221.813	0.0084
0.5	2.0%	2.5%	0.48	0.479	0.478	0	0	0.4785	0.095	0.095	38.1875	38.1875	38.7188	38.7188	38.0313	38.0313	82.375	84.4375	82.375	84.4375	45.0234	0.0084
1	2.0%	2.5%	1.021	1.021	1.013	0	0	1.01725	0.135	0.135	38.2188	38.2188	38.3438	38.3438	38.3438	38.3438	96.875	94.4688	96.875	94.4688	64.438	0.0087
3	2.0%	2.5%	2.998	2.998	2.978	0	0	2.9815	0.19	0.195	37.6563	37.6563	38.3438	38.3438	38.3438	126.563	133.126	126.563	133.126	81.2579	0.0094	
5	2.0%	2.5%	5.012	5.015	5.004	0	0	5.0065	0.26	0.26	37.6563	37.6563	38.3438	38.3438	38.3438	161.126	168.689	161.126	168.689	101.249	0.0094	
7	2.0%	2.5%	7.063	7.063	7.073	0	0	7.073	0.295	0.295	37.6563	37.6563	38.3438	38.3438	38.3438	196.25	203.813	196.25	203.813	126.563	0.0094	
9	2.0%	2.5%	9.076	9.076	9.076	0	0	9.076	0.335	0.335	37.6563	37.6563	38.3438	38.3438	38.3438	231.375	238.938	231.375	238.938	149.219	0.0094	
10	2.0%	2.5%	11.089	11.089	11.089	0	0	11.089	0.375	0.375	37.6563	37.6563	38.3438	38.3438	38.3438	256.5	264.063	256.5	264.063	168.689	0.0094	
11	2.0%	2.5%	13.102	13.102	13.102	0	0	13.102	0.415	0.415	37.6563	37.6563	38.3438	38.3438	38.3438	281.625	289.188	281.625	289.188	188.689	0.0094	
0.5	2.0%	3.0%	0.483	0.484	0.483	0	0	0.483	0.095	0.095	39.25	39.25	39.25	39.25	39.25	82.375	82.375	82.375	82.375	43.9453	0.0122	
1	2.0%	3.0%	0.983	0.982	0.981	0	0	0.9815	0.1295	0.1295	38.4375	38.4375	38.4375	38.4375	38.4375	96.875	96.875	96.875	96.875	50.3438	0.0087	
3	2.0%	3.0%	3.005	3.004	3.003	0	0	3.00325	0.21	0.21	38.4375	38.4375	38.4375	38.4375	38.4375	121.813	121.813	121.813	121.813	64.5445	0.0094	
5	2.0%	3.0%	5.027	5.029	5.024	0	0	5.0255	0.2615	0.2615	38.4375	38.4375	38.4375	38.4375	38.4375	146.875	146.875	146.875	146.875	75.4063	0.0094	
7	2.0%	3.0%	7.046	7.046	7.046	0	0	7.046	0.3015	0.3015	38.4375	38.4375	38.4375	38.4375	38.4375	171.813	171.813	171.813	171.813	103.247	0.0094	
9	2.0%	3.0%	9.063	9.063	9.063	0	0	9.063	0.3415	0.3415	38.4375	38.4375	38.4375	38.4375	38.4375	196.75	196.75	196.75	196.75	126.063	0.0094	
10	2.0%	3.0%	11.080	11.080	11.080	0	0	11.080	0.3815	0.3815	38.4375	38.4375	38.4375	38.4375	38.4375	221.688	221.688	221.688	221.688	151.211	0.0094	
11	2.0%	3.0%	13.097	13.097	13.097	0	0	13.097	0.4215	0.4215	38.4375	38.4375	38.4375	38.4375	38.4375	246.625	246.625	246.625	246.625	176.166	0.0094	
0.5	2.0%	4.0%	0.506	0.505	0.514	0	0	0.50975	0.125	0.125	37.625	37.625	37.625	37.625	37.625	82.375	82.375	82.375	82.375	43.9453	0.0122	
1	2.0%	4.0%	1.014	1.015	1.005	0	0	1.01075	0.135	0.135	37.625	37.625	37.625	37.625	37.625	96.875	96.875	96.875	96.875	50.3438	0.0087	
3	2.0%	4.0%	2.991	2.991	2.989	0	0	2.98975	0.225	0.225	37.625	37.625	37.625	37.625	37.625	121.813	121.813	121.813	121.813	64.5445	0.0094	
5	2.0%	4.0%	5.002	5.001	5.005	0	0	5.00625	0.295	0.295	37.625	37.625	37.625	37.625	37.625	146.75	146.75	146.75	146.75	75.4063	0.0094	
7	2.0%	4.0%	7.017	7.017	7.017	0	0	7.017	0.335	0.335	37.625	37.625	37.625	37.625	37.625	171.688	171.688	171.688	171.688	103.247	0.0094	
9	2.0%	4.0%	9.032	9.032	9.032	0	0	9.032	0.375	0.375	37.625	37.625	37.625	37.625	37.625	196.625	196.625	196.625	196.625	126.063	0.0094	
10	2.0%	4.0%	11.047	11.047	11.047	0	0	11.047	0.415	0.415	37.625	37.625	37.625	37.625	37.625	221.563	221.563	221.563	221.563	151.211	0.0094	
11	2.0%	4.0%	13.062	13.062	13.062	0	0	13.062	0.455	0.455	37.625	37.625	37.625	37.625	37.625	246.5	246.5	246.5	246.5	176.166	0.0094	

Table B2.4 Asphalt surface data

Disching actual/ds	SL (%)		CFS		CFS		Depth (ft)		Curb Distance (ft)		Spread Dist T1 (ft)		Spread Dist T2 (ft)		AVG		n value	Geomet Integrator				
	Initial	Final	Initial	Final	Initial	Final	Initial	Final	Initial	Final	T1min	T1max	T2min	T2max	1st run	2nd run			1st run	2nd run		
	1st run	2nd run	1st run	2nd run	1st run	2nd run	1st run	2nd run	1st run	2nd run	1st run	2nd run	1st run	2nd run	1st run	2nd run	1st run	2nd run	In	In		
0.5	3.0%	1.5%	0.515	0.509	0.509	0.509	0.040	0.040	0.086	0.086	38.7188	38.0638	38.625	38.1875	38.6875	38.7188	38.6875	38.6875	38.6875	46.0468	0.0068	0.00124
1	3.0%	1.5%	1.039	1.044	1.044	1.039	0.104	0.104	0.112	0.112	38.1563	39.0625	39.1563	38.9	38.9	38.9	38.9	38.9	38.9	103.5633	0.0068	0.00132
3	3.0%	1.5%	3.018	3.017	3.017	3.018	0.432	0.432	0.432	0.432	38.6813	38.2188	38.2188	38.2188	38.2188	38.2188	38.2188	38.2188	38.2188	130.198	0.0068	0.00164
5	3.0%	1.5%	5.001	5.001	5.001	5.001	0.865	0.865	0.865	0.865	38.2188	38.2188	38.2188	38.2188	38.2188	38.2188	38.2188	38.2188	38.2188	179.8668	0.0068	0.00170
7	3.0%	1.5%	7.24	7.24	7.24	7.24	1.272	1.272	1.272	1.272	38.1875	38.1875	38.1875	38.1875	38.1875	38.1875	38.1875	38.1875	38.1875	218.611	0.0068	0.00176
9	3.0%	1.5%	2.805	2.8	2.8	2.805	0.278	0.278	0.278	0.278	37.6668	37.6668	37.6668	37.6668	37.6668	37.6668	37.6668	37.6668	37.6668	229.291	0.0068	0.00182
10	3.0%	1.5%	3.727	3.7	3.7	3.727	0.432	0.432	0.432	0.432	37.6668	37.6668	37.6668	37.6668	37.6668	37.6668	37.6668	37.6668	37.6668	233.688	0.0068	0.00186
11	3.0%	1.5%	4.481	4.481	4.481	4.481	0.509	0.509	0.509	0.509	37.6668	37.6668	37.6668	37.6668	37.6668	37.6668	37.6668	37.6668	37.6668	240.031	0.0068	0.00192
6.5	3.0%	2.0%	0.481	0.481	0.481	0.481	0.040	0.040	0.086	0.086	38.7188	38.0638	38.625	38.1875	38.6875	38.7188	38.6875	38.6875	38.6875	46.0468	0.0068	0.00124
1	3.0%	2.0%	1.044	1.044	1.044	1.039	0.104	0.104	0.112	0.112	38.1563	39.0625	39.1563	38.9	38.9	38.9	38.9	38.9	38.9	103.5633	0.0068	0.00132
3	3.0%	2.0%	3.029	3.03	3.03	3.029	0.432	0.432	0.432	0.432	38.6813	38.2188	38.2188	38.2188	38.2188	38.2188	38.2188	38.2188	38.2188	130.198	0.0068	0.00164
5	3.0%	2.0%	4.916	4.916	4.916	4.984	0.865	0.865	0.865	0.865	38.2188	38.2188	38.2188	38.2188	38.2188	38.2188	38.2188	38.2188	38.2188	179.8668	0.0068	0.00170
7	3.0%	2.0%	7.41	7.39	7.44	7.45	1.272	1.272	1.272	1.272	38.1875	38.1875	38.1875	38.1875	38.1875	38.1875	38.1875	38.1875	38.1875	218.611	0.0068	0.00176
9	3.0%	2.0%	2.615	2.618	2.693	2.681	0.278	0.278	0.278	0.278	37.6668	37.6668	37.6668	37.6668	37.6668	37.6668	37.6668	37.6668	37.6668	229.291	0.0068	0.00182
10	3.0%	2.0%	3.747	3.751	3.705	3.706	0.432	0.432	0.432	0.432	37.6668	37.6668	37.6668	37.6668	37.6668	37.6668	37.6668	37.6668	37.6668	233.688	0.0068	0.00186
11	3.0%	2.0%	4.791	4.788	4.787	4.787	0.509	0.509	0.509	0.509	37.6668	37.6668	37.6668	37.6668	37.6668	37.6668	37.6668	37.6668	37.6668	240.031	0.0068	0.00192
0.5	3.0%	2.5%	0.501	0.489	0.497	0.489	0.040	0.040	0.086	0.086	38.7188	38.0638	38.625	38.1875	38.6875	38.7188	38.6875	38.6875	38.6875	46.0468	0.0068	0.00124
1	3.0%	2.5%	1.005	1.008	1.013	1.013	0.104	0.104	0.112	0.112	38.1563	39.0625	39.1563	38.9	38.9	38.9	38.9	38.9	38.9	103.5633	0.0068	0.00132
3	3.0%	2.5%	2.992	2.99	2.989	2.987	0.432	0.432	0.432	0.432	38.6813	38.2188	38.2188	38.2188	38.2188	38.2188	38.2188	38.2188	38.2188	130.198	0.0068	0.00164
5	3.0%	2.5%	5.005	5.01	5.003	5.002	0.865	0.865	0.865	0.865	38.2188	38.2188	38.2188	38.2188	38.2188	38.2188	38.2188	38.2188	38.2188	179.8668	0.0068	0.00170
7	3.0%	2.5%	7.96	7.96	7.98	7.98	1.272	1.272	1.272	1.272	38.1875	38.1875	38.1875	38.1875	38.1875	38.1875	38.1875	38.1875	38.1875	218.611	0.0068	0.00176
9	3.0%	2.5%	2.69	2.691	2.692	2.689	0.278	0.278	0.278	0.278	37.6668	37.6668	37.6668	37.6668	37.6668	37.6668	37.6668	37.6668	37.6668	229.291	0.0068	0.00182
10	3.0%	2.5%	3.817	3.815	3.812	3.81	0.432	0.432	0.432	0.432	37.6668	37.6668	37.6668	37.6668	37.6668	37.6668	37.6668	37.6668	37.6668	233.688	0.0068	0.00186
11	3.0%	2.5%	4.756	4.76	4.759	4.762	0.509	0.509	0.509	0.509	37.6668	37.6668	37.6668	37.6668	37.6668	37.6668	37.6668	37.6668	37.6668	240.031	0.0068	0.00192
0.5	3.0%	3.0%	0.505	0.504	0.508	0.509	0.040	0.040	0.086	0.086	38.7188	38.0638	38.625	38.1875	38.6875	38.7188	38.6875	38.6875	38.6875	46.0468	0.0068	0.00124
1	3.0%	3.0%	0.985	0.988	0.987	0.989	0.104	0.104	0.112	0.112	38.1563	39.0625	39.1563	38.9	38.9	38.9	38.9	38.9	38.9	103.5633	0.0068	0.00132
3	3.0%	3.0%	2.955	2.952	2.951	2.95	0.432	0.432	0.432	0.432	38.6813	38.2188	38.2188	38.2188	38.2188	38.2188	38.2188	38.2188	38.2188	130.198	0.0068	0.00164
5	3.0%	3.0%	4.965	4.98	4.984	4.985	0.865	0.865	0.865	0.865	38.2188	38.2188	38.2188	38.2188	38.2188	38.2188	38.2188	38.2188	38.2188	179.8668	0.0068	0.00170
7	3.0%	3.0%	6.622	6.624	6.629	6.629	1.272	1.272	1.272	1.272	38.1875	38.1875	38.1875	38.1875	38.1875	38.1875	38.1875	38.1875	38.1875	218.611	0.0068	0.00176
9	3.0%	3.0%	2.796	2.793	2.778	2.78	0.278	0.278	0.278	0.278	37.6668	37.6668	37.6668	37.6668	37.6668	37.6668	37.6668	37.6668	37.6668	229.291	0.0068	0.00182
10	3.0%	3.0%	3.823	3.835	3.717	3.715	0.432	0.432	0.432	0.432	37.6668	37.6668	37.6668	37.6668	37.6668	37.6668	37.6668	37.6668	37.6668	233.688	0.0068	0.00186
11	3.0%	3.0%	4.81	4.807	4.775	4.776	0.509	0.509	0.509	0.509	37.6668	37.6668	37.6668	37.6668	37.6668	37.6668	37.6668	37.6668	37.6668	240.031	0.0068	0.00192
0.5	3.0%	4.0%	0.508	0.507	0.489	0.5	0.040	0.040	0.086	0.086	38.7188	38.0638	38.625	38.1875	38.6875	38.7188	38.6875	38.6875	38.6875	46.0468	0.0068	0.00124
1	3.0%	4.0%	0.997	1.0	0.984	0.985	0.104	0.104	0.112	0.112	38.1563	39.0625	39.1563	38.9	38.9	38.9	38.9	38.9	38.9	103.5633	0.0068	0.00132
3	3.0%	4.0%	3.027	3.024	3.01	3.007	0.432	0.432	0.432	0.432	38.6813	38.2188	38.2188	38.2188	38.2188	38.2188	38.2188	38.2188	38.2188	130.198	0.0068	0.00164
5	3.0%	4.0%	5.059	5.055	5.04	5.075	0.865	0.865	0.865	0.865	38.2188	38.2188	38.2188	38.2188	38.2188	38.2188	38.2188	38.2188	38.2188	179.8668	0.0068	0.00170
7	3.0%	4.0%	7.729	7.73	7.733	7.732	1.272	1.272	1.272	1.272	38.1875	38.1875	38.1875	38.1875	38.1875	38.1875	38.1875	38.1875	38.1875	218.611	0.0068	0.00176
9	3.0%	4.0%	2.765	2.766	2.756	2.754	0.278	0.278	0.278	0.278	37.6668	37.6668	37.6668	37.6668	37.6668	37.6668	37.6668	37.6668	37.6668	229.291	0.0068	0.00182
10	3.0%	4.0%	3.749	3.757	3.748	3.746	0.432	0.432	0.432	0.432	37.6668	37.6668	37.6668	37.6668	37.6668	37.6668	37.6668	37.6668	37.6668	233.688	0.0068	0.00186
11	3.0%	4.0%	4.757	4.752	4.762	4.762	0.509	0.509	0.509	0.509	37.6668	37.6668	37.6668	37.6668	37.6668	37.6668	37.6668	37.6668	37.6668	240.031	0.0068	0.00192

Table B2.5 Asphalt surface data

Discharge actual CFS	SX (%)	GWAALL (CFS)				Color (CFS)				Total AVG CFS	Depth (ft)				Spread Dist T1 (in)				Curb Distance (in)				Spread Dist T2 (in)				AVG Spread in	n value Geomet integrate		
		Initial 1st run	Final 1st run	2nd run 1st run	2nd run 2nd run	Initial 1st run	Final 1st run	2nd run 1st run	2nd run 2nd run		Max	Min	1st run	2nd run	1st run	2nd run	1st run	2nd run	1st run	2nd run	1st run	2nd run	1st run	2nd run	T1min	T1max			1st run	2nd run
0.5	4.0%	0.49	0.49	0.49	0.49	0	0	0	0	0.4905	0.091	0.091	0.091	0.091	0.056	38.5313	38.5313	38.5313	38.5313	38.5313	38.5313	38.5313	38.5313	80.0313	91.3125	89.25	91.5	51.5659	0.0068	0.0068
1	4.0%	1.5%	0.994	0.996	1.001	1.002	0	0	0	0.99625	0.0875	0.0875	0.0875	0.0875	0.0725	39.8438	39.8438	39.8438	39.8438	39.8438	39.8438	39.8438	39.8438	126.135	126.135	126.135	126.135	66.923	0.0184	0.0184
3	4.0%	1.5%	3.007	3.011	3.011	3.004	0	0	0	3.00675	0.12	0.12	0.12	0.12	0.12	39.8563	39.8563	39.8563	39.8563	39.8563	39.8563	39.8563	39.8563	163.375	163.375	163.375	163.375	168.638	0.0181	0.0181
5	4.0%	1.5%	5.017	5.018	5.014	5.016	0	0	0	5.01625	0.1635	0.1635	0.1635	0.1635	0.17	39.5313	39.5313	39.5313	39.5313	39.5313	39.5313	39.5313	39.5313	40.75	40.75	40.75	40.75	154.288	0.0162	0.0162
7	4.0%	1.5%	0.728	0.728	0.728	0.728	0	0	0	0.728	0.205	0.205	0.205	0.205	0.205	39.2188	39.2188	39.2188	39.2188	39.2188	39.2188	39.2188	39.2188	201.594	201.594	201.594	201.594	160.333	0.0124	0.0124
9	4.0%	1.5%	2.812	2.812	2.796	2.796	0	0	0	2.807	0.205	0.205	0.205	0.205	0.205	39.2188	39.2188	39.2188	39.2188	39.2188	39.2188	39.2188	39.2188	227.75	227.75	227.75	227.75	186.944	0.0147	0.0147
10	4.0%	1.5%	3.742	3.747	3.746	3.743	0	0	0	3.744	0.235	0.235	0.235	0.235	0.235	39.4063	39.4063	39.4063	39.4063	39.4063	39.4063	39.4063	39.4063	230.25	230.25	230.25	230.25	193.375	0.0144	0.0144
11	4.0%	1.5%	4.751	4.75	4.746	4.743	0	0	0	4.748	0.235	0.235	0.235	0.235	0.235	39.4063	39.4063	39.4063	39.4063	39.4063	39.4063	39.4063	39.4063	242.281	242.281	242.281	242.281	200.02	0.0142	0.0142
0.5	4.0%	2.0%	0.51	0.51	0.51	0.51	0	0	0	0.51	0.0775	0.0775	0.0775	0.0775	0.0775	38.5313	38.5313	38.5313	38.5313	38.5313	38.5313	38.5313	38.5313	86.2813	86.2813	86.2813	86.2813	47.625	0.0147	0.0147
1	4.0%	2.0%	0.98	0.983	0.978	0.981	0	0	0	0.9805	0.1075	0.1075	0.1075	0.1075	0.1075	38.5313	38.5313	38.5313	38.5313	38.5313	38.5313	38.5313	38.5313	88.175	88.175	88.175	88.175	102.625	0.0141	0.0141
3	4.0%	2.0%	3.022	3.023	3.016	3.017	0	0	0	3.0195	0.1525	0.1525	0.1525	0.1525	0.1525	37.9688	37.9688	37.9688	37.9688	37.9688	37.9688	37.9688	37.9688	133.125	133.125	133.125	133.125	134.064	0.0143	0.0143
5	4.0%	2.0%	4.988	4.992	4.98	4.987	0	0	0	4.9895	0.1925	0.1925	0.1925	0.1925	0.1925	37.7188	37.7188	37.7188	37.7188	37.7188	37.7188	37.7188	37.7188	153.488	153.488	153.488	153.488	115.609	0.0114	0.0114
7	4.0%	2.0%	0.685	0.686	0.688	0.689	0	0	0	0.6875	0.215	0.215	0.215	0.215	0.215	38.375	38.375	38.375	38.375	38.375	38.375	38.375	38.375	160.688	160.688	160.688	160.688	170	0.0077	0.0077
9	4.0%	2.0%	2.779	2.78	2.765	2.767	0	0	0	2.7765	0.2625	0.2625	0.2625	0.2625	0.2625	37.25	37.25	37.25	37.25	37.25	37.25	37.25	37.25	181.75	181.75	181.75	181.75	146.042	0.0151	0.0151
10	4.0%	2.0%	3.785	3.792	3.755	3.777	0	0	0	3.784	0.2625	0.2625	0.2625	0.2625	0.2625	37.25	37.25	37.25	37.25	37.25	37.25	37.25	37.25	187.063	187.063	187.063	187.063	150.018	0.0123	0.0123
11	4.0%	2.0%	4.772	4.774	4.771	4.774	0	0	0	4.773	0.2625	0.2625	0.2625	0.2625	0.2625	37.25	37.25	37.25	37.25	37.25	37.25	37.25	37.25	187.063	187.063	187.063	187.063	150.018	0.0123	0.0123
0.5	4.0%	2.5%	0.482	0.483	0.483	0.483	0	0	0	0.48275	0.0965	0.0965	0.0965	0.0965	0.0965	39.6663	39.6663	39.6663	39.6663	39.6663	39.6663	39.6663	39.6663	102.625	102.625	102.625	102.625	50.9141	0.0065	0.0065
1	4.0%	2.5%	0.92	0.92	0.92	0.92	0	0	0	0.92	0.119	0.119	0.119	0.119	0.119	40	40	40	40	40	40	40	40	112.375	112.375	112.375	112.375	60.5	0.0075	0.0075
3	4.0%	2.5%	2.99	2.992	2.984	2.988	0	0	0	2.991	0.1725	0.1725	0.1725	0.1725	0.1725	38.625	38.625	38.625	38.625	38.625	38.625	38.625	38.625	144.9688	144.9688	144.9688	144.9688	109	0.0075	0.0075
5	4.0%	2.5%	4.997	4.997	4.994	4.994	0	0	0	4.998	0.214	0.214	0.214	0.214	0.214	38.375	38.375	38.375	38.375	38.375	38.375	38.375	38.375	163.375	163.375	163.375	163.375	130.75	0.0096	0.0096
7	4.0%	2.5%	0.74	0.739	0.745	0.734	0	0	0	0.7405	0.232	0.232	0.232	0.232	0.232	39.0313	39.0313	39.0313	39.0313	39.0313	39.0313	39.0313	39.0313	181.75	181.75	181.75	181.75	148.625	0.0118	0.0118
9	4.0%	2.5%	2.75	2.75	2.748	2.75	0	0	0	2.7495	0.254	0.254	0.254	0.254	0.254	38.0313	38.0313	38.0313	38.0313	38.0313	38.0313	38.0313	38.0313	160.688	160.688	160.688	160.688	159.219	0.0094	0.0094
10	4.0%	2.5%	3.736	3.739	3.74	3.741	0	0	0	3.7395	0.2575	0.2575	0.2575	0.2575	0.2575	38	38	38	38	38	38	38	38	160.688	160.688	160.688	160.688	169.25	0.0149	0.0149
11	4.0%	2.5%	4.805	4.804	4.801	4.801	0	0	0	4.8025	0.2775	0.2775	0.2775	0.2775	0.2775	38	38	38	38	38	38	38	38	160.688	160.688	160.688	160.688	170	0.0123	0.0123
0.5	4.0%	3.0%	0.504	0.503	0.505	0.507	0	0	0	0.5035	0.0925	0.0925	0.0925	0.0925	0.0925	38.625	38.625	38.625	38.625	38.625	38.625	38.625	38.625	102.625	102.625	102.625	102.625	50.9141	0.0065	0.0065
1	4.0%	3.0%	0.986	0.987	0.981	0.981	0	0	0	0.98675	0.105	0.105	0.105	0.105	0.105	38.5313	38.5313	38.5313	38.5313	38.5313	38.5313	38.5313	38.5313	112.375	112.375	112.375	112.375	60.5	0.0075	0.0075
3	4.0%	3.0%	3.033	3.029	3.031	3.039	0	0	0	3.033	0.1725	0.1725	0.1725	0.1725	0.1725	38.5313	38.5313	38.5313	38.5313	38.5313	38.5313	38.5313	38.5313	144.9688	144.9688	144.9688	144.9688	109	0.0075	0.0075
5	4.0%	3.0%	5.02	5.021	5.018	5.019	0	0	0	5.0445	0.22	0.22	0.22	0.22	0.22	38.625	38.625	38.625	38.625	38.625	38.625	38.625	38.625	163.375	163.375	163.375	163.375	130.75	0.0096	0.0096
7	4.0%	3.0%	0.842	0.84	0.836	0.835	0	0	0	0.8395	0.245	0.245	0.245	0.245	0.245	38.375	38.375	38.375	38.375	38.375	38.375	38.375	38.375	163.375	163.375	163.375	163.375	130.75	0.0096	0.0096
9	4.0%	3.0%	2.791	2.792	2.779	2.779	0	0	0	2.7905	0.265	0.265	0.265	0.265	0.265	38	38	38	38	38	38	38	38	160.688	160.688	160.688	160.688	169.25	0.0149	0.0149
10	4.0%	3.0%	3.761	3.763	3.773	3.768	0	0	0	3.7675	0.2675	0.2675	0.2675	0.2675	0.2675	38	38	38	38	38	38	38	38	160.688	160.688	160.688	160.688	169.25	0.0149	0.0149
11	4.0%	3.0%	4.725	4.727	4.72	4.722	0	0	0	4.7265	0.2775	0.2775	0.2775	0.2775	0.2775	38	38	38	38	38	38	38	38	160.688	160.688	160.688	160.688	170	0.0123	0.0123
0.5	4.0%	4.0%	0.49	0.499	0.487	0.486	0	0	0	0.498	0.099	0.099	0.099	0.099	0.099	38.625	38.625	38.625	38.625	38.625	38.625	38.625	38.625	102.625	102.625	102.625	102.625	50.9141	0.0065	0.0065
1	4.0%	4.0%	0.983	0.982	0.983	0.982	0	0	0	0.9825	0.138	0.138	0.138	0.138	0.138	38.625	38.625	38.625	38.625	38.625	38.625	38.625	38.625	102.625	102.625	102.625	102.625	50.9141	0.0065	0.0065
3	4.0%	4.0%	3.009	3.009	3.005	3.005	0	0	0	3.00875	0.181	0.181	0.181	0.181	0.181	38.625	38.625	38.625	38.625	38.625	38.625	38.625	38.625	133.125	133.125	133.125	133.125	115.609	0.0114	0.0114
5	4.0%	4.0%	5.009	5.009	5.015	5.014	0	0	0	5.0115	0.24	0.24	0.24	0.24	0.24	38	38	38	38	38	38	38	38	160.688	160.688	160.688	160.688	170	0.0123	0.0123
7	4.0%	4.0%	0.812	0.811	0.814	0.815	0	0	0	0.813	0.2875	0.2875	0.2875	0.2875	0.2875	37.7188	37.7188	37.7188	37.7188	37.7188	37.7188	37.7188	37.7188	160.688	160.688	160.688	160.688	170	0.0123	0.0123
9	4.0%	4.0%	2.868	2.866	2.862	2.861	0	0	0	2.865	0.302	0.302	0.302	0.302	0.302	37.9688	37.9688	37.9688	37.9688	37.9688	37.9688	37.9688	37.9688	181.75	181.75	181.75	181.75</			

Table B3.4 TxDOT concrete surface data

SL (%)		SX (%)		DWALL (CFS)		Othor (CFS)		Chiral		Reinft (gpm)		Depth (ft)		Max		Spread Dist T1 (ft)		Cup Distance (ft)		Spread Dist T2 (ft)		AVG		in value							
1st sun	2nd sun	1st sun	2nd sun	1st sun	2nd sun	1st sun	2nd sun	1st sun	2nd sun	1st sun	2nd sun	1st sun	2nd sun	1st sun	2nd sun	1st sun	2nd sun	1st sun	2nd sun	1st sun	2nd sun	1st sun	2nd sun	1st sun	2nd sun	1st sun	2nd sun				
0.03	0.04	0.999	0.999	0.986	0.999	0.989	0.999	6.868	6.868	6.868	6.868	0.155	0.155	0.155	0.155	46.8125	46.8125	46.8125	46.8125	46.8125	46.8125	46.8125	46.8125	91.625	91.375	92	91.6875	0.014819	0.014819		
0.03	0.04	3.011	3.011	3.012	3.011	3.011	3.011	3.011	3.011	3.011	3.011	0.22	0.22	0.22	0.22	46.8125	46.8125	46.8125	46.8125	46.8125	46.8125	46.8125	46.8125	116.375	116.375	117	116.6944	0.014819	0.014819		
0.03	0.04	0.884	0.884	0.884	0.884	0.884	0.884	0.884	0.884	0.884	0.884	0.34	0.34	0.34	0.34	46.8125	46.8125	46.8125	46.8125	46.8125	46.8125	46.8125	46.8125	141.25	141.25	142.875	142.875	142.875	142.875	0.014819	0.014819
0.03	0.04	0.772	0.772	0.772	0.772	0.772	0.772	0.772	0.772	0.772	0.772	0.34	0.34	0.34	0.34	46.8125	46.8125	46.8125	46.8125	46.8125	46.8125	46.8125	46.8125	153.0625	152.625	153.5	153.0625	0.014819	0.014819		
0.03	0.04	4.753	4.748	4.752	4.741	6.278	6.267	6.274	6.262	6.274	6.262	0.36	0.36	0.36	0.36	46.8125	46.8125	46.8125	46.8125	46.8125	46.8125	46.8125	46.8125	158.3125	156.9375	158.2625	156.9375	0.014819	0.014819		
0.03	0.04	0.956	0.956	0.956	0.956	0.956	0.956	0.956	0.956	0.956	0.956	0.15	0.15	0.15	0.15	46.8125	46.8125	46.8125	46.8125	46.8125	46.8125	46.8125	46.8125	93	93	93	93	0.014819	0.014819		
0.03	0.04	2.983	2.982	2.982	2.984	2.982	2.984	2.982	2.984	2.982	2.984	0.20	0.20	0.20	0.20	46.8125	46.8125	46.8125	46.8125	46.8125	46.8125	46.8125	46.8125	116.1875	116.1875	117.25	116.1875	0.014819	0.014819		
0.03	0.04	0.864	0.862	0.863	0.863	0.863	0.861	0.862	0.862	0.863	0.862	0.31	0.31	0.31	0.31	46.8125	46.8125	46.8125	46.8125	46.8125	46.8125	46.8125	46.8125	142.1875	142.1875	142.75	142.1875	0.014819	0.014819		
0.03	0.04	3.714	3.714	3.714	3.714	6.268	6.264	6.264	6.264	6.268	6.264	0.34	0.34	0.34	0.34	46.8125	46.8125	46.8125	46.8125	46.8125	46.8125	46.8125	46.8125	152.25	152.25	153.5	152.25	0.014819	0.014819		
0.03	0.04	4.683	4.683	4.683	4.683	6.273	6.273	6.273	6.273	6.273	6.273	0.36	0.36	0.36	0.36	46.8125	46.8125	46.8125	46.8125	46.8125	46.8125	46.8125	46.8125	154.625	154.625	155.5	154.625	0.014819	0.014819		
0.03	0.04	0.964	0.966	0.964	0.964	0.964	0.964	0.964	0.964	0.964	0.964	0.22	0.22	0.22	0.22	46.8125	46.8125	46.8125	46.8125	46.8125	46.8125	46.8125	46.8125	97.5	97.4	97.4	97.4	0.014819	0.014819		
0.03	0.04	2.927	2.928	2.928	2.942	2.928	2.942	2.928	2.942	2.928	2.942	0.18	0.18	0.18	0.18	46.8125	46.8125	46.8125	46.8125	46.8125	46.8125	46.8125	46.8125	119.1875	119.1875	123	119.1875	0.014819	0.014819		
0.03	0.04	0.648	0.651	0.649	0.652	0.649	0.652	0.649	0.652	0.649	0.652	0.31	0.31	0.31	0.31	46.8125	46.8125	46.8125	46.8125	46.8125	46.8125	46.8125	46.8125	142	142	142	142	0.014819	0.014819		
0.03	0.04	3.679	3.671	3.686	3.675	6.266	6.266	6.266	6.266	6.270	6.266	0.34	0.34	0.34	0.34	46.8125	46.8125	46.8125	46.8125	46.8125	46.8125	46.8125	46.8125	149.75	149.75	151	149.75	0.014819	0.014819		
0.03	0.04	4.621	4.623	4.626	4.626	6.261	6.261	6.261	6.261	6.266	6.261	0.36	0.36	0.36	0.36	46.8125	46.8125	46.8125	46.8125	46.8125	46.8125	46.8125	46.8125	153.125	153.125	155	153.125	0.014819	0.014819		
0.02	0.04	0.981	0.981	0.986	0.982	6.266	6.266	6.266	6.266	6.266	6.266	0.18	0.18	0.18	0.18	46.8125	46.8125	46.8125	46.8125	46.8125	46.8125	46.8125	46.8125	96.875	96.875	98.5	96.875	0.014819	0.014819		
0.02	0.04	2.975	2.983	2.976	2.984	2.975	2.984	2.975	2.984	2.975	2.984	0.25	0.25	0.25	0.25	46.8125	46.8125	46.8125	46.8125	46.8125	46.8125	46.8125	46.8125	122.3125	122.3125	123.75	122.3125	0.014819	0.014819		
0.02	0.04	3.004	3.004	3.006	3.004	6.266	6.266	6.266	6.266	6.266	6.266	0.33	0.33	0.33	0.33	46.8125	46.8125	46.8125	46.8125	46.8125	46.8125	46.8125	46.8125	150.9375	150.9375	151.875	150.9375	0.014819	0.014819		
0.02	0.04	0.718	0.718	0.717	0.718	6.268	6.272	6.274	6.274	6.268	6.272	0.23	0.23	0.23	0.23	46.8125	46.8125	46.8125	46.8125	46.8125	46.8125	46.8125	46.8125	117	117	117	117	0.014819	0.014819		
0.02	0.04	0.986	0.986	0.987	0.987	6.268	6.268	6.268	6.268	6.268	6.268	0.31	0.31	0.31	0.31	46.8125	46.8125	46.8125	46.8125	46.8125	46.8125	46.8125	46.8125	149.625	149.625	152.5	149.625	0.014819	0.014819		
0.02	0.04	3.731	3.733	3.735	3.735	6.268	6.268	6.268	6.268	6.268	6.268	0.37	0.37	0.37	0.37	46.8125	46.8125	46.8125	46.8125	46.8125	46.8125	46.8125	46.8125	154	154	154	154	0.014819	0.014819		
0.02	0.04	4.731	4.733	4.733	4.735	6.268	6.268	6.268	6.268	6.268	6.268	0.4	0.4	0.4	0.4	46.8125	46.8125	46.8125	46.8125	46.8125	46.8125	46.8125	46.8125	165.125	165.125	165	165.125	0.014819	0.014819		
0.02	0.04	0.961	0.961	0.961	0.961	6.266	6.266	6.266	6.266	6.266	6.266	0.18	0.18	0.18	0.18	46.8125	46.8125	46.8125	46.8125	46.8125	46.8125	46.8125	46.8125	96.875	96.875	98.5	96.875	0.014819	0.014819		
0.02	0.04	2.975	2.975	2.975	2.975	6.266	6.266	6.266	6.266	6.266	6.266	0.25	0.25	0.25	0.25	46.8125	46.8125	46.8125	46.8125	46.8125	46.8125	46.8125	46.8125	117	117	117	117	0.014819	0.014819		
0.02	0.04	3.014	3.014	3.014	3.014	6.266	6.266	6.266	6.266	6.266	6.266	0.31	0.31	0.31	0.31	46.8125	46.8125	46.8125	46.8125	46.8125	46.8125	46.8125	46.8125	149.625	149.625	152.5	149.625	0.014819	0.014819		
0.02	0.04	4.678	4.678	4.678	4.678	6.266	6.266	6.266	6.266	6.266	6.266	0.36	0.36	0.36	0.36	46.8125	46.8125	46.8125	46.8125	46.8125	46.8125	46.8125	46.8125	165.125	165.125	166	165.125	0.014819	0.014819		
0.02	0.04	0.969	0.969	0.969	0.969	6.266	6.266	6.266	6.266	6.266	6.266	0.18	0.18	0.18	0.18	46.8125	46.8125	46.8125	46.8125	46.8125	46.8125	46.8125	46.8125	96.875	96.875	98.5	96.875	0.014819	0.014819		
0.02	0.04	2.986	2.986	2.986	2.986	6.266	6.266	6.266	6.266	6.266	6.266	0.25	0.25	0.25	0.25	46.8125	46.8125	46.8125	46.8125	46.8125	46.8125	46.8125	46.8125	117	117	117	117	0.014819	0.014819		
0.02	0.04	0.986	0.986	0.986	0.986	6.266	6.266	6.266	6.266	6.266	6.266	0.18	0.18	0.18	0.18	46.8125	46.8125	46.8125	46.8125	46.8125	46.8125	46.8125	46.8125	96.875	96.875	98.5	96.875	0.014819	0.014819		
0.02	0.04	2.986	2.986	2.986	2.986	6.266	6.266	6.266	6.266	6.266	6.266	0.25	0.25	0.25	0.25	46.8125	46.8125	46.8125	46.8125	46.8125	46.8125	46.8125	46.8125	117	117	117	117	0.014819	0.014819		
0.02	0.04	0.986	0.986	0.986	0.986	6.266	6.266	6.266	6.266	6.266	6.266	0.18	0.18	0.18	0.18	46.8125	46.8125	46.8125	46.8125	46.8125	46.8125	46.8125	46.8125	96.875	96.875	98.5	96.875	0.014819	0.014819		
0.02	0.04	4.678	4.678	4.678	4.678	6.266	6.266	6.266	6.266	6.266	6.266	0.36	0.36	0.36	0.36	46.8125	46.8125	46.8125	46.8125	46.8125	46.8125	46.8125	46.8125	165.125	165.125	166	165.125	0.014819	0.014819		
0.02	0.04	0.969	0.969	0.969	0.969	6.266	6.266	6.266	6.266	6.266	6.266	0.18	0.18	0.18	0.18	46.8125	46.8125	46.8125	46.8125	46.8125	46.8125	46.8125	46.8125	96.875	96.875	98.5	96.875	0.014819	0.014819		
0.02	0.04	2.986	2.986	2.986	2.986	6.266	6.266	6.266	6.266	6.266	6.266	0.25	0.25	0.25	0.25	46.8125	46.8125	46.8125	46.8125	46.8125	46.8125	46.8125	46.8125	117	117	117	117	0.014819	0.014819		
0.02	0.04	0.986	0.986	0.986	0.986	6.266	6.266	6.266	6.266	6.266	6.266	0.18	0.18	0.18	0.18	46.8125	46.8125	46.8125	46.8125	46.8125	46.8125	46.8125	46.8125	96.875	96.875	98.5	96.875	0.014819	0.014819		

Table B3.5 TxDOT concrete surface data

SL (%)	SX (%)	Raw Data - Smooth Concrete			Finish (CFS)			Other (CFS)			Ravall (gpm)			Depth (ft)			Spread Dist T1 (ft)			Curb Distance (ft)			Spread Dist T2 (ft)			AVG Spread	In value	Grade/Integrat				
		1st run	2nd run	Final	1st run	2nd run	Final	1st run	2nd run	Final	Min	2nd run	Final	1st run	2nd run	Final	1st run	2nd run	Final	1st run	2nd run	Final	1st run	2nd run	Final				1st run	2nd run	Final	
0.02	0.02	0.979	0.975	0.98	0.976	0.978	0.979	0.975	0.976	0.977	0.978	0.979	0.975	0.976	0.977	0.978	0.975	0.976	0.977	0.978	0.975	0.976	0.977	0.978	0.975	0.976	0.977	0.978	121.9003	0.013014	0.01584	
0.02	0.02	3.066	3.04	3.007	3.005	3.006	3.005	3.006	3.005	3.006	3.005	3.006	3.005	3.006	3.005	3.006	3.005	3.006	3.005	3.006	3.005	3.006	3.005	3.006	3.005	3.006	3.005	3.006	199.0625	0.012302	0.01646	
0.02	0.02	0.684	0.695	0.695	0.695	0.695	0.695	0.695	0.695	0.695	0.695	0.695	0.695	0.695	0.695	0.695	0.695	0.695	0.695	0.695	0.695	0.695	0.695	0.695	0.695	0.695	0.695	0.695	197.125	0.00618	0.01149	
0.02	0.02	3.724	3.721	3.721	3.721	3.721	3.721	3.721	3.721	3.721	3.721	3.721	3.721	3.721	3.721	3.721	3.721	3.721	3.721	3.721	3.721	3.721	3.721	3.721	3.721	3.721	3.721	3.721	211.5625	0.010389	0.01545	
0.02	0.02	4.739	4.729	4.739	4.739	4.739	4.739	4.739	4.739	4.739	4.739	4.739	4.739	4.739	4.739	4.739	4.739	4.739	4.739	4.739	4.739	4.739	4.739	4.739	4.739	4.739	4.739	4.739	222.375	0.01192	0.01324	
0.02	0.02	0.972	0.971	0.97	0.97	0.972	0.971	0.97	0.97	0.972	0.971	0.97	0.97	0.972	0.971	0.97	0.97	0.972	0.971	0.97	0.97	0.972	0.971	0.97	0.97	0.972	0.971	0.97	126.9375	0.01456	0.01737	
0.02	0.02	2.972	2.973	2.971	2.971	2.972	2.973	2.971	2.971	2.972	2.973	2.971	2.971	2.972	2.973	2.971	2.971	2.972	2.973	2.971	2.971	2.972	2.973	2.971	2.971	2.972	2.973	2.971	158.5625	0.01259	0.01472	
0.02	0.02	3.624	3.622	3.624	3.624	3.624	3.624	3.624	3.624	3.624	3.624	3.624	3.624	3.624	3.624	3.624	3.624	3.624	3.624	3.624	3.624	3.624	3.624	3.624	3.624	3.624	3.624	3.624	186.5625	0.00849	0.01307	
0.02	0.02	3.624	3.622	3.624	3.624	3.624	3.624	3.624	3.624	3.624	3.624	3.624	3.624	3.624	3.624	3.624	3.624	3.624	3.624	3.624	3.624	3.624	3.624	3.624	3.624	3.624	3.624	3.624	186.5625	0.01427	0.01904	
0.02	0.02	4.691	4.697	4.693	4.693	4.694	4.693	4.693	4.693	4.694	4.693	4.693	4.693	4.693	4.693	4.693	4.693	4.693	4.693	4.693	4.693	4.693	4.693	4.693	4.693	4.693	4.693	4.693	224	0.00925	0.01544	
0.02	0.02	0.965	0.968	0.969	0.969	0.969	0.969	0.969	0.969	0.969	0.969	0.969	0.969	0.969	0.969	0.969	0.969	0.969	0.969	0.969	0.969	0.969	0.969	0.969	0.969	0.969	0.969	0.969	186.5625	0.01231	0.01594	
0.02	0.02	2.947	2.944	2.943	2.944	2.944	2.944	2.944	2.944	2.944	2.944	2.944	2.944	2.944	2.944	2.944	2.944	2.944	2.944	2.944	2.944	2.944	2.944	2.944	2.944	2.944	2.944	2.944	192.75	0.01168	0.01472	
0.02	0.02	3.624	3.625	3.624	3.624	3.624	3.624	3.624	3.624	3.624	3.624	3.624	3.624	3.624	3.624	3.624	3.624	3.624	3.624	3.624	3.624	3.624	3.624	3.624	3.624	3.624	3.624	3.624	186.5625	0.01125	0.01586	
0.02	0.02	3.624	3.625	3.624	3.624	3.624	3.624	3.624	3.624	3.624	3.624	3.624	3.624	3.624	3.624	3.624	3.624	3.624	3.624	3.624	3.624	3.624	3.624	3.624	3.624	3.624	3.624	3.624	186.5625	0.01125	0.01586	
0.02	0.02	4.729	4.739	4.739	4.739	4.739	4.739	4.739	4.739	4.739	4.739	4.739	4.739	4.739	4.739	4.739	4.739	4.739	4.739	4.739	4.739	4.739	4.739	4.739	4.739	4.739	4.739	4.739	200.5	0.00925	0.01594	
0.02	0.02	0.956	0.958	0.958	0.958	0.958	0.958	0.958	0.958	0.958	0.958	0.958	0.958	0.958	0.958	0.958	0.958	0.958	0.958	0.958	0.958	0.958	0.958	0.958	0.958	0.958	0.958	0.958	122.6875	0.01155	0.01521	
0.02	0.02	2.843	2.859	2.849	2.856	2.849	2.856	2.849	2.856	2.849	2.856	2.849	2.856	2.849	2.856	2.849	2.856	2.849	2.856	2.849	2.856	2.849	2.856	2.849	2.856	2.849	2.856	2.849	169	0.00525	0.00838	
0.02	0.02	0.958	0.959	0.957	0.957	0.957	0.957	0.957	0.957	0.957	0.957	0.957	0.957	0.957	0.957	0.957	0.957	0.957	0.957	0.957	0.957	0.957	0.957	0.957	0.957	0.957	0.957	0.957	186.5625	0.01285	0.01707	
0.02	0.02	3.624	3.621	3.625	3.625	3.625	3.625	3.625	3.625	3.625	3.625	3.625	3.625	3.625	3.625	3.625	3.625	3.625	3.625	3.625	3.625	3.625	3.625	3.625	3.625	3.625	3.625	3.625	202.5	0.010325	0.01526	
0.02	0.02	4.691	4.688	4.688	4.688	4.688	4.688	4.688	4.688	4.688	4.688	4.688	4.688	4.688	4.688	4.688	4.688	4.688	4.688	4.688	4.688	4.688	4.688	4.688	4.688	4.688	4.688	4.688	200.5	0.010325	0.01526	
0.02	0.02	0.958	0.958	0.958	0.958	0.958	0.958	0.958	0.958	0.958	0.958	0.958	0.958	0.958	0.958	0.958	0.958	0.958	0.958	0.958	0.958	0.958	0.958	0.958	0.958	0.958	0.958	0.958	186.5625	0.01125	0.01592	
0.02	0.02	3.029	3.028	3.025	3.028	3.028	3.028	3.028	3.028	3.028	3.028	3.028	3.028	3.028	3.028	3.028	3.028	3.028	3.028	3.028	3.028	3.028	3.028	3.028	3.028	3.028	3.028	3.028	200.5	0.01125	0.01592	
0.02	0.02	0.99	0.992	0.991	0.993	0.992	0.993	0.992	0.993	0.992	0.993	0.992	0.993	0.992	0.993	0.992	0.993	0.992	0.993	0.992	0.993	0.992	0.993	0.992	0.993	0.992	0.993	0.992	158.5625	0.01708	0.01937	
0.02	0.02	2.953	2.952	2.952	2.952	2.952	2.952	2.952	2.952	2.952	2.952	2.952	2.952	2.952	2.952	2.952	2.952	2.952	2.952	2.952	2.952	2.952	2.952	2.952	2.952	2.952	2.952	2.952	210.4375	0.01046	0.01477	
0.02	0.02	0.01	0.01	0.01	0.01	0.01	0.01	0.01	0.01	0.01	0.01	0.01	0.01	0.01	0.01	0.01	0.01	0.01	0.01	0.01	0.01	0.01	0.01	0.01	0.01	0.01	0.01	0.01	0.01	0.01	0.01	
0.02	0.02	0.01	0.01	0.01	0.01	0.01	0.01	0.01	0.01	0.01	0.01	0.01	0.01	0.01	0.01	0.01	0.01	0.01	0.01	0.01	0.01	0.01	0.01	0.01	0.01	0.01	0.01	0.01	0.01	0.01	0.01	
0.02	0.02	0.01	0.01	0.01	0.01	0.01	0.01	0.01	0.01	0.01	0.01	0.01	0.01	0.01	0.01	0.01	0.01	0.01	0.01	0.01	0.01	0.01	0.01	0.01	0.01	0.01	0.01	0.01	0.01	0.01	0.01	
0.02	0.02	0.92	0.923	0.92	0.92	0.92	0.92	0.92	0.92	0.92	0.92	0.92	0.92	0.92	0.92	0.92	0.92	0.92	0.92	0.92	0.92	0.92	0.92	0.92	0.92	0.92	0.92	0.92	158.5625	0.011975	0.01675	
0.02	0.02	2.884	2.887	2.888	2.888	2.888	2.888	2.888	2.888	2.888	2.888	2.888	2.888	2.888	2.888	2.888	2.888	2.888	2.888	2.888	2.888	2.888	2.888	2.888	2.888	2.888	2.888	2.888	210.4375	0.01428	0.01949	
0.02	0.02	0.99	0.998	0.998	0.998	0.998	0.998	0.998	0.998	0.998	0.998	0.998	0.998	0.998	0.998	0.998	0.998	0.998	0.998	0.998	0.998	0.998	0.998	0.998	0.998	0.998	0.998	0.998	200.5	0.01125	0.01592	
0.02	0.02	0.005	0.005	0.005	0.005	0.005	0.005	0.005	0.005	0.005	0.005	0.005	0.005	0.005	0.005	0.005	0.005	0.005	0.005	0.005	0.005	0.005	0.005	0.005	0.005	0.005	0.005	0.005	0.005	0.005	0.005	
0.02	0.02	0.005	0.005	0.005	0.005	0.005	0.005	0.005	0.005	0.005	0.005	0.005	0.005	0.005	0.005	0.005	0.005	0.005	0.005	0.005	0.005	0.005	0.005	0.005	0.005	0.005	0.005	0.005	0.005	0.005	0.005	0.005
0.02	0.02	0.005	0.005	0.005	0.005	0.005	0.005	0.005	0.005	0.005	0.005	0.005	0.005	0.005	0.005	0.005	0.005	0.005	0.005	0.005	0.005	0.005	0.005	0.005	0.005	0.005	0.005	0.005	0.005	0.005	0.005	0.005
0.02	0.02	0.005	0.005																													

Table B3.7 TxDOT concrete surface data

Pave Data	Smooth Concrete		Crown (FPS)		Dhoor (FPS)		Ravitt (gpm)		Depth (%)		Mer		Curb Distances (ft)		Spread Dist Tz (ft)		Thrus		AVG Speed	z-value	Geometric Margrets		
	SL (%)	St (%)	Final	1st	Final	1st	Final	1st	Final	1st	2nd	1st	2nd	1st	2nd	1st	2nd	1st				2nd	
0.015	0.01	0.976	0.976	0.977	0.976		0.99875	0	0.117	0.11	0.119	0.115	49.4375	49.4375	49.4375	167.75	163.075	172.25	163.075	186.5975	0.017133	0.014465	
0.015	0.01	2.969	2.967	2.97	2.966		2.99825	2.99825	0.163	0.16	0.165	0.165	49.4375	49.4375	49.4375	218.5	219.1975	218.25	219.25	219.25	219.25	0.015464	0.017446
0.015	0.01						0	0												0			
0.015	0.01						0	0												0			
0.015	0.01	0.989	0.987	1.001	0.996		0.99875	0	0.115	0.11	0.117	0.115	49.4375	49.4375	49.4375	171.375	169.8975	172.375	171.8975	171.2613	0.017273	0.015207	
0.015	0.01	2.993	2.988	2.996	2.999		2.99825	2.99825	0.17	0.16	0.17	0.165	49.4375	49.4375	49.4375	219.875	219.875	220.875	220.875	220.375	0.019369	0.017625	
0.015	0.01						0	0											0				
0.015	0.01						0	0											0				
0.015	0.01	0.989	0.992	0.99	0.99		0.99025	26.84	0.119	0.114	0.12	0.118	49.4375	49.4375	49.4375	174.125	174.4375	175.125	174.5113	0.015276	0.015986		
0.015	0.01	2.989	2.989	2.97	2.974		2.97025	26.78	0.165	0.165	0.17	0.17	49.4375	49.4375	49.4375	221.5	218.125	221.5	221.5	220.6693	0.015979	0.015931	
0.015	0.01						0	0											0				
0.015	0.01						0	0											0				
0.015	0.01	0.99	0.99	0.999	0.99		0.99975	52.91	0.121	0.115	0.121	0.12	49.4375	49.4375	49.4375	178.75	178.3975	178.75	178.3975	177.6406	0.015483	0.016	
0.015	0.01	3.003	3.004	3.005	3.004		3.004	51.74	0.165	0.168	0.17	0.17	49.4375	49.4375	49.4375	227.0625	227.0625	227.0625	227.0625	222.9975	0.017541	0.017541	
0.015	0.01						0	0											0				
0.015	0.01						0	0											0				
0.015	0.005	0.496	0.496	0.495	0.496		0.49575	0	0.075	0.075	0.075	0.075	49.4375	49.4375	49.4375	187.625	188.5	187.625	188.5	187.7813	0.01762	0.020877	
0.015	0.005	0.984	0.984	0.993	0.993		0.9935	0	0.091	0.092	0.092	0.092	49.4375	49.4375	49.4375	224.5	224.5	224.5	224.5	224.75	0.017299	0.015486	
0.015	0.005						0	0											0				
0.015	0.005						0	0											0				
0.015	0.005	0.469	0.467	0.469	0.469		0.469	7.636	0.092	0.092	0.092	0.092	49.4375	49.4375	49.4375	197.3125	196.625	196.625	196.625	196.7999	0.01644	0.019673	
0.015	0.005	0.976	0.976	0.977	0.976		0.976	7.09	0.099	0.099	0.099	0.099	49.4375	49.4375	49.4375	227	227	227	227	227	0.019399	0.016285	
0.015	0.005						0	0											0				
0.015	0.005						0	0											0				
0.015	0.005	0.504	0.503	0.504	0.504		0.50375	26.44	0.065	0.09	0.087	0.095	49.4375	49.4375	49.4375	162.625	162.625	162.625	162.625	162.625	0.017272	0.021165	
0.015	0.005	0.985	0.984	0.994	0.996		0.9945	26.62	0.095	0.097	0.095	0.097	49.4375	49.4375	49.4375	241.9375	241.9375	241.9375	241.9375	241.9375	0.017594	0.01981	
0.015	0.005						0	0											0				
0.015	0.005						0	0											0				
0.015	0.005	0.506	0.505	0.506	0.506		0.5065	51.43	0.089	0.089	0.089	0.089	49.4375	49.4375	49.4375	162.625	162.625	162.625	162.625	162.625	0.017115	0.020876	
0.015	0.005	0.999	1	0.998	1.01		0.99825	52.23	0.099	0.099	0.099	0.099	49.4375	49.4375	49.4375	241.9375	241.9375	241.9375	241.9375	241.563	0.017469	0.015962	
0.015	0.005						0	0											0				
0.015	0.005						0	0											0				

Table B4.2 Asphalt treatment surface data

Discharge actual Q dfs	SL (%)	SX (%)	OWALL (CFS)		Orflor (CFS)		Ortal		Depth (ft)		Spread Dist T (in)		Curb Distance (in)		Spread Dist Z (in)		AVG Spread In	n value Geometr Integrater	
			Initial	Final	Initial	Final	1st run	2nd run	1st run	2nd run	1st run	2nd run	1st run	2nd run	1st run	2nd run			1st run
0.5	3.0%	1.5%	0.50	0.50	0.00	0.00	0.50	0.50	0.105	0.100	38.168	37.938	39.999	38.838	114.438	114.438	78.375	0.0203	
1	3.0%	1.5%	0.99	0.99	0.00	0.00	0.99	0.99	0.115	0.125	38.031	38.188	39.156	38.156	135.156	135.156	97.068	0.0231	
3	3.0%	1.5%	3.01	3.01	0.00	0.00	3.00	3.00	0.200	0.210	37.813	37.688	37.875	37.761	179.313	179.313	141.462	0.0175	
5	3.0%	1.5%	5.01	5.01	0.00	0.00	5.01	5.01	0.215	0.225	37.658	37.531	37.719	37.563	223.563	223.563	165.961	0.0217	
7	3.0%	1.5%	0.80	0.80	0.00	0.00	0.80	0.80	0.255	0.265	37.504	37.813	37.658	37.658	243.531	243.656	206.876	0.0207	
8	3.0%	1.5%																	
10	3.0%	1.5%																	
11	3.0%	1.5%																	
0.5	3.0%	2.0%	0.50	0.49	0.00	0.00	0.50	0.50	0.110	0.120	37.875	37.656	39.906	38.313	39.000	38.781	95.469	0.0187	
1	3.0%	2.0%	0.99	0.99	0.00	0.00	0.99	0.99	0.135	0.145	37.631	37.875	37.656	38.688	38.781	123.688	123.750	86.008	0.0226
3	3.0%	2.0%	2.96	2.96	0.00	0.00	2.96	2.96	0.205	0.215	37.500	37.594	37.469	38.593	38.500	38.594	38.625	143.188	0.0173
5	3.0%	2.0%	4.97	4.97	0.00	0.00	4.97	4.97	0.250	0.258	37.469	37.219	37.531	37.313	38.625	38.468	168.563	0.0162	
7	3.0%	2.0%	0.79	0.78	0.00	0.00	0.79	0.79	0.285	0.295	37.188	37.031	38.313	38.500	38.375	38.375	192.625	0.0189	
8	3.0%	2.0%	2.79	2.79	0.00	0.00	2.79	2.79	0.315	0.325	37.215	37.250	37.406	37.344	38.688	38.594	219.531	0.0231	
10	3.0%	2.0%	3.80	3.80	0.00	0.00	3.80	3.80	0.335	0.345	37.168	37.044	37.750	38.094	38.313	38.156	237.875	0.0189	
11	3.0%	2.0%	4.77	4.77	0.00	0.00	4.77	4.77	0.345	0.355	37.156	37.000	37.000	37.219	38.468	38.468	230.375	0.0226	
0.5	3.0%	2.5%	0.56	0.56	0.00	0.00	0.56	0.56	0.115	0.114	38.344	38.219	38.375	38.313	39.406	39.344	89.906	0.0174	
1	3.0%	2.5%	1.04	1.04	0.00	0.00	1.04	1.04	0.133	0.133	38.438	38.261	38.438	38.313	39.438	39.313	103.188	0.0187	
3	3.0%	2.5%	3.09	3.09	0.00	0.00	3.09	3.09	0.210	0.210	37.906	37.719	37.906	38.969	39.000	38.969	142.375	0.0176	
5	3.0%	2.5%	5.00	5.00	0.00	0.00	5.00	5.00	0.253	0.258	37.875	37.750	37.875	38.906	38.875	38.875	147.219	0.0163	
7	3.0%	2.5%	0.74	0.74	0.00	0.00	0.74	0.74	0.283	0.280	37.688	37.644	37.719	38.875	38.875	38.844	176.906	0.0180	
8	3.0%	2.5%	2.77	2.76	0.00	0.00	2.77	2.76	0.323	0.323	37.625	37.625	37.469	38.688	38.594	38.625	181.594	0.0189	
10	3.0%	2.5%	3.75	3.76	0.00	0.00	3.75	3.76	0.333	0.343	37.406	37.406	37.250	38.531	38.594	38.594	206.250	0.0176	
11	3.0%	2.5%	4.84	4.84	0.00	0.00	4.84	4.84	0.360	0.370	37.469	37.444	37.500	37.344	38.625	38.625	217.531	0.0220	
0.5	3.0%	3.0%	0.57	0.57	0.00	0.00	0.57	0.57	0.114	0.113	37.644	37.969	37.644	38.813	38.875	38.875	86.281	0.0189	
1	3.0%	3.0%	1.06	1.06	0.00	0.00	1.06	1.06	0.160	0.165	37.688	37.688	37.688	38.594	38.594	38.906	98.906	0.0188	
3	3.0%	3.0%	3.04	3.04	0.00	0.00	3.04	3.04	0.235	0.240	37.406	37.313	37.250	38.438	38.438	38.438	124.594	0.0183	
5	3.0%	3.0%	4.97	4.97	0.00	0.00	4.97	4.97	0.275	0.283	37.261	37.156	37.344	37.219	38.500	38.593	147.469	0.0162	
7	3.0%	3.0%	0.73	0.73	0.00	0.00	0.73	0.73	0.320	0.315	37.031	36.938	36.875	38.156	38.219	38.219	149.313	0.0175	
8	3.0%	3.0%	2.81	2.82	0.00	0.00	2.81	2.82	0.338	0.343	37.000	37.000	38.094	38.125	38.156	38.125	163.531	0.0182	
10	3.0%	3.0%	3.79	3.79	0.00	0.00	3.79	3.79	0.348	0.353	36.944	36.719	36.875	38.094	38.094	38.094	170.531	0.0186	
11	3.0%	3.0%	4.75	4.75	0.00	0.00	4.75	4.75	0.360	0.360	36.875	36.656	36.813	38.188	38.188	38.188	189.438	0.0186	
0.5	3.0%	4.0%	0.53	0.53	0.00	0.00	0.53	0.53	0.128	0.128	38.375	38.594	38.438	39.156	39.000	39.219	78.688	0.0182	
1	3.0%	4.0%	1.05	1.05	0.00	0.00	1.05	1.05	0.176	0.175	38.044	37.969	38.156	38.969	39.188	39.188	88.281	0.0183	
3	3.0%	4.0%	2.97	2.97	0.00	0.00	2.97	2.97	0.258	0.260	37.844	37.719	37.938	38.444	38.656	38.444	112.969	0.0181	
5	3.0%	4.0%	5.01	5.01	0.00	0.00	5.01	5.01	0.308	0.313	38.031	38.094	37.906	38.750	38.625	38.781	123.750	0.0173	
7	3.0%	4.0%	0.77	0.77	0.00	0.00	0.77	0.77	0.348	0.348	37.858	37.813	37.625	39.063	38.969	38.969	134.531	0.0189	
8	3.0%	4.0%	2.73	2.73	0.00	0.00	2.73	2.73	0.373	0.373	38.000	37.938	38.094	38.094	38.156	38.156	140.313	0.0166	
10	3.0%	4.0%	3.78	3.77	0.00	0.00	3.78	3.77	0.398	0.413	37.944	38.219	37.906	38.381	38.381	38.381	144.656	0.0162	
11	3.0%	4.0%	4.75	4.75	0.00	0.00	4.75	4.75	0.418	0.428	37.800	37.219	37.531	37.261	38.594	38.438	161.281	0.0165	

Table B4.3 Asphalt treatment surface data

Disch/actual SL (%)	SX (%)	OWALL (CFS)		Offhor (CFS)		Ortal		Depth (ft)		Spread Dist T1 (in)		Curb Distance (in)		Spread Dist T2 (in)		AVG Spread in	n value Geomem Integrate						
		Initial	Final	Initial	Final	AVG	CFS	Min	Max	T1min	T1max	1st run	2nd run	Cmin	Cmax			T1min	T2max				
0.5	2.0%	0.50	0.50	0.00	0.00	0.00	0.00	0.50	0.103	0.103	39.219	39.281	40.313	40.250	40.344	117.500	117.563	78.221	0.0177				
1	2.0%	1.00	1.00	0.00	0.00	0.00	0.00	1.00	0.140	0.141	38.250	38.313	39.063	38.906	38.031	38.813	143.125	143.250	104.977	0.0194			
3	2.0%	3.02	3.02	0.00	0.00	0.00	0.00	3.02	0.186	0.186	36.375	36.125	36.406	36.219	36.063	38.969	183.969	183.688	150.031	0.0166			
5	2.0%	4.99	4.99	0.00	0.00	0.00	0.00	4.99	0.255	0.260	37.875	37.844	38.969	38.969	38.875	216.719	229.563	186.234	0.0179				
7	2.0%	1.5%																		0.0213			
9	2.0%	1.5%																					
10	2.0%	1.5%																					
11	2.0%	1.5%																					
1	2.0%	2.0%	0.50	0.00	0.00	0.00	0.00	0.50	0.118	0.119	38.281	38.188	38.313	38.250	38.938	38.969	101.688	101.688	83.430	0.0162			
3	2.0%	3.01	3.01	0.00	0.00	0.00	0.00	3.01	0.223	0.230	37.813	37.688	37.906	37.719	38.000	38.975	38.063	151.219	158.938	117.268	0.0136		
5	2.0%	5.00	5.01	0.00	0.00	0.00	0.00	5.00	0.265	0.275	37.719	37.594	37.813	37.531	38.781	38.975	38.781	180.375	189.563	147.297	0.0154		
7	2.0%	0.76	0.76	0.76	0.76	6.26	6.26	7.01	0.295	0.305	37.438	37.500	37.650	37.650	38.656	38.313	38.719	207.281	222.250	177.289	0.0215		
9	2.0%	2.76	2.76	2.76	2.76	6.25	6.25	6.25	0.325	0.335	37.500	37.281	37.469	37.344	38.531	38.688	227.250	238.844	195.414	0.0216			
10	2.0%	3.80	3.80	3.80	3.80	6.23	6.23	10.04	0.348	0.358	37.500	37.281	37.625	37.313	38.781	38.688	38.750	236.500	242.000	201.920	0.0177		
11	2.0%	2.0%	0.49	0.49	0.00	0.00	0.00	0.49	0.153	0.153	37.969	37.844	37.806	37.813	38.250	38.609	38.375	38.478	90.000	85.500	50.892	0.0133	
1	2.0%	2.5%	1.05	1.05	0.00	0.00	0.00	1.05	0.178	0.178	38.219	38.094	38.188	38.188	38.875	38.875	113.281	113.281	75.078	0.0175	0.0208		
3	2.0%	2.98	2.97	0.00	0.00	0.00	0.00	2.98	0.288	0.288	36.000	37.813	38.031	37.750	38.844	38.906	38.844	148.813	148.344	110.655	0.0176	0.0210	
5	2.0%	4.95	4.96	0.00	0.00	0.00	0.00	4.95	0.324	0.328	36.969	36.875	37.000	36.875	39.000	39.000	39.000	163.156	167.489	128.359	0.0154	0.0164	
7	2.0%	0.80	0.80	0.81	0.80	6.24	6.24	7.05	0.350	0.340	36.875	36.719	36.875	36.781	38.844	38.813	38.813	177.469	187.438	145.841	0.0153	0.0182	
9	2.0%	2.83	2.83	2.83	2.83	6.18	6.18	6.21	0.393	0.400	36.781	36.656	36.844	36.750	38.750	38.813	200.438	208.938	166.938	0.0172	0.0204		
10	2.0%	3.73	3.73	3.73	3.73	6.19	6.21	9.93	0.420	0.428	36.781	36.625	36.666	36.666	38.813	38.844	38.844	207.500	214.000	174.168	0.0174	0.0206	
11	2.0%	4.80	4.81	4.82	4.81	6.18	6.17	10.89	0.443	0.450	36.625	36.531	36.656	36.563	38.875	38.875	38.750	219.344	220.719	180.461	0.0173	0.0206	
0.5	2.0%	0.53	0.53	0.00	0.00	0.00	0.00	0.53	0.143	0.143	37.938	37.813	38.000	37.844	38.938	38.875	38.031	38.875	87.906	87.906	50.009	0.0158	0.0188
1	2.0%	3.0%	1.04	1.04	0.00	0.00	0.00	1.04	0.173	0.173	37.813	37.688	37.844	37.750	39.063	39.000	39.000	103.750	103.750	65.984	0.0169	0.0200	
3	2.0%	3.02	3.03	0.00	0.00	0.00	0.00	3.02	0.245	0.250	37.261	37.188	37.344	37.125	38.625	38.688	136.281	144.469	104.448	0.0197	0.0234		
5	2.0%	4.96	4.96	0.00	0.00	0.00	0.00	4.95	0.290	0.300	36.906	37.063	36.969	36.875	38.719	38.563	150.750	155.156	115.929	0.0160	0.0190		
7	2.0%	0.76	0.76	0.76	0.76	6.20	6.20	6.96	0.330	0.338	36.938	36.781	36.938	36.781	38.594	38.531	38.563	162.469	170.093	129.689	0.0153	0.0182	
9	2.0%	2.82	2.82	2.82	2.82	6.19	6.20	6.20	0.385	0.393	36.625	36.469	36.531	36.500	38.656	38.531	38.563	175.438	180.093	141.203	0.0148	0.0176	
10	2.0%	3.84	3.84	3.84	3.84	6.16	6.16	10.00	0.403	0.413	36.500	36.344	36.563	36.375	38.500	38.406	38.563	180.281	189.906	148.848	0.0153	0.0182	
11	2.0%	5.08	5.08	5.08	5.08	6.15	6.14	11.22	0.413	0.423	36.500	36.313	36.563	36.375	38.125	38.031	38.031	186.094	186.625	155.938	0.0155	0.0185	
0.5	2.0%	0.53	0.53	0.00	0.00	0.00	0.00	0.53	0.148	0.148	37.750	37.594	37.750	37.625	38.813	38.844	38.781	79.906	79.906	47.221	0.0161	0.0192	
1	2.0%	0.99	0.99	0.00	0.00	0.00	0.00	0.99	0.200	0.200	37.156	36.969	36.969	36.875	38.656	38.688	38.000	89.219	89.219	52.133	0.0151	0.0179	
3	2.0%	3.04	3.04	0.00	0.00	0.00	0.00	3.04	0.273	0.275	37.063	36.813	37.031	36.875	38.663	38.438	38.563	127.750	127.750	85.905	0.0166	0.0222	
5	2.0%	5.01	5.01	0.00	0.00	0.00	0.00	5.01	0.330	0.333	36.750	36.666	36.761	36.666	38.594	38.500	38.566	134.313	139.094	99.930	0.0170	0.0202	
7	2.0%	0.85	0.85	0.85	0.85	6.16	6.15	6.14	0.405	0.410	36.469	36.313	36.469	36.313	38.438	38.344	38.438	147.938	152.063	109.464	0.0155	0.0184	
9	2.0%	2.82	2.83	2.83	2.83	6.14	6.14	8.97	0.433	0.443	36.438	36.281	36.438	36.281	38.438	38.469	38.469	150.313	160.625	119.094	0.0151	0.0180	
10	2.0%	4.0%	3.95	3.96	3.95	6.11	6.12	10.07	0.460	0.475	36.344	36.344	36.313	36.306	38.344	38.250	38.313	163.500	163.500	122.492	0.0146	0.0173	
11	2.0%	4.0%																					

Table B4.4 Asphalt treatment surface data

Discharge actual cfs	SL (%)	SX (%)	QWALL (CFS)		Qfloor (CFS)		Qtotal		Depth (ft)		Spread Dist T1 (in)		Curb Distance (in)		Spread Dist T2 (in)		AVG Spread in	n value	
			Initial	Final	Initial	Final	AVG	Max	T1min	T1max	Cmin	Cmax	T1min	T1max	T2min	T2max			
			1st run	2nd run	1st run	2nd run	1st run	2nd run	1st run	2nd run	1st run	2nd run	1st run	2nd run	1st run	2nd run			
0.5	1.0%	1.5%	0.49	0.49	0.00	0.00	0.49	0.49	0.145	0.145	39.500	39.500	39.500	39.500	118.750	118.750	80.363	0.0167	
1	1.0%	1.5%	0.99	0.99	0.00	0.00	0.99	0.99	0.180	0.180	39.500	39.500	39.500	39.500	148.031	148.031	109.656	0.0184	
3	1.0%	1.5%	2.99	2.99	0.00	0.00	2.99	2.99	0.250	0.250	39.031	37.939	39.031	39.250	39.313	215.094	215.094	177.063	0.0219
5	1.0%	1.5%																	
7	1.0%	1.5%																	
9	1.0%	1.5%																	
10	1.0%	1.5%																	
11	1.0%	1.5%																	
0.5	1.0%	2.0%	0.50	0.50	0.00	0.00	0.50	0.50	0.120	0.120	39.313	38.031	39.250	39.969	39.281	109.969	110.000	71.938	0.0161
1	1.0%	2.0%	1.00	1.00	0.00	0.00	1.00	1.00	0.155	0.155	39.625	38.888	39.625	39.625	39.625	132.500	132.500	93.945	0.0164
3	1.0%	2.0%	3.01	3.01	0.00	0.00	3.01	3.01	0.263	0.270	39.156	38.063	39.156	39.406	39.406	173.594	173.594	136.477	0.0144
5	1.0%	2.0%	5.02	5.01	0.00	0.00	5.02	5.02	0.315	0.325	37.844	37.719	39.188	39.156	39.188	218.689	221.125	182.139	0.0227
7	1.0%	2.5%	0.75	0.75	0.00	0.00	0.75	0.75	0.345	0.345	39.000	37.781	39.688	39.500	39.500	235.500	242.125	200.898	0.0213
9	1.0%	2.0%																	
10	1.0%	2.0%																	
11	1.0%	2.0%																	
0.5	1.0%	2.5%	0.50	0.50	0.00	0.00	0.50	0.50	0.123	0.123	39.156	38.094	39.219	39.125	39.125	99.125	99.406	61.117	0.0150
1	1.0%	2.5%	0.99	0.99	0.00	0.00	0.99	0.99	0.193	0.197	37.844	37.669	37.906	39.031	39.031	121.125	121.125	83.344	0.0207
3	1.0%	2.5%	3.01	3.01	0.00	0.00	3.01	3.01	0.271	0.276	37.469	37.315	37.500	37.813	39.969	161.063	162.688	124.609	0.0198
5	1.0%	2.5%	4.98	4.98	0.00	0.00	4.98	4.98	0.309	0.313	37.188	37.281	37.656	39.813	39.813	185.000	192.094	152.227	0.0201
7	1.0%	2.5%	0.75	0.75	0.00	0.00	0.75	0.75	0.353	0.358	37.094	36.969	37.000	39.656	39.656	202.844	214.188	171.438	0.0201
9	1.0%	2.5%	2.79	2.79	0.00	0.00	2.79	2.79	0.394	0.399	39.938	39.613	39.781	39.781	39.781	223.063	223.094	189.625	0.0204
10	1.0%	2.5%	3.83	3.83	0.00	0.00	3.83	3.83	0.406	0.410	39.875	39.688	39.906	39.750	39.750	230.625	237.656	197.068	0.0203
11	1.0%	2.5%																	
0.5	1.0%	3.0%	0.49	0.49	0.00	0.00	0.49	0.49	0.158	0.158	37.500	38.031	38.031	38.844	38.844	90.281	90.281	52.344	0.0161
1	1.0%	3.0%	1.00	1.00	0.00	0.00	1.00	1.00	0.194	0.194	37.500	37.669	37.669	38.844	38.844	113.031	113.031	75.391	0.0211
3	1.0%	3.0%	2.98	2.97	0.00	0.00	2.97	2.97	0.275	0.277	37.531	37.469	37.669	39.750	39.906	147.188	147.188	108.688	0.0193
5	1.0%	3.0%	4.98	4.98	0.00	0.00	4.98	4.98	0.313	0.315	37.188	37.219	37.188	39.781	39.688	185.281	171.000	139.938	0.0165
7	1.0%	3.0%	0.82	0.82	0.00	0.00	0.82	0.82	0.400	0.401	37.094	36.969	36.969	39.781	39.625	177.594	190.656	147.068	0.0189
9	1.0%	3.0%	2.84	2.84	0.00	0.00	2.84	2.84	0.427	0.430	39.430	39.688	39.688	39.688	39.688	200.844	209.469	168.391	0.0167
10	1.0%	3.0%	3.81	3.80	0.00	0.00	3.81	3.81	0.450	0.455	39.625	39.625	39.625	39.188	39.188	203.563	214.750	172.578	0.0167
11	1.0%	3.0%	4.82	4.83	0.00	0.00	4.82	4.82	0.487	0.487	39.656	39.656	39.656	39.656	39.656	211.469	221.875	180.070	0.0165
0.5	1.0%	4.0%	0.50	0.50	0.00	0.00	0.50	0.50	0.155	0.156	39.188	38.094	39.250	39.156	39.188	83.406	83.406	45.289	0.0145
1	1.0%	4.0%	1.01	1.01	0.00	0.00	1.01	1.01	0.238	0.238	39.219	38.000	39.219	39.344	39.250	98.281	98.281	60.195	0.0182
3	1.0%	4.0%	2.98	2.98	0.00	0.00	2.98	2.98	0.332	0.332	37.531	37.669	37.469	39.625	39.625	126.594	126.594	90.438	0.0163
5	1.0%	4.0%	4.98	4.98	0.00	0.00	4.98	4.98	0.403	0.408	37.188	37.188	37.188	39.063	39.063	147.094	147.219	109.644	0.0169
7	1.0%	4.0%	0.82	0.82	0.00	0.00	0.82	0.82	0.445	0.441	39.675	39.675	39.675	39.675	39.675	157.688	162.875	123.289	0.0149
9	1.0%	4.0%	2.84	2.84	0.00	0.00	2.84	2.84	0.469	0.469	39.688	39.688	39.688	39.688	39.688	167.750	174.594	134.289	0.0146
10	1.0%	4.0%																	
11	1.0%	4.0%																	

Table B4.5 Asphalt treatment surface data

Discharge actual Q cfs	SL (%)	SX (%)	QWALL (CFS)		Qfloor (CFS)		Qtotal		Depth (ft)		Spread Dist T1 (lin)		Curb Distance (in)		Spread Dist T2 (in)		AVG Spread in	n value Geometri Integrator							
			Initial	Final	Initial	Final	AVG	Max	T1min	T2max	Cmin	Cmax	T1min	T2max	T1min	T2max									
			1st run	2nd run	1st run	2nd run	1st run	2nd run	1st run	2nd run	1st run	2nd run	1st run	2nd run	1st run	2nd run									
0.5	0.5%	1.5%	0.48	0.48	0.00	0.00	0.48	0.136	0.136	0.136	39.281	38.344	39.313	38.156	39.469	123.625	128.438	128.563	88.508	0.0127	0.0151				
1	0.5%	1.5%	1.01	1.01	0.00	0.00	1.01	0.180	0.180	0.180	39.219	38.063	39.406	38.031	39.406	159.938	169.938	160.031	160.156	0.0140	0.0167				
3	0.5%	1.5%																							
5	0.5%	1.5%																							
7	0.5%	1.5%																							
9	0.5%	1.5%																							
10	0.5%	1.5%																							
11	0.5%	1.5%																							
0.5	0.5%	2.0%	0.49	0.49	0.00	0.00	0.49	0.153	0.153	0.153	37.719	37.844	37.969	38.375	38.438	121.375	121.375	121.313	121.344	83.538	0.0172	0.0204			
1	0.5%	2.0%	1.05	1.05	0.00	0.00	1.05	0.198	0.198	0.198	37.656	38.094	37.906	38.125	38.438	143.863	146.281	144.094	146.375	107.234	0.0157	0.0187			
3	0.5%	2.0%	2.95	2.95	0.00	0.00	2.95	0.308	0.313	0.310	37.281	37.625	37.344	37.813	38.688	192.188	188.094	182.250	198.188	157.664	0.0156	0.0185			
5	0.5%	2.0%																							
7	0.5%	2.0%																							
9	0.5%	2.0%																							
10	0.5%	2.0%																							
11	0.5%	2.0%																							
0.5	0.5%	2.5%	0.50	0.50	0.00	0.00	0.50	0.173	0.173	0.172	37.688	37.781	37.688	37.813	38.719	38.219	104.631	104.094	104.094	68.570	0.0133	0.0159			
1	0.5%	2.5%	1.03	1.03	0.00	0.00	1.03	0.220	0.225	0.220	37.469	37.688	38.000	38.906	38.188	135.500	135.500	135.438	137.719	97.719	0.0181	0.0215			
3	0.5%	2.5%	2.98	2.98	0.00	0.00	2.98	0.368	0.373	0.373	37.031	37.375	37.031	37.063	38.063	39.000	172.719	177.094	173.719	176.906	137.734	0.0154	0.0184		
5	0.5%	2.5%	5.01	5.01	0.00	0.00	5.01	0.398	0.405	0.398	37.438	37.063	37.438	38.719	38.906	213.688	216.969	243.750	216.500	185.464	0.0210	0.0250			
7	0.5%	2.5%	0.88	0.87	0.87	6.15	6.17	7.03	0.455	0.460	36.250	37.125	36.156	36.313	39.000	36.375	39.031	229.688	237.313	229.625	237.344	198.820	0.0170	0.0203	
9	0.5%	2.5%																							
10	0.5%	2.5%																							
11	0.5%	2.5%																							
0.5	0.5%	3.0%	0.49	0.50	0.00	0.00	0.49	0.180	0.180	0.180	37.938	38.781	37.906	38.781	38.500	38.656	38.531	38.656	38.781	98.781	61.422	0.0147	0.0175		
1	0.5%	3.0%	1.00	1.00	0.00	0.00	1.00	0.240	0.243	0.241	37.500	38.063	38.156	38.344	38.688	125.750	125.750	125.875	125.875	87.862	0.0168	0.0224			
3	0.5%	3.0%	3.02	3.03	0.00	0.00	3.02	0.338	0.343	0.343	36.989	37.344	38.313	38.486	38.844	162.406	162.406	162.406	162.406	124.981	0.0159	0.0190			
5	0.5%	3.0%	4.98	4.98	0.00	0.00	4.98	0.408	0.415	0.408	36.375	37.094	38.688	38.031	38.688	38.625	187.688	194.000	187.719	194.094	154.164	0.0168	0.0201		
7	0.5%	3.0%	0.82	0.82	0.82	6.15	6.18	6.98	0.473	0.480	0.474	0.481	36.375	36.406	38.719	39.063	208.563	210.375	208.625	210.469	173.103	0.0164	0.0196		
9	0.5%	3.0%																							
10	0.5%	3.0%																							
11	0.5%	3.0%																							
0.5	0.5%	4.0%	0.50	0.49	0.00	0.00	0.49	0.203	0.203	0.203	37.688	38.031	37.688	38.031	38.469	38.688	38.469	38.656	38.469	89.375	89.406	89.375	51.523	0.0146	0.0174
1	0.5%	4.0%	1.00	1.00	0.00	0.00	1.00	0.245	0.248	0.245	37.406	38.000	37.469	37.938	38.531	38.875	187.719	187.719	187.719	107.719	70.016	0.0164	0.0195		
3	0.5%	4.0%	3.03	3.03	0.00	0.00	3.03	0.370	0.375	0.375	36.781	37.688	38.625	37.719	38.844	38.844	147.625	150.188	147.625	150.125	111.688	0.0188	0.0225		
5	0.5%	4.0%	4.98	4.98	0.00	0.00	4.98	0.455	0.460	0.455	38.281	37.375	38.281	37.656	38.313	38.938	185.813	170.125	165.813	170.125	131.070	0.0175	0.0208		
7	0.5%	4.0%																							
9	0.5%	4.0%																							
10	0.5%	4.0%																							
11	0.5%	4.0%																							

APPENDIX C

MANNING'S N-VALUES ESTIMATED BY PRANDTL-VON KARMAN VELOCITY METHOD

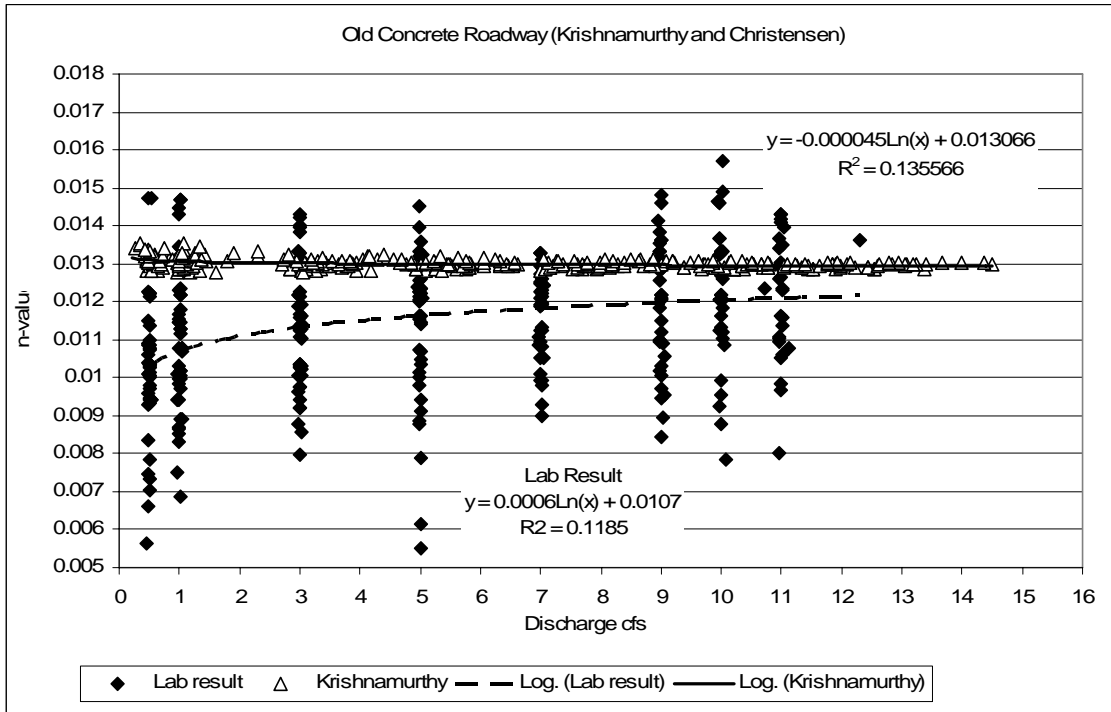


Figure C1.1 Manning's n-value and discharge of smooth concrete surface estimated by Krishnamurthy and Christensen's equation

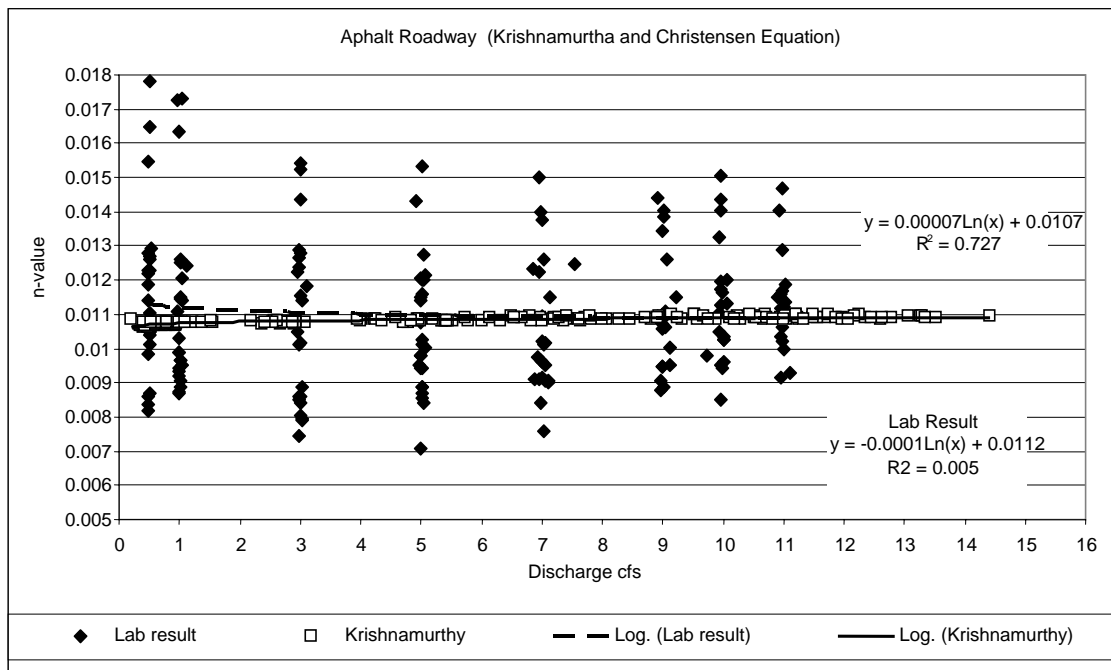


Figure C1.2 Manning's n-value and discharge of asphalt surface estimated by Krishnamurthy and Christensen's equation

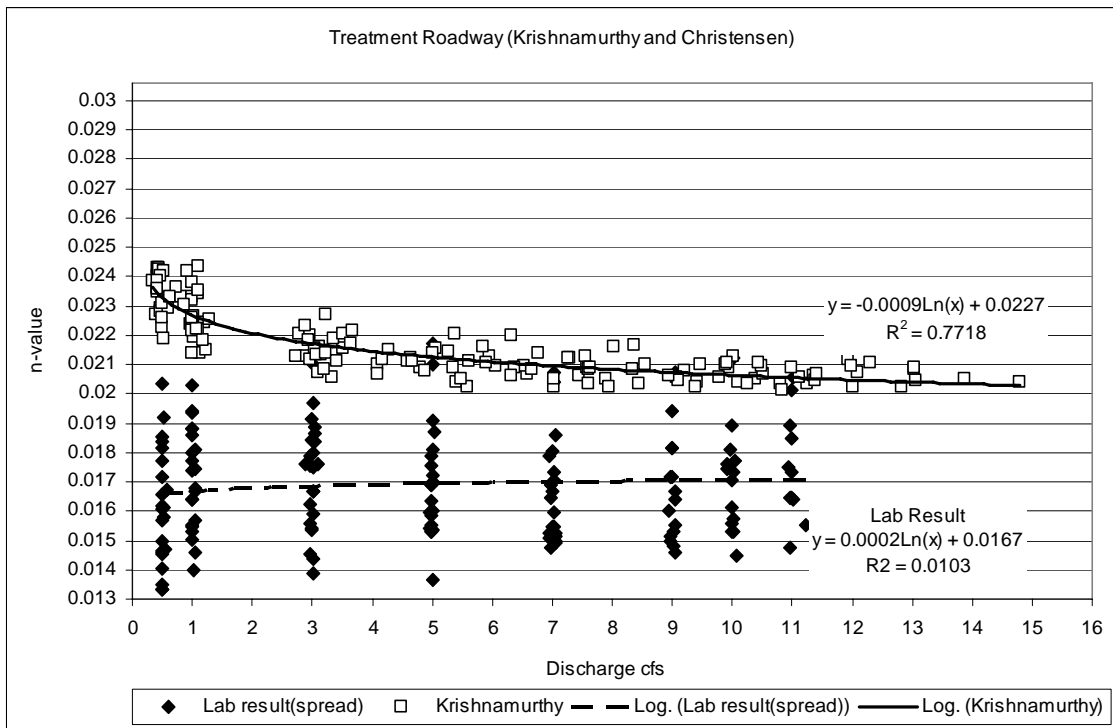


Figure C1.3 Manning's n-value and discharge of asphalt treatment surface estimated by Krishnamurthy and Christensen's equation

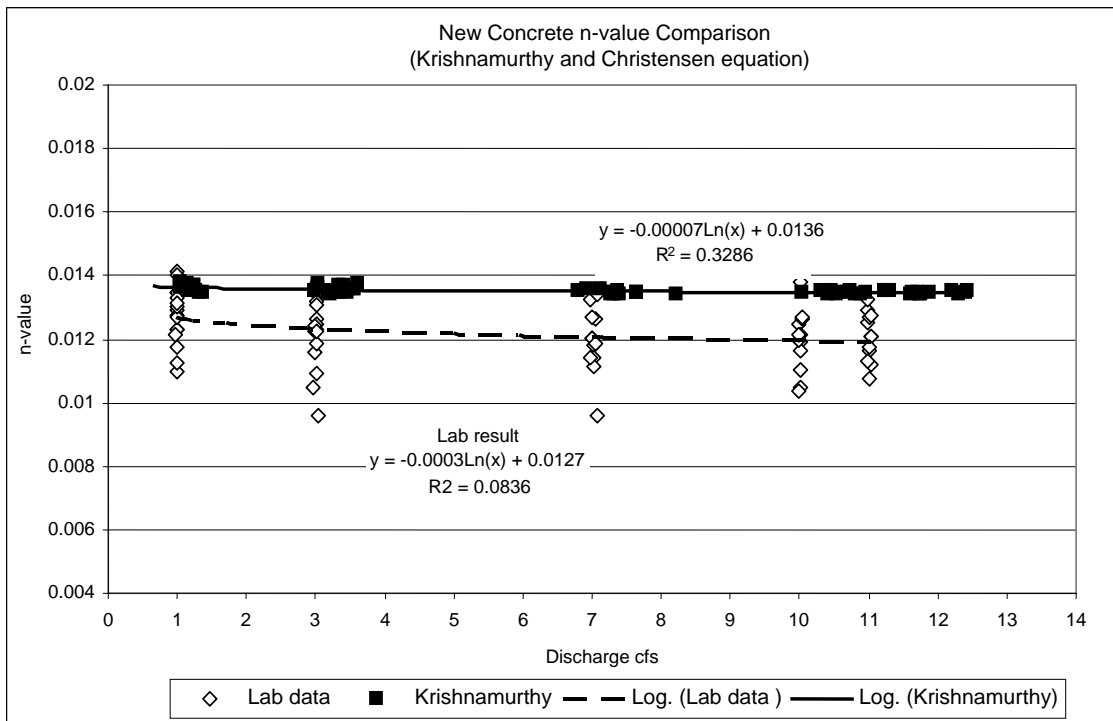


Figure C1.4 Manning's n-value and discharge of TxDOT concrete surface estimated by Krishnamurthy and Christensen's equation

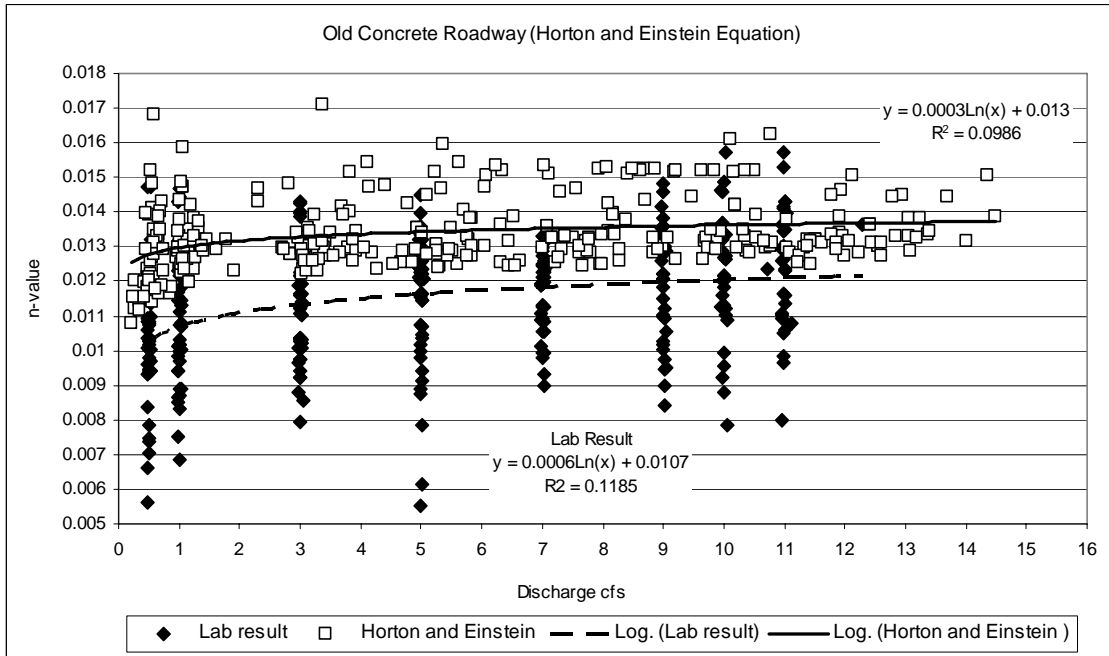


Figure C2.1 Manning's n-value and discharge of smooth concrete surface estimated by Horton and Einstein's equation

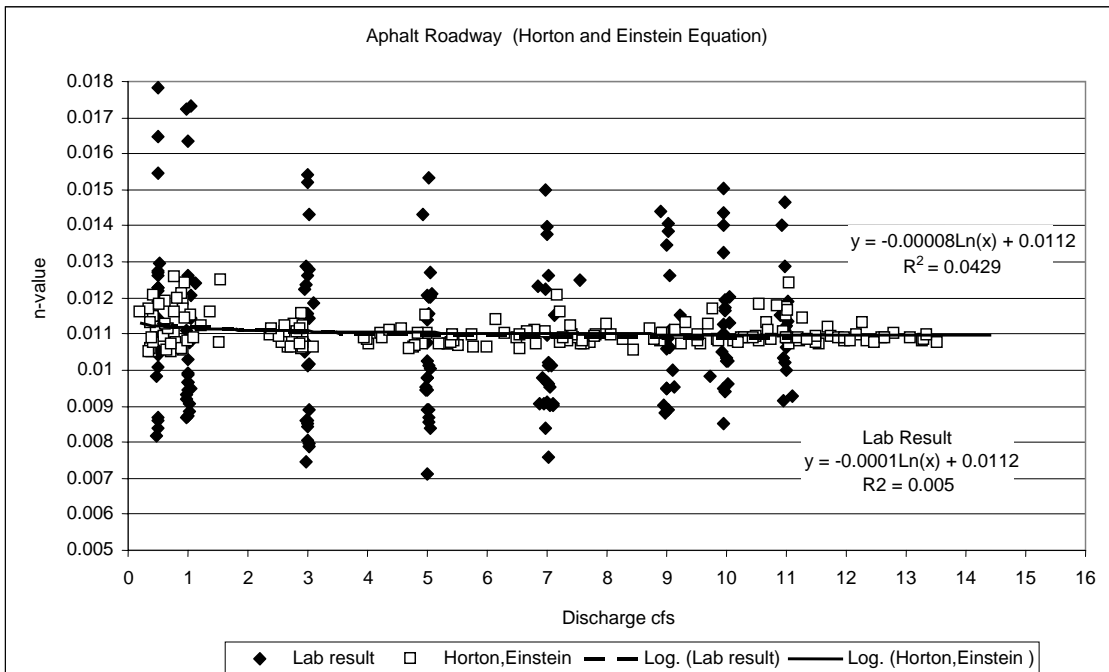


Figure C2.2 Manning's n-value and discharge of asphalt surface estimated by Horton and Einstein's equation

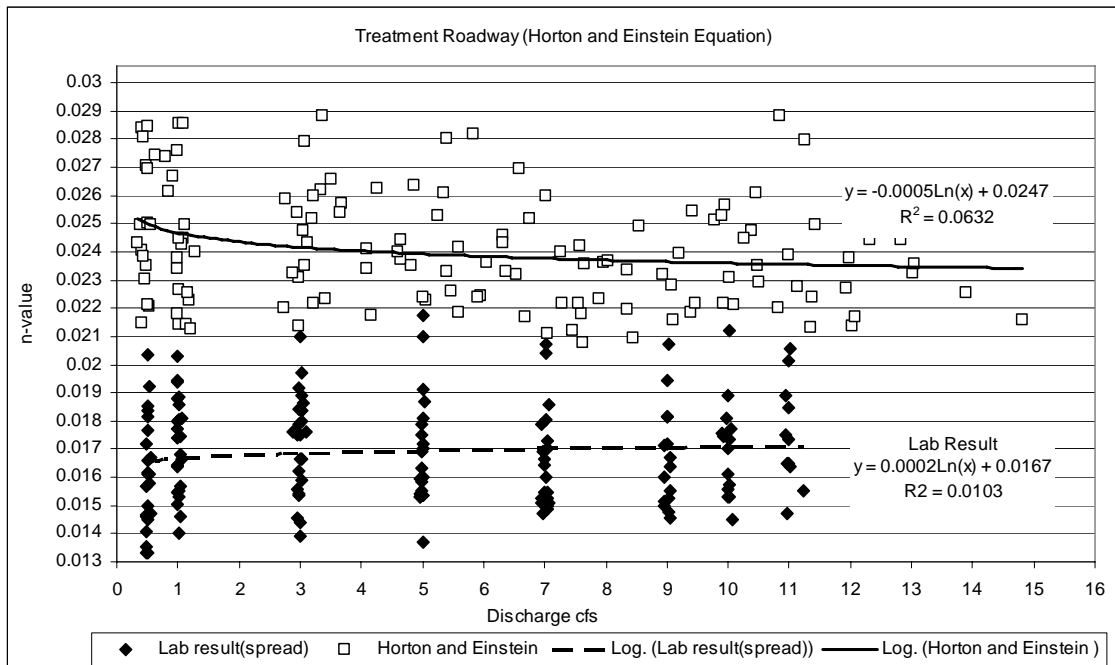


Figure C2.3 Manning's n-value and discharge of asphalt treatment surface estimated by Horton and Einstein's equation

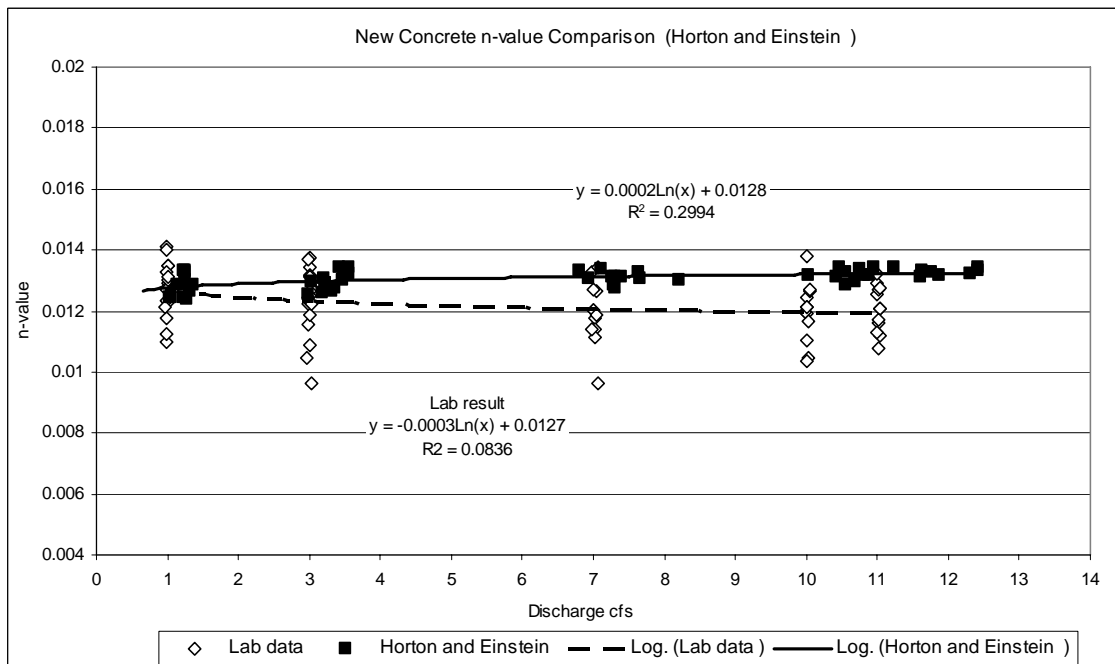


Figure C2.4 Manning's n-value and discharge of TxDOT concrete surface estimated by Horton and Einstein's equation

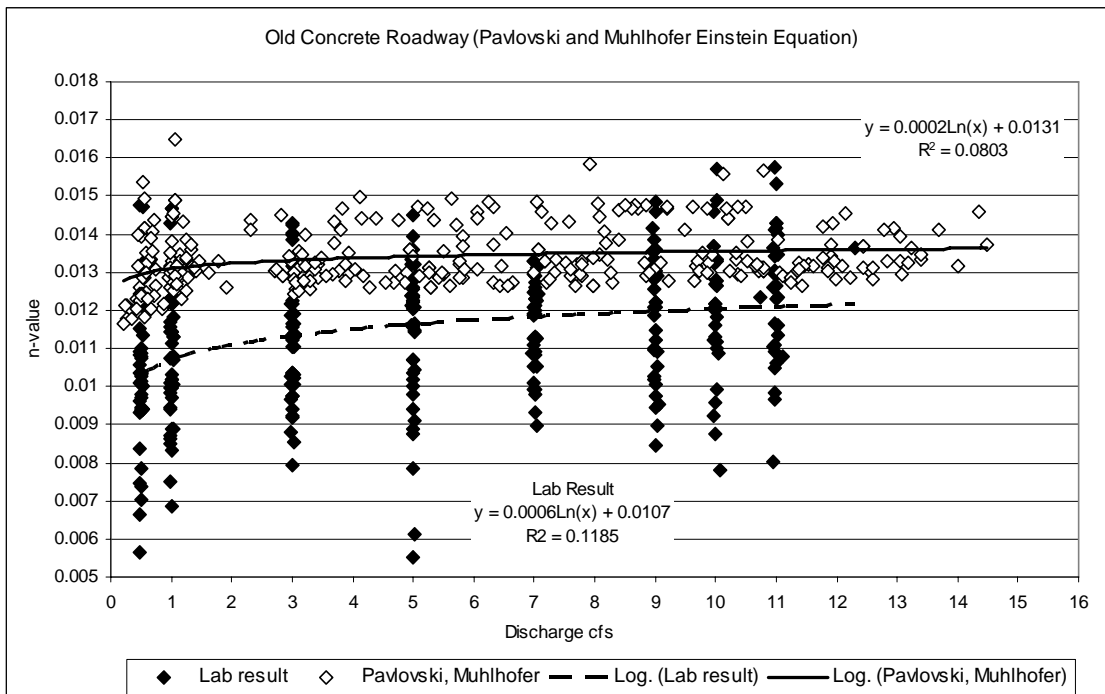


Figure C3.1 Manning's n-value and discharge of smooth concrete roadway estimated by Pavlovski, Muhlhofer, Einstein and Banks's equation

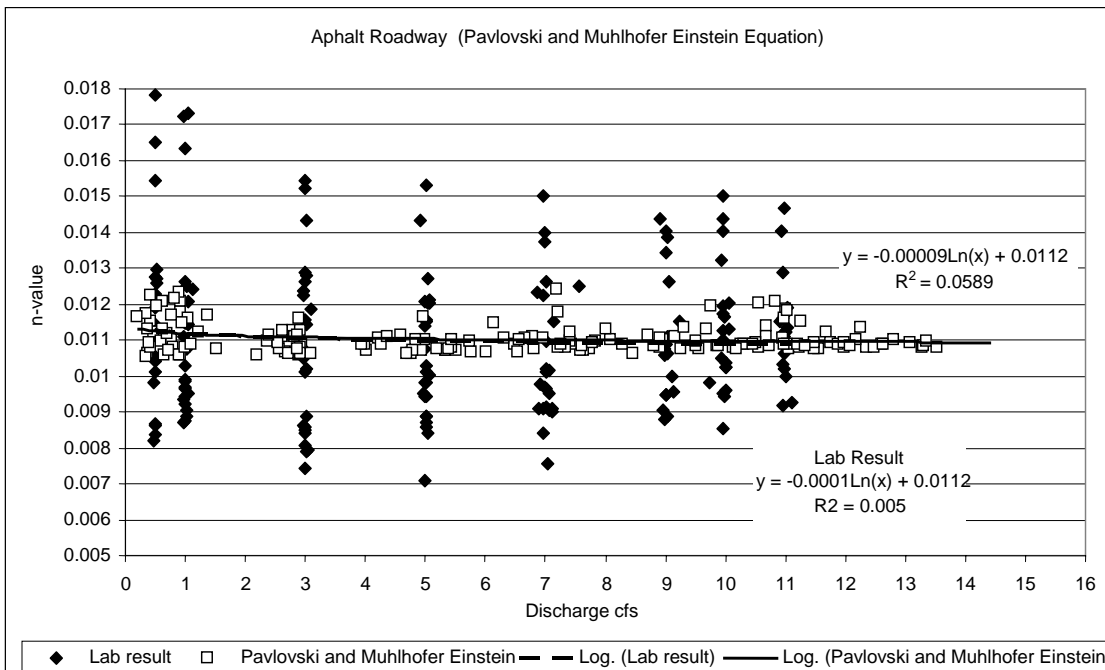


Figure C3.2 Manning's n-values and discharges of asphalt Roadway estimated by Pavlovski, Muhlhofer, Einstein and Banks's equation

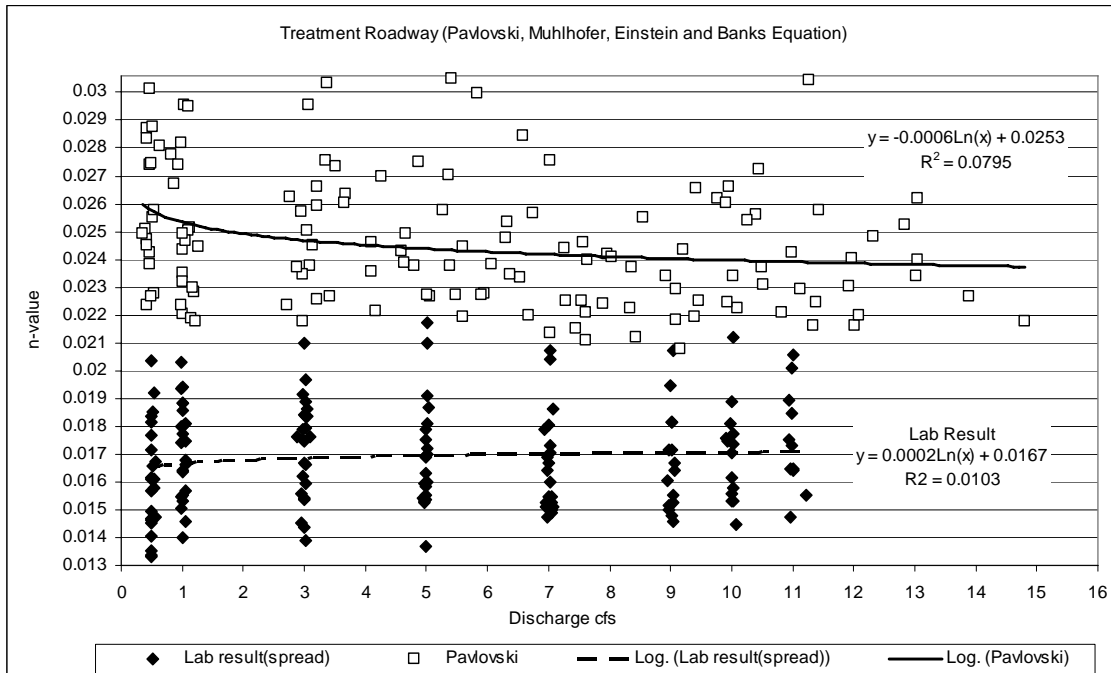


Figure C3.3 Manning's n-values and discharges of asphalt treatment roadway estimated by Pavlovski, Muhlhofer, Einstein and Banks's equation

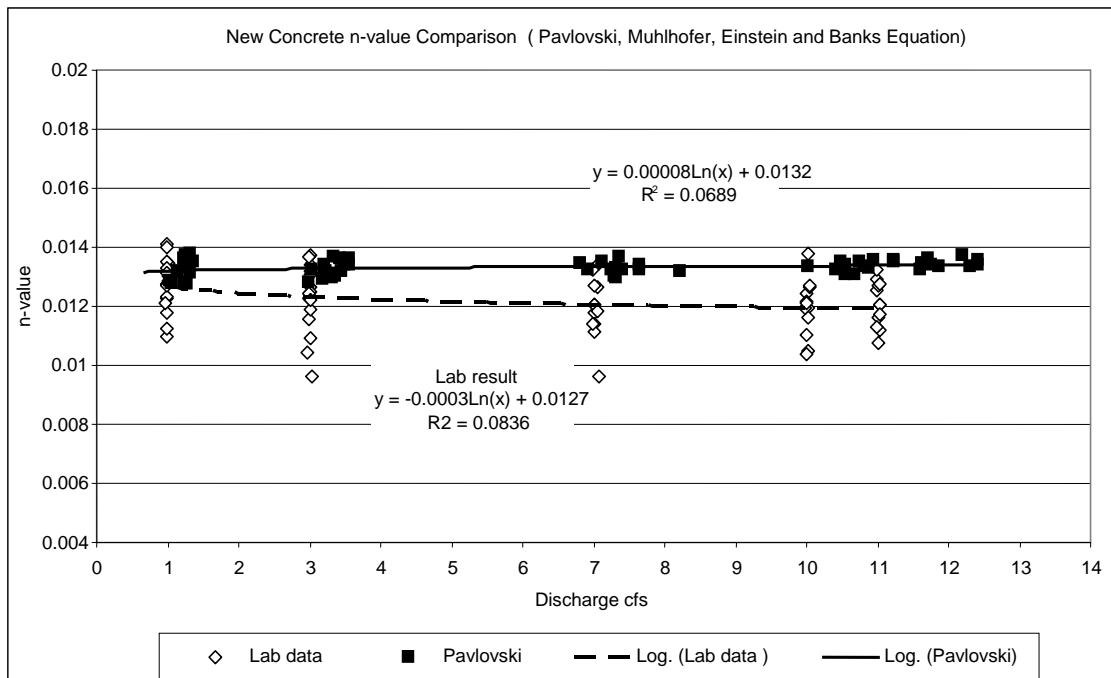


Figure C3.4 Manning's n-values and discharges of TxDOT concrete roadway estimated by Pavlovski, Muhlhofer, Einstein and Banks's equation

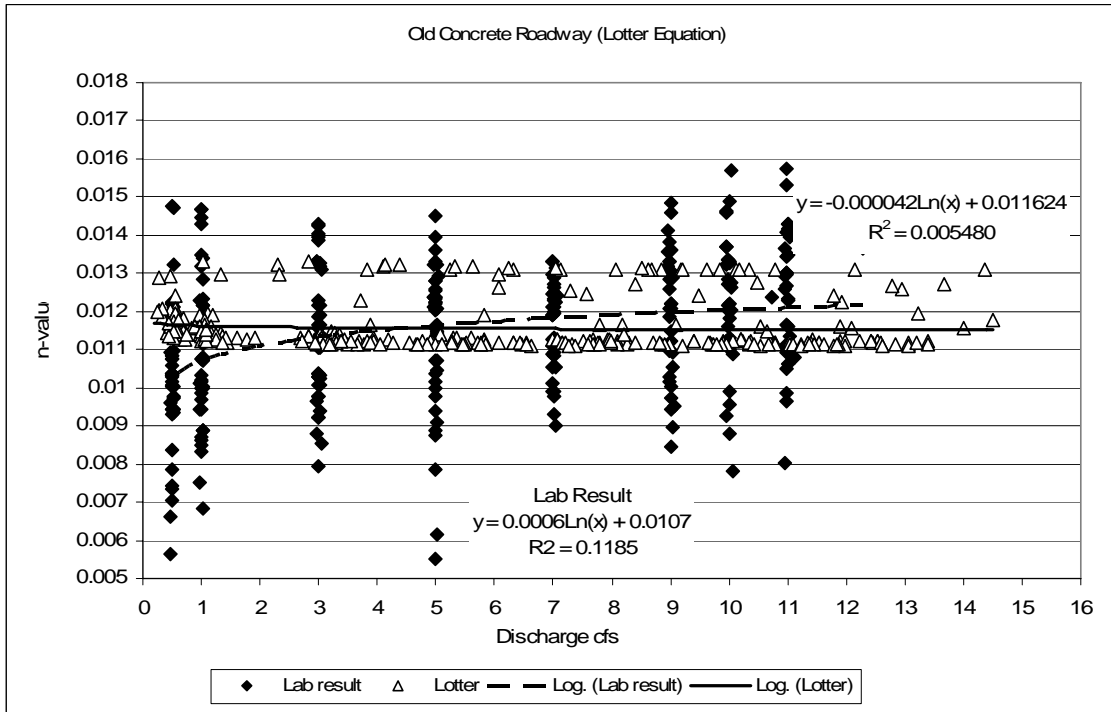


Figure C4.1 Manning's n-values and discharges of smooth concrete roadway estimated by Lotter's equation

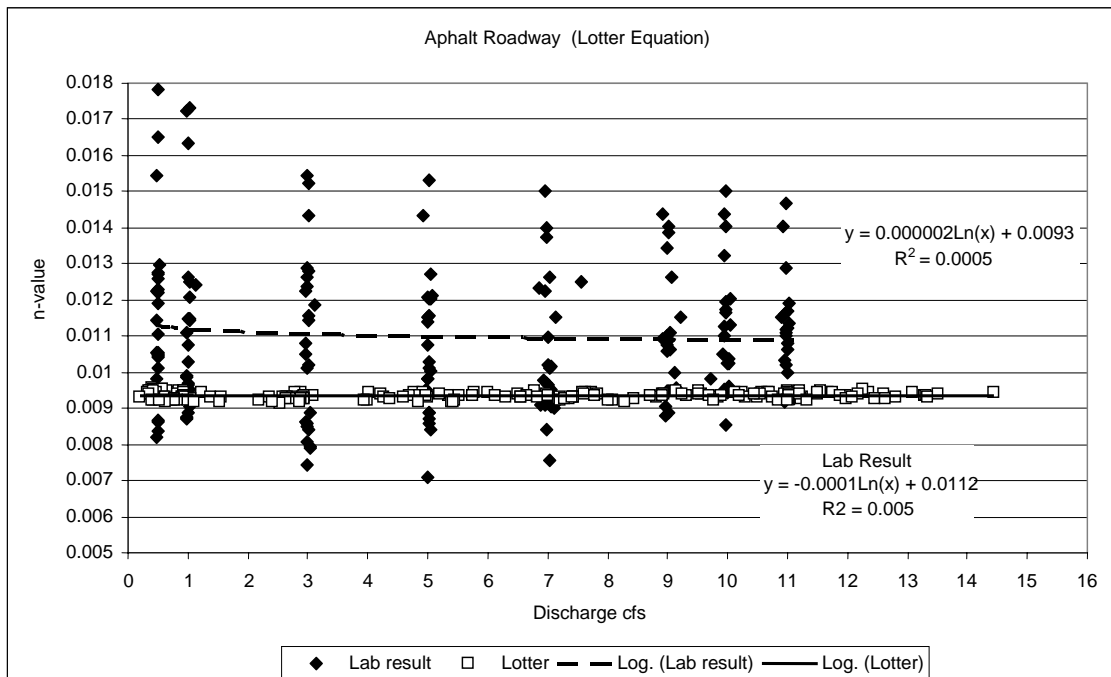


Figure C4.2 Manning's n-values and discharges of asphalt roadway estimated by Lotter's equation

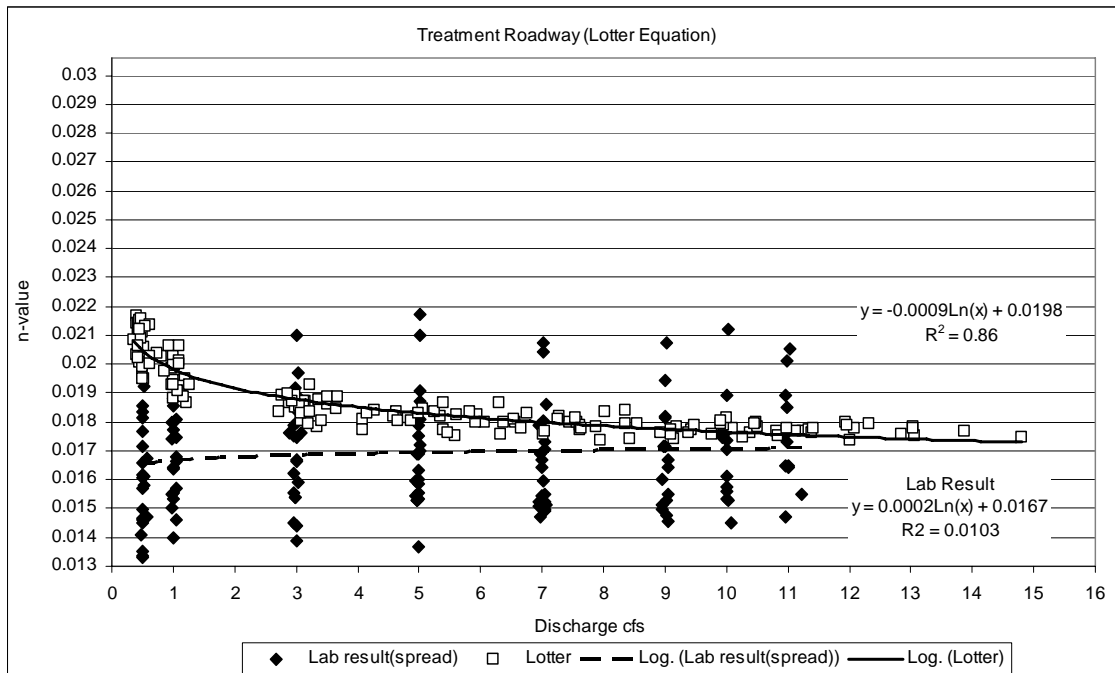


Figure C4.3 Manning's n-values and discharges of asphalt treatment roadway estimated by Lotter's equation

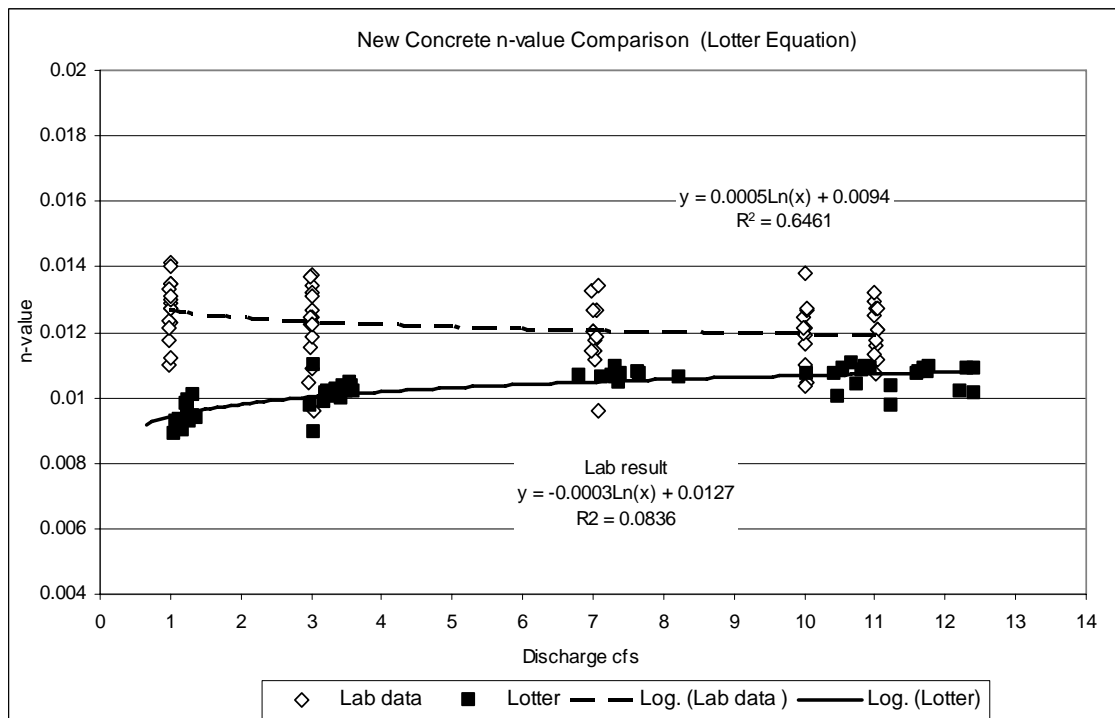


Figure C4.4 Manning's n-values and discharges of TxDOT concrete roadway estimated by Lotter's equation

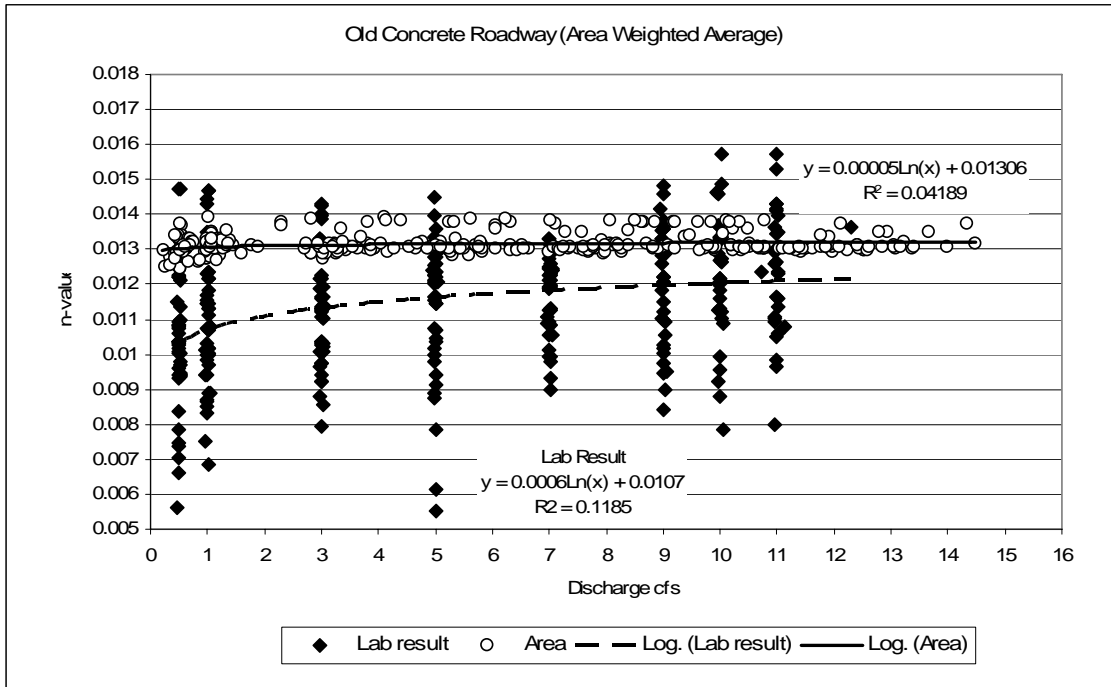


Figure C5.1 Manning's n-values and discharges of smooth concrete surface estimated by Area-Weight averaging method

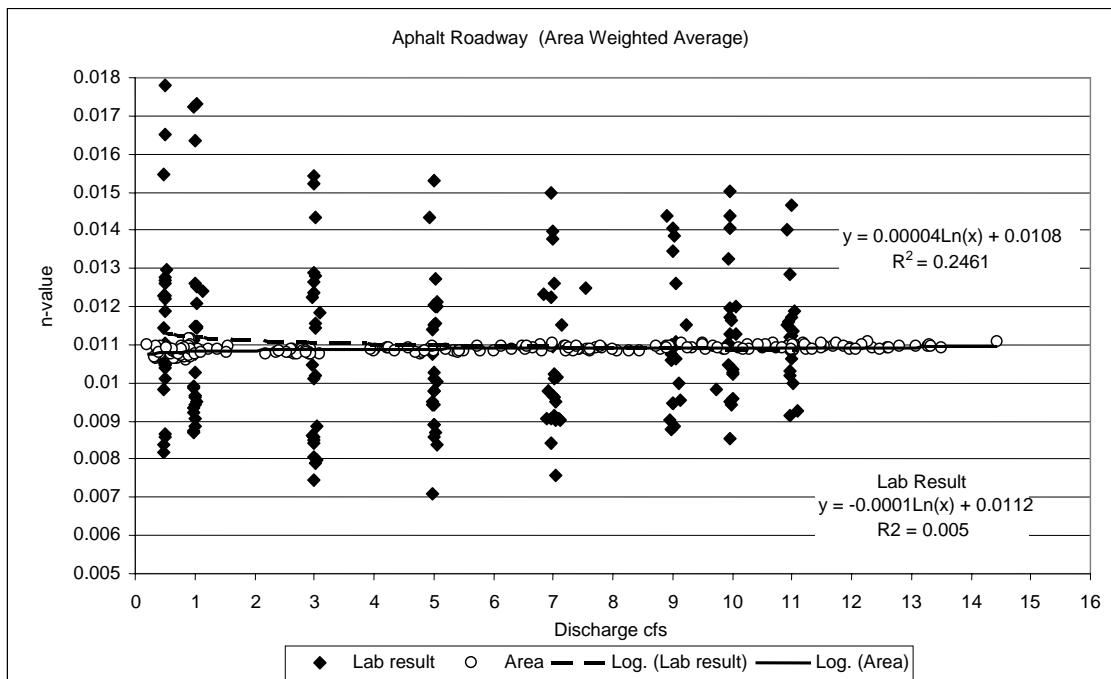


Figure C5.2 Manning's n-values and discharges of asphalt surface estimated by area-weight averaging method

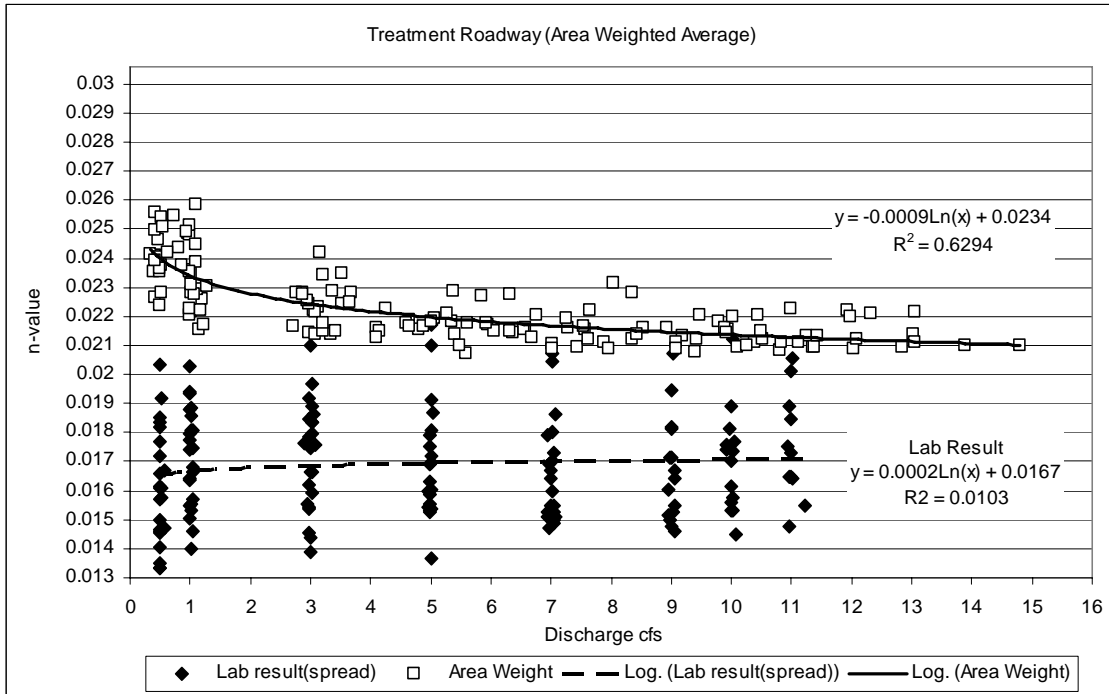


Figure C5.3 Manning's n-values and discharges of asphalt treatment surface estimated by area-weight averaging method

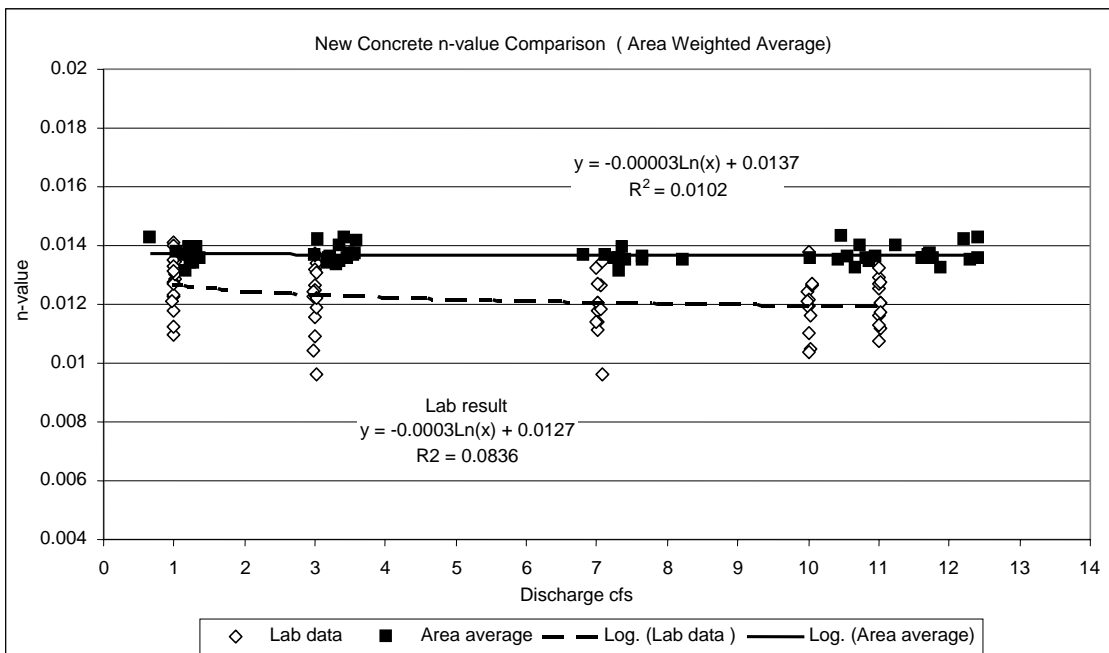


Figure C5.4 Manning's n-values and discharges of TxDOT concrete surface estimated by area-weight averaging method

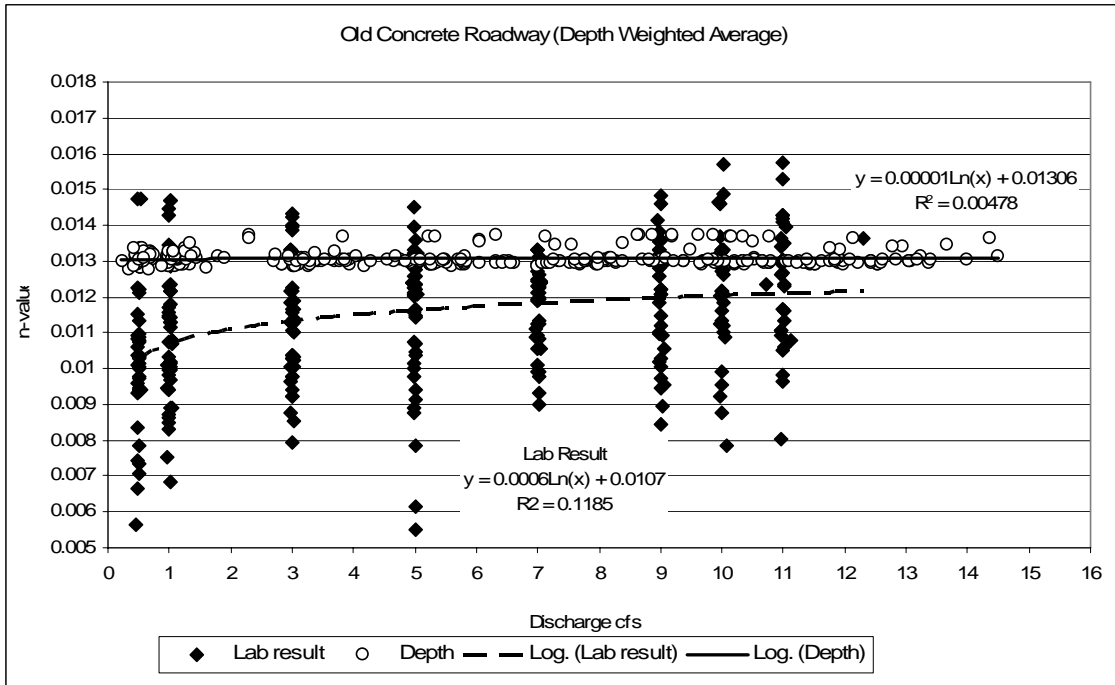


Figure C6.1 Manning's n-values and discharges of smooth concrete surface estimated by depth-weight averaging method

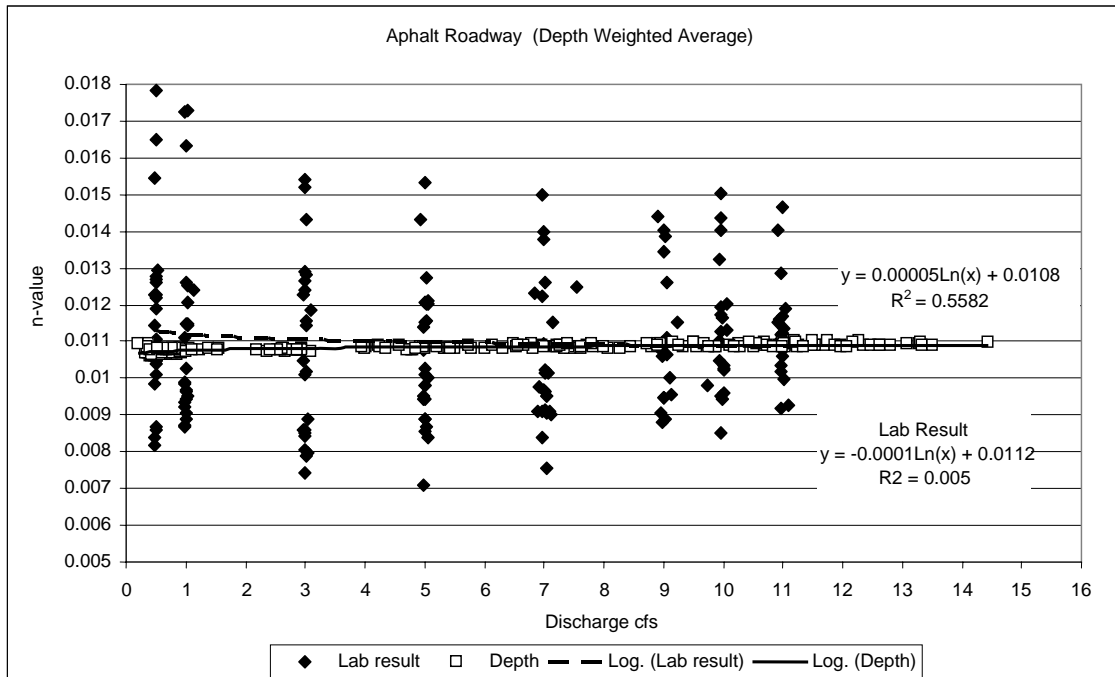


Figure C6.2 Manning's n-values and discharges of asphalt surface estimated by depth-weight averaging method

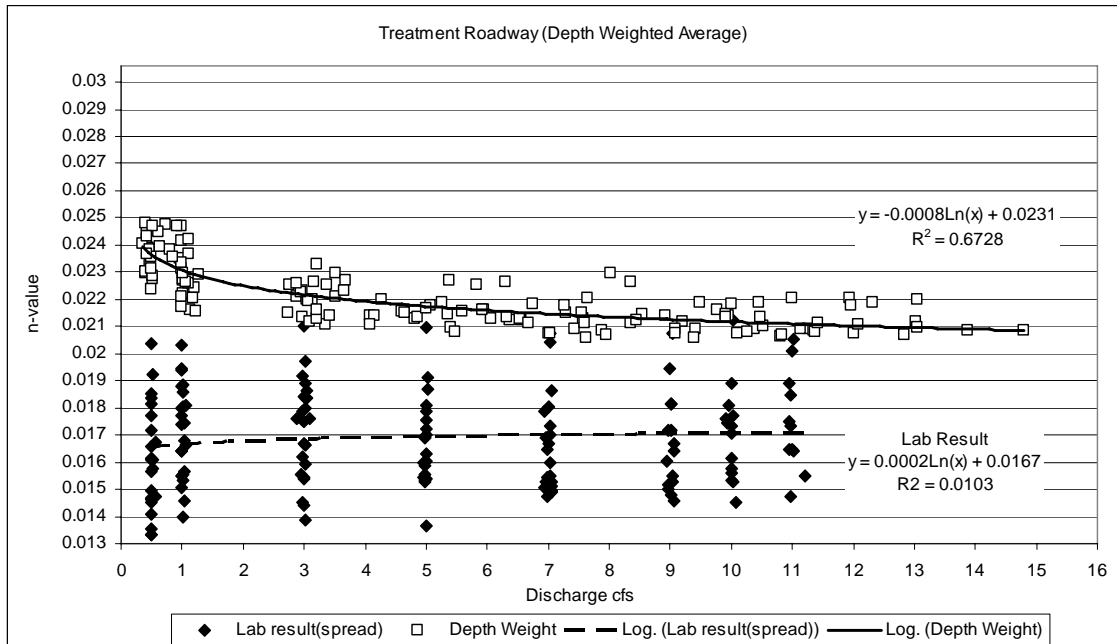


Figure C6.3 Manning's n-values and discharges of asphalt treatment surface estimated by depth-weight averaging method

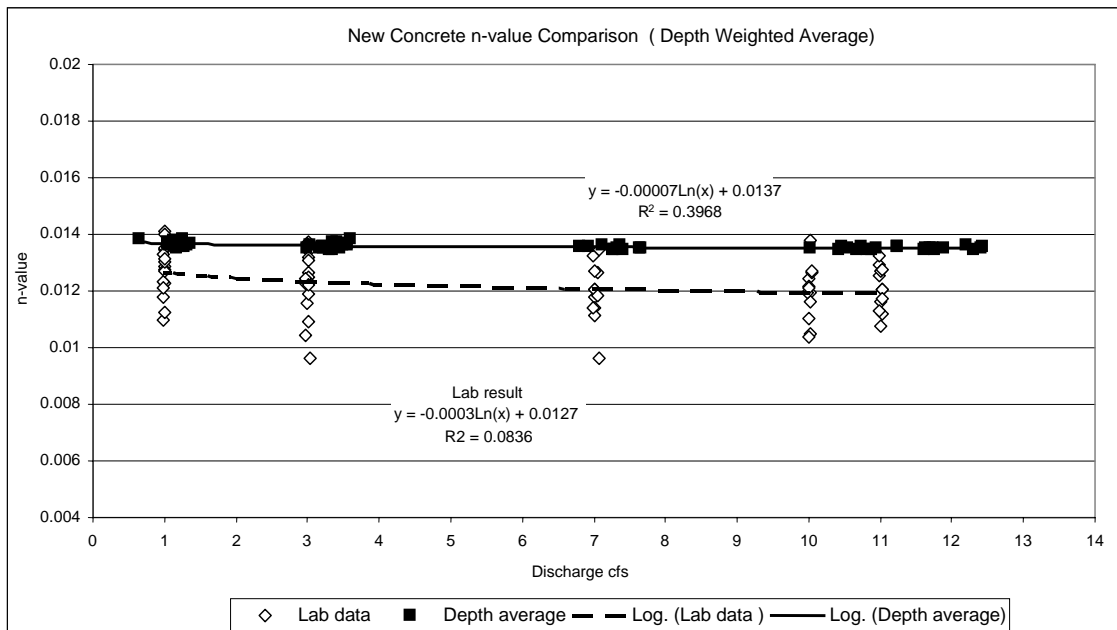


Figure C6.4 Manning's n-values and discharges of TxDOT concrete surface estimated by depth-weight averaging method

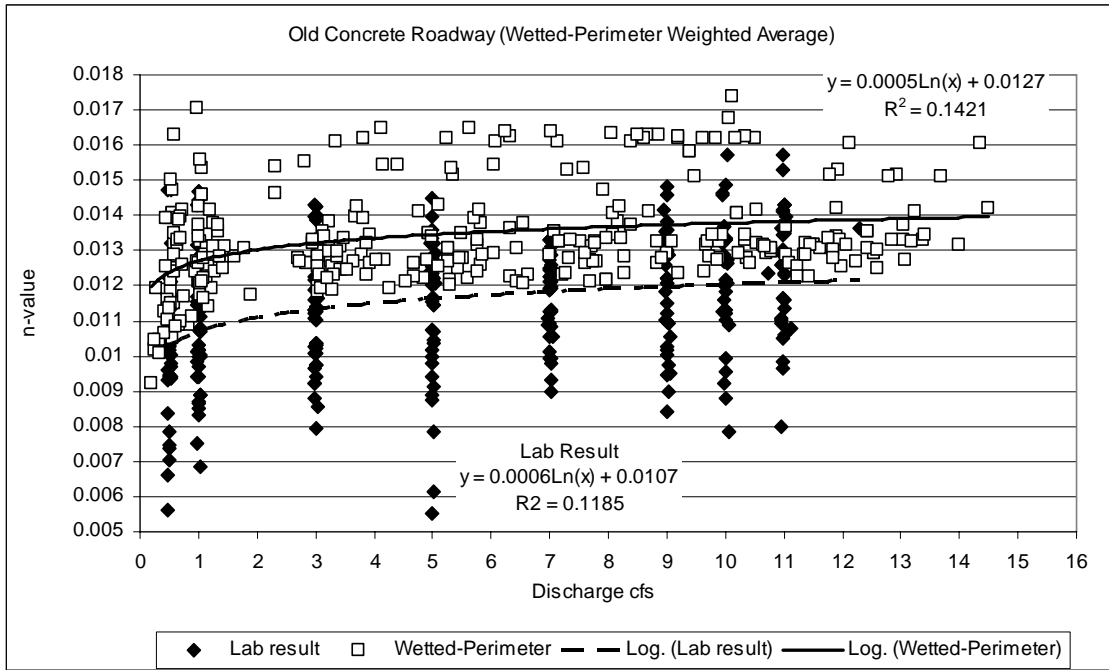


Figure C7.1 Manning's n-values and discharges of smooth concrete surface estimated by wetted-perimeter weighted averaging method

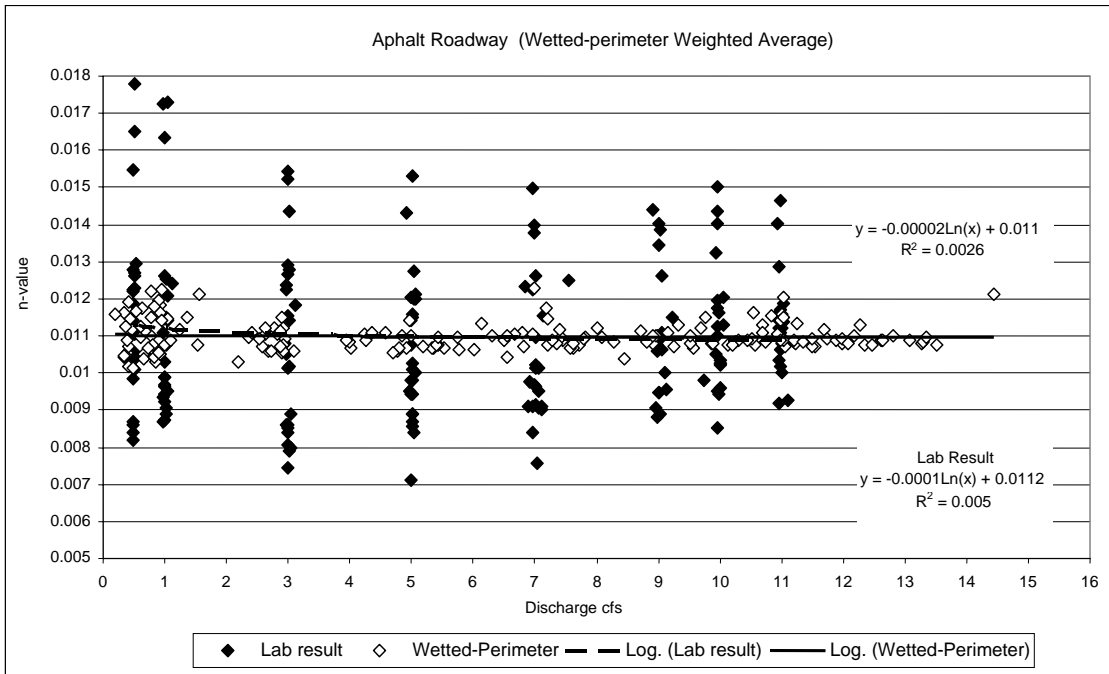


Figure C7.2 Manning's n-values and discharges of asphalt surface estimated by wetted-perimeter weighted averaging method

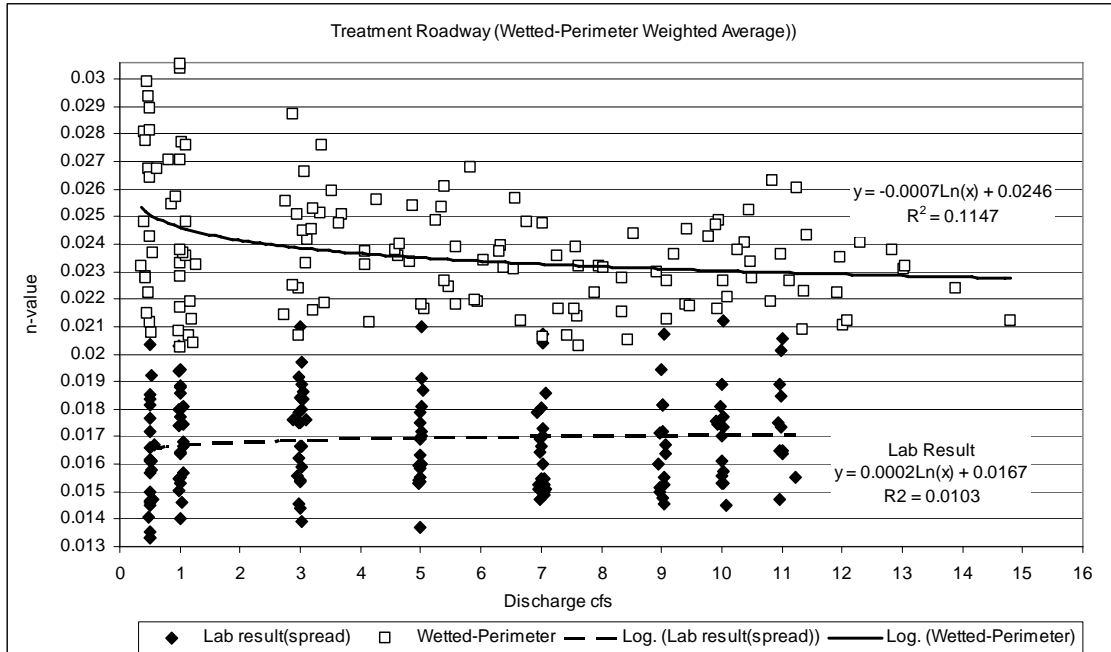


Figure C7.3 Manning's n-values and discharges of asphalt treatment surface estimated by wetted-perimeter weighted averaging method

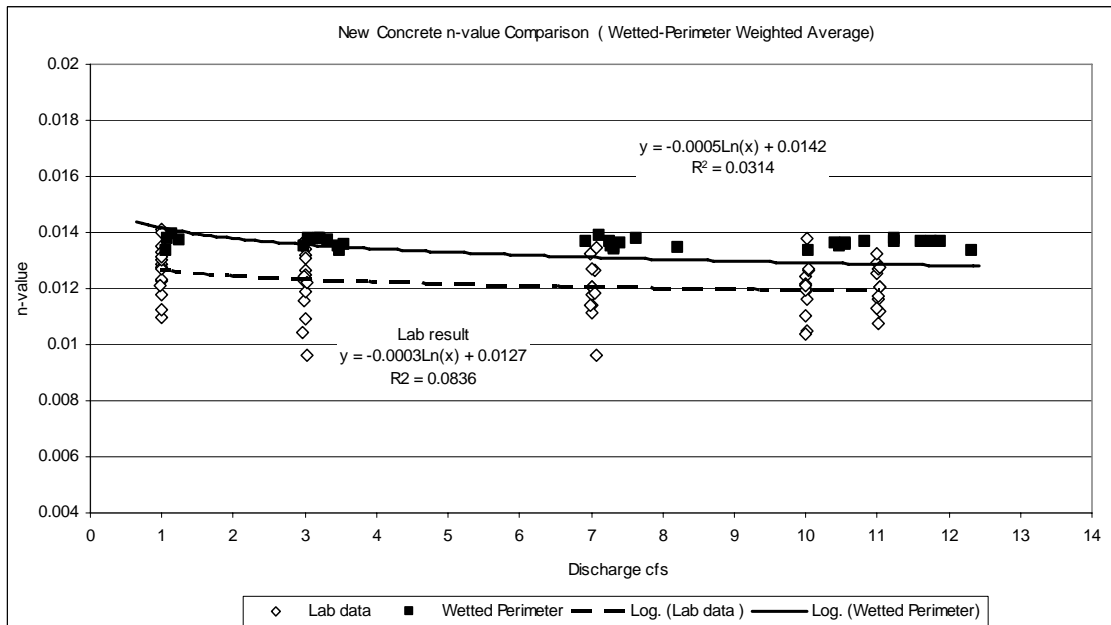


Figure C7.4 Manning's n-values and discharges of TxDOT concrete surface estimated by wetted-perimeter weighted averaging method

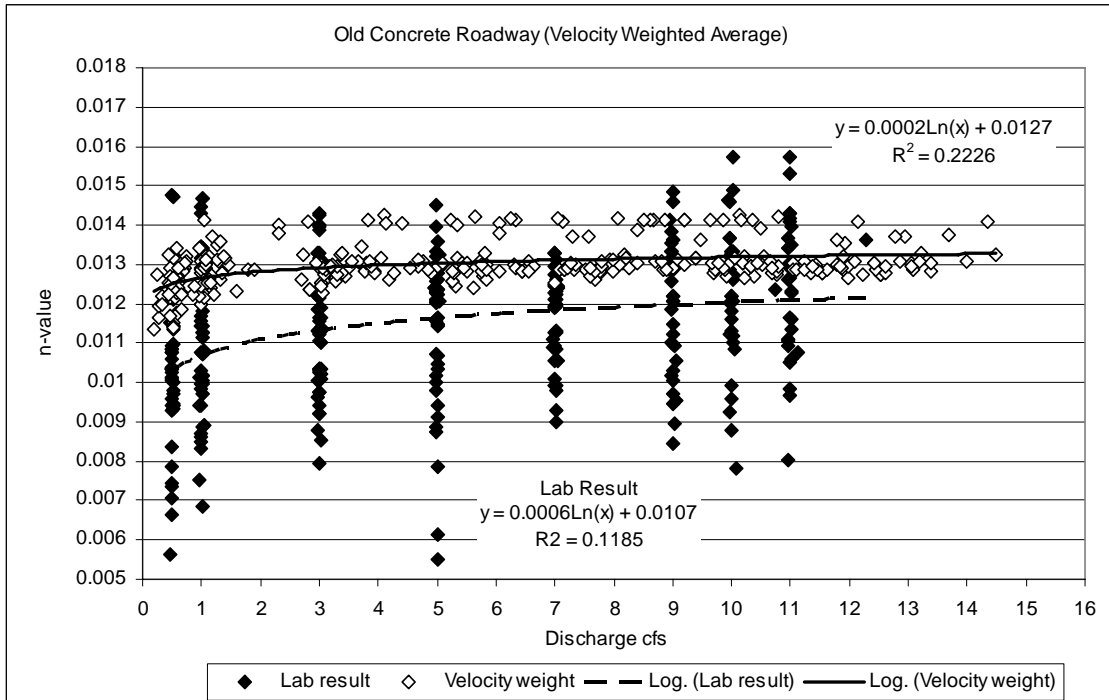


Figure C8.1 Manning's n-values and discharges of smooth concrete surface estimated by velocity-weight averaging method

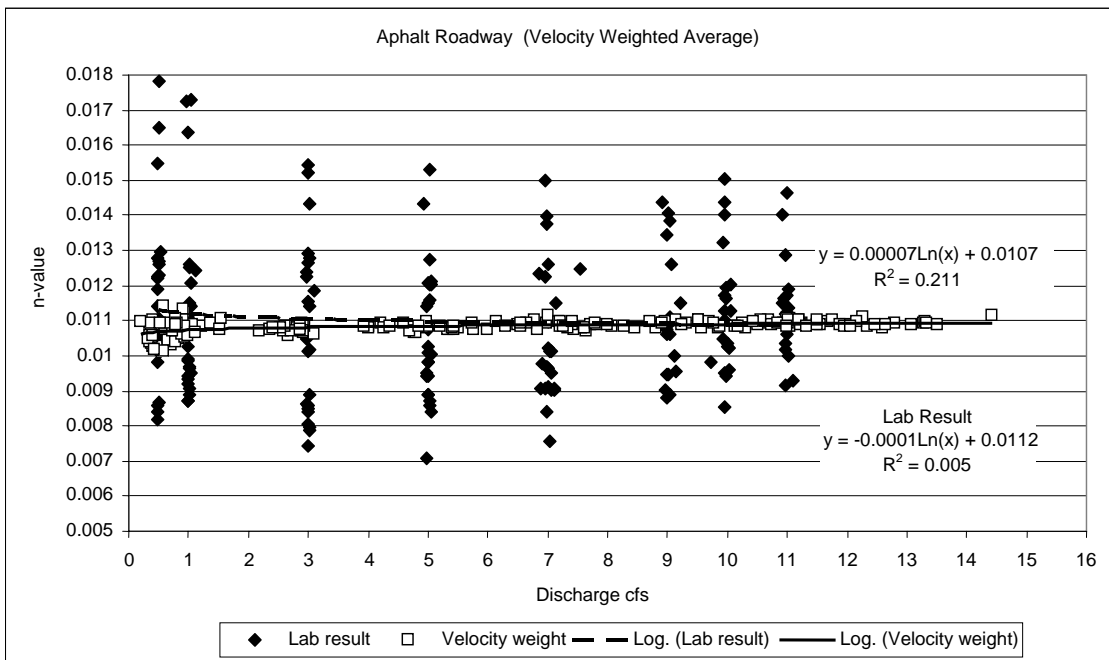


Figure C8.2 Manning's n-values and discharges of asphalt surface estimated by velocity-weight averaging method

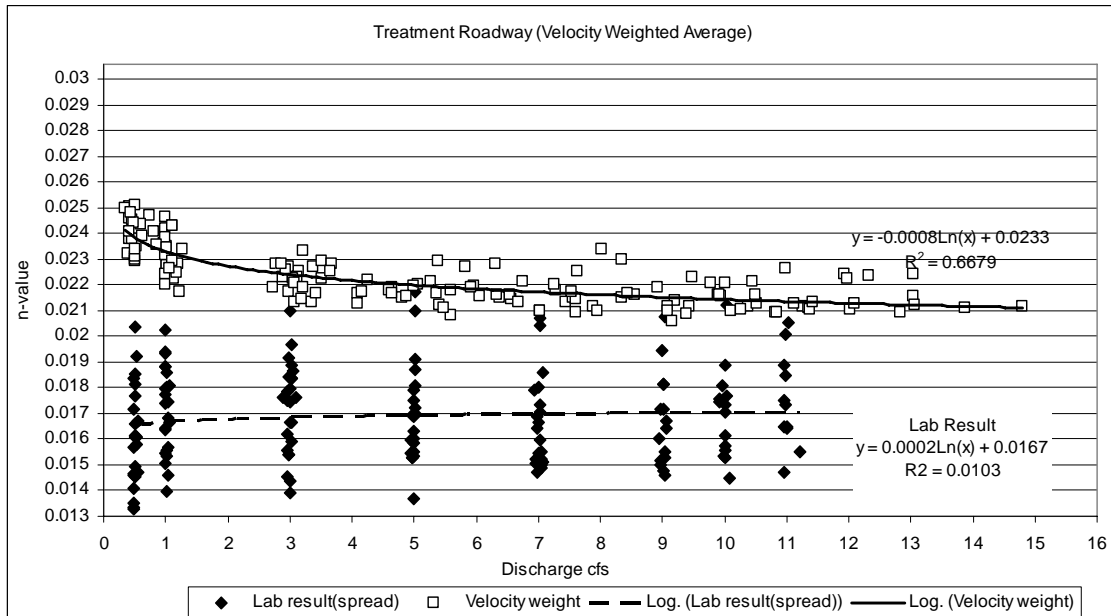


Figure C8.3 Manning's n-values and discharges of asphalt treatment surface estimated by velocity-weight averaging method

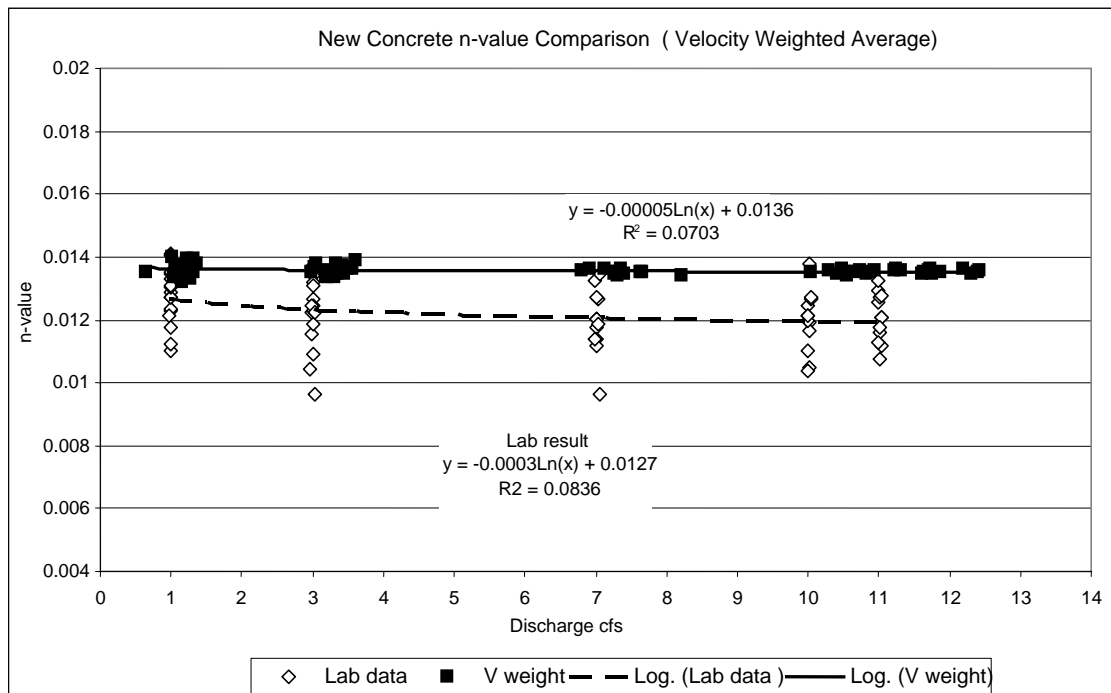


Figure C8.4 Manning's n-values and discharges of TxDOT concrete surface estimated by velocity-weight averaging method

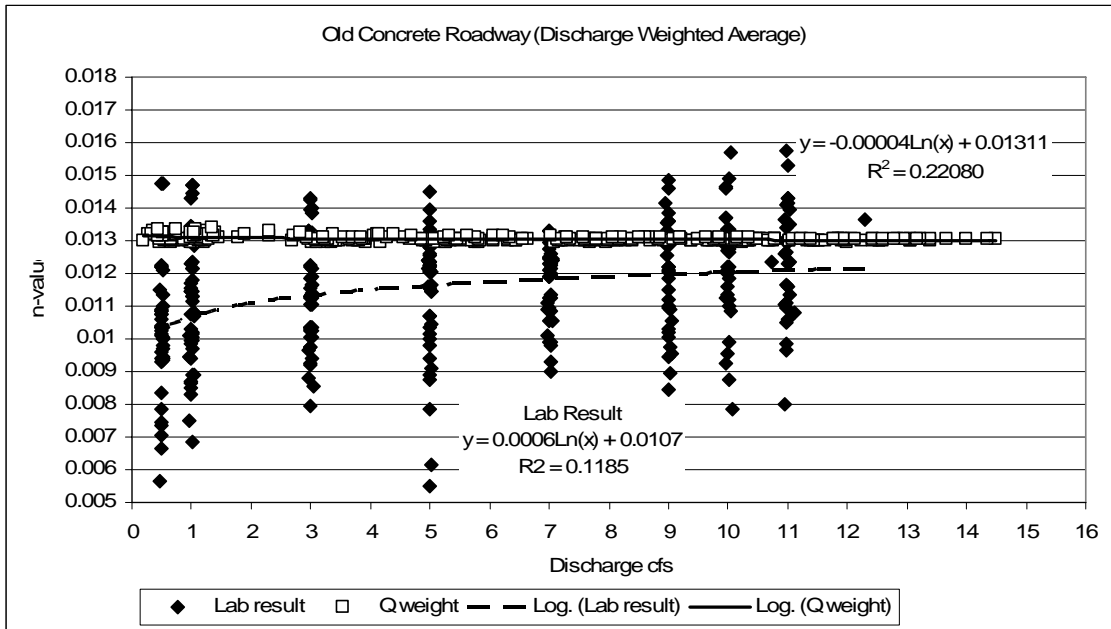


Figure C9.1 Manning's n-values and discharges of smooth concrete surface estimated by discharge-weight averaging method

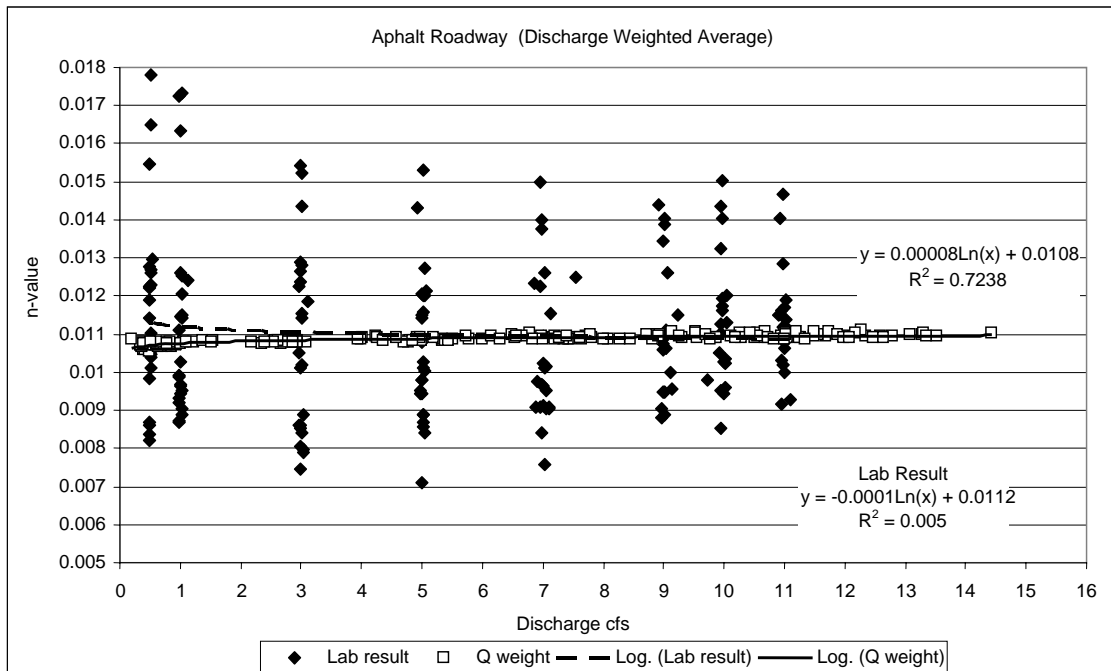


Figure C9.2 Manning's n-values and discharges of asphalt surface estimated by discharge-weight averaging method

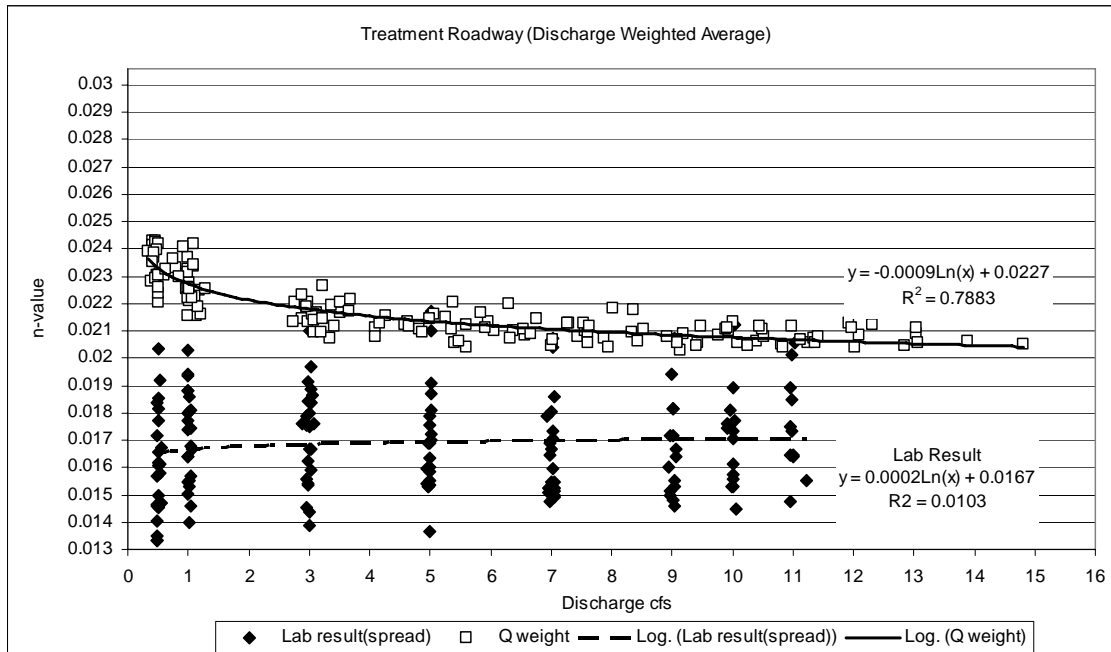


Figure C9.3 Manning's n-values and discharges of asphalt treatment surface estimated by discharge-weight averaging method

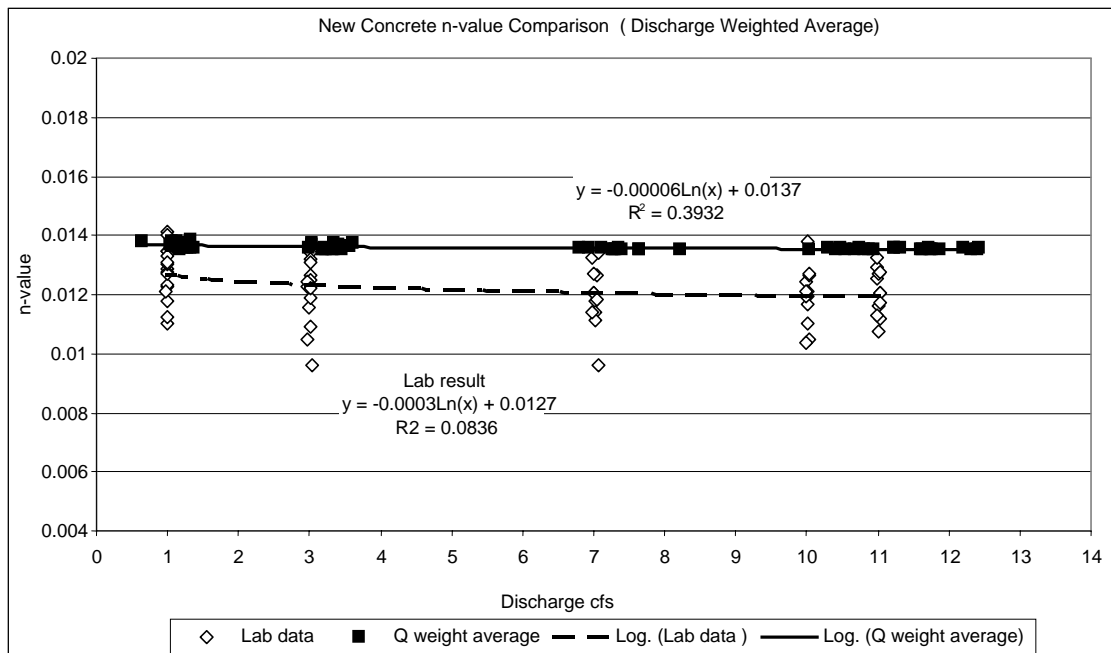


Figure C9.4 Manning's n-values and discharges of TxDOT concrete surface estimated by discharge-weight averaging method

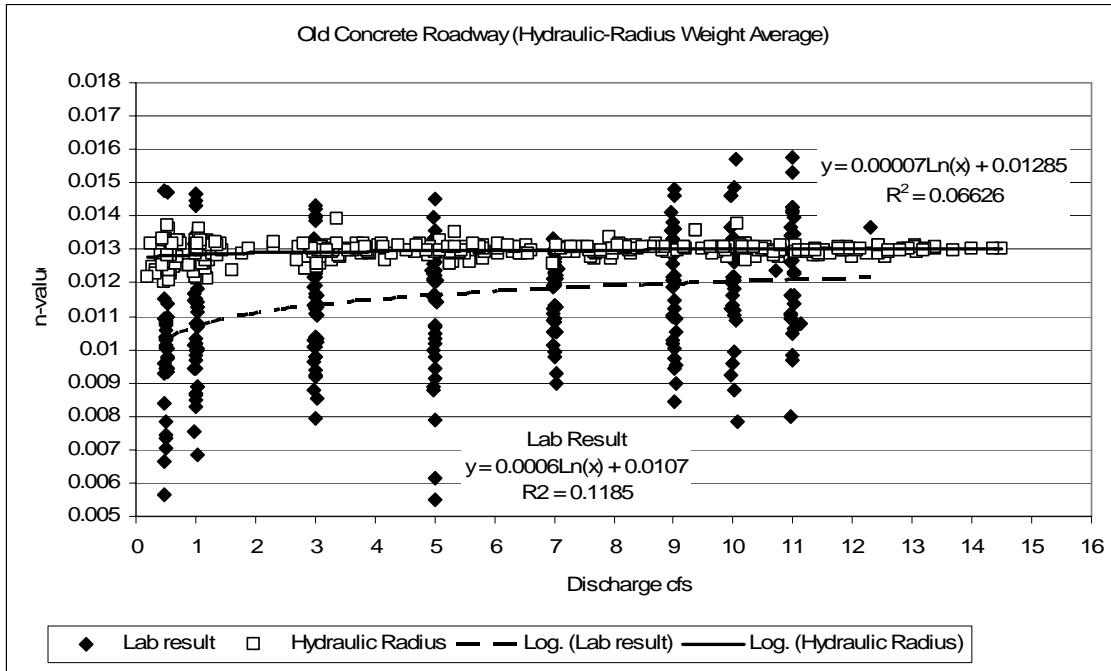


Figure C10.1 Manning's n-values and discharges of smooth concrete surface estimated by hydraulic-radius weighted averaging method

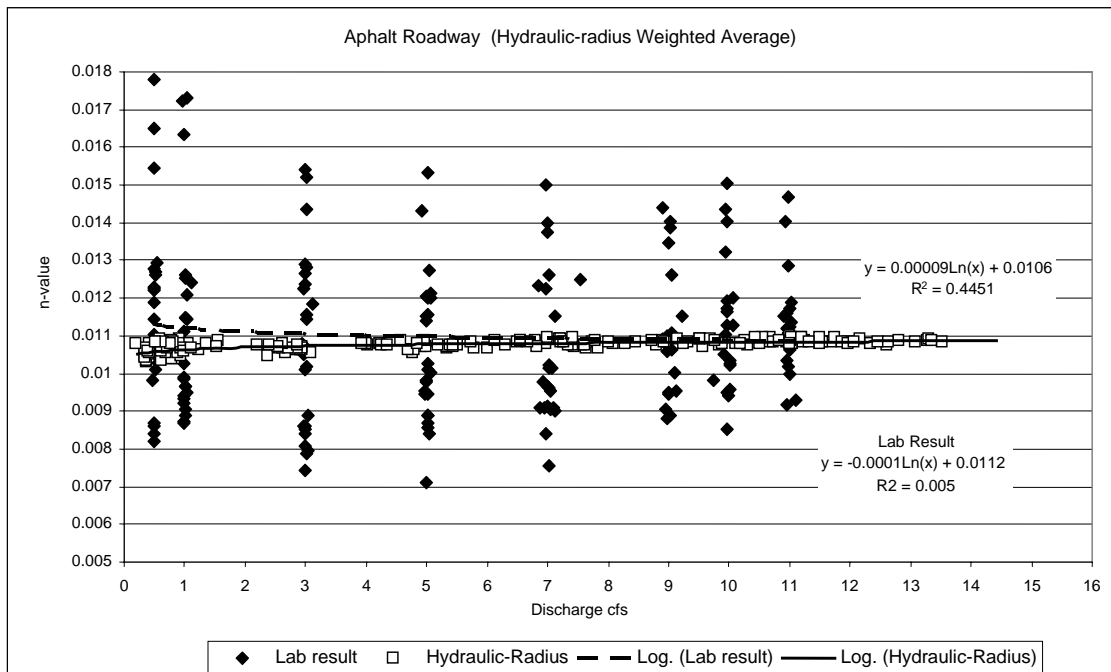


Figure C10.2 Manning's n-values and discharges of asphalt surface estimated by hydraulic-radius weighted averaging method

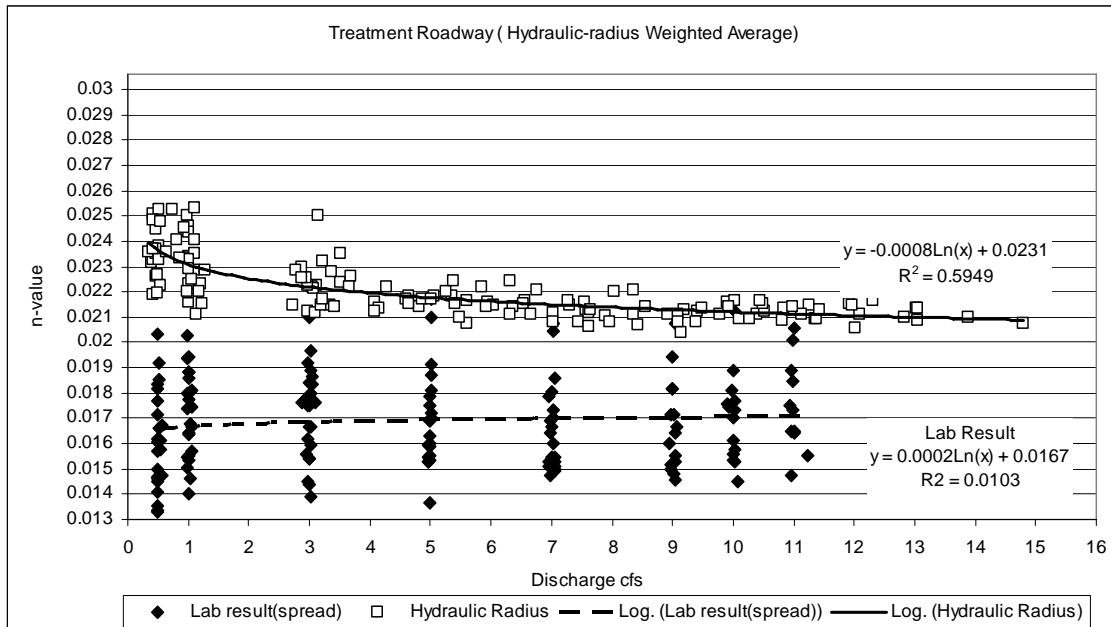


Figure C10.3 Manning's n-values and discharges of asphalt treatment surface estimated by hydraulic-radius weighted averaging method

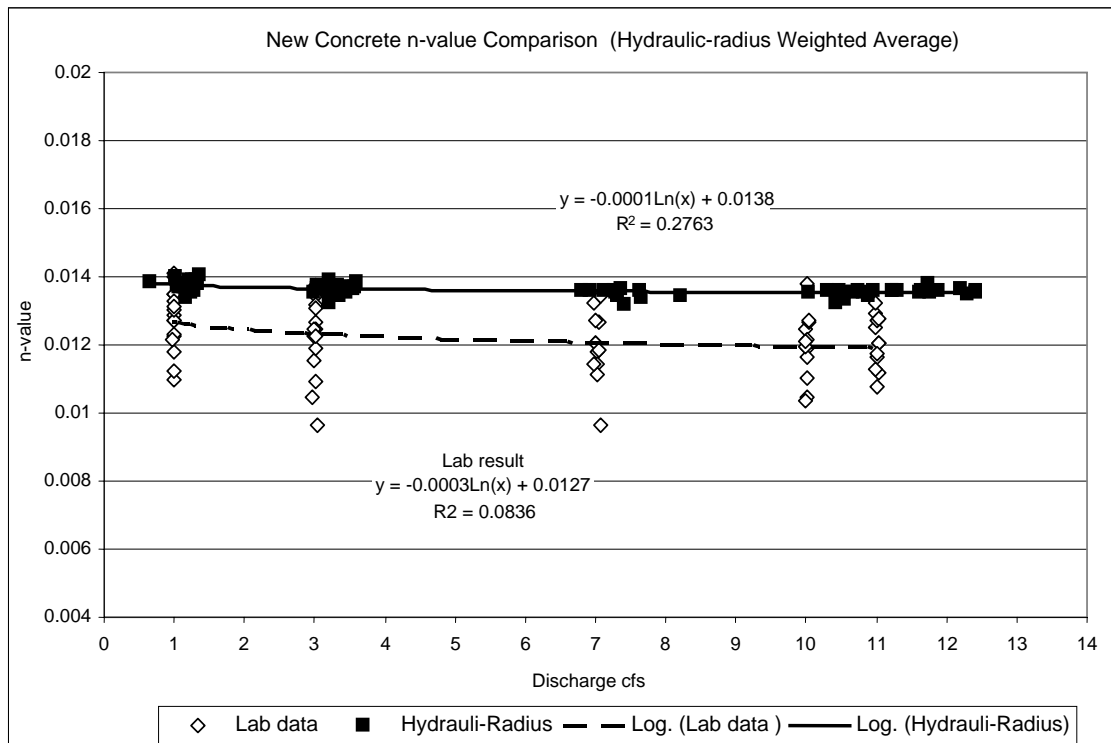


Figure C10.4 Manning's n-values and discharges of TxDOT concrete surface estimated by hydraulic-radius weighted averaging method

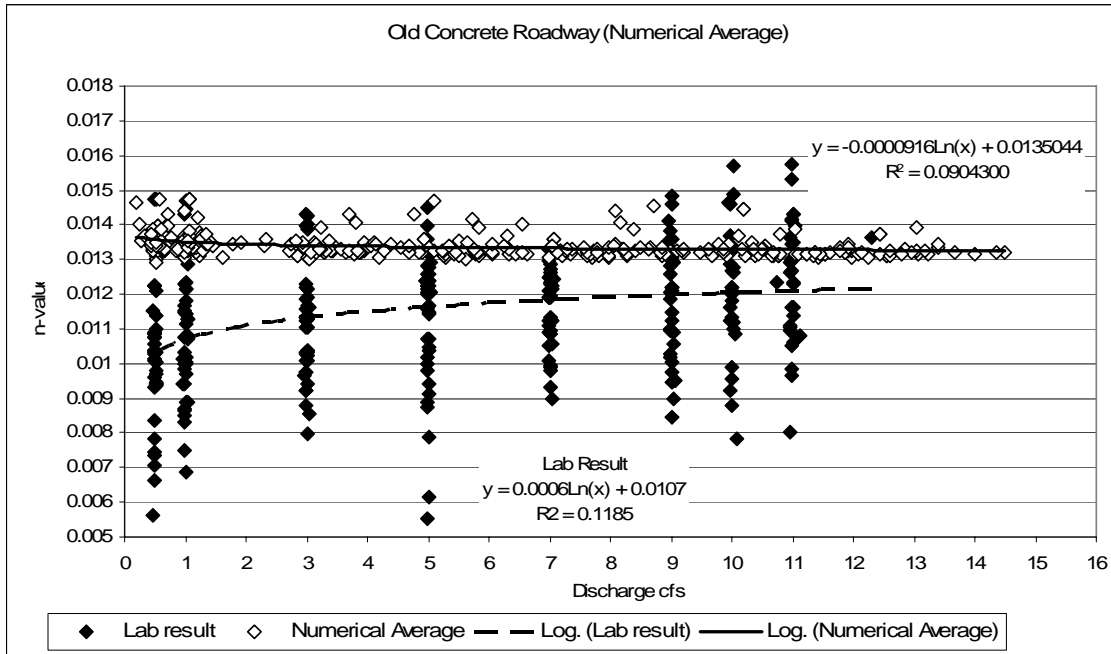


Figure C11.1 Manning's n-values and discharges of smooth concrete surface estimated by numerical average

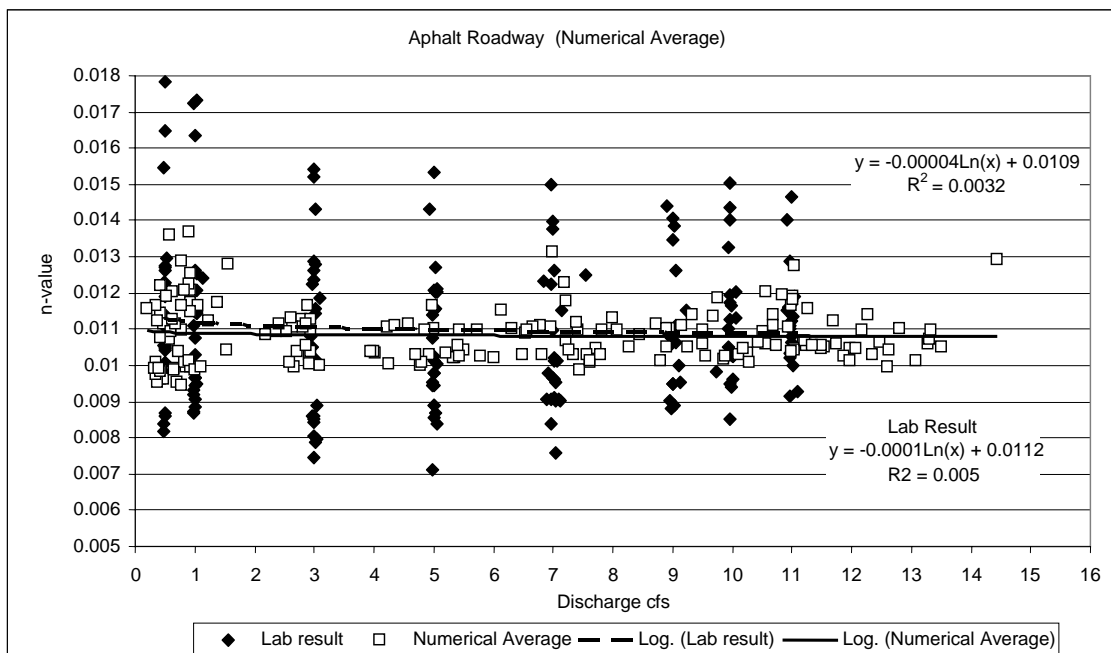


Figure C11.2 Manning's n-values and discharges of asphalt surface estimated by numerical average

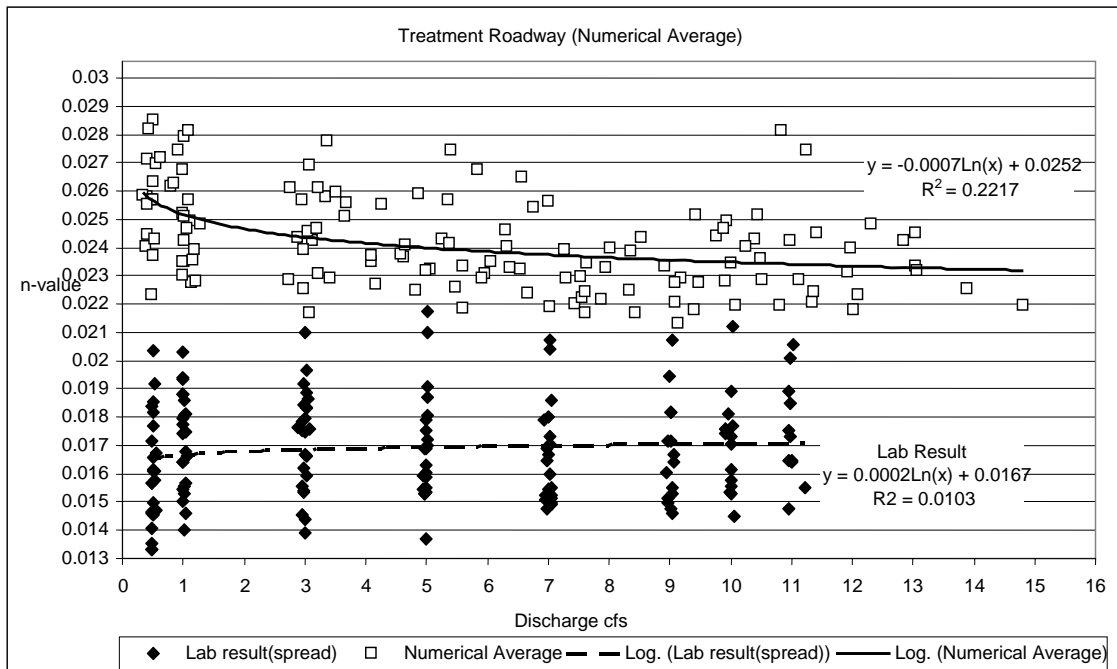


Figure C11.3 Manning's n-values and discharges of asphalt treatment surface estimated by numerical average

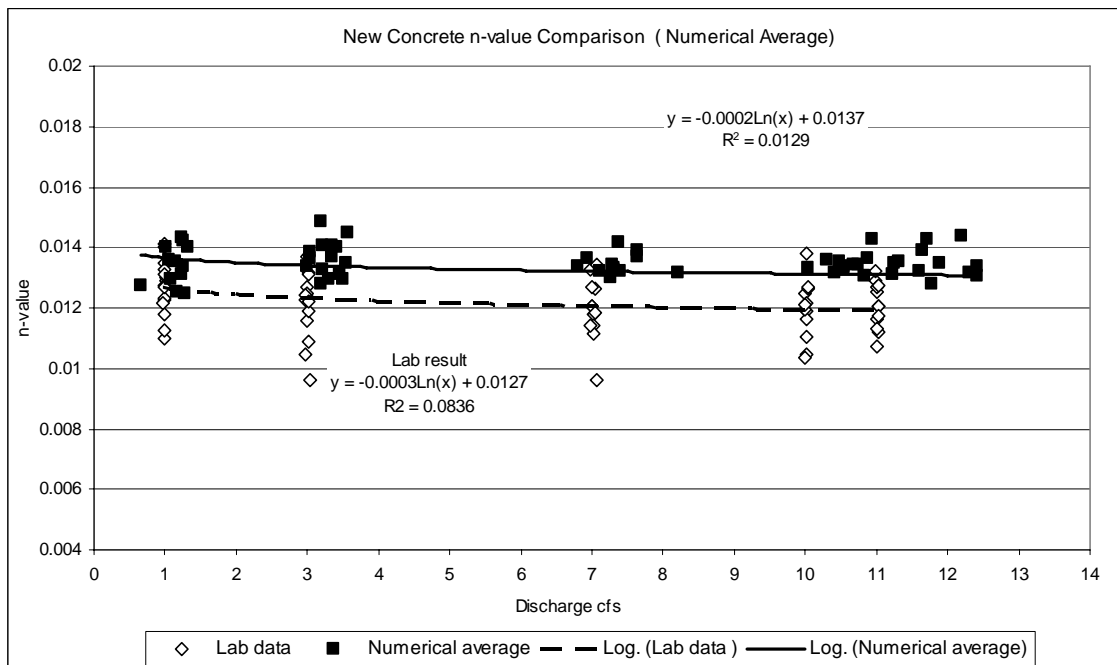


Figure C11.4 Manning's n-values and discharges of TxDOT concrete surface estimated by numerical average

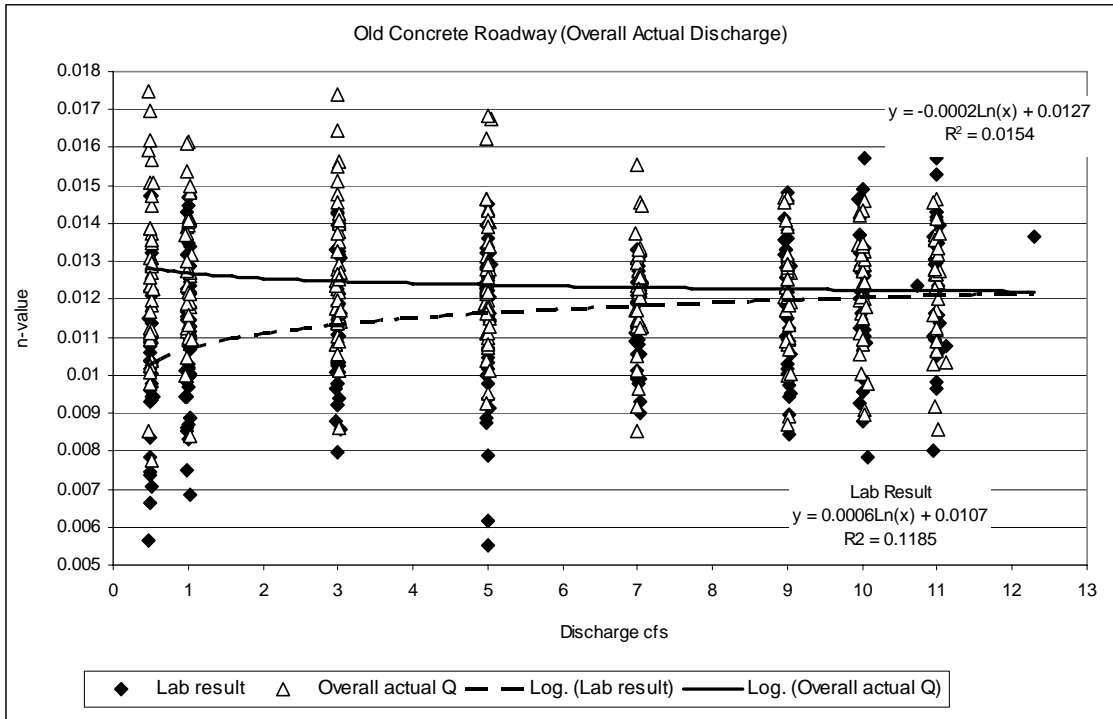


Figure C12.1 Manning's n-values and discharges of smooth concrete surface estimated by Manning's equation and using measured discharge

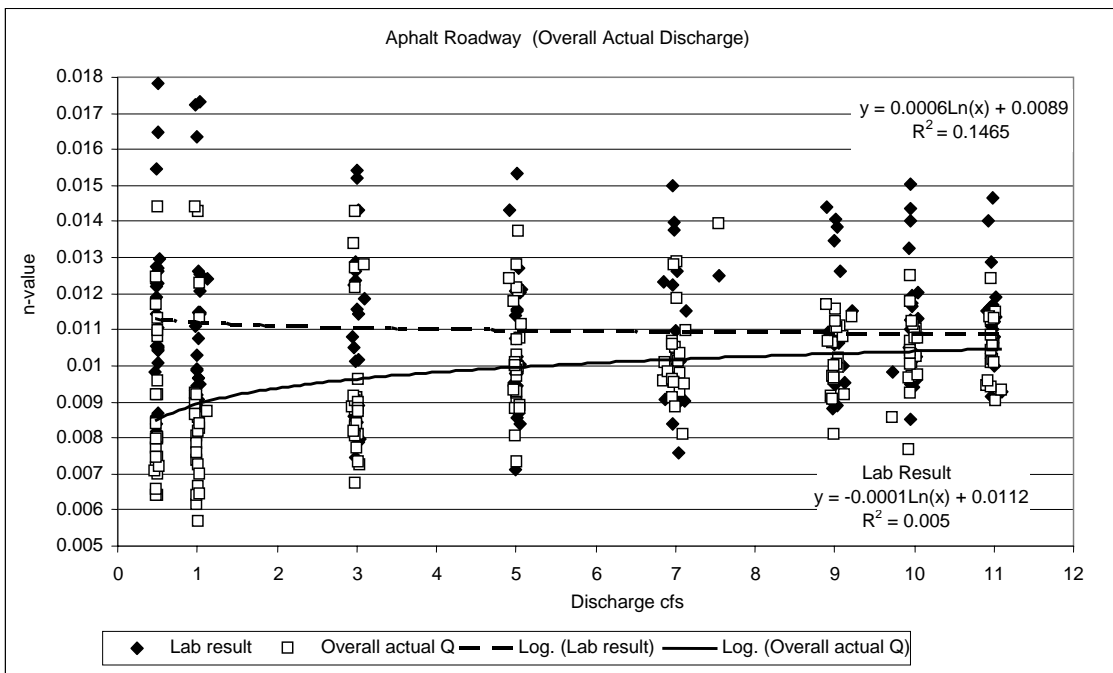


Figure C12.2 Manning's n-values and discharges of asphalt surface estimated by Manning's equation and using measured discharge

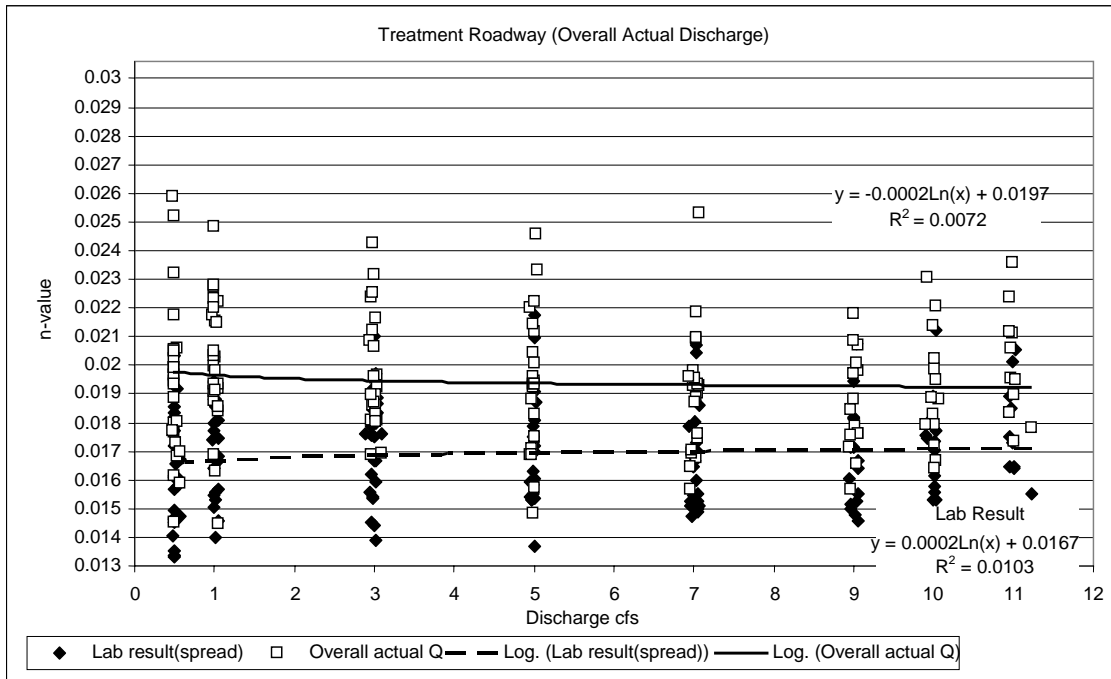


Figure C12.3 Manning's n-values and discharges of asphalt treatment surface estimated by Manning's equation and using measured discharge

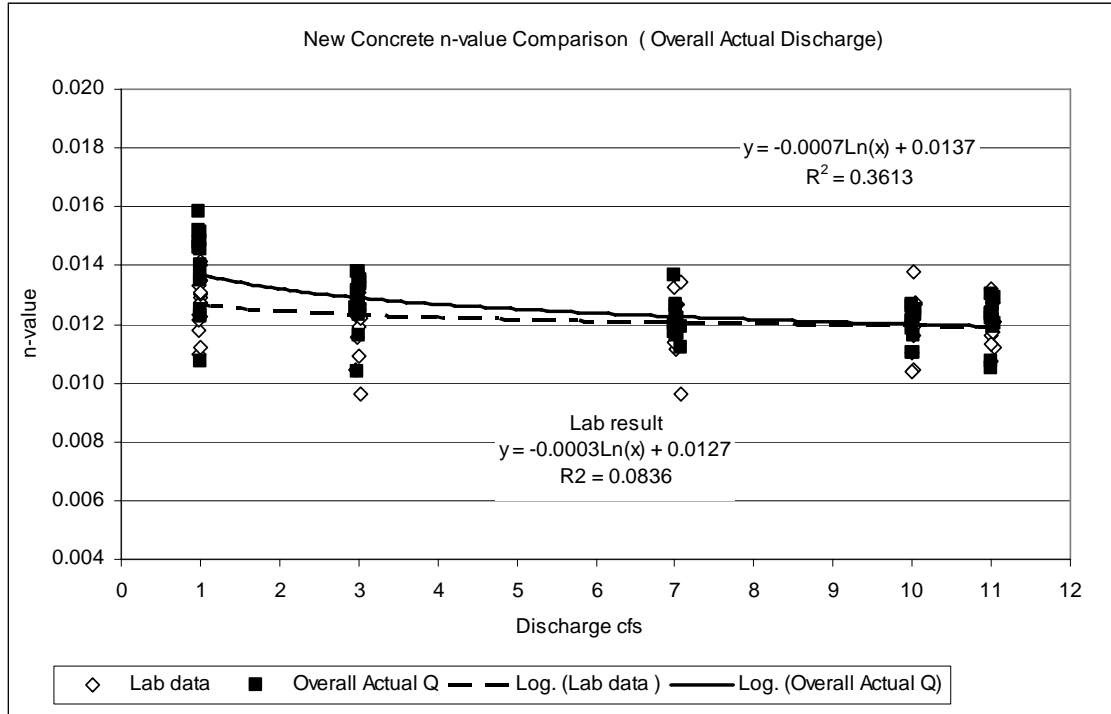


Figure C12.4 Manning's n-values and discharges of TxDOT concrete surface estimated by Manning's equation and using measured discharge

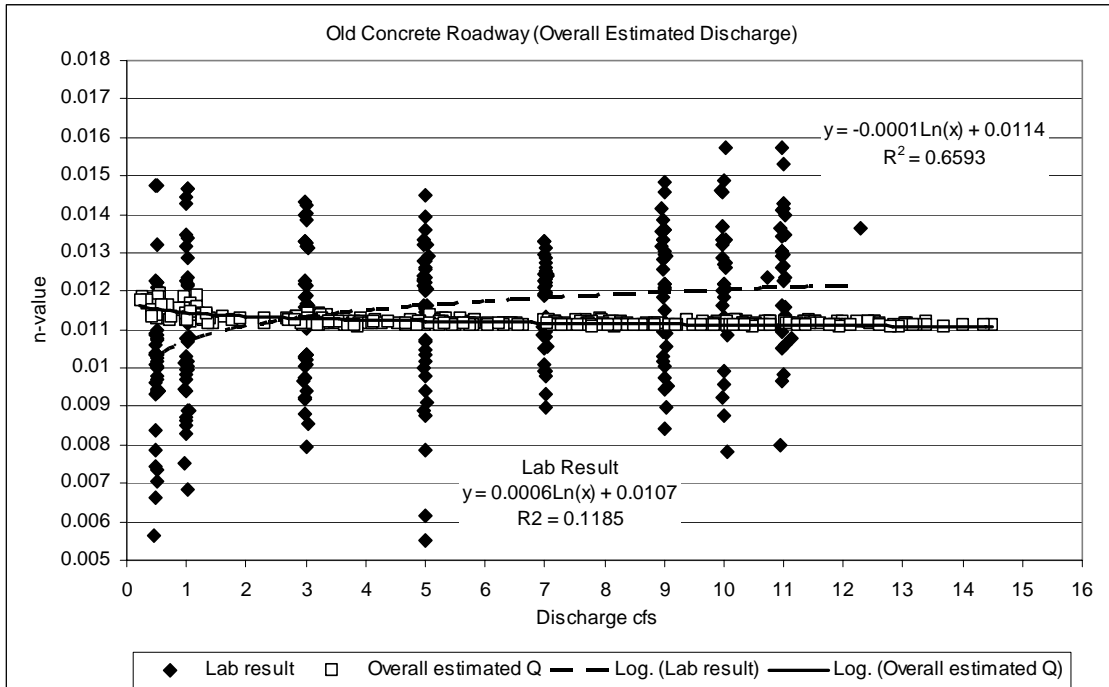


Figure C13.1 Manning's n-values and discharges of smooth concrete surface estimated by Manning's equation and using Prandtl-von Karman estimated discharge

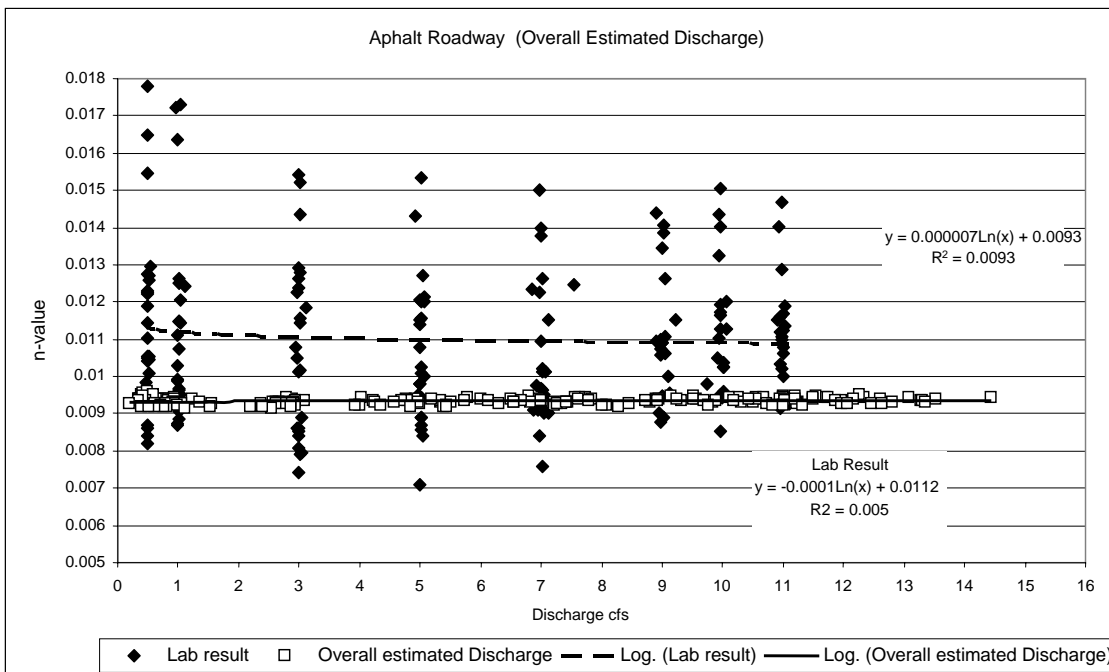


Figure C13.2 Manning's n-values and discharges of asphalt surface estimated by Manning's equation and using Prandtl-von Karman estimated discharge

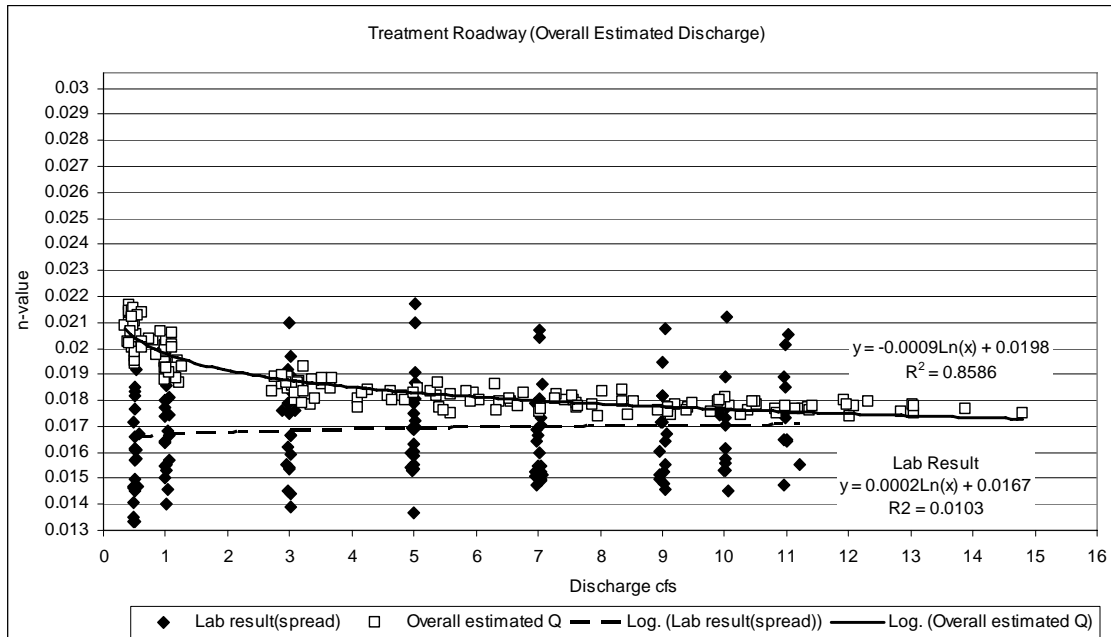


Figure C13.3 Manning's n-values and discharges of asphalt treatment surface estimated by Manning's equation and using Prandtl-von Karman estimated discharge

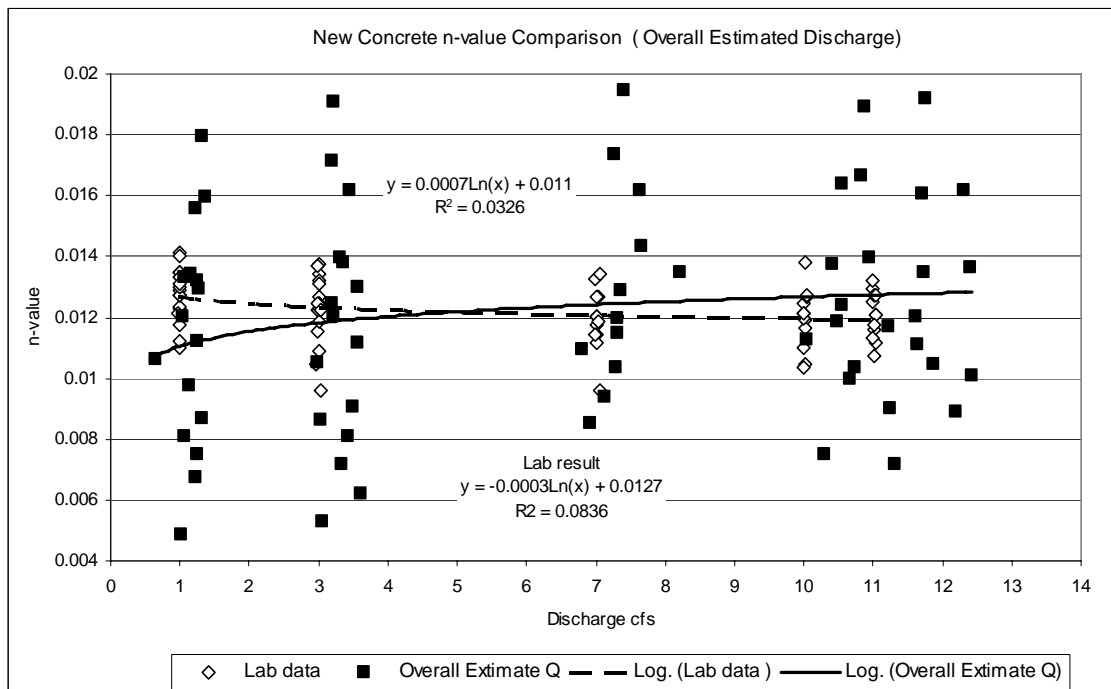


Figure C13.4 Manning's n-values and discharges of TxDOT concrete surface estimated by Manning's equation and using Prandtl-von Karman estimated discharge

APPENDIX D

COMPARISON BETWEEN MEASURD AND PRANDTL-VON KARMAN VELOCITY METHOD DISCAHRGES

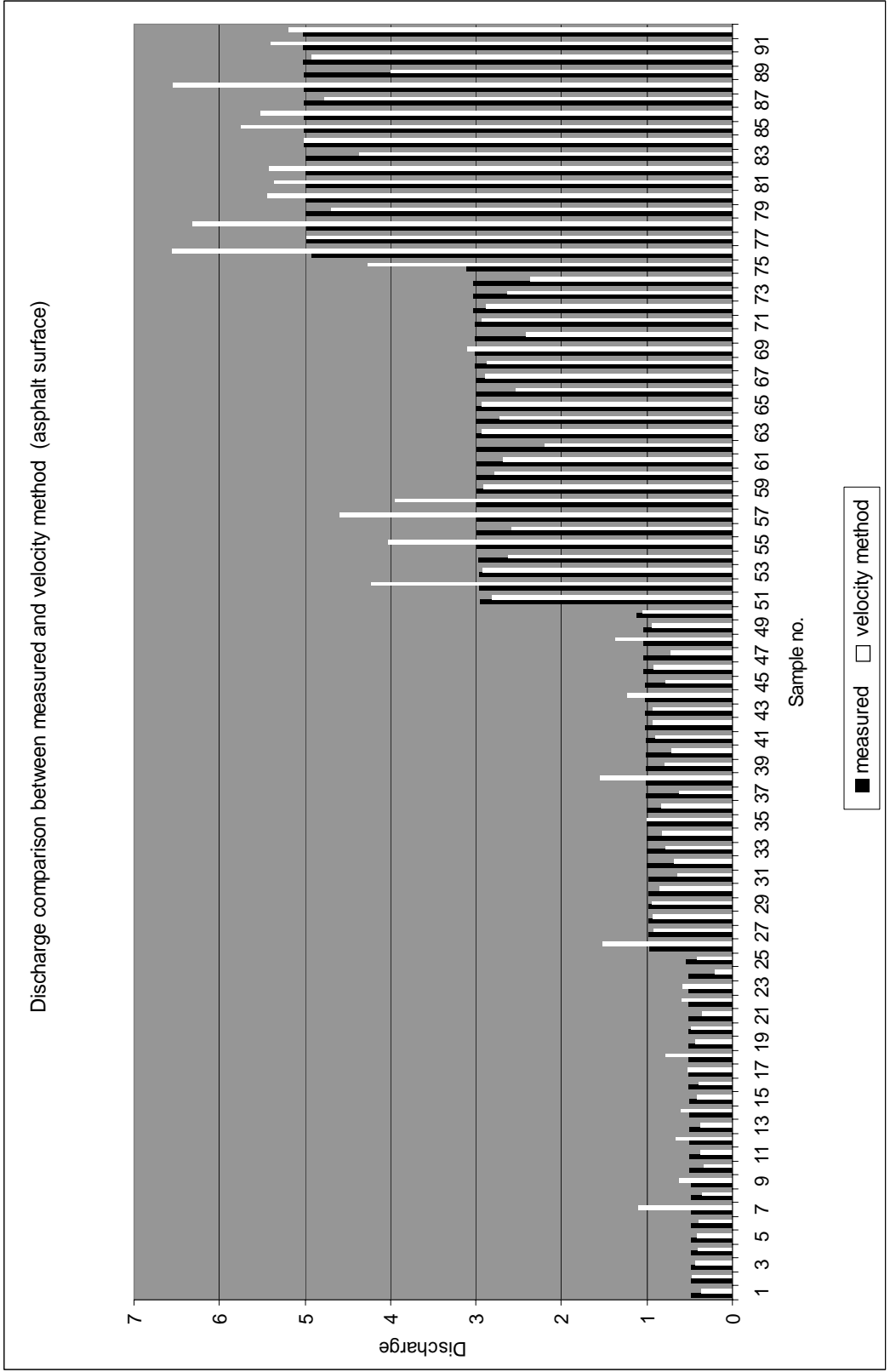


Figure D1.1 Comparison between measured and Prandtl and Von Karman velocity method discharges for asphalt surface (before remove outliers)

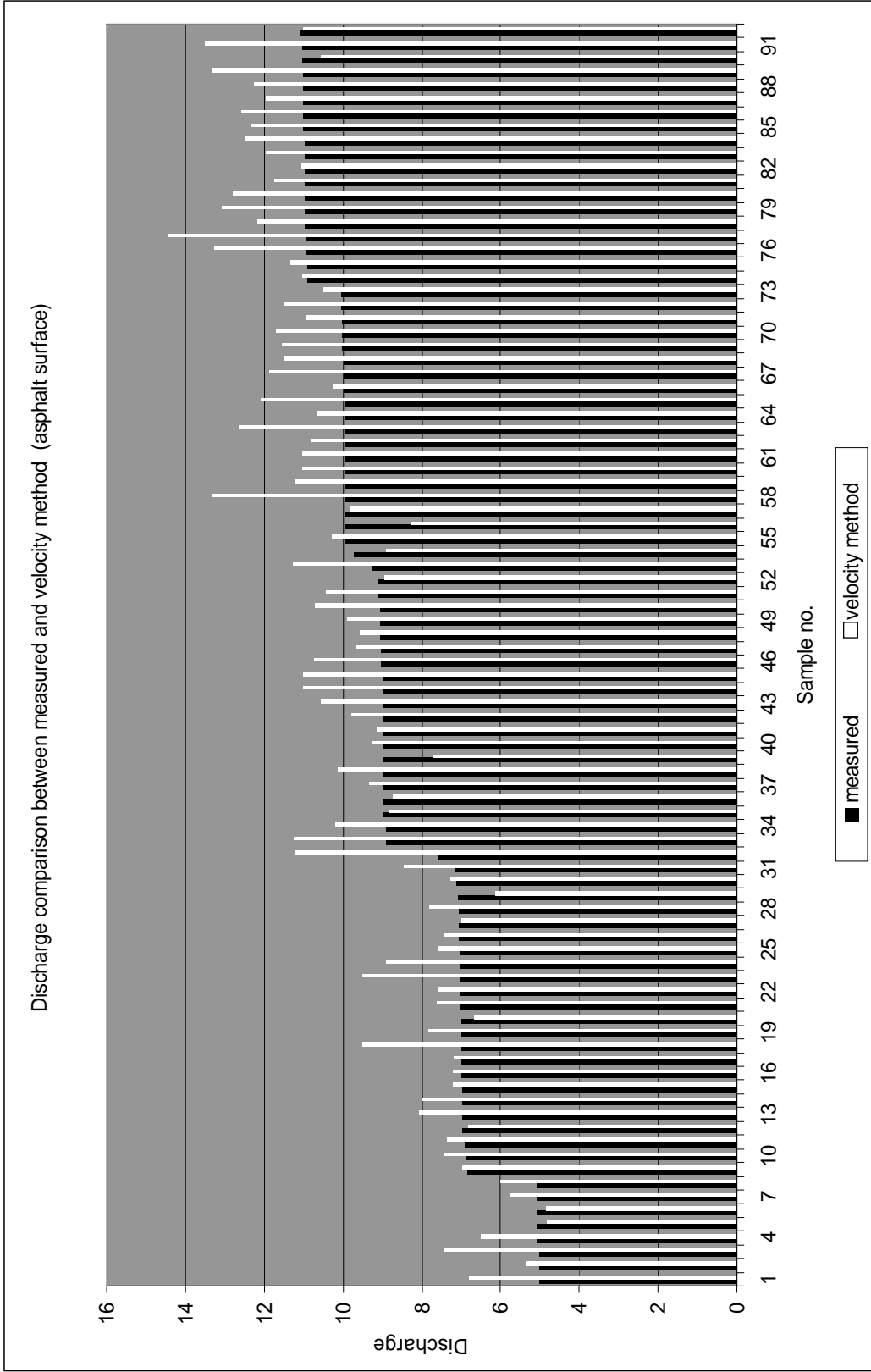


Figure D1.2 Comparison of discharge between measured and Prandtl and Von Karman velocity method for asphalt surface (before remove outliers)

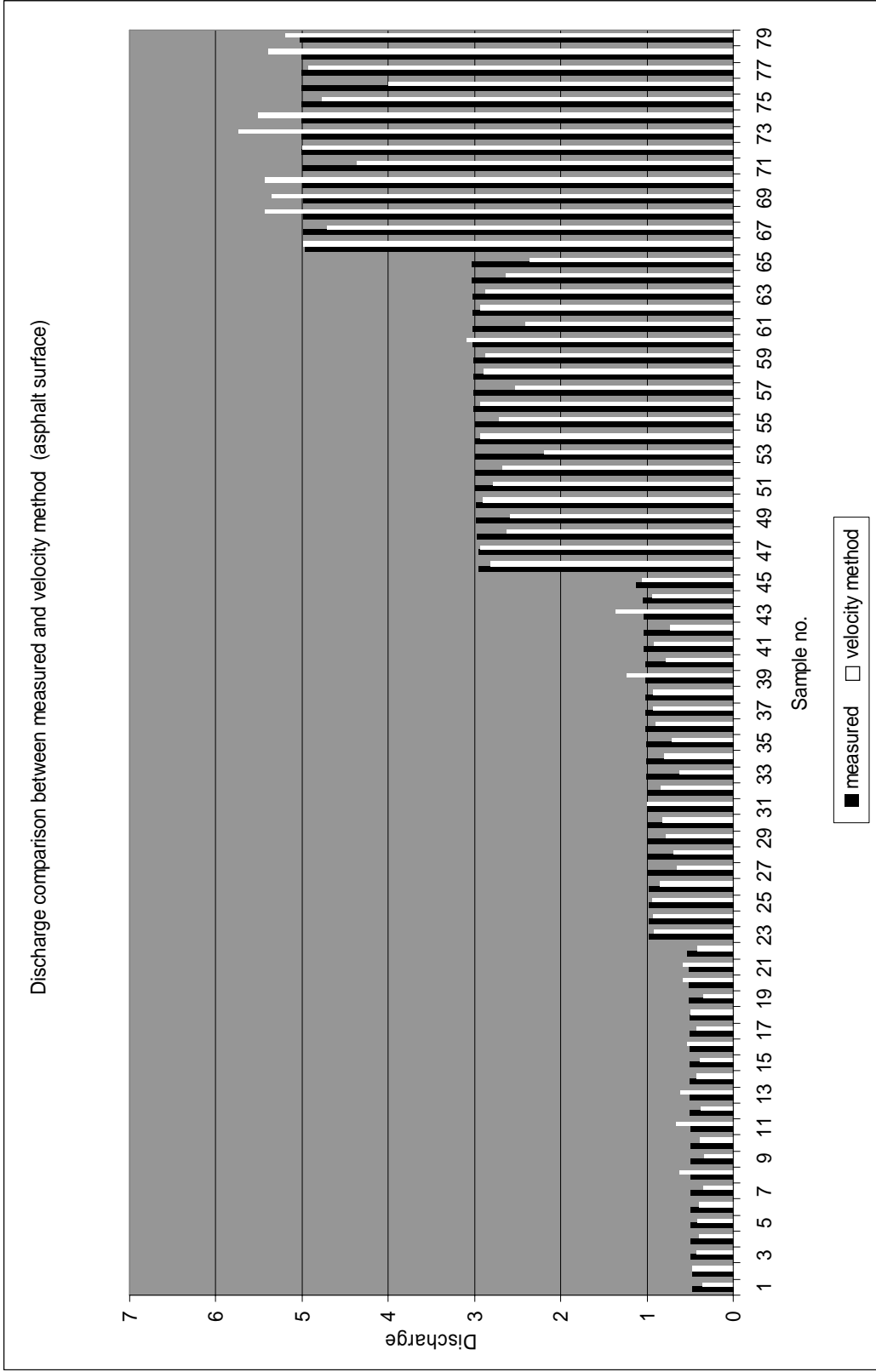


Figure D1.3 Comparison of discharge between measured and Prandtl and Von Karman velocity method for asphalt surface (after remove outliers)

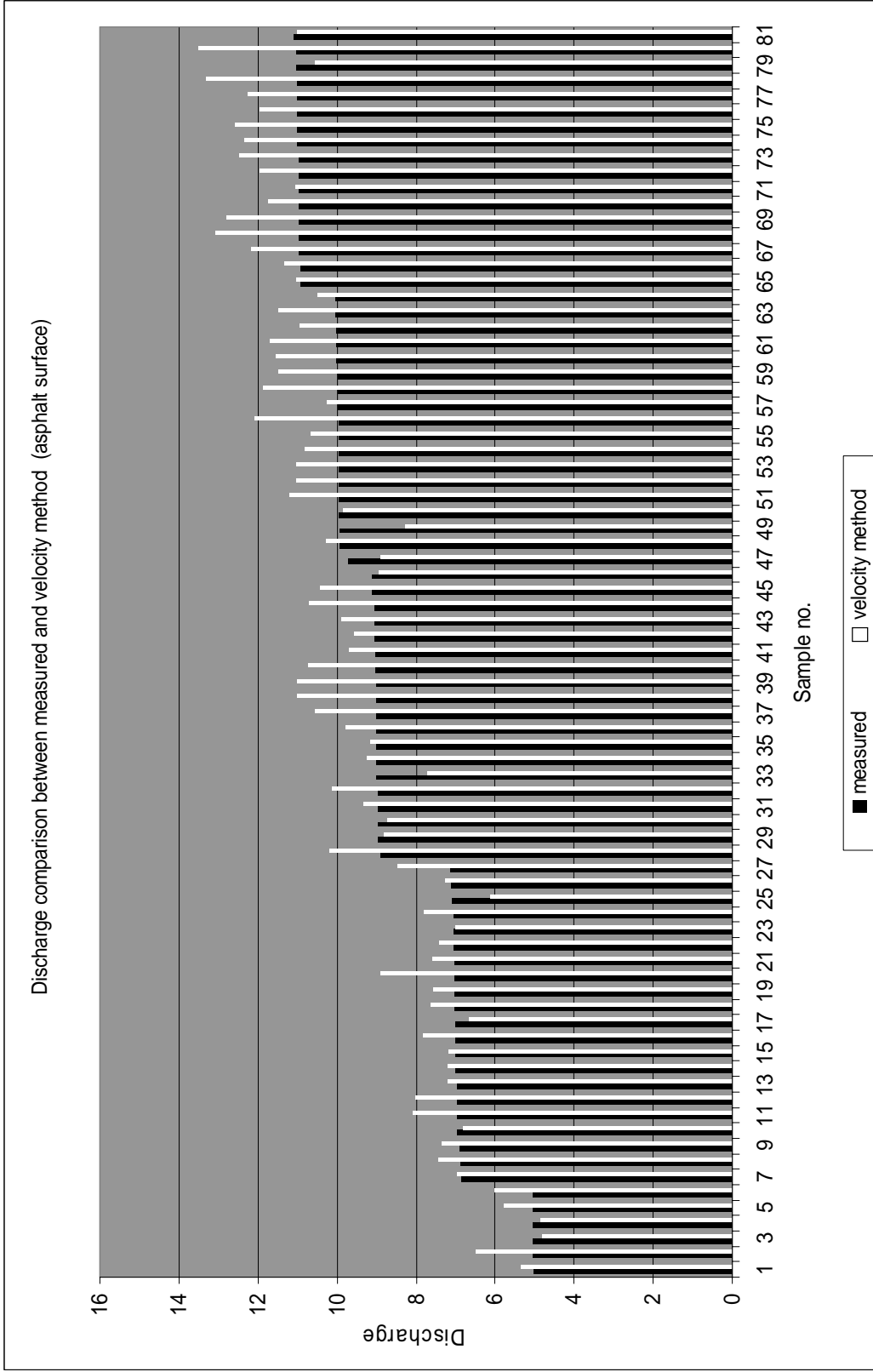


Figure D1.4 Comparison of discharge between measured and Prandtl and Von Karman velocity method for asphalt surface (after remove outliers)

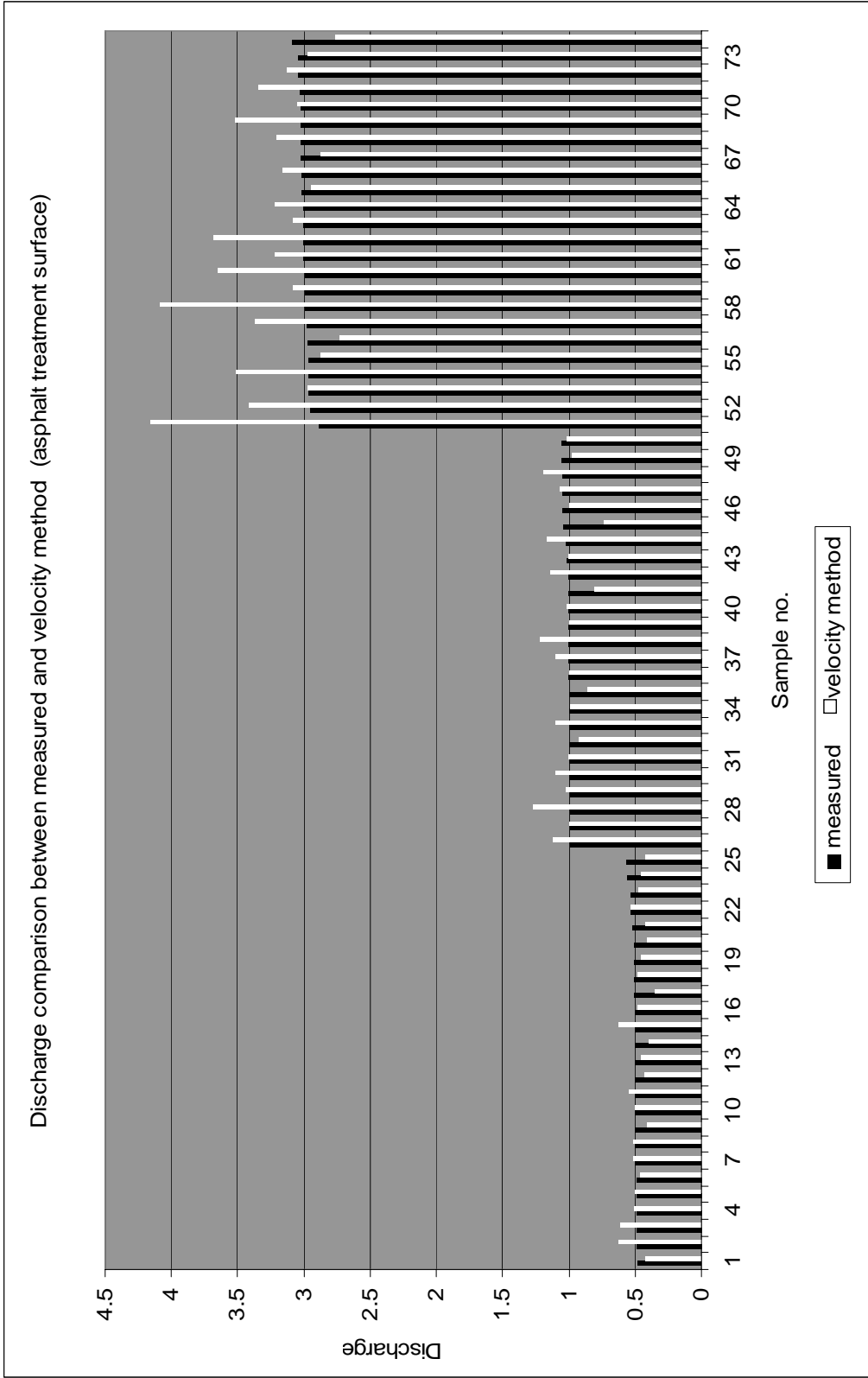


Figure D2.1 Comparison of discharge between measured and Prandtl and Von Karman velocity method for asphalt treatment surface (before remove outliers)

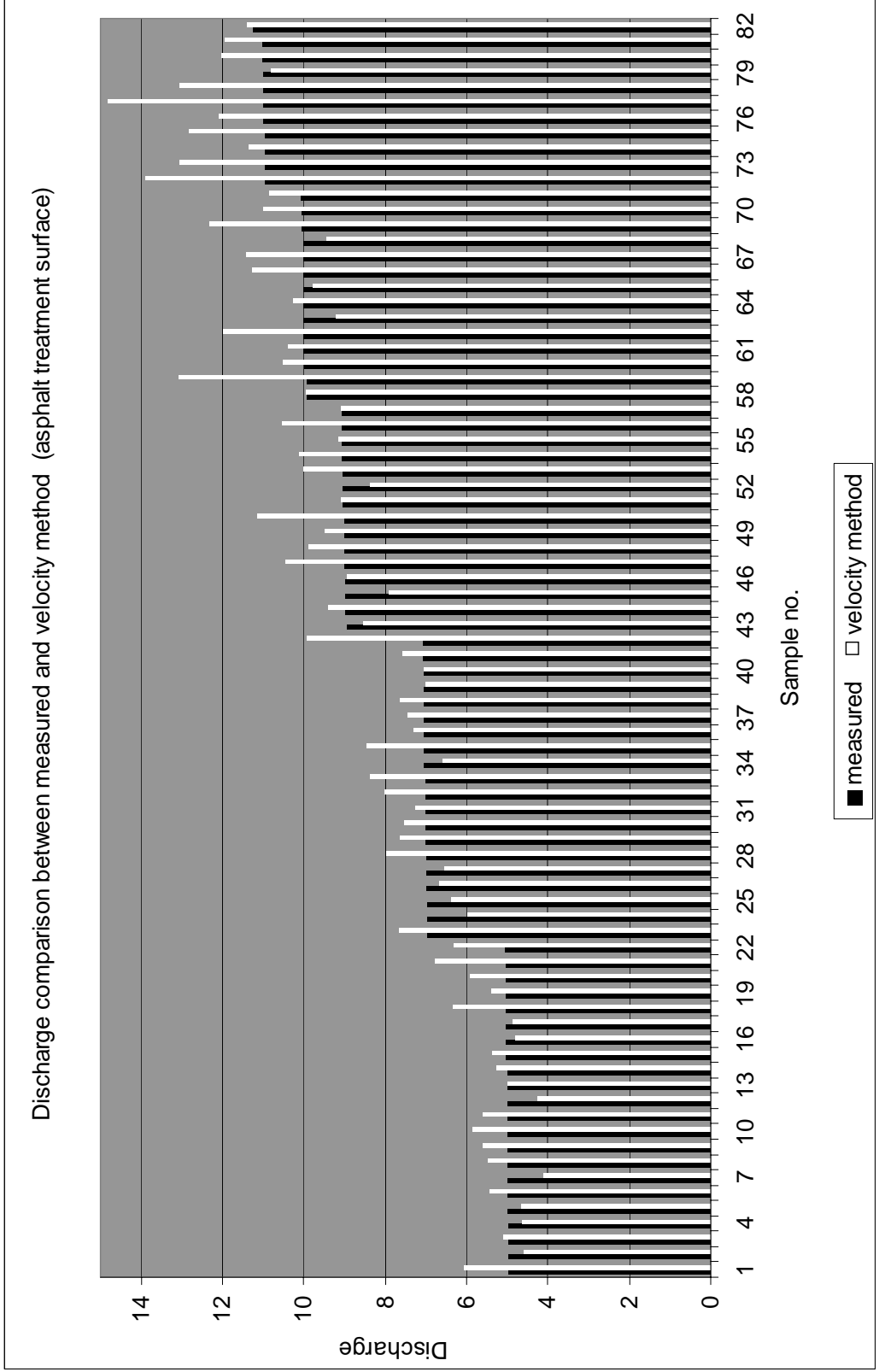


Figure D2.2 Comparison of discharge between measured and Prandtl and Von Karman velocity method for asphalt treatment surface (before remove outliers)

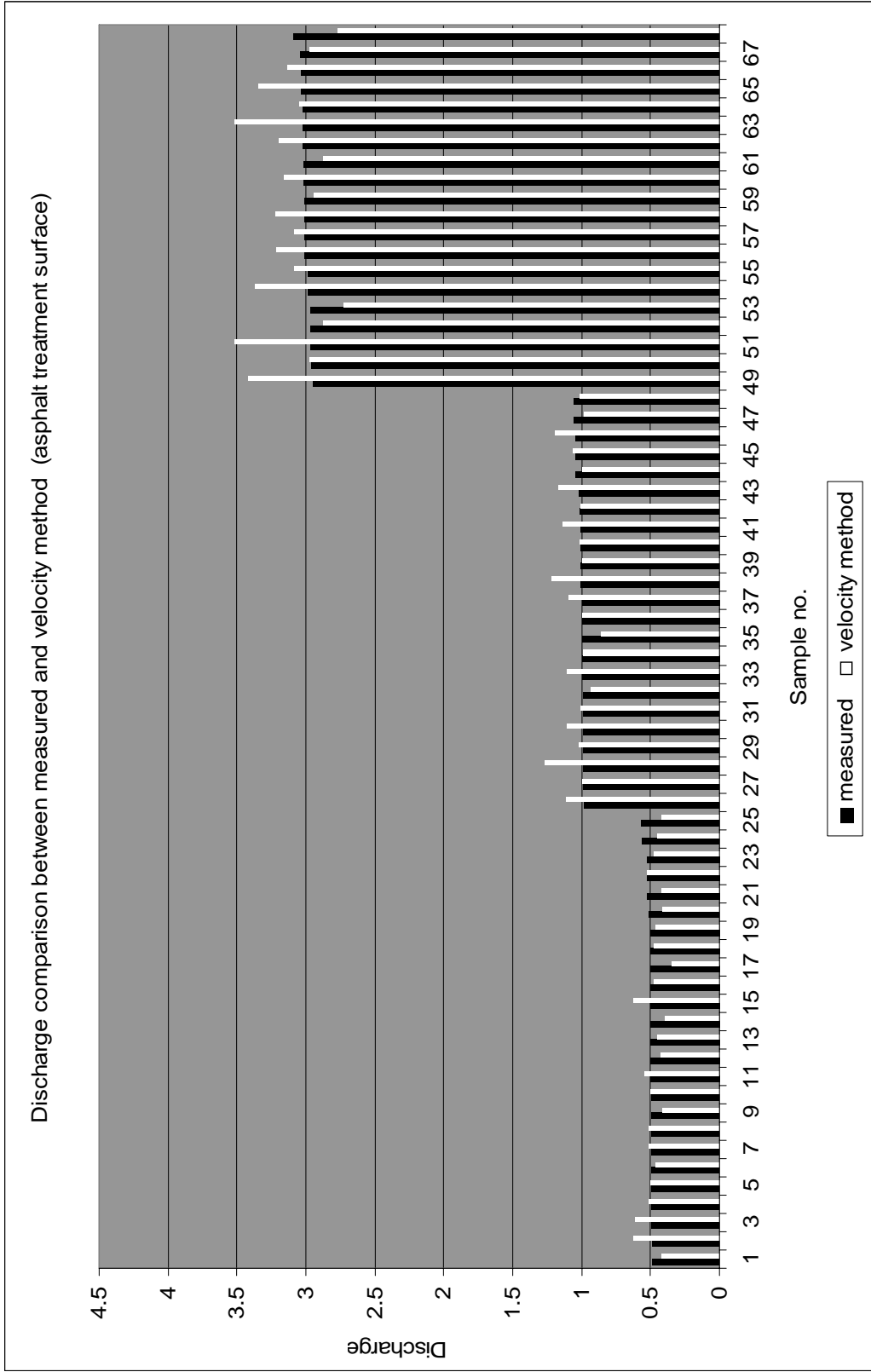


Figure D2.3 Comparison of discharge between measured and Prandtl and Von Karman velocity method for asphalt treatment surface (after remove outliers)

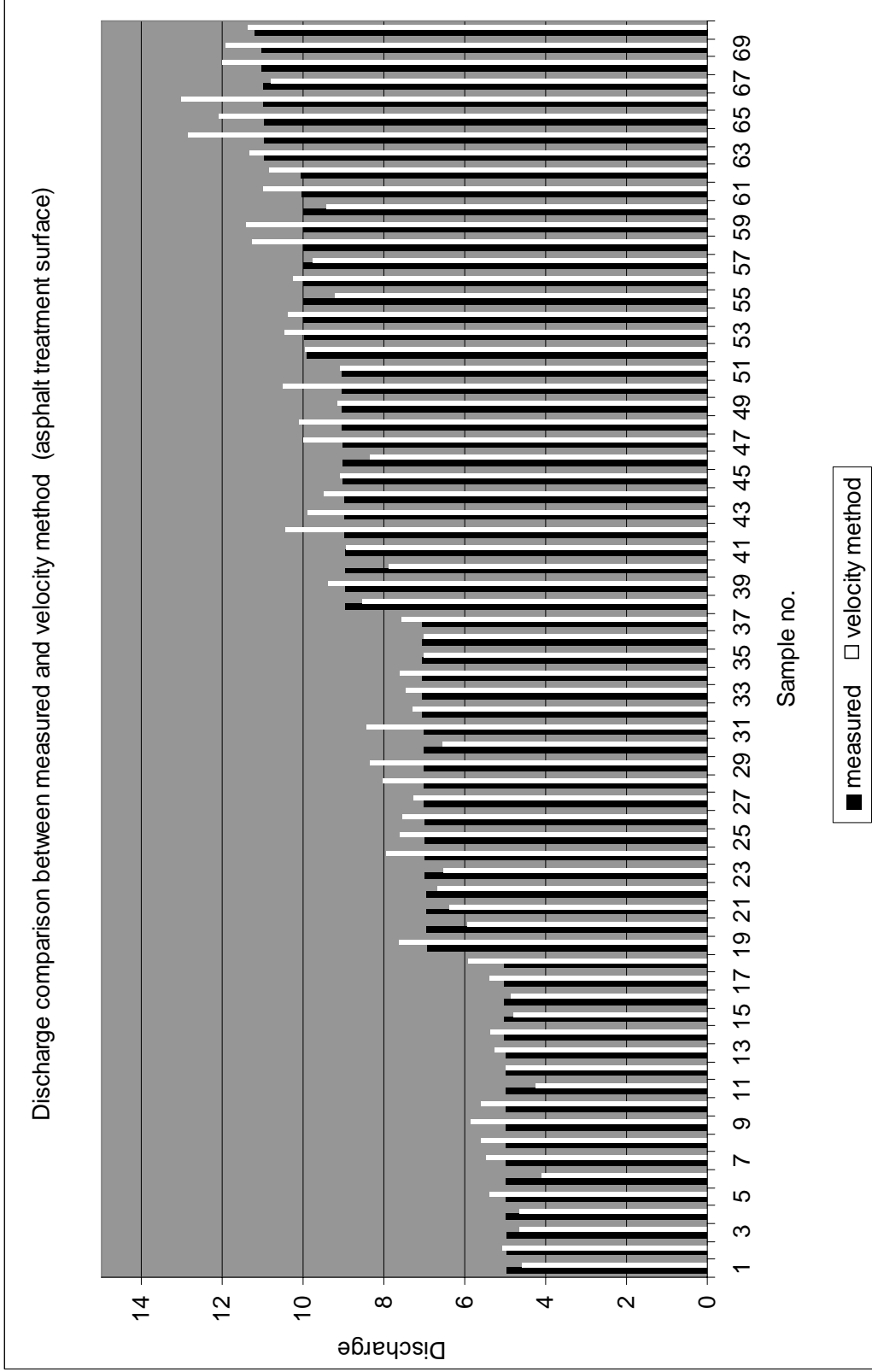


Figure D2.4 Comparison of discharge between measured and Prandtl and Von Karman velocity method for asphalt treatment surface (after remove outliers)

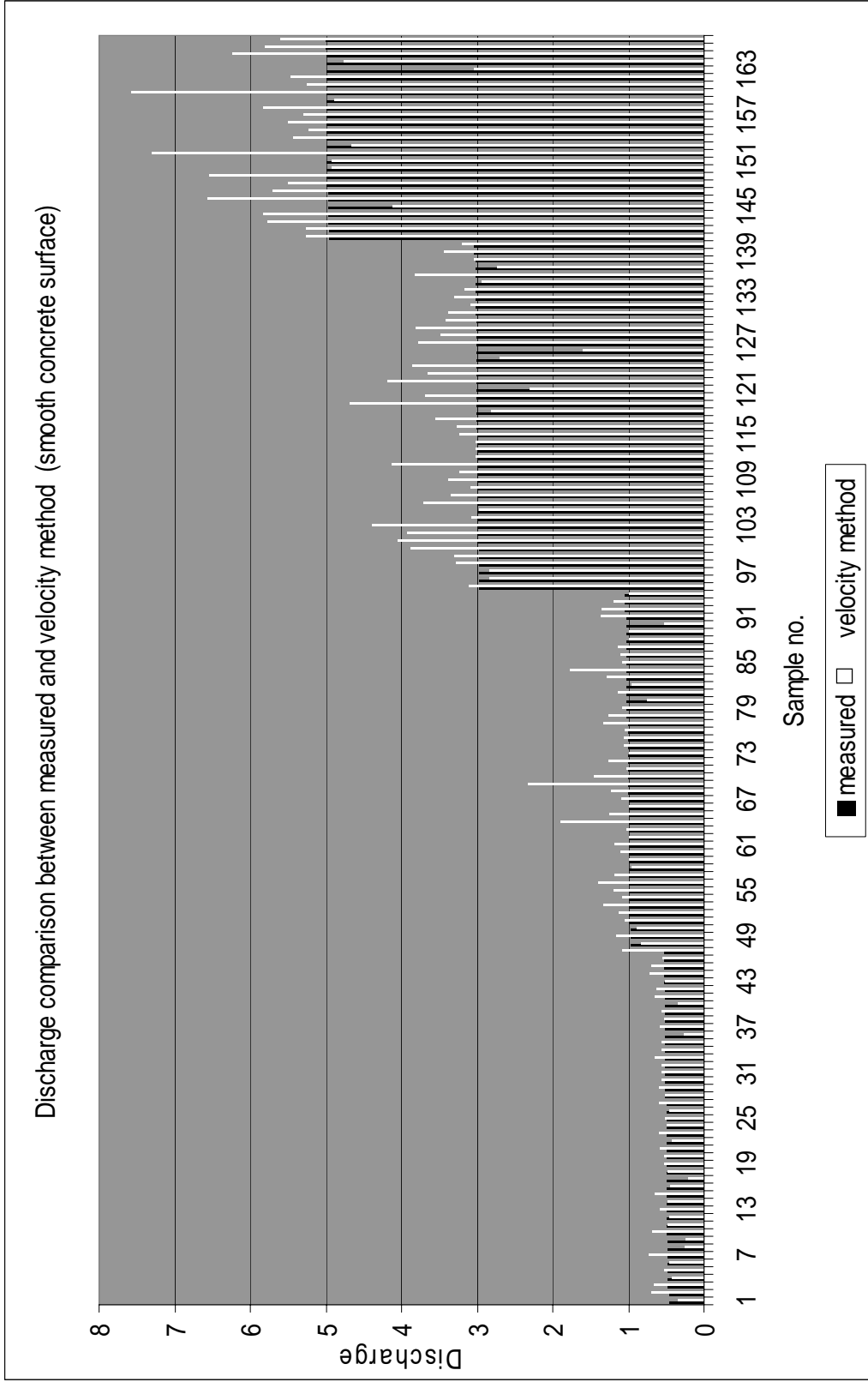


Figure D3.1 Comparison of discharge between measured and Prandtl and Von Karman velocity method for smooth concrete surface (before remove outliers)

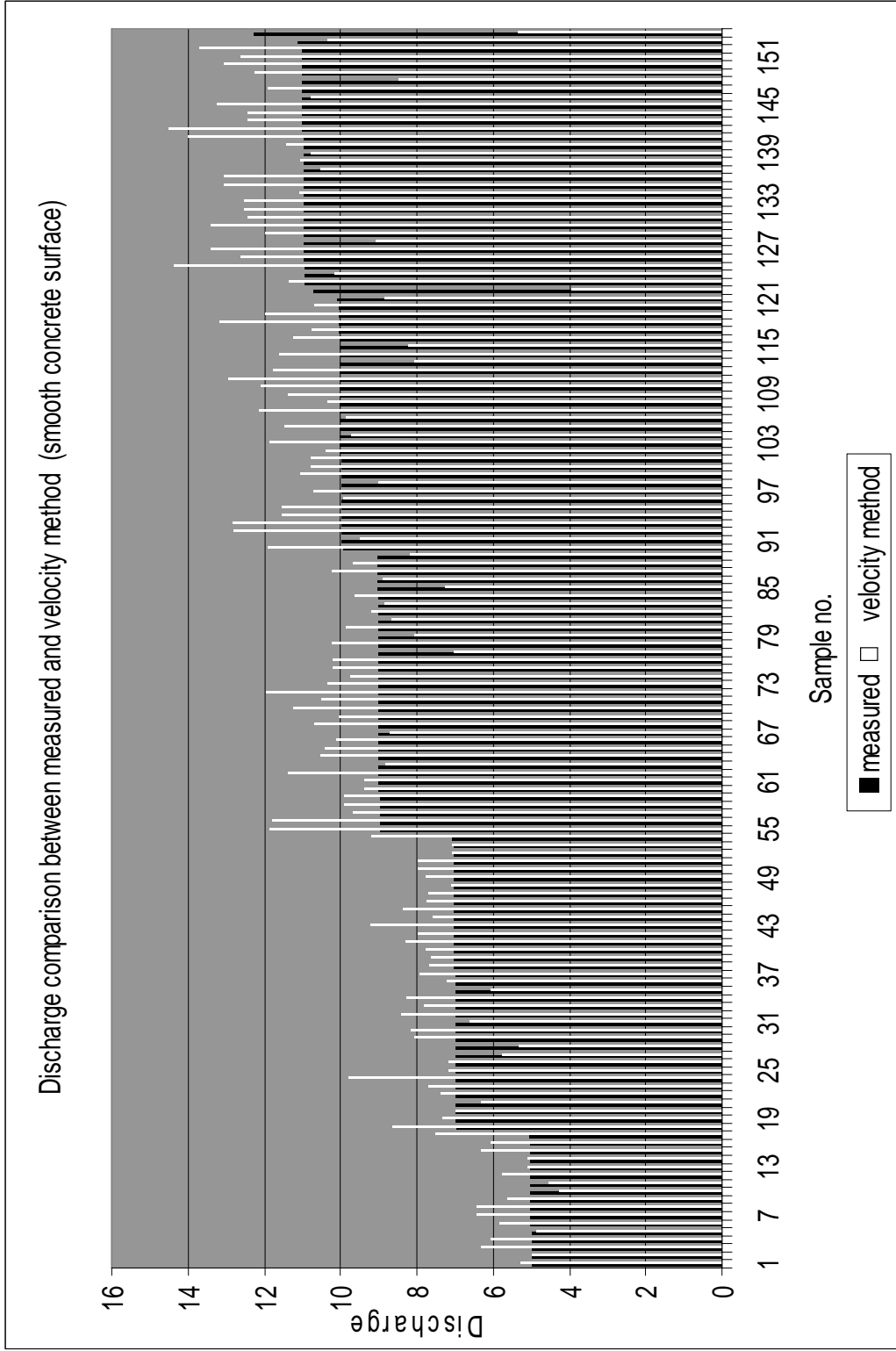


Figure D3.2 Comparison of discharge between measured and Prandtl and Von Karman velocity method for smooth concrete surface (before remove outliers)

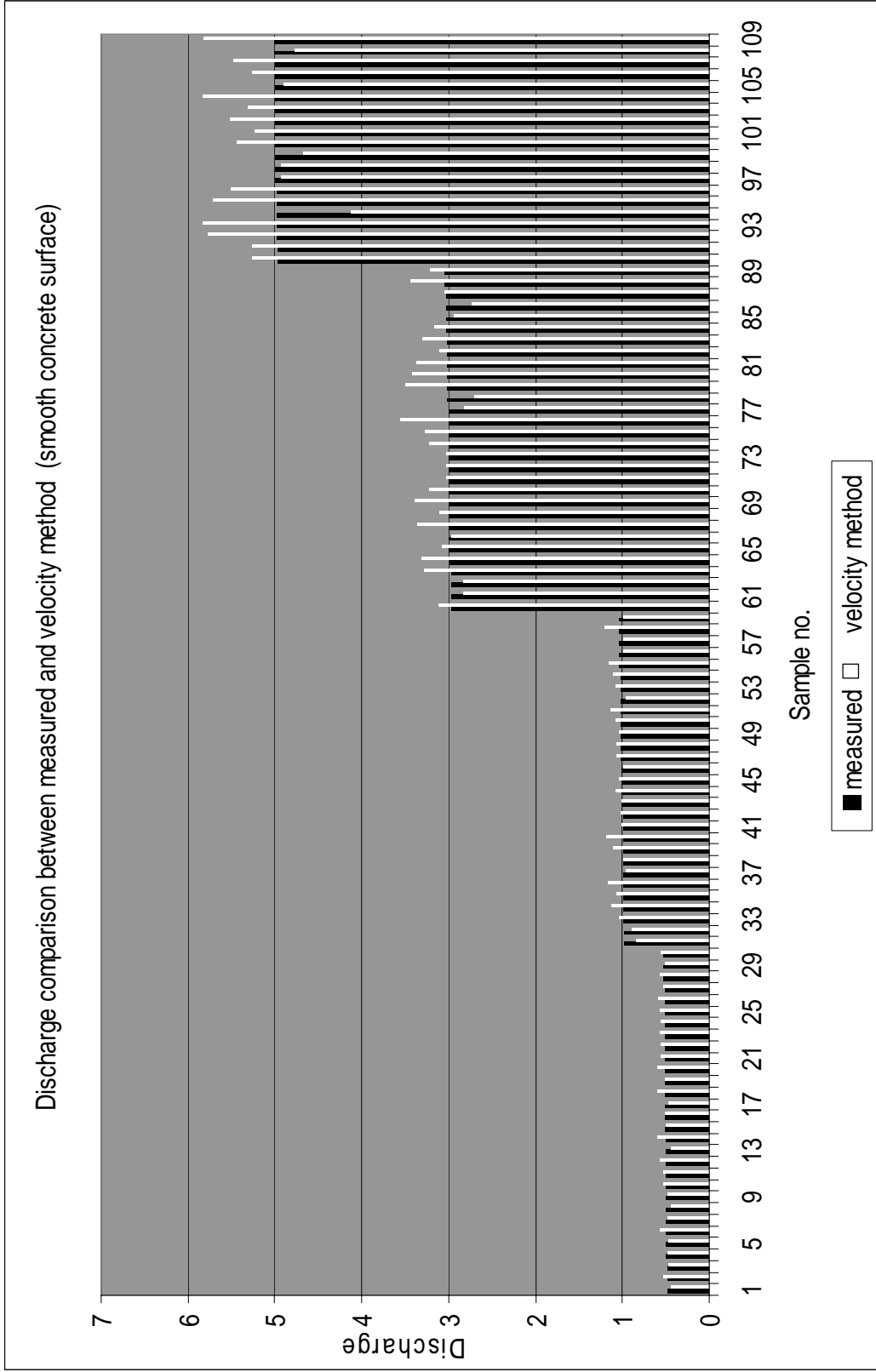


Figure D3.3 Comparison of discharge between measured and Prandtl and Von Karman velocity method for smooth concrete surface (after remove outliers)

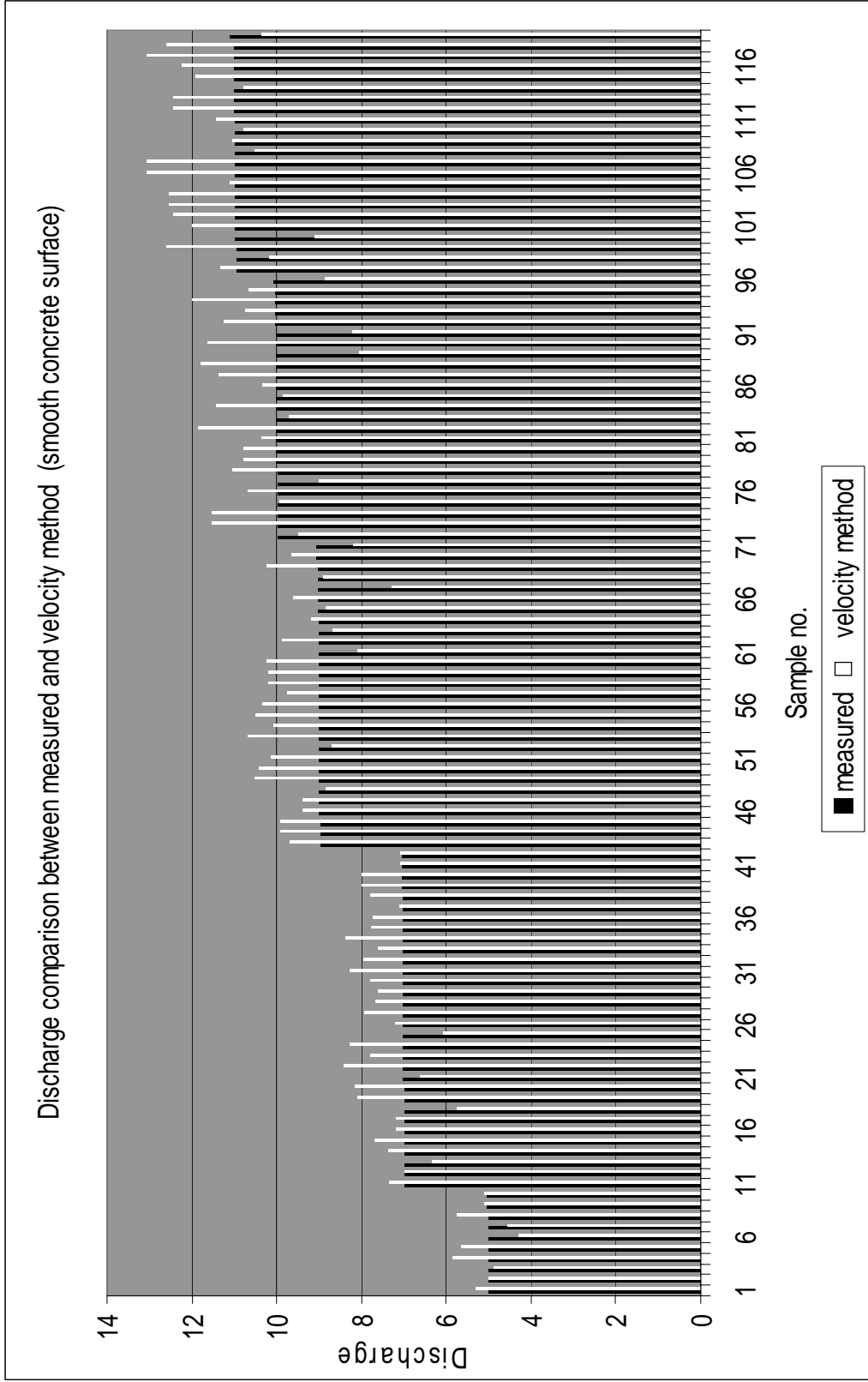


Figure D3.4 Comparison of discharge between measured and Prandtl and Von Karman velocity method for smooth concrete surface (after remove outliers)

APPENDIX E

HISTOGRAM PLOTS OF MANNING'S N-VALUES

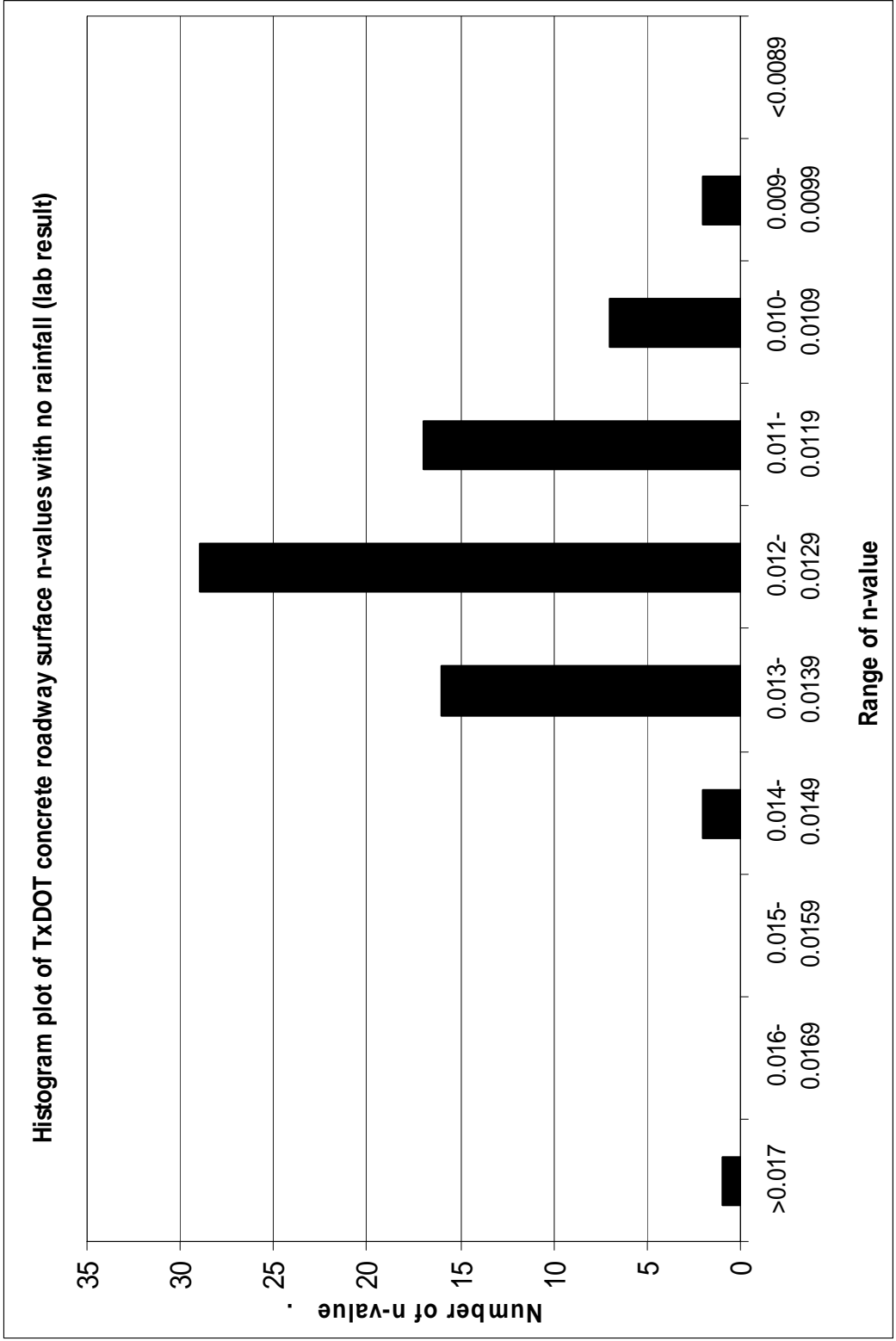


Figure E1.1 Histogram plot of TxDOT concrete roadway surface n-values with no-rainfall (lab result)

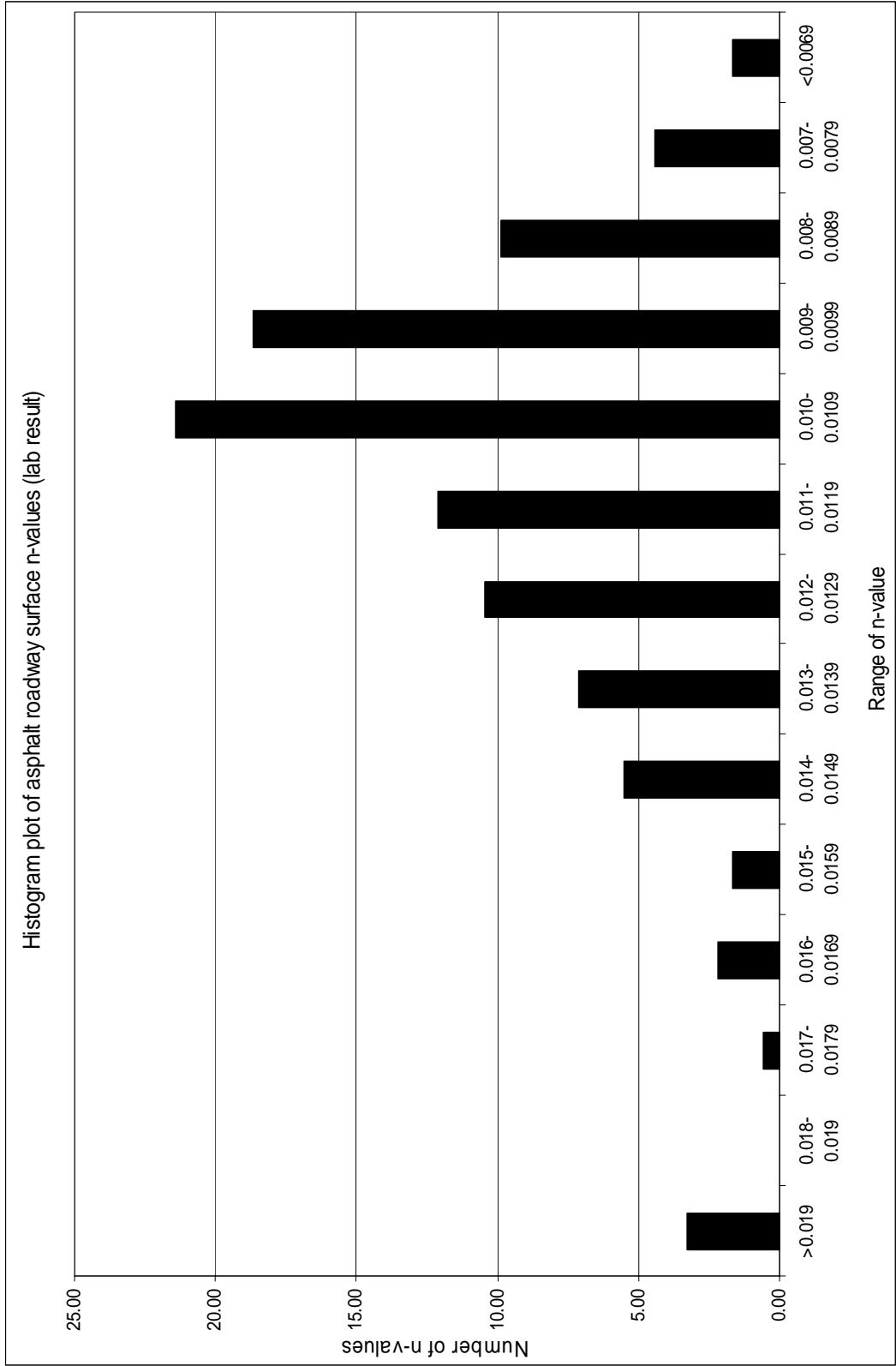


Figure E1.2 Histogram plot of asphalt roadway surface n-values (lab result)

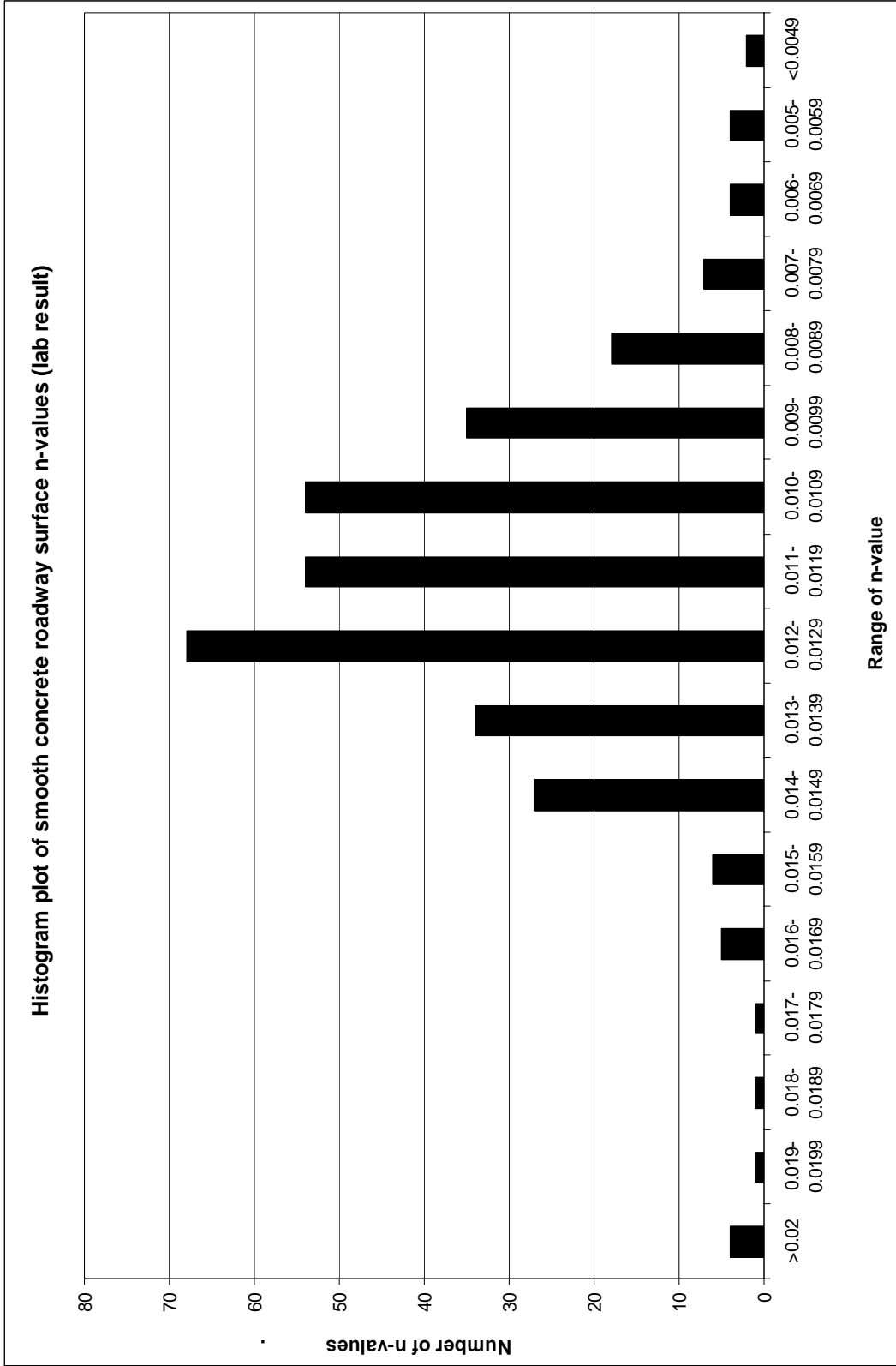


Figure E1.3 Histogram plot of smooth concrete roadway surface n-values (lab result)

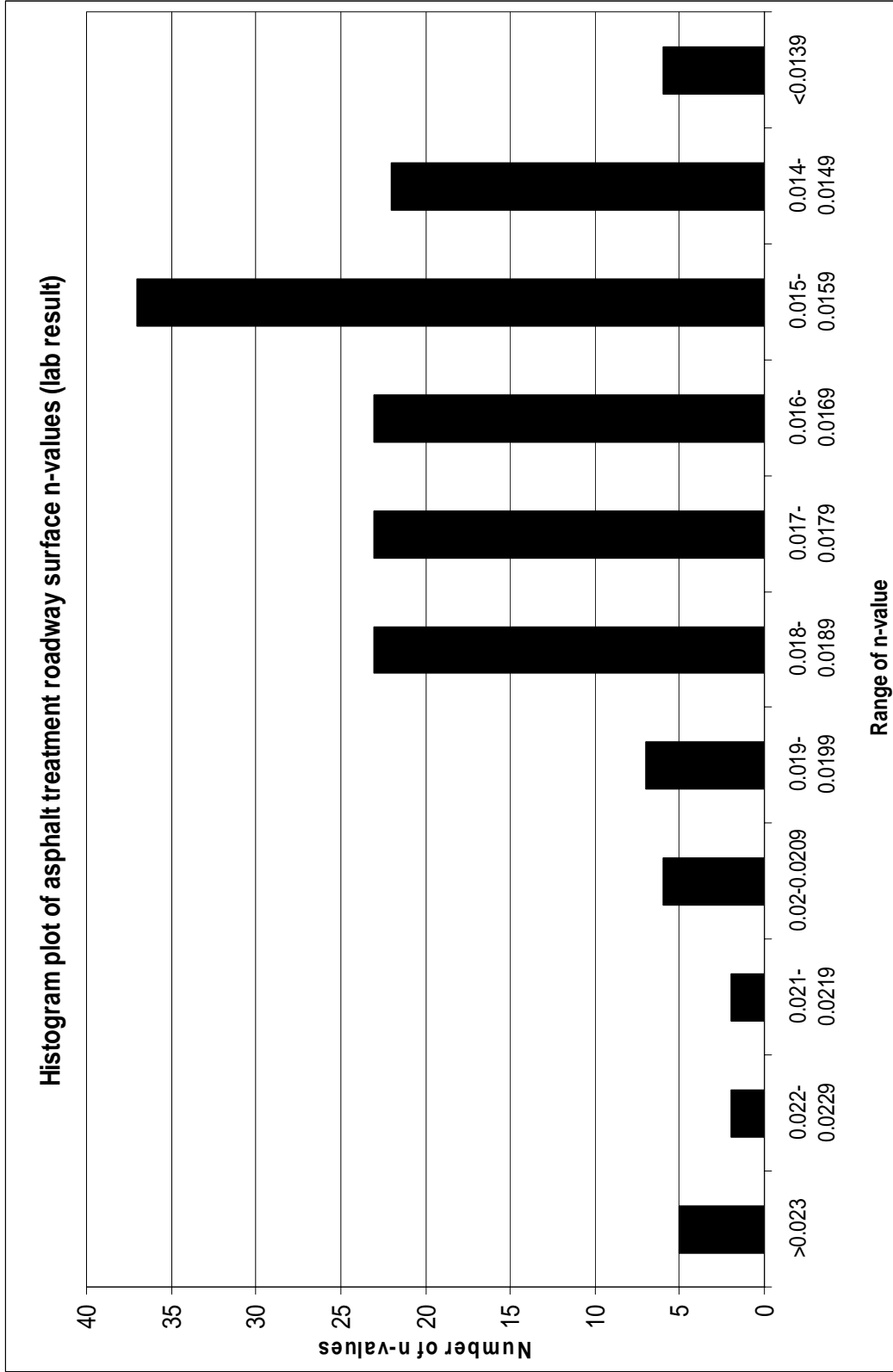


Figure E1.4 Histogram plot of asphalt treatment roadway surface n-values (lab result)

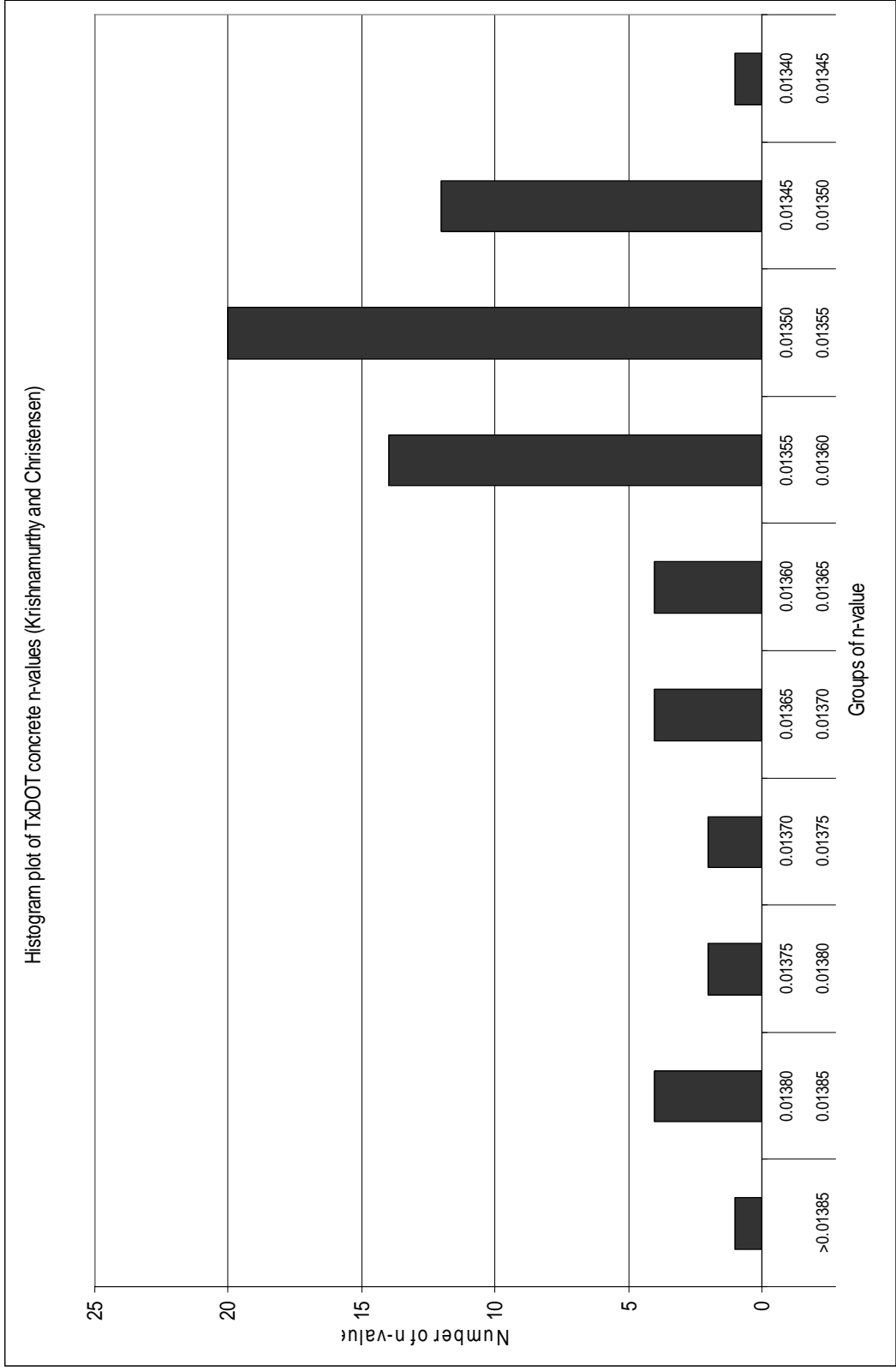


Figure E2.1 Histogram plot of TxDOT roadway surface n-values (Krishnamurthy and Christensen)

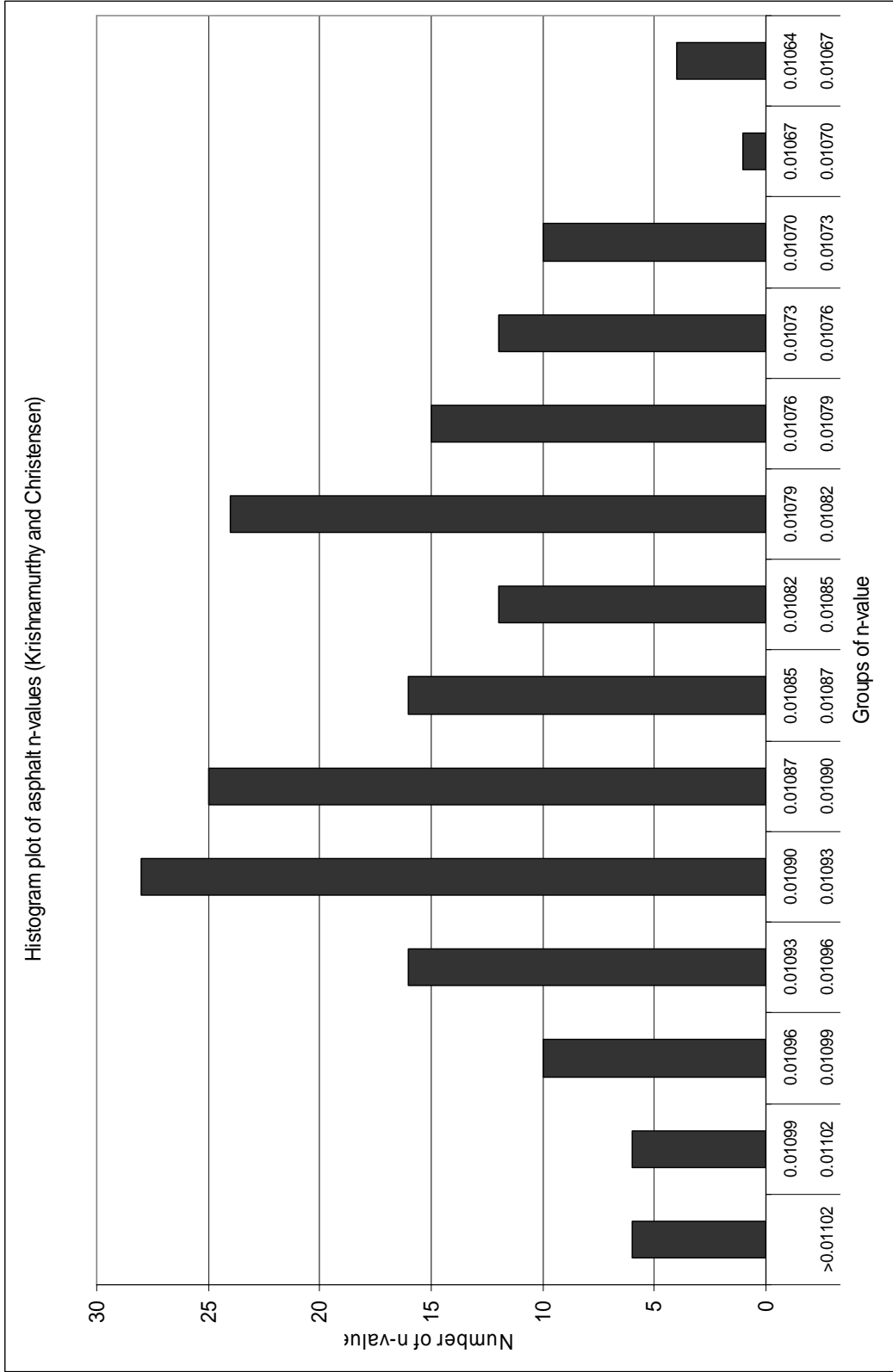


Figure E2.2 Histogram plot of asphalt roadway surface n-values (Krishnamurthy and Christensen)

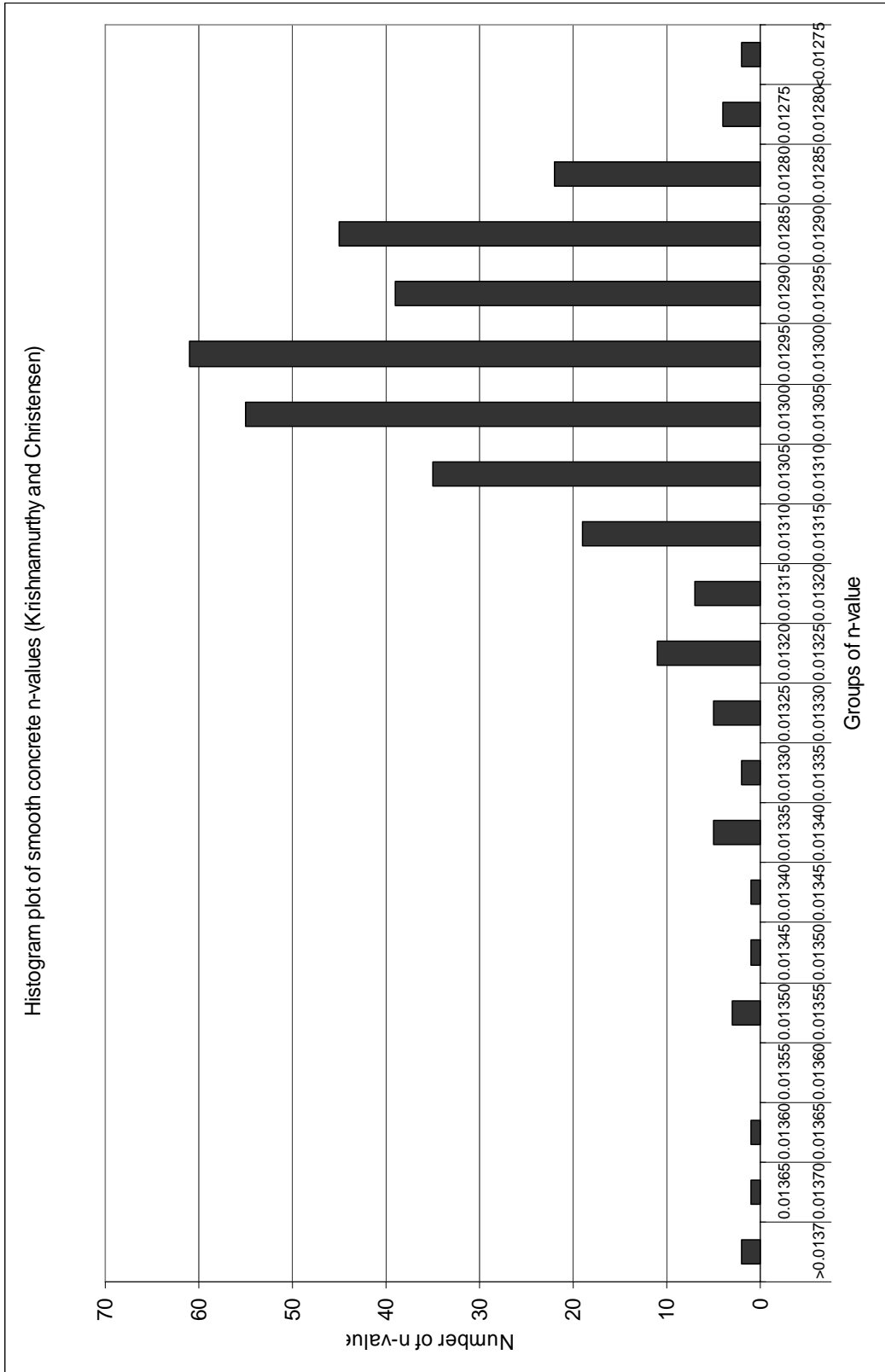


Figure E2.3 Histogram plot of smooth concrete roadway surface n-values (Krishnamurthy and Christensen)

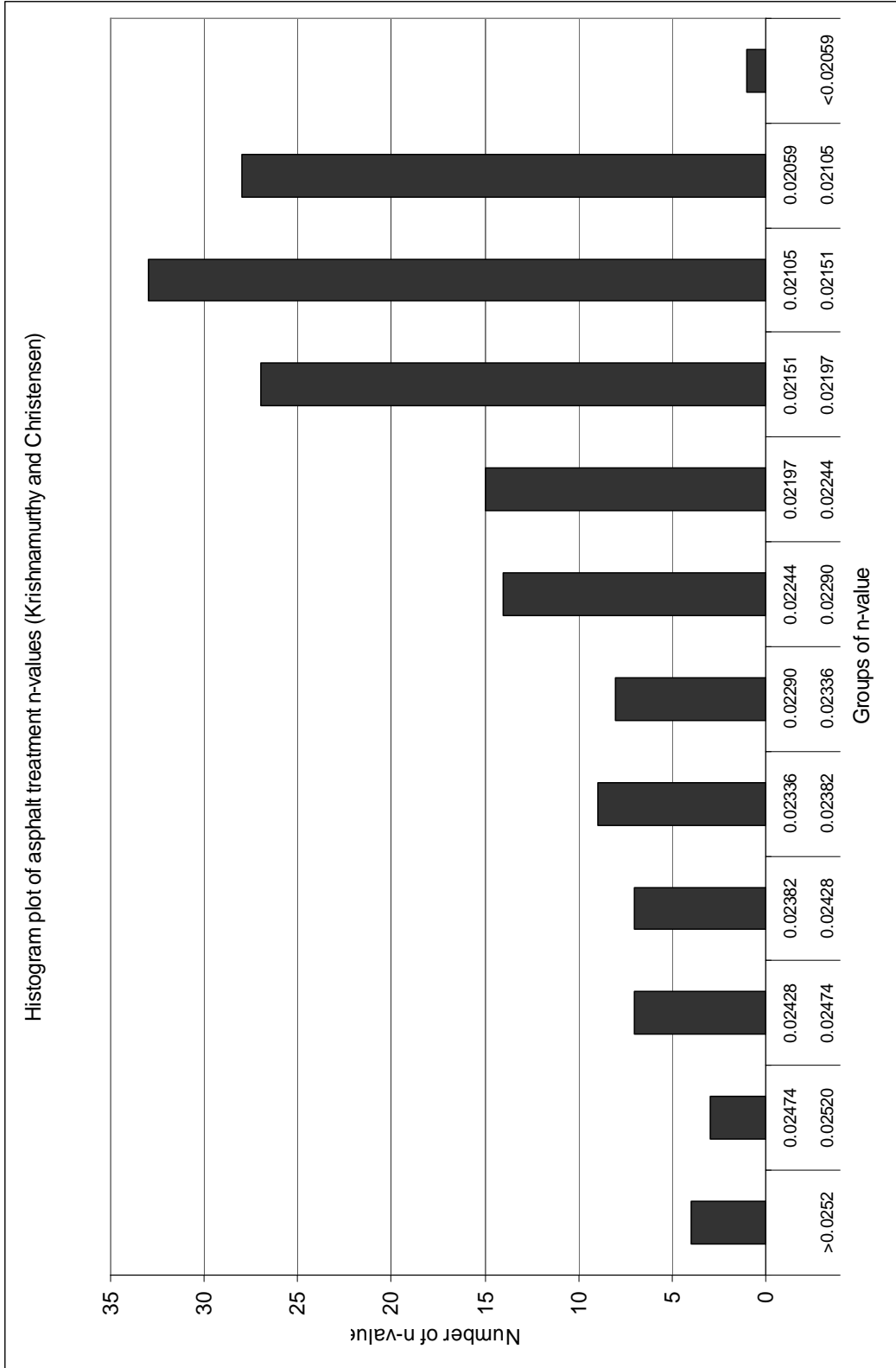


Figure E2.4 Histogram plot of asphalt treatment roadway surface n-values (Krishnamurthy and Christensen)

REFERENCES

1. Bathurst, J.C., 2002. *At-a-site variation and minimum flow resistance for mountain rivers*, Journal of Hydrology 269, September.
2. Bathurst, J.C., Li, R.M., Simons, D.B., 1981. *Resistance equation for large-scale roughness*. Proc. ASCE, Journal of Hydraulic Division. 107(HY12), 1593-1613.
3. Bathurst, J.C., 1985. *Flow resistance estimation in mountain rivers*, Proc ASCE, Journal of Hydraulic Engineering, 111(4), pp 625-643.
4. Bettess, Roger, 2002. *Flow resistance equation for gravel bed-rivers*, International Association of Hydraulic Engineering and Research.
5. Boyer, M.C., 1954. *Estimating the Manning coefficient from an average bed roughness in open channels*, Transactions, American Geophysical Union. Vol. 35, Number 6.
6. Bray, D.I., 1979. *Estimating average velocity in gravel-bed rivers*, Proc ASCE, J of Hydraulic Division, 105(9) pp1103-1122.
7. Charlton, F.G., Brown, P.M. and Benson, R.W., 1978. *The hydraulic geometry of some gravel rivers in Britain*, HR Wallingford Report IT 180.
8. Chow, V.T., 1959. *Open-channel hydraulics* McGraw-Hill Book, Page192-211

9. Colebrook, C.F., 1939. *Turbulent flow in pipes, with particular reference to the transition region between the smooth and rough pipe laws*, J. Intuition of Civil Engineering, 11, pp 113.
10. Colebrook, C.F. and White, C.M., 1937. *Experiments with fluid friction in roughened pipes*, Proc Roy Soc (A), 161.
11. Coon, W.F., 1995. *Estimates of roughness coefficients for selected natural stream channels with vegetated banks in New York*. US Geology Survey, Lake Wood, CO, pp 127.
12. Daniel, M.K., F.J. Watts, and E. R. Burroughs., 1995. *Effect of surface roughness and rainfall impact on overland flow*, Journal of Hydraulic Engineering, pp 546-553.
13. Filliben, J.J., 1975. The probability plot correlation coefficient test for normality, Technometrics, 17, no.1 (1975), 111-117.
14. Griffith, G.A., 1981. *Flow resistance in coarse gravel bed rivers*, Proc ASCE, J of Hydraulic Division, 107(7), pp899-918.
15. Golubtsov, V.V., 1969. *Hydraulic resistance formula for computing the average flow velocity of mountain rivers*. Soc. Hydrology, Am. Geophysics 5, 500-511.
16. Hey, R.D., 1979. *Flow resistance in gravel bed rivers*, Proc ASCE, J of Hydraulics Division, 105(4), pp365-379.
17. Horton, R.E., 1933. *Separate roughness coefficients for channel bottom and sides*, *Engineering News-Record*, vol. 111, no 22, pp 652-653.

18. Jarret, R.D., 1983. *Hydraulic of high gradient stream*. ASCE Journal of Hydraulic Engineering 110(11): 1519-1539.
19. Johnson, R.A. and Wichern, D.W., 2002. *Applied multivariate statistical analysis*, 5th edition. Prentice Hall.
20. Joseph B.F, Finnemore, E. J., 1997. *Fluid mechanics with engineering applications*, Ninth Edition. McGraw Hill.
21. Krishnamurthy, M. and B.A. Christensen. 1972. *Equivalent roughness for shallow channels*, J. Hyd. Div., ASCE 98, no. HY12. pp. 2257-63.
22. Lane, E.W. and Carlson, E.J. 1953. *Some factors affecting the stability of canals constructed in coarse granular materials*, Proceedings, Minnesota International Hydraulics Convention, Minneapolis, MN, 1-4 September.
23. Langbein, W.B., 1940. *Determination of Manning's n from vertical-velocity curves*, Transactions, American Geophysical Union. pp.618-620.
24. Limerinos, J.T., 1970. *Determination of the Manning coefficient from measured bed roughness in natural channels*, Water Supply Paper 1898-B, US Geological Survey, Washington.
25. Lotter, G.K., 1933. *Considerations on hydraulic design of channels with different roughness of walls*, Transactions, All-union Scientific Research Institute of Hydraulic Engineering, Leningrad, vol. 9, pp. 238-241.
26. Prandtl, Ludwig., 1926. *Uber die ausgebildete Turbulenz (On fully developed turbulence)*, Proceedings of the 2nd International Congress of Applied Mechanics, Zurich, pp62-74.

27. Montgomery, D.C., Runger, G.C., Hubele, N.F., 2004. *Engineering statistics*, Third Ed. John Wiley.
28. Meyer-Peter, E. and Müller, R. (1948). *Formulas for bed-load transport*. Proc., 2nd Meeting, M IAHR, Stockholm, Sweden, 39-64.
29. O'Brien, M.P., 1937. *The vertical distribution of velocity in wide rivers*, Hydrology pp467-470.
30. Pavlovski, N.N., 1931. *On a design formula for uniform movement in channels with nonhomogeneous walls*. Transactions, All-union Scientific Research Institute of Hydraulic Engineering , Leningrad, vol. 3, pp. 157-164.
31. Rickenmann, D., 1996. *An alternative equation for the mean velocity in gravel-bed river and mountain rivers*, ASCE Hydraulic Engineering, pp. 672-676.
32. Singh, V.P., 1996. Kinematic wave modeling in water resources (Surface water hydrology), Wiley Interscience. 254-357.
33. Scobey, F.C., 1915. *The flow of water in irrigation channels*. U.S. Department of Agriculture. Paper Bulletin, 194.
34. Streeter, V.L., 1958. *Fluid mechanics*, Fifth Ed. McGraw-hill Book.
35. Strickler, A., 1923. *Beiträge zur Frage der Geschwindigkeitsformel und der Rauigkeitszahlen für Ströme, Kanäle, und geschlossene Leitungen*, Mitteilung Nr. 16 des Amtes für Wasserwirtschaft, Eidgenössisches Department des Innern, Bern; 77.
36. Sturm, T.W., 2001. *Open channel hydraulics*, McGraw Hill Book.

37. Von Karman, T., 1930. *Mechanische Aehnlich und Turbulenz (Mechanical similarity and turbulence)*, Proceedings of the 3ed. International Congress of Applied Mechanics, Stockholm, Vol. 1, pp. 85-92.
38. Wahl, K.L., Thomas, W.O., Jr., and Hirsch, R.M., 1995. *Stream-gagging program of the U.S. Geological Survey*.
39. Wiberg, P.L., Smith, J.D., 1991. *Velocity distribution and bed roughness in high-gradient stream*. Water Resources. Res. 27, (5), 825-838,
40. Yen, B.C., 1992. *Hydraulic resistance in open channels (channel flow resistance: centennial of Manning's formula)*, ed. B.C. Yen. Littleton, CO: Water Resources Publications, pp241-257.

BIOGRAPHICAL INFORMATION

Chirakarn received an undergraduate degree in Irrigation Engineering from Kasetsart University, (Thailand) in July 2001. He continued study in water resources area at Civil and Environment department, The University of Texas at Arlington. He worked as a graduate research assistant in Texas Department of Transportation (TxDOT) roadway roughness project from 2002-2005. He received his Master Degree in Civil Engineering in December 2003.

After his Master Degree, he began his research in velocity distribution modeling and worked as a graduate teaching assistant in Civil and Environment Department. He received his Philosophy Degree in Civil Engineering from The University of Texas at Arlington in August 2007. His area of expertise is Water Resources Engineering.